UNIVERSITY OF CALIFORNIA,
IRVINE

Enhancing functional properties of self-assembled neomenisci and neocartilage toward their implantation in a suitable preclinical large animal model

DISSERTATION

Submitted in partial satisfaction of the requirements for the degree of

DOCTOR OF PHILOSOPHY

in Biomedical Engineering

by

Erik Gonzalez-Leon

Dissertation Committee:
Distinguished Professor Dr. Kyriacos Athanasiou, Chair
Associate Professor Dr. Tim Downing
Dr. Jerry Hu

2022

DEDICATION

To

My parents, Monica Leon and Carlos Gonzalez, and stepmom, Claudia Curti, who have always given me love, helped shape me into the person I am today, and have always been model examples of resiliency through turbulent times.

My family, especially my grandparents Gricelda Contreras, Gustavo Leon, and Sergio Gonzalez who are no longer here with us in person but will always be with us in spirit.

My siblings, Jorge and Sofia. Always strive for excellence and be kind to those around you; the next generation will be better because of you two.

Taylor Brown, a kind soul with a brilliant mind who left us much too soon. We continue to hold you in our memories, and you will always be remembered as a shining light with a contagious smile.

Table of Contents

Acknowledgments

My academic journey has reached heights I never could have imagined. I was fortunate that my hard work and dedication in high school led me to the beautiful UC San Diego campus, making me the first in my family to attend a university. During my early undergrad years, while in the process of trying to pass my classes and meeting a myriad of amazing people, I was first introduced to research in the bioengineering field. Funnily, I had no idea what a PhD or doctorate was until I realized I was being taught by professors with PhDs the entire time. Coming from humble roots in Chula Vista, this concept of advanced education was new to me and, thus, my eyes were opened to incredible opportunities. Years later, despite several peaks and valleys that were traversed in life, I find myself at the precipice of earning my own doctoral degree and the culmination of my academic career at UC Irvine. Reflecting on this journey reassures me that I can take on monumental challenges in life, and that these achievements could not have been accomplished without the unwavering support of very special people in my life.

First and foremost, I would like to thank my advisor, Dr. Kyriacos Athanasiou, who believed in me enough to give me a chance to join his lab and prove myself. I am grateful that you saw something in me because your mentorship, patience, and advice have helped me develop incredibly as a researcher. Never did I imagine that I would be the recipient of a national fellowship, much less two, and that I would present an award-winning abstract to some of the most brilliant minds in biomedical engineering. Also, I would like to thank Dr. Jerry Hu for his mentorship and blunt honesty throughout the years. My writing would not have improved without our countless editing sessions, and I

am grateful for all the training you provided me in addition to the many conversations about our dogs and their quirks.

Also, while graduate school was crucial to my development, this journey began with the help of several people at UCSD. Specifically, I would like to thank Drs. Marcelo Rivera-Aguilar, Todd Coleman, and Shu Chien for their mentorship and setting the foundation for my research endeavors. I would also like to thank Drs. Valita Jones and Antonio DeMaio for guiding me during my time with IMSD.

My time in this laboratory has allowed me to rub shoulders with some of the most brilliant and driven people I have ever met, much less work with. I would like to thank Dr. Evelia Salinas, Dr. Jarrett Link, Gaston Otarola, Ryan Donahue, Ben Bielajew, Dr. Wendy Brown, Dr. Heenam Kwon, Dr. Gabriela Espinosa, and Dr. Rachel Nordberg for all the moments we have shared together, both professionally and outside of the lab.

Finally, I would like to thank my partner Caitlin Semper, parents Monica Leon and Carlos Gonzalez, stepmom Claudia Curti, brother Jorge, sister Sofia, extended family, closest friends, and dogs Cleo and Toffee for their unconditional support, patience, and their propensity for putting a smile on my face. Without you all, reaching the end of this academic journey would not have been possible.

Curriculum Vitae

Erik Gonzalez-Leon

2013-2014, Undergraduate Student Researcher, Molecular Vascular Bioengineering Lab, Advisors: Shu Chien & David Brafman, University of California, San Diego

2015-2016, Undergraduate Student Researcher, Neural Interaction Lab, Advisor: Todd Coleman, University of California, San Diego

2016, BS in Bioengineering (Minor in Business), University of California, San Diego

2016, University of California, Irvine Eugene Cota-Robles (ECR) Fellowship Awardee

2017-2022, Graduate Student Researcher, DELTA*i*, Advisor: Kyriacos A. Athanasiou, University of California, Irvine

2018, Teaching Assistant, University of California, Irvine

2018-2022, National Science Foundation Graduate Research Fellowship Program Awardee

2018-2021, Howard Hughes Medical Institute Gilliam Fellowship Awardee

2019, Biomedical Engineering Society (BMES) Student Design and Research Award Recipient

2020, MS in Biomedical Engineering, University of California, Irvine

2022, PhD in Biomedical Engineering, University of California, Irvine

Field of Study

Enhancing functional properties of self-assembled neomenisci and neocartilage toward their implantation in a suitable preclinical large animal model

Publications

1. Salinas, EY*, **Gonzalez-Leon, EA***, Hu, JC, & Athanasiou, KA. *Improving mechanical properties of neocartilage with a combination of uniaxial tension and fluid-induced shear stress during tissue culture* (manuscript currently in preparation), *indicates co-first authorship.

2. Espinosa, MG, **Gonzalez-Leon, EA**, Hu, JC, & Athanasiou, KA. *Hyperelastic mechanical properties correlate to biochemical composition of native and tissue-engineered knee menisci* (manuscript currently in preparation).

3. **Gonzalez-Leon, EA**, Hu, JC, & Athanasiou, KA. *Yucatan minipig knee meniscus regional biomechanics and biochemical structure support its suitability as a large animal model for translational research.* Frontiers in Biomedical Engineering and Biotechnology. (2022).

4. Wang, D, **Gonzalez-Leon, EA**, Rodeo, SA, & Athanasiou, KA. *Clinical Replacement Strategies for Meniscus Tissue Deficiency.* Cartilage (2021)

5. **Gonzalez-Leon, EA**, Bielajew, BJ, Hu, JC, & Athanasiou, KA. *Engineering self-assembled neomenisci through combination of matrix augmentation and directional remodeling.* Acta Biomaterialia (2020)

6. Donahue, RP*, **Gonzalez-Leon, EA***, Hu, JC, & Athanasiou, KA. *Considerations for translation of tissue engineered fibrocartilage from bench to bedside. Journal of Biomechanical Engineering* (2018), *indicates co-first authorship.

Abstract

Enhancing functional properties of self-assembled neomenisci and neocartilage toward their implantation in a suitable preclinical large animal model

by

Erik Gonzalez-Leon

Doctor of Philosophy in Biomedical Engineering

University of California, Irvine, 2022

Distinguished Professor Kyriacos Athanasiou, Chair

Knee meniscus injury is frequent, resulting in over 1 million surgeries annually in the United States and Europe. Loss of meniscus tissue has been associated with early onset knee osteoarthritis due to an increase in joint contact pressures in meniscectomized knees; thus, meniscal injury also leads to damage on articular cartilage surfaces within the knee joint. Clinically available replacement strategies range from allograft transplantation to synthetic implants. Although short-term efficacy has been demonstrated with some of these treatments, factors such as long-term durability and chondroprotective efficacy remain unpredictable. Because of the near-avascularity of this fibrocartilaginous tissue and its intrinsic lack of healing, tissue engineering has been proposed as a solution for meniscus repair and replacement. In particular, bioactive and mechanical stimulation during culture can be used to enhance mechanical properties and drive extracellular matrix content toward native tissue levels. Before an effective tissue-engineering strategy for treating meniscal lesions can be translated to the clinic, the United States Food and Drug Administration (FDA) requires rigorous preclinical testing of

the safety and efficacy of these technologies in a large animal model. However, guidance documents for meniscus repair technologies are nonexistent and no gold-standard animal model has been established for preclinical meniscus research. Thus, toward translating tissue engineering technologies to clinical applications, the global objectives of this research are: 1) to enhance self-assembled neomeniscus and neocartilage mechanical and biochemical properties through application of bioactive or mechanical stimuli, and 2) to identify appropriate implantation and integration methods in a large animal model to validate the repair capacity of the tissue-engineering strategies developed *in vitro*.

To address these objectives, this research: 1) enhanced the mechanical and extracellular matrix properties of neomenisci using bioactive factors TGF-β1, chondroitinase ABC, and lysyl oxidase-like 2 (collectively termed "TCL"), in addition to lysophosphatidic acid (LPA); 2) improved neocartilage mechanical and biochemical properties through sequential application of two forms of mechanical stimuli (uniaxial tension and fluid-induced shear); 3) established the Yucatan minipig as a suitable preclinical animal model for meniscus research by showing that several gross morphological, mechanical, and biochemical properties were within ranges of values reported in human menisci; and 4) evaluated the efficacy of neocartilage implanted in the medial meniscus of Yucatan minipigs toward repairing meniscal lesions.

An approach employing bioactive stimuli to enhance both extracellular matrix content and organization of neomenisci toward augmenting their mechanical properties was investigated. Specifically, self-assembled neomenisci were treated with TCL+LPA. Supporting our hypothesis, TCL+LPA treatment synergistically improved circumferential tensile stiffness and strength, significantly enhanced collagen and pyridinoline crosslink

contents per dry weight by 61% and 81% over controls, respectively, and achieved tensile anisotropy (circumferential/radial) values of neomenisci close to 4. This study utilized a combination of bioactive stimuli for use in neomeniscus tissue engineering studies that improved functional properties to achieve anisotropic tensile properties, which is a crucial mechanical aspect of the native meniscus, providing a promising path toward deploying these neomenisci as functional repair and replacement tissues.

To investigate whether a hyperelastic model could capture changes to native and engineered meniscus functional properties to better inform meniscus tissue engineering strategies, three different hyperelastic models were applied to mechanical and biochemical data from native tissue treated with bioactive treatments, namely collagenase. Experimental data from neomenisci treated with bioactive factors in a previously published study, specifically TCL+LPA treated neomenisci, were also examined using hyperelastic analysis. Small-strain analysis, which is largely phenomenological, is typically used to model the meniscus; however, the meniscus experiences large strains (~40%) under normal loading conditions. Collagenase treatment on native meniscus samples led to significant decreases in tensile properties and collagen content compared to untreated controls. The three hyperelasticity models examined were Neo-Hookean, Yeoh, and fiber-reinforced neo-Hookean models; it was hypothesized that a microstructural, hyperelastic model would best describe the experimental data and provide model parameters that would correlate with the biochemical content of both engineered and native tissues. Out of the three, the fiber-reinforced Neo-Hookean model, which incorporates tissue microstructural properties, was found to be the best model based on goodness-of-fit. Positive correlations between

both collagen content (ρ=0.81) and pyridinoline crosslinking (ρ=0.69) and the fiber modulus (γ), which is a stress-like material property determined from mechanical tests of the tissue, were identified. Interestingly, the strongest correlation existed between the collagen to GAG ratio (ρ=0.84) and the nonlinearity parameter (α). Together, these data provide a hyperelastic model that allows for deeper understanding of meniscal function with regard to its structural properties, and aids tissue engineers in the design of functional neomenisci toward their use in repair and replacement technologies.

The manipulation of neocartilage construct mechanical properties toward native tissue values can also be achieved with applied mechanical stimuli during culture. Uniaxial tensile stress, for example, has been found to improve tensile stiffness and strength of bovine-derived neocartilage constructs, while fluid-induced shear (FIS) improved constructs' compressive stiffness. It was hypothesized, first, that combining two mechanical stimulation strategies, specifically, uniaxial tension and FIS, would improve multiple neocartilage mechanical properties more effectively compared to using one stimulus alone and, secondly, that order of stimulus application would lead to differences in neocartilage construct properties. It was found that the combination of both mechanical stimuli led to synergistic improvements to tensile properties and compressive stiffness. Specifically, constructs exhibited tensile Young's modulus, ultimate tensile strength, and compressive aggregate modulus values that were 180%, 161%, and 131% higher than nonstimulated controls, respectively. Furthermore, combining the stimuli had additive effects on the extracellular matrix content of constructs, compared to unstimulated controls. Finally, it was determined that applying tension before FIS was more effective toward improving tissue mechanical properties, specifically tensile

properties, when compared to applying FIS before tension. Overall, the use of complementary dual mechanical stimuli synergistically increased neocartilage properties and a dependence on the order of application was identified; thus, researchers should consider applying these or other forms of complementary mechanical stimuli toward engineering neocartilage with robust properties.

The frequency of knee meniscus injuries and surgical procedures motivates tissue engineering attempts and the need for suitable animal models. Despite their extensive use in cardiovascular research and the existence of characterization data for the menisci of farm pigs, the farm pig may not be a desirable preclinical model for the meniscus due to its rapid weight gain. However, minipigs, such as the Yucatan breed, are suitable for *in vivo* experiments due to their slower growth rate compared to farm pigs and similarity in body weight to humans. Despite this, characterization of minipig knee menisci is lacking**.** Both medial and lateral Yucatan minipig knee menisci were extensively characterized in terms of structural and functional properties within different regions to inform the Yucatan minipig's suitability as a preclinical model for meniscal therapies. Gross morphological properties of minipig menisci that fell within ranges seen in native human tissue included meniscal width and peripheral height. Additionally, per wet weight, biochemical evaluation revealed 23.9-31.3% collagen (COL; 22% for human) and 1.20-2.57% glycosaminoglycans (GAG; 0.8% for human). Also, per dry weight, pyridinoline crosslinks (PYR) were 0.12-0.16% (0.12% for human). Biomechanical testing revealed circumferential Young's modulus of 78.4-116.2MPa (100-300MPa for human), circumferential ultimate tensile strength (UTS) of 18.2-25.9MPa (12-18MPa for human), radial Young's modulus of 2.5-10.9MPa (10-30MPa for human), radial UTS of 2.5-4.2MPa

(1-4MPa for human), aggregate modulus of 157-287kPa (100-150kPa for human), and shear modulus of 91-147kPa (120kPa for human). Anisotropy indices ranged from 11.2-49.4 and 6.3-11.2 for tensile stiffness and strength (approximately 10 for human), respectively. Regional differences in mechanical and biochemical properties within the minipig medial meniscus were observed; specifically, GAG, PYR, PYR/COL, radial stiffness, and Young's modulus anisotropy varied by region. The posterior region of the medial meniscus exhibited the lowest radial stiffness, which mirrors what is seen in humans and corresponds to the most prevalent location for meniscal lesions. Overall, similarities between minipig and human menisci support the use of minipigs for meniscus translational research.

Finally, to investigate the repair capacity of the approaches developed to this point, this work concluded with a large animal study examining the effects of tissue-engineered constructs in a meniscus defect. Allogeneic, self-assembled constructs were implanted into partial-thickness medial meniscus defects in the Yucatan minipig using novel surgical methods. Implants showed an exceptional safety profile and did not lead to a systemic immune response. As hypothesized, the surgical approach that was developed allowed for defect creation and implant delivery; additionally, implant treatment increased Young's modulus values for the interface between native tissue and repair tissue in the pocket where the tissue was embedded by 51% compared to untreated controls. However, the allogeneic implants did not lead to increased defect repair tissue mechanical and biochemical properties because defects in the untreated control group also exhibited robust healing. Thus, modifications to surgical techniques used to implant engineered tissues within preclinical animal models, in addition to changes to the defect model, might

be required to better investigate of the repair capacity of self-assembled constructs and translate our approach from the bench to the clinical bedside.

Introduction

Damage to the knee meniscus is common and can result from trauma and age-related degeneration. Meniscal lesions are the most common intra-articular knee injuries and are the most frequent cause of orthopaedic surgical procedures in the United States. Treatments involve either partial or complete removal of the meniscus, which may alleviate pain temporarily but virtually guarantees the emergence of osteoarthritis.

Knee menisci are semi-circular, wedge-shaped fibrocartilaginous tissues, located between the distal femur and the tibial plateau, that protect articular cartilage via load distribution and near-frictionless properties. Upon compressive loading, the meniscus functions by using its wedge shape to develop tension, which is resisted by the tissue's circumferentially aligned collagen. Collagen content, crosslinking, and organization are, thus, critical to the tensile properties of menisci and their function. The meniscus lacks intrinsic healing abilities due to the avascularity in its inner white zone and low vascularity in its outer red zone, making it a prime target for replacement via tissue-engineering.

To address these issues surrounding knee meniscus clinical indications, repair or replacement strategies need to be developed. Repair involves the resection of the torn tissue, and a biomaterial is then shaped and affixed into the defect site. Replacement is characterized by the removal of the entire meniscus in exchange for a meniscal prosthesis or allograft. *In vivo* meniscus tissue-engineering studies are scarce, and, of these, few report any alleviation of articular cartilage degeneration. Although scarce in number, these studies are immensely important as they all illustrate the need for appropriate biomechanical properties for an engineered tissue. Existing repair and replacement techniques using biomaterials do not offer long-term relief, leading to

osteoarthritis; for the healing of meniscal defects researchers have turned to cell-based therapies, such as tissue engineering.

At present, surgical interventions aimed at meniscal repair or replacement may be deficient due to inappropriate mechanical properties of the biomaterial/graft and lack of donor tissue. Our laboratory has an established track record in generating mechanically functional musculoskeletal tissues, such as the temporomandibular joint (TMJ) disc and articular cartilage. For example, anisotropic neomenisci that also recapitulate the shape of native tissue have been tissue engineered using a cell-based, self-assembling process that forms tissues *in vitro* without the use of scaffolds. Yet, compared to articular cartilage, meniscus tissue-engineering has been less studied in general. With the addition of biochemical stimuli during *in vitro* culture, self-assembled neomenisci have exhibited compressive mechanical properties similar to those of native tissue. However, tensile properties still require improvement before engineered menisci can be deployed as functional tissues. As we aim to reach tensile properties on par with native tissue, the proposed work is significant as it will go a long way toward providing a mechanically functional construct critical to the restoration of meniscus function *in vivo*.

Ultimately, following the translational paradigm, *in vivo* preclinical assessments in a representative animal model are required before deployment of engineered technologies in humans. The pillars of the preclinical assessment criteria are safety and efficacy. Especially for allogeneic implants, first establishing the safety of the approach in a small cohort of animals is a viable and ethical strategy. The minipig has emerged as an attractive animal model for assessing the safety of neocartilage implants due to its anatomical and physiologic similarities to humans, docile nature, and success as a model

for allogeneic temporomandibular joint disc repair. Demonstrating that an allogeneic approach to meniscal defect repair is safe would indicate that approaches of this nature can proceed toward preclinical studies geared more toward assessing durability and efficacy.

Considering the desire for translation of promising meniscus repair and replacement techniques, this work aimed to improve neomeniscus and neocartilage functionality *in vitro,* and sought to establish a newly characterized large-animal meniscus model as suitable for future preclinical research. The global objectives of this work were two-fold: 1) to enhance neomeniscus and neocartilage mechanical and biochemical properties through application of bioactive or mechanical stimuli, and 2) to identify appropriate implantation and integration methods in a large animal model to validate the repair capacity of the tissue-engineering strategies developed *in vitro*. Toward these objectives, three specific aims were investigated:

Specific Aim 1: To enhance tensile properties of neomenisci via application of bioactive stimuli. This aim will combine, for the first time, four stimuli that have separately been shown to enhance the tensile properties of engineered tissues (e.g., articular cartilage). The objective of this aim is to use this combination of stimuli to enhance the tensile properties of neomenisci as well. This work is motivated by our prior work applying combinations of bioactive stimuli to neomenisci; combining transforming growth factor beta-1 (TGF-β1) and chondroitinase ABC (C-ABC) increased circumferential and radial tensile modulus values of neomenisci. Separately, we have also shown that phospholipid lysophosphatidic acid (LPA) increased tensile properties and collagen organization of neomenisci. For the native meniscus, collagen cross-linking agent lysyl oxidase-like 2

(LOXL2) has been shown to preserve tensile properties. *It was hypothesized that the combination of TGF-β1, C-ABC, LOXL2 (TCL) treatments with LPA will lead to the greatest increase in neomeniscus tensile properties.*

Specific Aim 2: To enhance functional properties of neocartilage via mechanical stimuli. The objective of this aim is to use a sequential combination of complementary mechanical stimuli, namely uniaxial tension and fluid-induced shear (FIS), to enhance neocartilage tensile and compressive properties, respectively. Additionally, the effect of the order in which the two stimuli are applied on properties of neocartilage constructs will be investigated. Uniaxial tension and FIS regimens previously used during culture of self-assembled neocartilage were modified to investigate their sequential application in two separate bioreactors; this aim also employed uniaxial tensile stimulus in minipig-derived neocartilage while previous studies utilized bovine and human models. *It is hypothesized that the combination of uniaxial tension and FIS will be more effective than either stimulus alone toward increasing neocartilage mechanical and biochemical properties, and that the order of application for these two stimuli has an effect on neocartilage properties.*

Specific Aim 3: To develop novel surgical fixation techniques to implant allogeneic neocartilage in the minipig to assess efficacy toward repair of meniscal tissue. The objective of this aim is to develop novel surgical implantation methods that enable fixation without direct suturing, then use that method to implant allogeneic neomenisci in the minipig to assess efficacy toward repair of meniscal tissue. Once functional properties of Yucatan minipig-derived neomenisci or neocartilage have sufficiently approached those of native tissue, the next focus will be to implant and integrate the engineered tissue *in vivo*. In a series of pilot studies, the surgical techniques will be developed with Dr. Dean

Wang, orthopaedic surgeon for UC Irvine Health. It is expected that a medial parapatellar approach will allow access to the medial meniscus for defect creation and subsequent implantation of self-assembled neocartilage. Minipigs will receive implants in a full, statistically-powered study and will be sacrificed after 8 weeks for quantitative assessment of biochemical (extracellular matrix content) and mechanical (tensile Young's modulus, UTS) properties. Implant safety will be ensured by assessing immunological responses with histology and a full blood panel. *It is hypothesized that implanted constructs will repair injured meniscal tissue in vivo and retain or improve their tensile properties 8 weeks after implantation.*

The aims have been completed as proposed, and this dissertation describes all work that contributed to their fulfillment. Chapters 1 and 2 establish background information and techniques related to meniscus tissue engineering and surgical replacement. Chapter 1 describes scaffold-free and scaffold-based tissue engineering approaches in the context of translating tissue-engineered technologies, with perspectives based on two fibrocartilaginous tissues that share structure-function relationship similarities, namely the knee meniscus and TMJ disc; methods for obtaining engineered tissue design criteria from native tissues, the FDA translational paradigm, the need for fibrocartilage guidance documents, and possible large-animal models for preclinical studies are introduced. Chapter 2 presents information pertaining to technologies that are currently used clinically to repair the knee meniscus in addition to those that are currently undergoing clinical trials; meniscal allografts, synthetic options, and cell-based approaches, such as self-assembled neomenisci, are discussed. These two chapters guided the execution of the specific aims laid out in this thesis.

For the investigation of Aim 1, Chapter 3 presents research that developed new strategies for enhancing the functional properties of self-assembled neomenisci closer to those of the native knee meniscus. To augment tensile properties, this study utilized bioactive factors known to augment matrix content in combination with a soluble factor that enhances matrix organization and anisotropy via cell traction forces. Specifically, the effect of a bioactive factor cocktail termed “TCL” consisting of transforming growth factor beta-1 (TGF-β1), chondroitinase ABC (C-ABC), and lysyl oxidase like 2 (LOXL2) in combination with lysophosphatidic acid (LPA) on neomeniscus structure-function properties was examined. TCL + LPA treatment synergistically improved neomenisci circumferential tensile stiffness and strength, significantly enhanced collagen and pyridinoline crosslink content per dry weight, and achieved tensile anisotropy (circumferential/radial) values of neomenisci close to 4.

In addition, to better understand how bioactive agents can influence tissue-engineering of the knee meniscus, it is pertinent to utilize appropriate models for the examination of structure-function relationships within native and engineered tissues. To this end, Chapter 4 presents a study that aimed to model both the native knee meniscus and engineered neomenisci at strains that are seen under normal loading conditions (~40% strain); values used for modeling of engineered neomenisci were previously reported in Chapter 3. Hyperelastic modeling of native bovine menisci successfully reflected biochemical and mechanical changes due to bioactive treatments; specifically, a fiber-reinforced Neo-Hookean model also was effective in reflecting changes to self-assembled neomenisci properties that stemmed from TCL+LPA treatment in a previous

study. The work presented in Chapter 4 advances the fields of musculoskeletal biomechanics, tissue engineering, and orthopedics.

Aim 2 is addressed in Chapter 5, which describes the sequential application of two forms of mechanical stimuli, namely uniaxial tension and fluid-induced shear (FIS), on self-assembled neocartilage constructs. These two forms of mechanical stimuli, applied on their own, had previously been identified as effective toward increasing mechanical and biochemical properties of neocartilage constructs. First, it was identified that combining uniaxial tension and FIPS synergistically improved minipig-derived neocartilage mechanical properties and was more effective compared to using one stimulus alone. Secondly, it was determined that applying tension before FIS was more effective toward improving tissue mechanical properties when compared to applying FIS before tension. Together, these findings imply that combining complementary mechanical stimuli, especially in the correct order of application, can be used towards engineering robust neocartilage.

Finally, to address Aim 3, Chapter 6 examined the suitability of the Yucatan minipig as a large animal model for translational meniscus research by characterizing regional mechanics and biochemical structure of medial and lateral menisci and comparing them to human values from the literature. Yucatan minipig menisci were found to have gross morphological, mechanical, and biochemical properties that fell within ranges seen in humans, making them a suitable model for preclinical meniscus studies. Subsequently, Chapter 7 described the development of novel surgical implantation methods that enabled fixation of neocartilage constructs without direct suturing in the knee meniscus, such that the efficacy of implanted constructs toward repair of minipig meniscal tissue could be

assessed. Neocartilage implants were shown to be safe as no systemic immune response was incurred. Implant treatment did not increase mechanical or biochemical properties of repair tissue found within an orthotopic defect, while integration of native to repair tissue was also not improved as shown by a lack of increase to interfacial tensile properties; however, neocartilage implants improved the integration between native tissue laminae that were created to accommodate and retain the implant within the meniscal body.

The product of this body of work and potential future directions it has illuminated are contained in the Conclusions Chapter. Particularly, this work has provided a foundation upon which additional studies to enhance functional properties of engineered neomeniscus and neocartilage tissue through application of bioactive or mechanical stimuli can be conducted. Additionally, this work established a suitable large-animal model for preclinical meniscus research and provided insight into the effectiveness of novel surgical methods used for implantation of tissue constructs toward healing meniscus lesions.

Chapter 1: Considerations for translation of tissue engineered fibrocartilage from bench to bedside

Abstract

Fibrocartilage is found in the knee meniscus, the temporomandibular joint (TMJ) disc, the pubic symphysis, the annulus fibrosus of intervertebral disc, tendons, and ligaments. These tissues are notoriously difficult to repair due to their avascularity, and limited clinical repair and replacement options exist. Tissue engineering has been proposed as a route to repair and replace fibrocartilages. Using the knee meniscus and TMJ disc as examples, this review describes how fibrocartilages can be engineered toward translation to clinical use. Presented are fibrocartilage anatomy, function, epidemiology, pathology, and current clinical treatments because they inform design criteria for tissue engineered fibrocartilages. Methods for how native tissues are characterized histomorphologically, biochemically, and mechanically to set gold standards are described. Then, provided is a review of fibrocartilage-specific tissue engineering strategies, including the selection of cell sources, scaffold or scaffold-free methods, and biochemical and mechanical stimuli. In closing, the Food and Drug Administration paradigm is discussed to inform researchers of both the guidance that exists and the questions that remain to be answered with regard to bringing a tissue engineered fibrocartilage product to the clinic.

Published as: Donahue, RP*, Gonzalez-Leon, EA*, Hu, JC, & Athanasiou, KA. *Considerations for translation of tissue engineered fibrocartilage from bench to bedside. Journal of Biomechanical Engineering* (2018), *indicates co-first authorship.

1.1. Introduction

Cartilage is a connective tissue that is classified by its biochemical properties into hyaline, elastic, and fibrous cartilage (also referred to as fibrocartilage). Of these, fibrocartilage is marked by the presence of type I collagen and traces of type II collagen. Glycosaminoglycans (GAGs) are present in fibrocartilage, albeit in lower amounts than in hyaline articular cartilage [1]. Areas in the body containing fibrocartilage include the knee meniscus [2], the temporomandibular joint (TMJ) disc [3], the pubic symphysis, the annulus fibrosus of the intervertebral disc, tendons, and ligaments. Fibrocartilage undergoes a range of stresses including tension, compression, and shear in different areas of the body. Much like hyaline articular cartilage, fibrocartilage has a naturally low regenerative capacity due to its avascularity [1]. Fibrocartilages are notoriously difficult to repair with limited clinical options. Tissue engineering may be a route to provide novel clinical treatments, but the pathway for these products can be ill-defined due to the low number of FDA-approved cellular products. While Food and Drug Administration (FDA) guidance documents exist for human cells, tissues, and cellular and tissue-based products (HCT/Ps) in general [4] and, specifically, for products intended to repair or replace hyaline articular cartilage [5], an equivalent document for fibrocartilage does not exist. Formation of clinically relevant, tissue engineered fibrocartilages would require satisfying a variety of design criteria and regulatory requirements. This review uses the knee meniscus and TMJ disc fibrocartilages as two examples to discuss how tissue engineered fibrocartilages may be translated from the bench to bedside.

In the following sections, anatomy and structure-function relationships of the knee meniscus and TMJ disc will be presented. Epidemiology of these tissues and the causal pathologies that lead to specific indications for current clinical treatments will be provided.

Assays for characterization for histomorphological, biochemical, and mechanical properties of fibrocartilages will be explained. Together, anatomy, function, epidemiology, pathology, current clinical treatments, and characterization studies inform design criteria for tissue engineered fibrocartilages. In context to these design criteria, current tissue engineering methods for fibrocartilage, specifically the meniscus and TMJ disc, will be discussed via subsections on the selection of cell source, a scaffolding or scaffold-free approach, biochemical stimuli, and mechanical stimuli. In addition, evaluation of tissue engineered fibrocartilages and discussion of engineering a fibrocartilage spectrum will be provided. The final section of this paper will look toward the translation of tissue engineered fibrocartilage and how this type of product may be shepherded through the FDA paradigm. A focus will be considerations for preclinical animal models and clinical trials. Future directions will be recommended, motivation for FDA guidance will be discussed, and remaining questions or concerns will be presented.

1.2. Fibrocartilage Types, Epidemiology, Pathology, and Clinical Treatments

Fibrocartilage anatomy, function, epidemiology, and pathology all inform how tissue engineered fibrocartilage should be designed and made. Current clinical options and practices can inform how tissue engineered fibrocartilage may be deployed in the clinical setting and can, thus, inform design criteria as well. These are provided below.

1.2.1 The Knee Meniscus and TMJ Disc

In 2005, more than 46 million adults incurred over $353 billion in direct healthcare costs related to different rheumatic conditions in the United States alone [6]. These conditions encompass those affecting fibrocartilages. Two fibrocartilages of high clinical relevance are the knee menisci and TMJ disc. Knee menisci are semi-circular, wedge-shaped

fibrocartilaginous tissues, located between the distal femur and the tibial plateau (Fig. 1.1), that protect articular cartilage via load distribution. The knee contains a medial and a lateral meniscus (Fig. 1.1). Under compressive load, the menisci's wedge shape causes tension to develop, which is resisted by circumferentially aligned collagen. A gradient of healing capabilities in the knee meniscus correlates with the degree of vascularity, with the capacity for healing decreasing as one moves closer to the innermost, avascular region (Fig. 1.1, white-white region).

The TMJ is a ginglymoarthrodial joint that contains a fibrocartilaginous disc situated between the mandibular condyle on the inferior side, and articular eminence and mandibular fossa on the superior side (Fig. 1.1). The TMJ disc is biconcave and consists of the anterior and posterior bands as well as the lateral, central, and medial zones that are collectively referred to as the intermediate zone (Fig. 1.1) [7]. The TMJ disc serves to increase congruity between the eminence and fossa, to distribute load, and to aid in joint lubrication [8]. The movement of the TMJ disc serves the rotational motion of the joint primarily in the rotational axis during normal mastication and the translational motion of the joint when the mouth is opened wide. During typical movements of the joint, loading patterns in the anterior portion of the mandibular condyle and posterior portion of the articular eminence lead to complex shear, compressive, and tensile forces on the fibrocartilaginous disc.

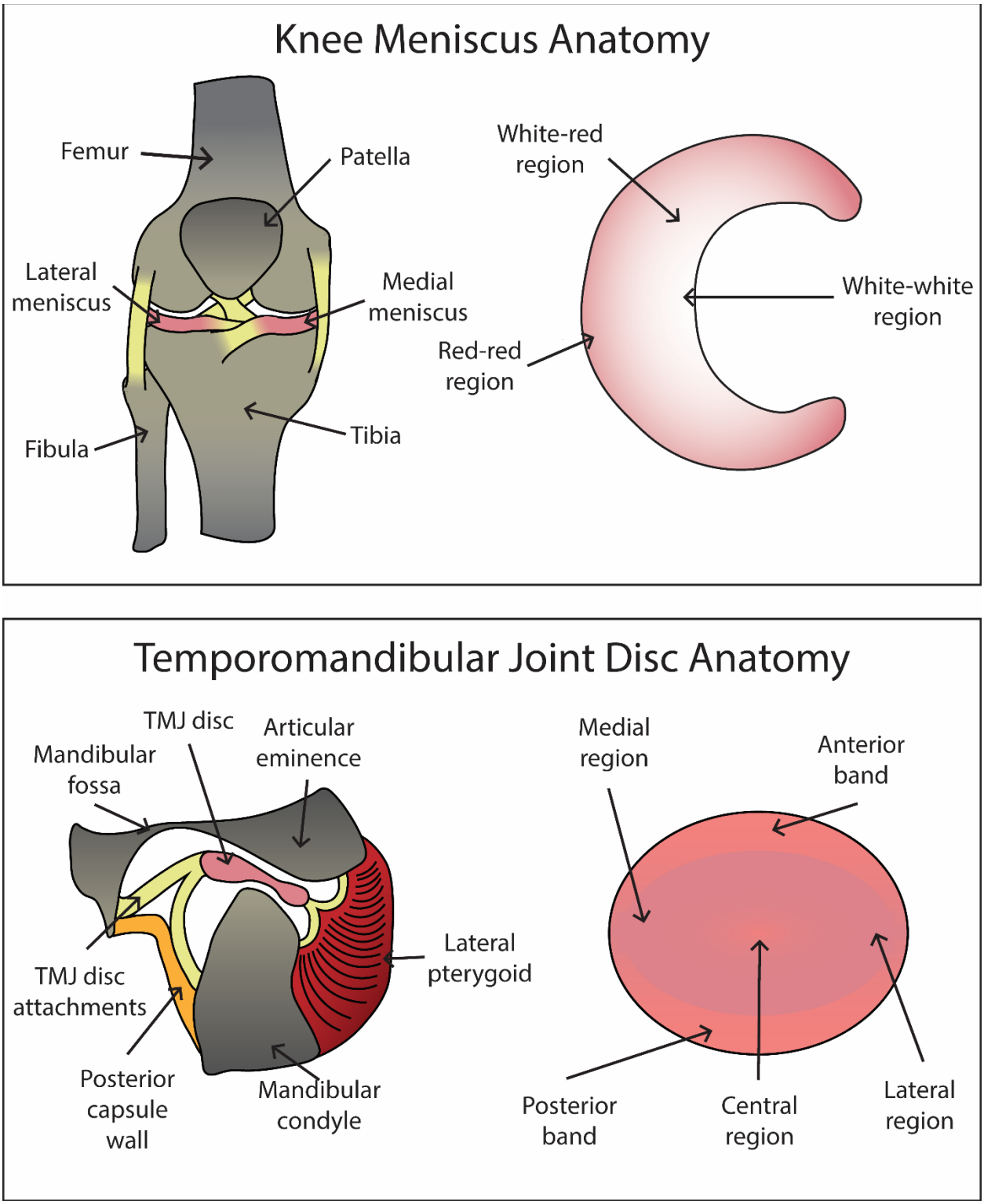

Figure 1.1. Anatomy of the knee meniscus and TMJ disc. The anatomical structures of the knee are shown, with the menisci depicted between the femur and tibia. The

transverse view is shown in the right panel, indicating the different vascular regions of each meniscus. The TMJ disc is shown from a sagittal view between the mandibular condyle and the articular eminence in an open jaw position. The disc from a transverse view is depicted in the right-hand panel.

1.2.2 Epidemiology and Pathology

Meniscal lesions are the most common intra-articular knee injuries and most frequent cause of orthopedic surgical procedures in the U.S. [9]. This is reflected by the size of the meniscus repair market, which in 2008 was anticipated to increase at a compound annual growth rate of 10.6% to an estimated $318 million in 2015 [10]. Previously reported incidences of meniscal injury leading to meniscectomy were noted at 61 per 100,000 persons [11], but damage to the medial meniscus is significantly more prevalent than in the lateral meniscus (81% and 19%, respectively) [11–17]. Injury to the lateral meniscus, while less frequent, leads to the degeneration of knee function, lower Lysholm scale scores—a scale from 0-100 that measures patient-reported pain where 100 represents a better outcome with fewer symptoms or disability, and a higher rate of instability when treated via meniscectomy as compared to meniscectomy of the medial meniscus [16,17]. Meniscal lesions are classified by their spatial alignment as vertical longitudinal (or longitudinal), radial, oblique, complex (or degenerative), and horizontal tears (Fig. 1.2). Complex tears are more likely to arise with increasing age, while other tears are more commonly attributed to traumatic injury. Oblique and vertical longitudinal tears represent 81% of meniscal tears [18,19]. Vertical longitudinal tears run parallel to the long axis of the meniscus and are perpendicular to the tibial plateau (Fig. 1.2). These tears divide the circumferentially aligned collagen fibers and are categorized as either complete or

incomplete vertical longitudinal tears. The former is known as a bucket handle tear, which more commonly affects the medial meniscus. Bucket handle tears are often unstable and can cause mechanical symptoms or locking of the knee [18], and are more amenable to repair if found within a vascularized region of the meniscus [20].

TMJ disorders (TMDs) encompass any issue with the jaw and the muscles that control it. TMDs are the second most common musculoskeletal condition resulting in pain and disability [21] and cost an estimated $4 billion per annum in healthcare in the U.S. alone. TMDs may cause pain in 20-25% of adults worldwide [22]. A gender paradox exists with TMDs because a 3.5-fold higher prevalence is seen in women than men [23,24]. This gender paradox has been well studied and has been hypothesized to occur due to hormone differences between genders [24]. TMD symptoms are wide-ranging, including clicking, restricted or deviating range of motions, and cranial and/or muscular pain [22]. Up to 70% of TMD patients suffer from internal derangement (ID) of the disc [25], where the TMJ disc is displaced from its normal anatomic position. Severe cases of ID are often presented with focal thinning of the disc, with eventual progression to larger areas of thinning or disc perforation (DP) (Fig. 1.2) [26]. Osteoarthritis (OA) often accompanies TMDs [27], but there is conflicting evidence of a clear causal relationship between ID and OA [28].

Epidemiological and economic data make the knee meniscus and TMJ disc highly significant fibrocartilages for tissue engineering. When one considers the mechanical behaviors of the knee meniscus and TMJ disc, and how these functions fail due to pathology, many similarities begin to emerge. For example, both fibrocartilages function under large magnitudes of mechanical stress; engineered implants must be ready to bear

similar loads. While specific pathological features may differ for the knee meniscus and TMJ disc (tears for the meniscus and thinning or perforation for the TMJ disc), late-stage pathologies of both fibrocartilages are often treated by tissue removal without long-term options for replacement, leading to joint degeneration. The similarities lead to comparable design criteria for the tissue engineering of these fibrocartilages.

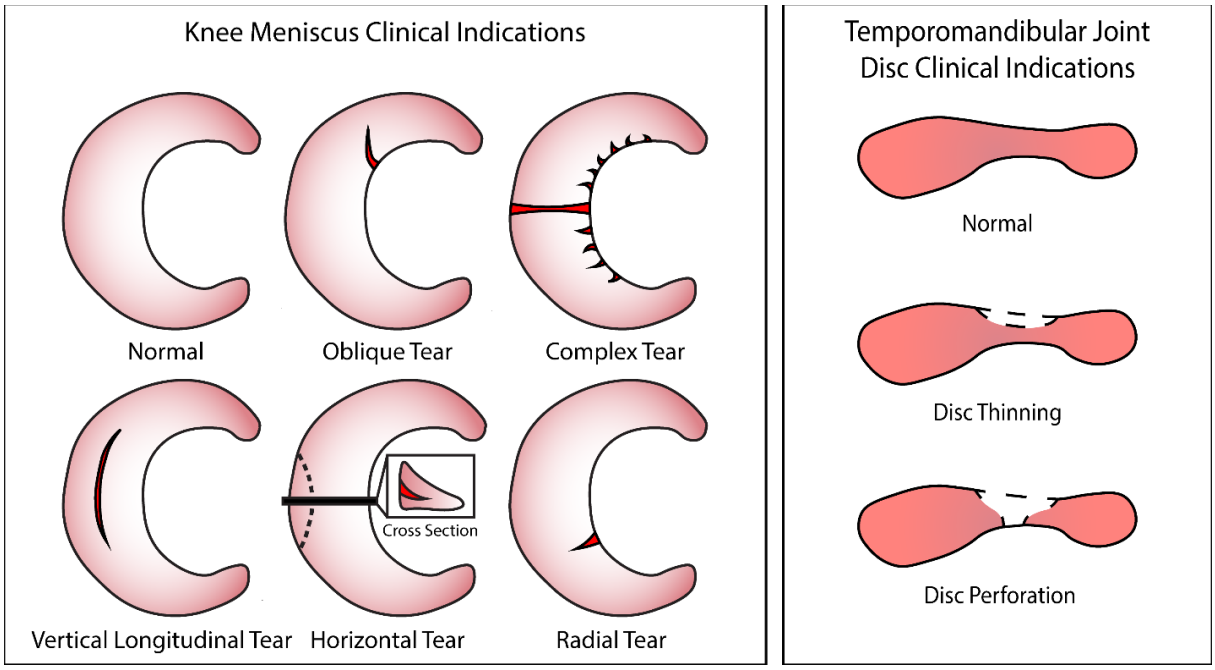

Figure 1.2. Clinical indications of the knee meniscus and TMJ disc. Different clinical indications for the meniscus are shown including five different tears: oblique, complex, vertical longitudinal, horizontal, and radial tears. For the TMJ disc, disc thinning and disc perforation are the clinical indications presented.

1.2.3 Current Clinical Treatments

Fibrocartilage treatments usually follow a path of two stages: nonsurgical methods followed by surgical intervention that range from minimally to highly invasive procedures. Nonsurgical methods may include physical therapy, analgesics for pain management, and behavioral modification, and are indicated for early disease stages. If no improvement

in symptoms is shown, surgery may be indicated. Surgical options for fibrocartilage are limited and progress rapidly to final stage options, such as arthroplasty, beyond which, even fewer options exist [29]. Tissue engineered fibrocartilage could potentially bridge the gap between the early and end stages of fibrocartilage pathology.

Initial diagnoses of knee meniscus injuries begin with clinical examination using a variety of tests [18]. If a meniscal tear is identified, the tear's severity is categorized to determine treatment which includes repair via arthroscopy, partial or full meniscectomy, and allograft transplantation [18]. Therapeutic efficacy varies by indication in part due to anatomy. For example, tears found in the red-white region of the meniscus are more amenable to repair than the white-white region due to the higher levels of vascularity in that region [20]. If possible, meniscectomy should be reserved for cases refractory to repair because meniscal repair tends to yield better clinical outcomes than meniscectomy [30].

Meniscectomy removes parts of the knee meniscus or cleans up degenerative debris, leading to immediate pain relief, although this is not always observed. Meniscectomy virtually guarantees the emergence of OA [31]. While some meniscectomy patients report pain relief, a statistically significant increase in quality of life after meniscectomy over alternatives such as physical therapy has not been observed, illustrating the limitations of fibrocartilage removal without replacement [32–34].

Diagnosis of TMDs follows patients' report of pain in the TMJ, headaches behind or around the eyes, and pain spreading to the temple, neck, ears, and shoulders [27]. Patients will often undergo a physical exam and multiple imaging modalities, such as MRI and/or computed tomography [22]. Although many TMJ symptoms can resolve

themselves [21,27], approximately 3-5% of TMD patients will require medical intervention in various forms.

Even in the most severe cases of TMDs, nonsurgical treatment is preferred [27]. Surgical options for TMDs are limited but include disc repositioning or discectomy with or without disc replacement [22,35]. Hemiarthroplasty is replacement of the articulating joint surface [36], most commonly the superior side in the TMJ with a vitallium alloy in the mandibular fossa-articular eminence region [37]. For certain indications such as ID, the disc can be repositioned in the correct anatomic position. Another option is discectomy, where the TMJ disc is removed. Postoperative follow-up in 3 years shows that discectomy increases mandibular motion [38] but is also associated with signs of degenerative changes including flattening of the articular surfaces and osteophytes [22,39]. Alloplastic disc replacements have been studied including Teflon-Proplast- [40] and silicone-based [22] implants. Biologic materials such as fat have also been explored [41], but all have required follow-up intervention. When a substantial portion of the joint is lost due to degeneration from trauma or significant degeneration in the articulating surfaces, total joint reconstruction may be indicated [22]. Costochondral grafts are used to replace the condyle in autologous TMJ reconstruction [42]. Alloplastic materials have been used in three FDA approved products [8,22] and often require secondary surgery due to the average patient age and resultant implant degradation [22].

As illustrated with the knee meniscus and TMJ disc, both nonsurgical and surgical options for fibrocartilage repair and replacement are lacking in long-term efficacy. Nonsurgical methods commonly treat symptoms and attempt to delay degeneration but are often unsuccessful in doing so. Surgical methods can cause degeneration in the joint

space and commonly require additional surgical follow-ups. An important consideration for tissue engineers will be where and how engineered products might fit into existing treatment modalities, such as serving as a bridge between early- and late-stage surgical interventions.

1.2.4 Using Tissue Engineering for Fibrocartilage

The need for interventions that can delay or arrest joint degeneration motivates the development of tissue engineered fibrocartilages. In early-to mid-stage pathologies, such as a partial vertical longitudinal tear in the knee meniscus or thinning of the TMJ disc, tissue engineered fibrocartilage implants may be used to bolster failing tissues to slow down or to arrest the degenerative process. Late-stage pathology where fibrocartilage removal by meniscectomy or discectomy is indicated may be combined with implantation of a tissue engineered fibrocartilage replacement. While there is hope for these strategies, there is currently a lack of tissue engineered fibrocartilage products on the market. Subsequent sections outline the process of fibrocartilage tissue engineering and examines the necessary steps for translating a tissue engineered fibrocartilage product to clinical use.

1.3. Characterization Studies of Fibrocartilages

Prior to carrying out tissue engineering studies, design criteria must be acquired. These are determined via characterization studies of the native fibrocartilage using histology, immunohistochemistry (IHC), biochemical testing, and mechanical testing (Fig. 1.3). Various animals commonly serve as models due to their anatomical, structural, and functional similarities to human tissues. Various reviews and comparative studies in the literature discuss different animal models and their similarities to human tissue for both

the knee meniscus [43,44] and TMJ disc [45,46] and should be referenced to determine comparability. Test results establish the gold standards toward which tissue engineers aim for in terms of histomorphological, biochemical, and mechanical properties of the engineered tissue. This section will provide guidance for the aforementioned testing and will provide values for native knee meniscus and TMJ disc properties that are relevant to tissue engineering.

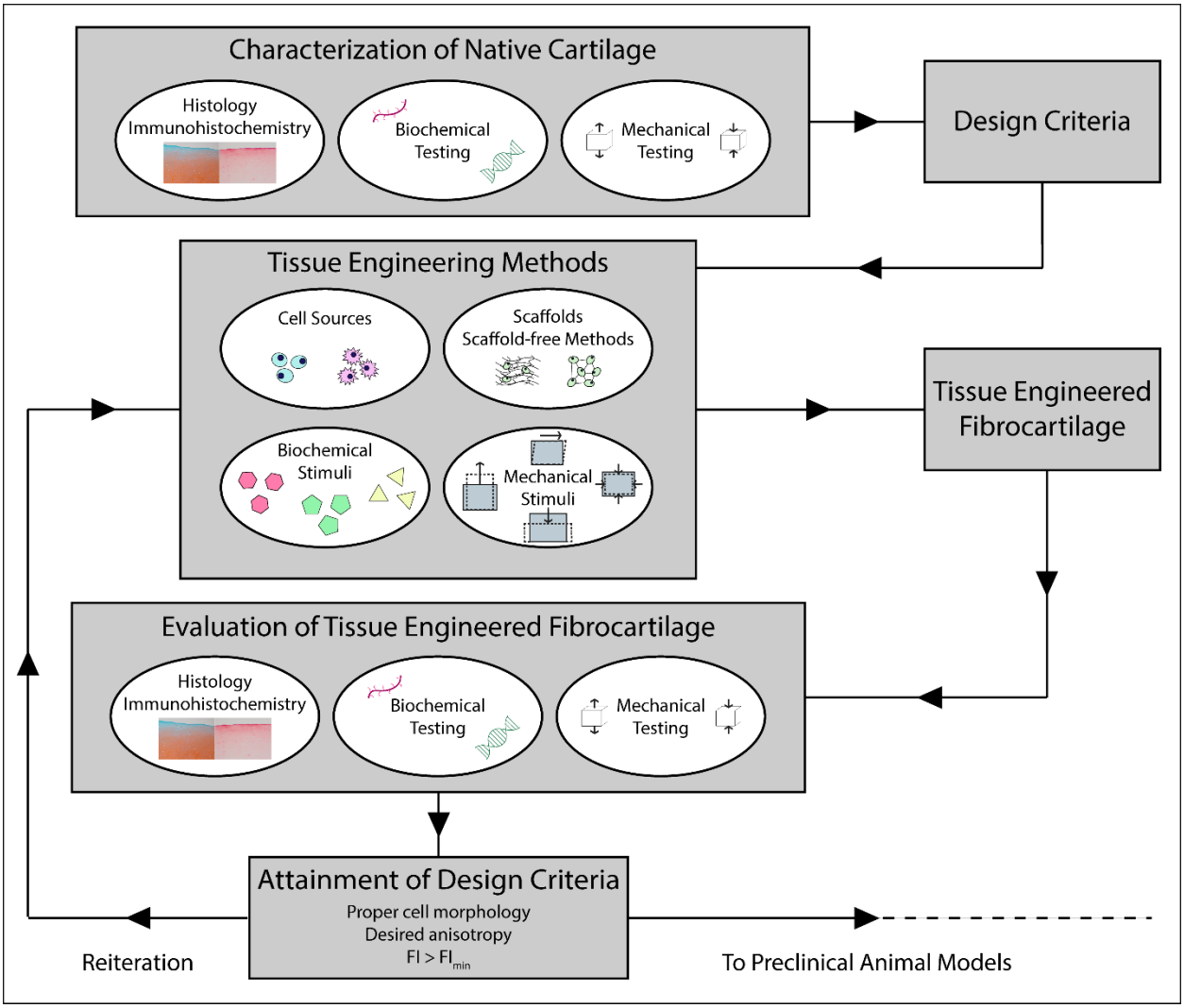

Figure 1.3. Tissue engineering of fibrocartilage. Tissue engineering requires characterization of native cartilage from which design criteria can be specified. Tissue

engineering parameters such as selection of a cell source, choice of scaffold or scaffold-free methodology, and use of biochemical or mechanical stimuli results in tissue engineered fibrocartilage which is subsequently tested for appropriate properties. If design criteria are met, the tissue engineered fibrocartilage and methodology used may move to preclinical animal models or the tissue engineering process might be reiterated to obtain improved tissue engineered fibrocartilage.

1.3.1 Histomorphological Properties

Histology and IHC allows for examination of a tissue's microscopic organization. In fibrocartilage, the distribution of different cell types [47–50], GAGs [48,50–54], and collagen [48,50,52–55] can be visualized using hematoxylin staining, Safranin O staining with a Fast Green counterstain, and Picrosirius Red staining, respectively. IHC uses antibodies for more specific visualization of the aforementioned items [53,56,57]. For example, multiple collagen types exist within fibrocartilages, and these can be discerned using IHC.

Histology, IHC, and microscopy techniques (e.g., polarized light, second harmonic generation) are used widely to elucidate fibrocartilage properties. For example, different cell types reside side-by-side in fibrocartilage, as seen in the meniscus where chondrocyte-like cells exist in its inner region and transition to a fibroblast-like phenotype in its outer region [58,59] (Fig. 1.4A). In the TMJ disc, the ratio of fibroblasts to chondrocyte-like cells varies by region as well, with the highest relative number of chondrocyte-like cells present in the intermediate zone [47] (Fig. 1.4C). GAGs were evenly distributed throughout young equine menisci, whereas samples from older horses showed distinct positive and negative staining locations [60]. IHC determined the

presence of hyaluronic acid backbone, keratan sulfate, and chondroitin sulfate in the primate TMJ disc [57]. In addition, collagen fibers in an equine knee meniscus model were shown to be randomly organized in the distal and proximal surface layers [60,61] (Fig. 1.4B), while the innermost layer exhibited circumferentially aligned collagen fibers with parallel alignment in the red-red region [60]. Polarized light microscopy [62] and scanning electron microscopy [56] showed that collagen aligned primarily circumferentially of the human and porcine TMJ discs, with the intermediate zone showing alignment anteroposteriorly (Fig. 1.4D). Finally, IHC showed greater type I collagen staining than type II collagen staining throughout the porcine TMJ disc [56].

Overall, histology and IHC are an adequate starting point for confirming presence and distribution of cells, GAGs, and collagen within fibrocartilage. While useful for the visualization of tissue organization, histology and IHC are qualitative assays and should be supported by sufficient sample sizes and quantitative assays, such as biochemical and mechanical testing.

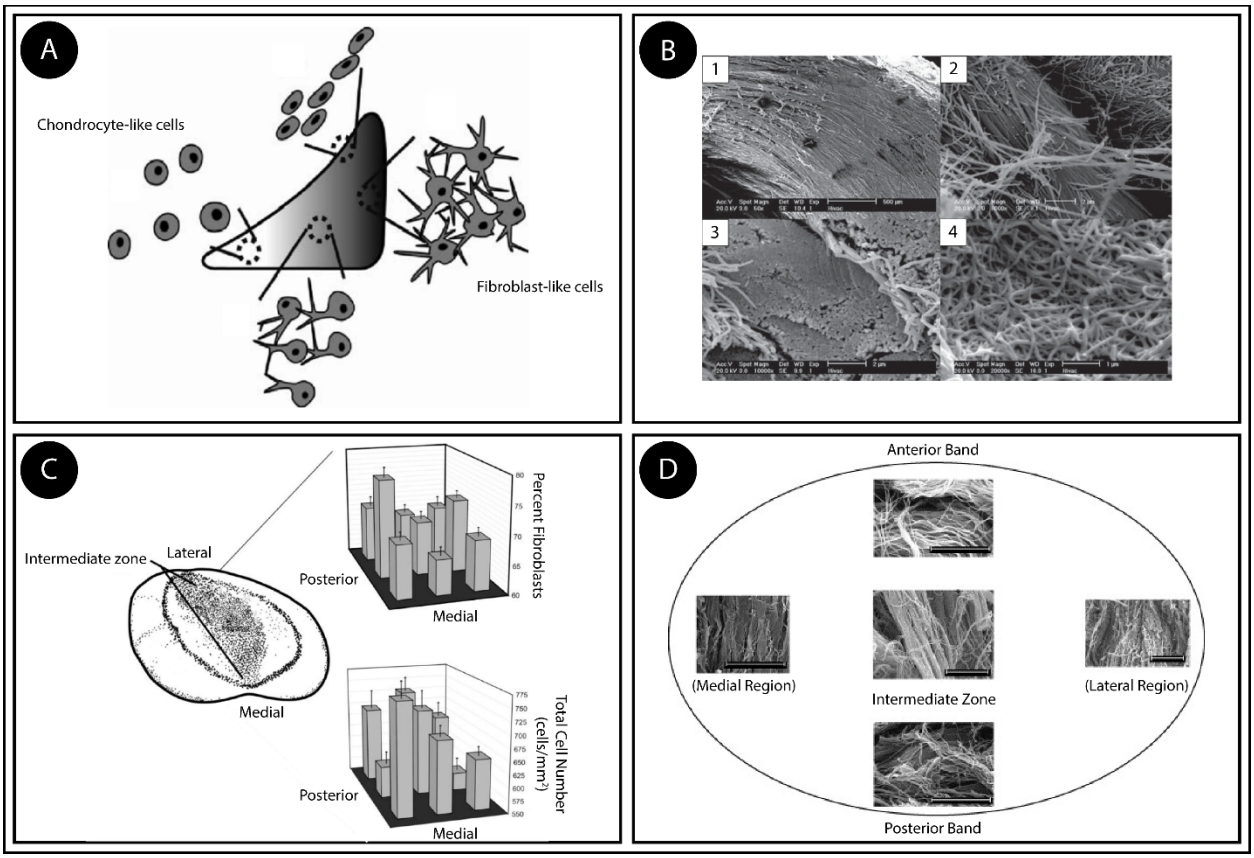

Figure 1.4. Cell morphology and collagen alignment of the knee meniscus and TMJ disc. A) A representation of the wedge-shape of the meniscus is depicted with the innermost region showing rounded, chondrocyte-like cells transitioning to spindle-shaped, fibroblast-like cells toward the outermost region. Figure reused with permission from Springer Nature: Cellular and Molecular Bioengineering [59]. B) Scanning electron micrographs showing (1) the circumferential collagen alignment, (2) a close-up view depicting individual collagen fibers, (3) a cross section of a collagen bundle, and (4) the random collagen orientation on the outer surfaces of the meniscus. Figure reused with permission from SAGE Publications: Proceedings of the Institution of Mechanical Engineers, Part H: Journal of Engineering in Medicine [61]. C) Ratio between fibroblasts and chondrocyte-like cells, and overall cellularity in the TMJ disc are reported, showing

the posterior and anterior bands have a higher proportion of fibroblasts when compared to the intermediate zone. Figure reused with permission from Elsevier: Journal of Oral and Maxillofacial Surgery [47]. D) Scanning electron micrographs of various regions of the TMJ disc showing primarily anteroposterior alignment in the intermediate zone, while the anterior and posterior bands show circumferential alignment. Scale bars are 10 microns except for the lateral region where the scale bar represents 200 microns. Figure reused with permission from Elsevier: Matrix Biology [56].

1.3.2 Biochemical Properties

Biochemical assays yield quantitative data that allow one to determine how similar properties of tissue engineered fibrocartilage are when compared with those of native tissue. DNA content can be quantified using, for example, PicoGreen [48,63]. Sulfated GAGs are often quantified using dimethyl methylene blue (DMMB) [48,54]. Collagen content can be measured by assaying for hydroxyproline [48,54,64]; a modified version of this assay which excludes use of perchloric acid to measure the collagen content has recently been published [64]. For quantification of specific types of collagen and GAG, enzyme-linked immunosorbent assay (ELISA) is used [53,56]. Pyridinoline content, a measure of collagen crosslinking, can also be quantified with high performance liquid chromatographic assays [48,54,65]. Much like histology and IHC, many of these biochemical assays can be performed to determine regional variation.

The knee meniscus extracellular matrix (ECM) is composed of water, fibrillar components, proteoglycans, and adhesion glycoproteins. Water, collagen, and GAGs account for the majority of components by mass and has been shown to be 72%, 22%,

and 0.8%, respectively in human menisci. The remainder of the tissue is made up of DNA (0.12%) and adhesion molecules. The distribution pattern of GAGs is as follows: 40% chondroitin 6-sulfate, 10-20% chondroitin 4-sulfate, 20-30% dermatan sulfate, and 15% keratan sulfate [66]. Collagen accounts for approximately 60-70% of the dry weight, and includes types I, II, III, V, and VI collagen [67]. Of these, type I collagen is by far the most predominant in the meniscus, accounting for more than 90% of total collagen [68]. The outer two-thirds of bovine menisci is composed primarily of type I collagen, whereas the inner one-third is 60% type II collagen and 40% type I collagen [69]. Pyridinoline collagen crosslinking has been shown to be highest in the inner region [70].

The biochemical composition of the TMJ disc is similar to the meniscus, being composed of primarily collagen and GAGs. Collagen is approximately 68.2% per dry weight in the porcine TMJ disc [71], while GAG content ranges from 0.273-0.936% per wet weight among species [51]. In a study on the structure-function relationship of the Yucatan minipig TMJ disc, the tissue showed regional variation in DNA content via PicoGreen assay ranging from 0.024%-0.041% per wet weight [48]. In a study on the porcine TMJ disc using ELISA to quantify GAGs, chondroitin sulfate was the most abundant GAG found, compromising 74% of the total GAG content [56]. For regional collagen variation, the intermediate zone had slightly more collagen per dry weight than the anterior and posterior bands of the disc, while in the mediolateral direction the central region contained significantly higher collagen than the lateral region [71]. In the Yucatan minipig TMJ disc, pyridinoline content was found to be significantly lower in the anterior and posterior bands than in the lateral and medial regions of the disc [48].

Biochemically, the knee meniscus and TMJ disc are similar due to their fibrocartilaginous nature. Both have similar ranges for collagen, GAG, and DNA content, and vary regionally as discussed above. In addition, the meniscus and TMJ disc both are composed of primarily type I collagen in relation to other collagen types. Uniform biochemical characterization can be used for fibrocartilages and is a required quantitative step after performing histomorphological studies. Although biochemical assays may provide insight on structure, they should be supplemented by mechanical testing to yield an understanding into fibrocartilage function.

1.3.3 Mechanical Properties

Inasmuch as fibrocartilages bear and distribute load, recapitulating the tissue's mechanical properties is a critical design criterion. Tension and compression tests are commonly used to derive target values. Uniaxial tensile testing provides tensile Young's modulus and ultimate tensile strength (UTS) [48,52,54,63,72]. For compression properties, creep indentation testing and incremental stress relaxation provide, among other properties, aggregate modulus [73–75] coefficient of viscosity [53,63,76], and instantaneous and relaxation moduli [48,51,54,62,63]. In addition to aggregate modulus, Poisson's ratio and permeability are also obtained from creep indentation testing [73,75,77]. These values can be derived from experimental data using different models based on linear elasticity, viscoelasticity including the standard linear solid model, poroelasticity, and mixture theories including the biphasic model. In-depth descriptions of these tests and their assumptions, performance, and mechanical models are available in the literature [1,78–82]. While no one testing modality is the gold-standard for measuring mechanical properties, tissue structure-function relationships dictate which testing

modality might be most informative when measuring characteristic properties of a native tissue. For example, the knee meniscus functions under compression, but its geometry causes tensile forces to develop within the tissue, and, thus, the tensile properties of a tissue engineered meniscus may be more indicative of whether it will be effective in replacing diseased tissue. Similarly, an analogous argument can be made for the TMJ disc which though it functions primarily under compression, the end result is principally tensile strain fields in the ECM. Values derived from mechanical testing of the meniscus and TMJ disc are provided below.

Since both the knee meniscus and the TMJ disc exhibit anisotropy, the mechanical properties depend on testing direction. The knee meniscus exhibits more robust tensile mechanical properties in the circumferential orientation rather than the radial due to the generally circumferentially aligned collagen fibers; this holds true throughout the depth of the tissue for the tissue's Young's modulus [72]. The Young's modulus is approximately 100-300 MPa in the circumferential direction and 10-fold lower in the radial direction [2]. The meniscus has been shown to have an aggregate modulus of 100-150 kPa [75]. Incremental stress relaxation testing of porcine knee menisci in synovial fluid have yielded instantaneous and relaxation moduli for 20% strain of 2.37-6.75 MPa and 0.07-0.15 MPa, respectively [83]. Values of mechanical properties can vary from species to species, as well as different testing modalities [77,84].

The mechanical properties of the TMJ disc display anisotropic, regional, and interspecies variations. Research on the Yucatan minipig TMJ disc revealed that UTS and tensile Young's modulus of the central region was highest in the anteroposterior direction, while the posterior band was stiffest and strongest in the mediolateral direction,

when determined by uniaxial tensile testing [48]. Creep indentation testing shows that the medial region of the TMJ disc had the largest aggregate modulus at 28.9 ± 12.3 kPa and was found to be significantly higher than the anterior, posterior, central, and lateral regions [73]. Instantaneous and relaxation moduli for 20% strain in the Yucatan minipig TMJ disc were found to be 216-1,540 kPa and 20.5-57.5 kPa, respectively dependent on region [48]. Uniaxial tensile testing, creep indentation testing, and incremental stress relaxation all provide valuable design criteria.

As tissues that undergo constant mechanical loading, the gold standard for fibrocartilage functionality should accordingly be mechanical testing. Appropriate characterization of not only mechanical properties, but histomorphological and biochemical properties, defines the design criteria to be used in tissue engineering studies. By defining native tissue values, tissue engineers know what criteria they need to strive for and mimic within tissue engineered fibrocartilages.

1.4. Tissue Engineering of Fibrocartilage

The tools developed to address the design criteria for tissue engineering fall into the general category of cells, scaffolds, and signals. For fibrocartilage, of particular interest are the issues of finding an appropriate cell source, choosing a scaffold or scaffold-free approach, and identifying both biochemical and mechanical stimuli as depicted in Figure 1.3. A selection of the most impactful studies outlined in Section 1.4 is summarized in Table 1.1. The following subsections will include information on each of the aforementioned components with a focus on approaches shown efficacious when applied with a scaffold-free, self-assembling process of tissue formation.

1.4.1 Cell Sources

Cell sources used in tissue engineering of fibrocartilage vary from tissue-specific, terminally differentiated cells to various stem cell types. In terms of tissue-specific cells for tissue engineering of the knee meniscus, meniscus cells (MCs) and hyaline articular chondrocytes (ACs) [53,63,76,85] have been explored. For engineering the TMJ disc, TMJ disc cells [86–98], articular eminence cells [87], mandibular condyle cells [99], costal chondrocytes (CCs) [89,100–104], ACs [54,102,105–107], MCs [54,106,107], and dermal fibroblasts [89] have been explored. Mesenchymal stem cells (MSCs) are the most heavily examined stem cell population for tissue engineering of both fibrocartilages. Factors to take into account for all cells are an autologous versus allogeneic approach, coculture of cells, and various cell expansion technologies. For stem cells, additional considerations include their theoretically infinite ability to expand and suboptimal differentiation efficiency.

Autologous tissue-specific, terminally differentiated cells directly from native tissue, such as TMJ disc cells or MCs, offer the lowest risk of rejection, but sourcing can be a difficulty due to insufficient healthy tissue. Other cell sources that can potentially be derived in an autologous fashion for tissue engineered fibrocartilages include cells from hyaline articular cartilage [54,102,105–107], costal cartilage [89,100–104], tendon, and ligament [108]. Autologous sources require two surgical procedures on the same patient: one for harvest of the donor tissue and another for implantation of engineered tissue. An allogeneic approach, which employs cells from a non-self donor, mitigates the issue of multiple surgeries for the patient and donor site morbidity but is limited by a possible immune response and rejection. Traditionally, articular cartilage has been considered to be an immunoprivileged tissue; immune response against cells within cartilage is rare due

to the dense ECM [1]. A recent minipig study showed minimal to no T cells, B cells, and macrophages within allogeneic, tissue engineered fibrocartilage implants in the TMJ disc [104], providing evidence that fibrocartilage, like hyaline articular cartilage, may also be immunoprivileged.

Cocultures of cells have been explored to recreate the various fibrocartilages that naturally contain different cell types and ECM composition. For example, a one-to-one coculture ratio of ACs and MCs [53,63,76], in comparison to other ratios, has been shown to be optimal in reconstituting the native meniscal cross section as well in providing adequate strength and stiffness [109]. Menisci that exhibit a more hyaline articular cartilage-like inner region and a more fibrous outer region have been engineered by seeding 100% ACs in the inner region and a one-to-one mix of ACs to MCs in the outer region. This regionally variant meniscus exhibited significantly higher compressive properties as well as GAG per dry weight in the inner region, while the outer region exhibited significantly higher circumferential tensile modulus and collagen per dry weight [110]. These compositional and functional properties mimic the biochemical and mechanical differences seen in native meniscus regions (Fig. 4B). For tissue engineering the TMJ disc, AC and MC cocultures [54,106,107], and CC and dermal fibroblast cocultures [89] have been examined. In AC and MC coculture, it was found that the presence of ACs is required to maintain a cylindrical shape by reducing contraction [106]. CC and dermal fibroblast coculture was inferior to CCs alone in terms of GAG content, total collagen, and type I collagen [89]. Coculture of multiple cell sources remains a viable option for creating more biomimetic tissue engineered fibrocartilages. Clinically, this may be more difficult to achieve using an autologous approach due to donor site morbidity and

increasing number of surgeries as previously discussed, but an allogeneic approach might be appropriate if coculture were used.

Advances in cell expansion technologies that preserve cell phenotype, in combination with an allogeneic approach, have the potential to mitigate the concerns that repeat surgeries, donor site morbidity, and cell sourcing pose. For example, a combination of transforming growth factor beta 1 (TGF-β1), basic fibroblast growth factor (bFGF), and platelet-derived growth factor (PDGF) increases the post-expansion chondrogenic potential of CCs by increasing GAG content, altering the ratios of collagen types, and improving compressive properties engineered using treated cells [111]. After expansion, the phenotype of CCs can be preserved by culturing them in three-dimensional (3D) aggregates [112]. During this aggregate redifferentiation process, application of TGF-β1, growth differentiation factor 5 (GDF-5), and bone morphogenetic protein 2 (BMP-2) also improves biochemical and mechanical properties of neocartilage using treated cells [113]. This process allows defined expansion of cells and preservation of phenotype by aggregate culture, and is extremely promising for allogeneic approaches, increasing the impact one donor can have.

Stem cells offer a solution to sourcing issues by having a theoretically infinite capability to expand. Synovial MSCs have been explored for the repair of the meniscus in scaffold-free culture methods [114] as well as via injection [115,116]. TMJ disc engineering has used both MSCs from bone marrow [117] and adipose tissue [118]. The current limitation of stem cells for tissue engineered fibrocartilage formation lies in their suboptimal differentiation protocols, which often lack efficiency (i.e., only a low percentage of cells attain the target phenotype) and may result in “chondrocyte-like” cells

[119] that may not form mechanically robust tissue engineered fibrocartilage. Additional concerns with stem cell use include tumorigenic potential and possible xenogeneic culture components. While stem cells for tissue engineered fibrocartilages have been used in research, their infinite expansion potential has yet to be realized clinically due to lack of efficiency.

To summarize, an autologous approach may be the ultimate goal because the cells are patient-specific, but not the most practical because the scarcity of healthy tissue remains an issue in these already diseased patients. An allogeneic approach may be the most translatable, especially with the advent of cell expansion technologies and evidence that suggests fibrocartilage as immunoprivileged. Allogeneic cells solve the issue of donor site morbidity and repeated surgeries from autologous approaches. Using stem cells may present the solution to the cell sourcing issue, but their translatability is not yet realized due to efficiency and possible tumorigenic potential. The selection of a cell source is among the most important choices a tissue engineer can make and should be well-informed by how a tissue engineered fibrocartilage will be translated.

1.4.2 Scaffold and Scaffold-free Methods

For 3D cell culture of tissue engineered fibrocartilage, both scaffold and scaffold-free methods exist. Scaffolds can be used to direct cell behavior by engineering specific biochemical and mechanical cues into the biomaterial. In addition, scaffolds also allow immediate cell attachment and provide support to the cells. Tissues can also be engineered without scaffolds. Scaffold-free tissue engineering is particularly useful when one wants to avoid scaffold degradation products and stress shielding cells. With scaffold-free methods, degradation products and residual byproducts from fabrication and their

associated toxicity to the cells do not need to be considered. Stress-shielding of cells via scaffolds is another consideration that is removed in scaffold-free approaches. While scaffolds retain the ability to directly alter cell behavior and support cells, for fibrocartilage tissue engineering, soluble and mechanical signals have both shown efficacy in directing cell performance in the absence of scaffolds.

A variety of scaffolding materials have been explored for tissue engineered fibrocartilages including alginate [86], polycaprolactone (PCL) [117], poly(glycolic acid) [86–88,93–98,105], decellularized matrix [120], polyamide [87], polytetrafluoroethylene (PTFE) [87], poly(glycerol sebacate) [100], type I collagen [91,99], poly(lactic acid) (PLA) [88,105,118], and poly(lactic-co-glycolic acid) (PLGA) [90,117]. Considerations for scaffold formulations include degradation rates and products, and fabrication methods and resulting residual byproducts. Also, a recently added consideration may be compatibility with 3D printing because the technology is conducive toward producing tissue engineered fibrocartilages that are anisotropic and regionally variant, characteristics important in the function of native fibrocartilages. For example, anisotropic collagen alignment has been produced in 3D printed menisci [121]. Similarly, a regionally variant TMJ disc has been produced using 3D printing with PCL and spatiotemporal delivery of PLGA microspheres with connective tissue growth factor (CTGF) and transforming growth factor, beta 3 (TGF-β3) encapsulated [117]. The wide range of scaffolds available for knee meniscus and TMJ disc tissue engineering has been reviewed elsewhere [2,45,122].

Self-organization and the self-assembling process are techniques that generate 3D structures in a scaffold-free manner, but they are distinctly different. Self-organization

is defined as any technique that produces biomimetic tissues with use of external forces or energy whereas the self-assembling process is defined as a spontaneous organization of cells that mimics native tissue structures without external forces or energy. Self-assembly occurs via the minimization of free energy through cell-cell interactions. Examples of self-organization includes cell sheet engineering and bioprinting of cells. Self-assembly is used across multiple tissue types, including fibrocartilage. Self-assembly addresses considerations of scaffold-based methods by the creation of robust tissue engineered fibrocartilages that can immediately bear load and do not shield the cells from various stresses present in the joint environment [123].

1.4.3 Biochemical Stimuli

Biochemical stimuli are used to target cells and ECM molecules to improve mechanical properties. This can occur, for example, via increased production of ECM, improved collagen fiber alignment, or increased collagen crosslinking. For the production of scaffold-free, tissue engineered fibrocartilage, prior studies have applied a variety of growth factors including TGF-β1, small molecules such as ascorbic acid and phospholipid lysophosphatidic acid (LPA), and matrix modifying enzymes chondroitinase ABC (C-ABC) and lysyl oxidase-like 2 (LOXL2) separately and in combination.

Growth factors have been extensively studied for tissue engineered fibrocartilages. TGF-β1 [54,76,124,125], TGF-β3 [88,90,117], CTGF [117], PDGF [92,126,127], bFGF [92–94,127], insulin-like growth factor 1 (IGF-1) [88,92–94,106,126,128], and epidermal growth factor (EGF) [126,127] are examples of growth factors that have shown various levels of efficacy in enhancing tissue engineered fibrocartilage formation. For example, TGF-β1 has been shown by microarray analysis to promote AC synthesis of ECM [129]

and has shown similar effects in fibrocartilage studies [54,76,124,125]. Small molecules such as LPA and ascorbic acid have been studied as well. LPA increased values of tensile Young's modulus from 247 ± 89 kPa in control groups to 503 ± 159 kPa in stimulated groups, along with collagen fiber density and organization in meniscal tissue engineered fibrocartilage [63]. Ascorbic acid is a vital component to cell culture media and was found to be optimal at 25 μg/mL for cell concentration, collagen deposition, and aggregate modulus values in a TMJ disc model [95]. Enzymes such as the GAG-depleting enzyme C-ABC and the collagen crosslinking enzyme LOXL2 have been previously shown to have a positive effect on mechanical properties. Specifically in articular cartilage, C-ABC has been shown to increase tensile properties exhibiting an increase of 121% and 80% compared to untreated controls in UTS and Young's modulus, and allow for more type II collagen deposition as a result of GAG depletion [130]. For the native knee meniscus, LOXL2 has been shown to increase tensile properties approximately 1.9-fold during explant culture [131]. More thorough and extensive reviews of various biochemical stimuli and their effects on tissue engineered fibrocartilage are available in the literature [2,132,133].

Various growth factors and enzymes have also been used in combinations to create synergistic effects between increased ECM and more mature ECM. For example, increases in radial tensile moduli by 5-fold over untreated controls of meniscal tissue engineered fibrocartilage were observed over untreated controls when a combination of TGF-β1 and C-ABC was applied [76]. A TGF-β1 and C-ABC combination can be used to tissue engineer other fibrocartilages as well because it has been observed to increase both tensile Young's modulus and UTS over unstimulated controls, reaching the lower

range of native values [124]. Combining TGF-β1, C-ABC, and LOXL2 treatments during the culture of tissue engineered fibrocartilage led to further significant improvement of tensile Young's modulus and UTS by 245% and 186%, respectively [54]. This combination has also been used to enhance mechanical properties and integration of TMJ disc tissue engineered fibrocartilages, resulting in values of tensile Young's modulus of over 6 MPa and compressive instantaneous modulus of over 1200 kPa after 8 weeks in culture [103]. The biochemical stimuli that have been used and their varying efficacy might warrant additional research into novel, synergistic combinations of stimuli.

1.4.4 Mechanical Stimuli

Mechanical forces exerted naturally on native fibrocartilage are critical in tissue development and homeostasis. Native fibrocartilages experience tension, compression, hydrostatic pressure, and shear, and each of these forces has been applied to tissue engineered fibrocartilage as well. Prior tissue engineering studies involving mechanical loading either alone or combined with biochemical stimuli have resulted in significant increases of mechanical properties and also anisotropy.

Tension and compression are two commonly applied mechanical stimuli for tissue engineered fibrocartilage. While typically applied as separate stimuli, in fibrocartilage they often work together. For example, in the meniscus when a compressive load is applied, tensile strains develop due to the meniscus' wedge shape [2]. Meniscal tissue engineered fibrocartilage comprised of a nanofibrous matrix seeded with MSCs was subjected to dynamic tensile loading, leading to an increase in tensile modulus by 16% [134]. Independently of tension, passive axial compression of 0.1 N in a TMJ disc model has been shown to increase collagen and GAG content significantly as well as increase

relaxation and tensile Young's modulus by 96% and 255%, respectively, over controls [135]. Combining TGF-β1 and C-ABC treatments with direct tension-compression loading during culture significantly increased instantaneous modulus (3-fold), relaxation modulus (2-fold), and tensile Young's modulus in the radial (6-fold) and circumferential (4-fold) directions of self-assembled meniscal fibrocartilage. The direct compression-tension bioreactor for menisci was fabricated such that the platens matched the curved surface and elliptical shape of the meniscal tissue engineered fibrocartilage, ensuring simultaneous compression and tension stimulation [53].

Although less often examined, hydrostatic pressure and shear also have been used to tissue engineer fibrocartilage. When subjected to a hydrostatic pressure loading regimen, PLA scaffolds seeded with MCs exhibited increases in ECM production exhibiting 3-fold higher GAG deposition and 4-fold higher collagen deposition [125]. In a study on TMJ disc cells on PLA scaffolds, hydrostatic pressure was applied at 10 MPa either intermittently at 1 Hz or continuously for 4 hours a day. Type I collagen was highest in the continuous stimulation group compared to the non-loaded and intermittent stimulation groups [98]. Fluid shear, while typically regarded as being a detrimental mechanical stimulus for the maintenance of a chondrocyte-like phenotype, may merit exploration for tissue engineered fibrocartilages. Exposing MCs to oscillatory fluid flow in parallel plate flow chambers has been shown to upregulate calcium signaling and GAG production [136]. Use of a rotating bioreactor in TMJ disc cell culture led to earlier and greater contraction compared to the control. This resulted in a denser ECM and cell composition; however, total ECM content and compressive stiffness were not significantly

different [97]. Overall, there is currently not enough evidence to conclude whether fluid-induced shear is beneficial for tissue engineered fibrocartilages.

Using mechanical stimuli on tissue engineered fibrocartilages is an effective way to increase ECM production and organization, which subsequently results in more robust mechanical properties. This in conjunction with a biochemical stimulus regimen may also lead to synergistic effects, further enhancing tissue engineered fibrocartilage functionality. While there are limited studies using mechanical stimuli on tissue engineered fibrocartilage, many of the stimuli discussed here have been extensively studied for hyaline articular neocartilage in other reviews [137]. Further examination of mechanical stimulus regimens for tissue engineered fibrocartilage is warranted because specific application times and load amounts can have either beneficial or detrimental effects.

1.4.5 Toward Tissue Engineering the Fibrocartilage Spectrum

Due to the spectrum of fibrocartilage structures in the body, each tissue engineering strategy will be slightly different. The outlined studies here provide insight into current tissue engineering methodology for the knee meniscus and the TMJ disc, but the approach to the pubic symphysis or annulus fibrosus of the intervertebral disc might require different methods. However, the concepts discussed in the prior sections can be used generally to approach tissue engineered fibrocartilages in a uniform manner. One way to tailor the tissue engineering approach used is application of multiple types of stimuli, varying the cell source, or using a different scaffolding or scaffold-free approach. Taking these considerations into account is critical when designing and carrying out tissue engineering studies. By properly considering these factors, a translational approach can be created and quickly shifted from basic research to preclinical animal models. This can

eventually result in transition to clinical trials and a tangible product that can be put through the FDA paradigm (Fig. 1.5).

1.4.6 Evaluation of Tissue Engineered Fibrocartilage

Histomorphological, biochemical, and mechanical testing of tissue engineered fibrocartilage yields properties that can be compared with those of native tissue to determine whether the tissue engineering design criteria have been met. All evaluation methods outlined in Section 3 can be applied to tissue engineered fibrocartilage (Fig. 1.3). The quantitative values derived from these assays can be statistically compared to each other to determine whether one tissue engineering modality is more efficacious than another. Quantitative values can also be normalized to native tissue values in the form of a functionality index (FI), Eq. (1). The FI accounts for biochemical and mechanical properties found in native tissue and normalizes tissue engineered values to those of native tissue. The FI provides a quantitative value that reflects the overall quality of tissue engineered constructs that can be compared to each other. For example, the TMJ disc FI accounts for GAG, total collagen, instantaneous modulus values, relaxation modulus values, tensile Young's modulus values, and UTS values. The FI in Equation 1 weighs each of the metrics equally [104,138]. The FI varies between 0% and 100%, where 100% is the value of native fibrocartilage.

$$FI(TE|N) = \frac{1}{6}\left[\begin{array}{l}\left(1-\left|\frac{GAG_N - GAG_{TE}}{GAG_N}\right|\right)+\left(1-\left|\frac{Col_N - Col_{TE}}{Col_N}\right|\right)+\left(1-\left|\frac{E_N^{20i}-E_{TE}^{20i}}{E_{MC}^{r}}\right|\right)\\ +\left(1-\left|\frac{E_N^{20r}-E_{TE}^{20r}}{E_N^{r}}\right|\right)+\left(1-\left|\frac{E_N^{T}-E_{TE}^{T}}{E_N^{T}}\right|\right)+\left(1-\left|\frac{UTS_N - UTS_{TE}}{UTS_N}\right|\right)\end{array}\right] * 100\% \qquad (1)$$

Similarly, a knee meniscus FI might include similar components with the addition of radial tensile modulus to account for the tissue's anisotropy.

It is important to note that a perfect FI of 100% is not necessarily needed for proper functioning of tissue engineered fibrocartilage *in vivo*. For example, an FI of 42% was adequate for a TMJ disc thinning model in the Yucatan minipig, where the implanted disc exhibited mechanical robustness *in situ*, adaptively remodeled, and improved integration stiffness [104]. For specific models of fibrocartilage injury, appropriate FI values need to be established for the translation of tissue engineered fibrocartilages that researchers can aim for

It is important to note that the tissue engineering approach must meet established design criteria (Fig. 1.3). As discussed, this can be measured by an index such as an FI, but other characteristics such as cell morphology and tissue anisotropy need to be evaluated qualitatively or using other measurements. If the tissue engineering approach does not meet design criteria in any of these categories, the process can be reiterated, and the approach can be modified to meet the target design criteria (Fig. 1.3). Upon meeting design criteria for the tissue engineering phase, researchers still need to demonstrate safety and efficacy in preclinical animal models and approved by the FDA before a tissue engineered fibrocartilage can be marketed as a therapy.

1.5. Toward Translation of Tissue Engineering

Tissue engineered fibrocartilage safety and efficacy must first be reviewed and cleared by the FDA before it can be marketed for clinical use. After tissue engineering studies, tissue engineered fibrocartilages should be demonstrated as safe and effective in animal models before examining the products' effects in humans. This section will present the FDA paradigm (Fig. 1.5), diving into preclinical animal models and clinical trials, and discussing considerations for both. Because there is lack of approved tissue engineered

fibrocartilage products existing for repair or replacement, this section uses existing articular cartilage guidance as a way to infer how tissue engineered fibrocartilage products might be regulated. This section closes with a discussion on areas where additional guidance from the FDA is desired, for example, through the creation of a fibrocartilage guidance document analogous to that which exists for articular cartilage.

1.5.1 The FDA Paradigm

Tissue engineered fibrocartilage products will be regulated as HCT/Ps, a category of products containing or consisting of human cells or tissues intended for implantation, transplantation, infusion, or transfer into humans [4]. Much like tissue engineered products for hyaline articular cartilage [5], tissue engineered fibrocartilage products will be regulated through two centers of the FDA: the Center for Biologics Evaluation and Research (CBER) and/or the Center for Devices and Radiological Health (CDRH). CBER and CDRH co-authored the FDA guidance document for products intended to repair or replace hyaline articular cartilage [5], and this document can give insight into how tissue engineered fibrocartilage products might be regulated given similarities between the two tissue types.

If an HCT/P is minimally manipulated, intended for homologous use, and uncombined with another object, then it is only subject to regulation under Section 361 of the Public Health Service (PHS) Act and Title 21 of the Code of Federal Regulations Section 1271.3(d)(1). These HCT/Ps are referred to as 361 products and do not require premarket approval. Examples of 361 products include bone (including demineralized bone), ligaments, tendons, and cartilage, which may have been sourced from cadaveric tissues. In terms of specific fibrocartilage products, cadaveric fibrocartilaginous tissue to

be used as an allograft such as the knee meniscus and TMJ disc would fall under the category of 361 products. Otherwise, HCT/Ps are regulated as drugs, and/or biological products under Section 351 of the PHS Act and/or the Federal Food, Drug, and Cosmetic (FD&C) Act and are referred to as 351 products. Examples as provided by the FDA include cultured cartilage cells, cultured nerve cells, and gene therapy products. For fibrocartilage, expanded TMJ disc cells or MCs might fall under this category as well as tissue engineered fibrocartilage cultured using the self-assembling process.

Under the CDRH, products are regulated as devices under the FD&C Act. Human collagen and preserved umbilical cord vein grafts are in this classification. Biomaterial scaffolds without combination of cells for fibrocartilage repair or replacement may fall into this category. In addition, certain HCT/Ps can be classified as combination products by the Office of Combination Products and assigned to CBER or CDRH for primary jurisdiction. One example is cultured cells on synthetic membranes or combined with collagen. This product has potential to be regulated as a device or biological product, but is currently under review and may be regulated by CBER under device or 351 product regulations [4]. Tissue engineered fibrocartilage with use of a scaffold and seeded chondrocytes may fit into this category. Due to the many ways and materials with which fibrocartilage can be engineered, the FDA's classification of tissue engineered fibrocartilage products can vary. Consultation with the FDA is recommended if there is confusion as to the categorization of a specific tissue engineered fibrocartilage product.

Following product classification, a sponsor seeking FDA approval may consult guidance documents and the regulation of other approved products to determine data that need to be collected and submitted to the FDA. Guidance documents specifically for

tissue engineered fibrocartilage products have not been published, but a guidance document has been published for products intended for repair or replacement of hyaline articular cartilage, which shares many similarities with fibrocartilage. In addition, autologous cultured chondrocytes on a porcine collagen membrane is an approved cellular and gene therapy product whose pathway to regulatory approval may offer insights for tissue engineered fibrocartilage products. The guidance document for articular cartilage products contains non-binding recommendations to the industry on preparation and submission of investigational device exemption (IDE) and/or an investigational new drug (IND) application. Recommendations for classification of products, preclinical data, biocompatibility testing, and clinical study protocols are described. For example, goats, sheep, and horses are listed as the most frequently used large animal models for testing biological response, durability, toxicology, dose response, lesion size and location, appropriate endpoints, and use of arthroscopic or MRI imaging evaluations for articular cartilage repair [5]. Fibrocartilage large animal models are similar to the ones employed for articular cartilage with the addition of the minipig, farm pig, and dog [43,46,48,139]. For clinical trials, design, controls, study populations, endpoints, implantation procedures, and patient follow-up are all discussed as well [5]. Examples of measures that may be used to assess endpoints for articular cartilage products are the Knee Injury and Osteoarthritis Outcome Score (KOOS), IKDC Subjective Knee Evaluation Form-2000, and Western Ontario and McMaster Universities Osteoarthritis Index (WOMAC) [5]. For fibrocartilage within the knee such as the meniscus, these scoring systems might be adaptable while the TMJ disc fibrocartilage might need new indices created. This

motivates the creation of a standardized scoring system for fibrocartilages throughout the body.

Guidance documents as well as meetings with the FDA help to provide clarity on the process by which a product receives FDA approval, and this process is briefly depicted in Figure 1.5. Tissue engineering studies yield a product candidate that is then tested in preclinical animal studies to generate data for submission of an IDE and/or IND application dependent on product classification. An IDE/IND is necessary for clinical trials. Clinical trials are conducted in phases, and considerations for clinical trials include defining and measuring endpoints, the surgical procedures used, and patient follow-up. Upon completion, data from the trials are submitted via a premarket approval (PMA) and/or a biologics license application (BLA) to the FDA. These applications will be under review for a time-period known as the premarket application phase where the FDA reviews the data for safety and efficacy of the product. FDA approval allows the product to be marketed. Product safety and efficacy continues to be monitored in the post-marketing phase, sometimes referred to Phase IV clinical trials. For more information on the FDA paradigm and general translation of tissue engineering products, readers are directed to a recent review [140].

1.5.2 Preclinical Animal Models

Currently, there are limited approved fibrocartilage HCT/Ps or clinical trials. Putting this in context of Figure 1.5, the general state of fibrocartilage tissue engineering currently straddles the phases of tissue engineering studies (discussed in Section 1.4) and preclinical animal studies. Animal studies provide preclinical data that show how the product functions *in vivo*. Animal studies are used to assess biological responses, the

durability of repair, toxicology, dose response, lesion size and location, appropriate endpoints mirroring those to be used in humans, and use of arthroscopic and/or MRI evaluations as has been previously outlined [5]. Aside from examining the host, testing modalities outlined in Section 1.3 should also be applied to the tissue engineered fibrocartilage implant both before and after implantation. Data on how the implant's biochemical, mechanical, and cellular properties change or remain the same will inform the success of the tissue engineering process and implant performance *in vivo*. Similar to using the FI to optimize tissue engineering procedures, the FI can be for *in vivo* studies to determine, for example, implant properties that correlate with a durable repair response. It is worth noting that, unlike suggestions found in the hyaline articular cartilage product guidance document which only touches on compressive testing modalities [5], an appropriate FI for fibrocartilage should include both tensile and compressive properties due to the way fibrocartilage functions. Correlation of the implant's FI to host response might further inform eventual release criteria for the manufacturing of tissue engineered fibrocartilage products. An index such as the FI for general fibrocartilage tissue engineering would be informative to the field and allow comparison of various tissue engineering strategies for different fibrocartilages.

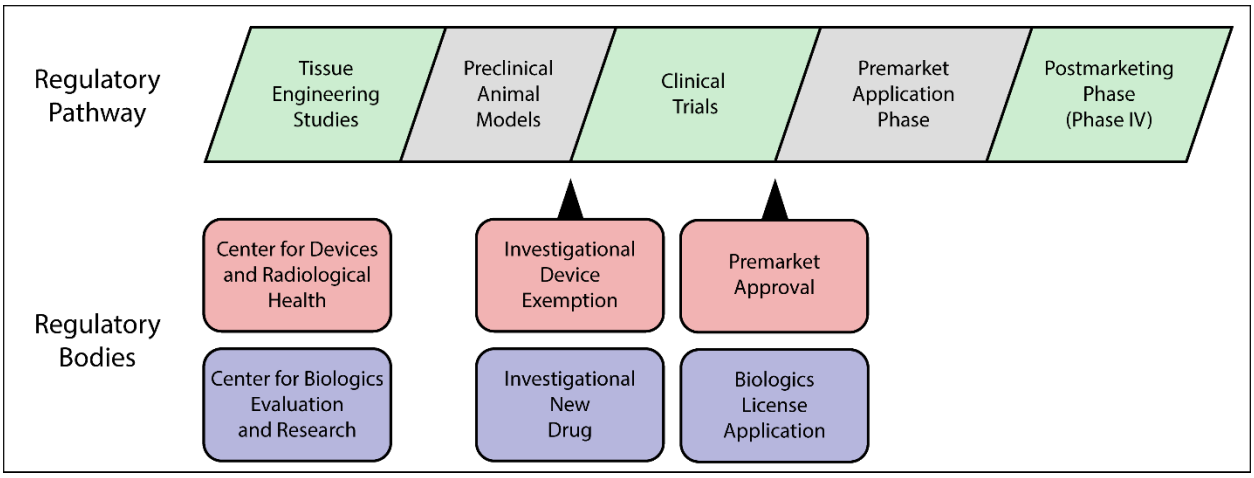

Figure 1.5. The FDA paradigm. The FDA paradigm is outlined from tissue engineering studies to the postmarketing phase with appropriate milestones for CBER and CDRH depicted.

Ideally, preclinical studies in animals would test a version of the product that is identical to that which will be used in clinical studies. Investigating a product that contains human cells in animal models could require immunosuppressive agents to avoid rejection upon implantation, and this can be difficult if not impossible to implement in certain animal models. Recently, a review on experimental immunosuppression and immunomodulation has been published and may help provide strategies by which these can be applied to xenogeneic or allogeneic animal models [141]. Alternatively, one can test an analogous cellular product in terms of cellular characteristics and biological activity, derived from the animal species used in studies in an allogeneic strategy.

Preclinical data can be obtained from a combination of small and large animal studies. Small animal models, such as rodent and leporine models, allow for larger, more economical studies. However, for fibrocartilage injuries, surgical procedures in small animals may become difficult due to small joints that provide little space for operating. Translational applications in humans for tissue engineered fibrocartilage are best modeled in large animals that replicate human biomechanics as much as possible. As noted above, goats, sheep, and horses are recommended for examining hyaline articular cartilage repair [5], but other species may suit fibrocartilage studies better. For example, menisci in pigs and sheep are most similar to humans' in terms of size and proportion [44], while ovine menisci are also similar to humans' in terms of composition and biomechanics [142]. For the TMJ disc, the Yucatan minipig has also been deemed a

suitable comparative model to humans in terms of its structure-function relationships [48], and has seen success in a regeneration study by our group which used CCs to tissue engineer allogeneic TMJ disc fibrocartilage [104]. As such, the pig (including minipigs) and sheep may prove useful as large animal models for fibrocartilage studies, especially in those regarding the knee meniscus and TMJ disc.

For each animal model, details such as the specific surgical procedure for implanting the fibrocartilage product, how that surgical procedure may translate to human studies, how the study models particular indications, and specialized recovery or post-operative care must all be considered. For example, in a recent study where a focal thinning defect model was used, there was careful consideration of the minipig's post-operative diet [104]. After TMJ surgery, a diet consisting of mainly soft foods or liquids as opposed to hard foods is more amenable to repair. Thus, even if an animal model displays anatomical and functional similarities to humans, it does not automatically mean that the model should be chosen if surgical, husbandry, or other aspects listed above cannot be adequately developed for the animal.

1.5.3 Clinical Trials

After obtaining preclinical data and approval of an IDE and/or IND, clinical trials can commence. Phase I and II trials commonly contain small patient cohorts compared to Phase III trials. Phase I trials are meant to determine safety and dosage of the tissue engineered fibrocartilage product. Phase II trials determine product efficacy and possible side effects of fibrocartilage therapies. Phase III trials examine long-term safety and efficacy in larger patient cohorts.

While animal models may inform endpoints in humans, it is ultimately clinical trial data that will be used in final approval for market. Because explanting implanted tissue engineered fibrocartilages would impair function, it is oftentimes not possible to test human implant properties as done in preclinical animal models. Therefore, endpoints are often defined via subjective scales, such as pain and range of motion testing. Development of a standard fibrocartilage scoring system would be of great value to clinical trials of tissue engineered fibrocartilage products. Arthroscopic evaluation, histologic evaluation, serological assessments for inflammation, and imaging might also inform endpoints [5].

Considerations that ensure successful repair in animals should likewise be thought out in clinical trials. For example, surgical approaches such as technique and post-operative care must be standardized and inspected particularly in multi-center trials to minimize center-to-center variability. In addition, for the indication that a tissue engineered fibrocartilage product intends to treat, participants that undergo current gold standard treatment should also be enrolled to demonstrate the tissue engineered product's efficacy over standard of care. For example, for late-stage pathology of the TMJ disc such as perforation, either discectomy or total joint reconstruction is often indicated. These two clinical treatments will ultimately be two treatments that a tissue engineered TMJ disc may be compared to. Lastly, follow-up of treatment with tissue engineered fibrocartilage will be required in these patient populations. It is common for the FDA to require safety and efficacy data over a number of years to compare short-term results of the tissue engineered fibrocartilage to current clinical treatments. The FDA will also use these data

to evaluate claims of the product. For successful execution of clinical trials, these considerations should be taken into account to gain FDA approval for commercialization.

1.5.4 Future Directions

Tissue engineering approaches of fibrocartilage have improved markedly within the last decade, allowing for the fabrication of more mechanically robust tissue engineered fibrocartilages. However, as previously discussed, current clinical treatments that address indications such as meniscal tears and TMJ disc perforation require follow-up clinical procedures within a short time frame. In addition, there is a lack of tissue engineered fibrocartilage products on the market. This may be due, in part, to a dearth of clarity on how tissue engineered fibrocartilage products can be translated.

Outlined here is the FDA paradigm as seen through current documentation and resources with numerous specific considerations for preclinical animal models and clinical trials of potential fibrocartilage products. The considerations discussed here are just an example of what must be taken into account when going through the FDA paradigm. Clarification of important considerations and guidelines must occur in order to allow translation of tissue engineered fibrocartilage products. As such, the field should gravitate toward studies that have translational implications and perhaps ask for the FDA to create a guidance document similar to the one that exists for articular cartilage products [5]. A guidance document would provide recommendations to researchers and streamline translational advances to tissue engineered fibrocartilage products used in the clinic.

There are a number of remaining questions and concerns surrounding the creation of such a guidance document. One concern is how such a document can be created when there are multiple types of fibrocartilaginous tissues in the body varying in function. As

examined earlier, there are actually significant similarities between meniscus and TMJ disc pathologies and current clinical treatments that allow for similar tissue engineering approaches to be used for both. These tissues are just two fibrocartilage examples. Hence, discussion and exploration of other fibrocartilaginous tissues like the pubic symphysis and annulus fibrosus of the intervertebral disc is warranted. Along those same lines, critics might question the inclusion of numerous different pathologies, ranging from early- to late-stage, within one document. One option might be to focus in on pathologies that are associated with degeneration of the tissue where tissue engineering might be able to bolster the early- to mid-stage degeneration via repair or replace the tissue completely for late-stage pathologies. Finally, as discussed with the FDA paradigm, clinical endpoints must be measured. A major hurdle remaining is the development of standardized indices or measurement systems for fibrocartilage in general. Evaluating tissue engineered fibrocartilage by an FI was suggested for tissue engineering and preclinical studies but remains a question for measurement of clinical endpoints in phased human trials.

In summary, tissue engineering of fibrocartilage addresses the limitations of current clinical treatments. There has been limited translation of tissue engineered fibrocartilage products from the bench to the bedside. Throughout the FDA paradigm, there are many considerations to be included in the guidance document as discussed earlier. However, there are still several hurdles and remaining questions before the creation of a fibrocartilage guidance document analogous to that which exists for articular cartilage can come to fruition.

1.6. Conclusion

This review has highlighted tissue engineering of fibrocartilage, using the knee meniscus and TMJ disc as primary examples. Anatomy, function, epidemiology, pathologies, and current clinical treatments were reviewed to elucidate the need for tissue engineered solutions that are both biochemically and mechanically reminiscent of native tissue. Prior to tissue engineering fibrocartilage, design criteria must be attained via characterization of native tissue in the species of interest. Design parameters such as cell sourcing, scaffold versus scaffold-free methods, as well as biochemical and mechanical stimuli alone or in combination were discussed to create a fibrocartilage spectrum. Evaluation of the resultant tissue engineered fibrocartilages was also examined for comparison to previously characterized properties of native tissue.

Navigation of the FDA paradigm was discussed to motivate the translation of studies from laboratory bench to bedside in the clinic. We have recommended collaboration and open communication with the FDA to create a fibrocartilage guidance document analogous to that which exists for articular cartilage. Regulation of tissue engineered fibrocartilage and considerations for preclinical animal models and clinical trials were highlighted to encourage standardization amongst the field. Ultimately, this review looks to the future of tissue engineered fibrocartilage products, which are the culmination of decades-long research efforts. While there remains much to be accomplished, the field is now closer than ever to alleviating prominent fibrocartilage conditions.

Nomenclature

GAG_N	Native glycosaminoglycan content

GAG_{TE}	Tissue engineered glycosaminoglycan content
Col_N	Native collagen content
Col_{TE}	Tissue engineered collagen content
E_N^{20i}	Native instantaneous modulus
E_{TE}^{20i}	Tissue engineered instantaneous modulus
E_N^{20r}	Native relaxation modulus
E_{TE}^{20r}	Tissue engineered relaxation modulus
E_N^T	Native tensile Young's modulus
E_{TE}^T	Tissue engineered tensile Young's modulus
UTS_N	Native ultimate tensile strength
UTS_{TE}	Tissue engineered ultimate tensile strength
FI (TE|N)	Functionality index of tissue engineered fibrocartilage in relation to native tissue

References

[1] Athanasiou, K. A., Darling, E. M., DuRaine, G. D., Hu, J. C., and Reddi, A. H., 2017, Articular Cartilage, Second Edition, CRC Press.

[2] Makris, E. A., Hadidi, P., and Athanasiou, K. A., 2011, "The Knee Meniscus: Structure-Function, Pathophysiology, Current Repair Techniques, and Prospects for Regeneration," Biomaterials, 32(30), pp. 7411–7431.

[3] Detamore, M. S., and Athanasiou, K. A., 2003, “Structure and Function of the Temporomandibular Joint Disc: Implications for Tissue Engineering,” J. Oral Maxillofac. Surg., 61(4), pp. 494–506.

[4] Food and Drug Administration, 2018, “FDA Regulation of Human Cells, Tissues, and Cellular and Tissue-Based Products (HCT/P’s) Product List” [Online]. Available: https://www.fda.gov/biologicsbloodvaccines/tissuetissueproducts/regulationoftissues/ucm150485.htm. [Accessed: 26-Jun-2018].

[5] Food and Drug Administration, 2011, “Guidance for Industry Preparation of IDEs and INDs for Products Intended to Repair or Replace Knee Cartilage.”

[6] Cisternas, M. G., Murphy, L. B., Yelin, E. H., Foreman, A. J., Pasta, D. J., and Helmick, C. G., 2009, “Trends in Medical Care Expenditures of US Adults with Arthritis and Other Rheumatic Conditions 1997 to 2005,” J. Rheumatol., 36(11), pp. 2531–2538.

[7] Alomar, X., Medrano, J., Cabratosa, J., Clavero, J. A., Lorente, M., Serra, I., Monill, J. M., and Salvador, A., 2007, “Anatomy of the Temporomandibular Joint,” Semin. Ultrasound, CT, MRI, 28(3), pp. 170–183.

[8] Willard, V. P., Zhang, L., and Athanasiou, K. A., 2011, “Tissue Engineering of the Temporomandibular Joint,” Comprehensive Biomaterials, pp. 221–235.

[9] Salata, M. J., Gibbs, A. E., and Sekiya, J. K., 2010, “A Systematic Review of Clinical Outcomes in Patients Undergoing Meniscectomy,” Am. J. Sports Med., 38(9), pp. 1907–1916.

[10] Shetty, A., 2009, U.S. Soft Tissue Repair Markets - Meniscus and Cartilage, N536, Frost & Sullivan.

[11] Baker, B. E., Peckham, A. C., Pupparo, F., and Sanborn, J. C., 1985, “Review of Meniscal Injury and Associated Sports,” Am. J. Sports Med., 13(1), pp. 1–4.

[12] Kim, S., Bosque, J., Meehan, J. P., Jamali, A., and Marder, R., 2011, “Increase in Outpatient Knee Arthroscopy in the United States: A Comparison of National Surveys of Ambulatory Surgery, 1996 and 2006,” J. Bone Jt. Surgery-American Vol., 93(11), pp. 994–1000.

[13] Englund, M., Guermazi, A., Gale, D., Hunter, D. J., Aliabadi, P., Clancy, M., and Felson, D. T., 2008, “Incidental Meniscal Findings on Knee MRI in Middle-Aged and Elderly Persons,” N. Engl. J. Med., 359(11), pp. 1108–1115.

[14] Hede, A., Jensen, D. B., Blyme, P., and Sonne-Holm, S., 1990, “Epidemiology of Meniscal Lesions in the Knee: 1,215 Open Operations in Copenhagen 1982-84,” Acta Orthop. Scand., 61(5), pp. 435–437.

[15] Fox, A. J. S., Wanivenhaus, F., Burge, A. J., Warren, R. F., and Rodeo, S. A., 2015, “The Human Meniscus: A Review of Anatomy, Function, Injury, and Advances in Treatment,” Clin. Anat., 28(2), pp. 269–287.

[16] Hede, A., Larsen, E., and Sandberg, H., 1992, “The Long Term Outcome of Open Total and Partial Meniscectomy Related to the Quantity and Site of the Meniscus Removed,” Int. Orthop., 16(2), pp. 122–125.

[17] Hede, A., Larsen, E., and Sandberg, H., 1992, “Partial versus Total Meniscectomy. A Prospective, Randomised Study with Long-Term Follow-Up,” J. Bone Jt. Surgery-British Vol., 74(1), pp. 118–121.

[18] Maffulli, N., Longo, U. G., Campi, S., and Denaro, V., 2010, “Meniscal Tears,” Open Access J. Sport. Med., 1, pp. 45–54.

[19] Greis, P. E., Bardana, D. D., Holmstrom, M. C., and Burks, R. T., 2002, “Meniscal Injury: I. Basic Science and Evaluation.,” J. Am. Acad. Orthop. Surg., 10(3), pp. 168–176.

[20] Barber-Westin, S. D., and Noyes, F. R., 2014, “Clinical Healing Rates of Meniscus Repairs of Tears in the Central-Third (Red-White) Zone,” Arthroscopy, 30(1), pp. 134–146.

[21] Srinivasan, P., 2015, Temporomandibular Disorders (TMD) and Use of Oral Appliance for Obstructive Sleep Apnea Syndrome in the United States, 9AD2/02, Frost & Sullivan.

[22] Murphy, M. K., MacBarb, R. F., Wong, M. E., and Athanasiou, K. A., 2013, “Temporomandibular Disorders: A Review of Etiology, Clinical Management, and Tissue Engineering Strategies,” Int. J. Oral Maxillofac. Implants, 28(6), pp. e393–e414.

[23] Isong, U., Gansky, S. A., and Plesh, O., 2008, “Temporomandibular Joint and Muscle Disorder-Type Pain in U.S. Adults: The National Health Interview Survey.,” J. Orofac. Pain, 22(4), pp. 317–322.

[24] Warren, M. P., and Fried, J. L., 2001, “Temporomandibular Disorders and Hormones in Women,” Cells, Tissues, Organs, 169(3), pp. 187–192.

[25] Farrar, W. B., and McCarty, W. L. J., 1979, “The TMJ Dilemma,” J. Alabama Dent. Assoc., 63(1), pp. 19–26.

[26] Muñoz-Guerra, M. F., Rodríguez-Campo, F. J., Escorial Hernández, V., Sánchez-Acedo, C., and Gil-Díez Usandizaga, J. L., 2013, “Temporomandibular Joint Disc Perforation: Long-Term Results after Operative Arthroscopy,” J. Oral Maxillofac. Surg., 71(4), pp. 667–676.

[27] American Society of Temporomandibular Joint Surgeons, 2003, “Guidelines for Diagnosis and Management of Disorders Involving the Temporomandibular Joint and Related Musculoskeletal Structures,” CRANIO, 21(1), pp. 68–76.

[28] Brooks, S. L., Westesson, P. L., Eriksson, L., Hansson, L. G., and Barsotti, J. B., 1992, “Prevalence of Osseous Changes in the Temporomandibular Joint of Asymptomatic Persons without Internal Derangement,” Oral Surg. Oral Med. Oral Pathol., 73(1), pp. 118–122.

[29] Burdick, J. A., and Mauck, R. L., eds., 2011, Biomaterials for Tissue Engineering Applications: A Review of the Past and Future Trends, SpringerWienNewYork.

[30] Xu, C., and Zhao, J., 2015, “A Meta-Analysis Comparing Meniscal Repair with Meniscectomy in the Treatment of Meniscal Tears: The More Meniscus, the Better Outcome?,” Knee Surgery, Sport. Traumatol. Arthrosc., 23(1), pp. 164–170.

[31] Rangger, C., Kathrein, A., Klestil, T., and Glötzer, W., 1997, “Partial Meniscectomy and Osteoarthritis. Implications for Treatment of Athletes.,” Sports Med., 23(1), pp. 61–68.

[32] Herrlin, S., Hållander, M., Wange, P., Weidenhielm, L., and Werner, S., 2007, “Arthroscopic or Conservative Treatment of Degenerative Medial Meniscal Tears: A Prospective Randomised Trial,” Knee Surgery, Sport. Traumatol. Arthrosc., 15(4), pp. 393–401.

[33] Katz, J., Brophy, R., Chaisson, C., Chaves, L., Cole, B., and Dahm, D., 2013, “Surgery versus Physical Therapy for a Meniscal Tear and Osteoarthritis,” N. Engl. J. Med., 368(18), pp. 1675–1684.

[34] Khan, M., Evaniew, N., Bedi, A., Ayeni, O. R., and Bhandari, M., 2014, “Arthroscopic Surgery for Degenerative Tears of the Meniscus: A Systematic Review and Meta-Analysis,” Can. Med. Assoc. J., 186(14), pp. 1057–1064.

[35] Dolwick, M. F., 1997, “The Role of Temporomandibular Joint Surgery in the Treatment of Patients with Internal Derangement,” Oral Surg. Oral Med. Oral Pathol. Oral Radiol. Endod., 83(1), pp. 150–155.

[36] Wolford, L. M., 2006, “Factors to Consider in Joint Prosthesis Systems,” Proc. (Baylor Univ. Med. Center), 19(3), pp. 232–238.

[37] McLeod, N. M. H., Saeed, N. R., and Hensher, R., 2001, “Internal Derangement of the Temporomandibular Joint Treated by Discectomy and Hemi-Arthroplasty with a Christensen Fossa-Eminence Prosthesis,” Br. J. Oral Maxillofac. Surg., 39(1), pp. 63–66.

[38] Bjørnland, T., and Larheim, T. A., 2003, “Discectomy of the Temporomandibular Joint: 3-Year Follow-up as a Predictor of the 10-Year Outcome,” J. Oral Maxillofac. Surg., 61(1), pp. 55–60.

[39] Eriksson, L., and Westesson, P.-L., 2001, “Discectomy as an Effective Treatment for Painful Temporomandibular Joint Internal Derangement: A 5-Year Clinical and Radiographic Follow-Up,” J. Oral Maxillofac. Surg., 59(7), pp. 750–758.

[40] Henry, C. H., and Wolford, L. M., 1993, “Treatment Outcomes for Temporomandibular Joint Reconstruction after Proplast-Teflon Implant Failure,” J. Oral Maxillofac. Surg., 51(4), pp. 352–358.

[41] Dimitroulis, G., 2011, “Condylar Morphology after Temporomandibular Joint Discectomy with Interpositional Abdominal Dermis-Fat Graft,” J. Oral Maxillofac. Surg., 69(2), pp. 439–446.

[42] Troulis, M. J., Tayebaty, F. T., Papadaki, M., Williams, W. B., and Kaban, L. B., 2008, “Condylectomy and Costochondral Graft Reconstruction for Treatment of Active Idiopathic Condylar Resorption,” J. Oral Maxillofac. Surg., 66(1), pp. 65–72.

[43] Deponti, D., Giancamillo, A. Di, Scotti, C., Peretti, G. M., and Martin, I., 2015, “Animal Models for Meniscus Repair and Regeneration,” J. Tissue Eng. Regen. Med., 9(5), pp. 512–527.

[44] Proffen, B. L., McElfresh, M., Fleming, B. C., and Murray, M. M., 2012, “A Comparative Anatomical Study of the Human Knee and Six Animal Species,” Knee, 19(4), pp. 493–499.

[45] Helgeland, E., Shanbhag, S., Pedersen, T. O., Mustafa, K., and Rosén, A., 2018, “Scaffold-Based TMJ Tissue Regeneration in Experimental Animal Models: A Systematic Review,” Tissue Eng. Part B Rev., 24(4), pp. 300–316.

[46] Almarza, A. J., Brown, B. N., Arzi, B., Ângelo, D. F., Chung, W., Badylak, S. F., and Detamore, M., 2018, “Preclinical Animal Models for Temporomandibular Joint Tissue Engineering,” Tissue Eng. Part B Rev., 24(3), pp. 171–178.

[47] Detamore, M. S., Hegde, J. N., Wagle, R. R., Almarza, A. J., Montufar-Solis, D., Duke, P. J., and Athanasiou, K. A., 2006, “Cell Type and Distribution in the Porcine Temporomandibular Joint Disc,” J. Oral Maxillofac. Surg., 64(2), pp. 243–248.

[48] Vapniarsky, N., Aryaei, A., Arzi, B., Hatcher, D. C., Hu, J. C., and Athanasiou, K. A., 2017, “The Yucatan Minipig Temporomandibular Joint Disc Structure–Function Relationships Support Its Suitability for Human Comparative Studies,” Tissue Eng. Part C Methods, 23(11), pp. 700–709.

[49] Zhao, J., Huang, S., Zheng, J., Zhong, C., Tang, C., Zheng, L., Zhang, Z., and Xu, J., 2014, “Changes of Rabbit Meniscus Influenced by Hyaline Cartilage Injury of Osteoarthritis,” Int. J. Clin. Exp. Med., 7(9), pp. 2948–2956.

[50] Pauli, C., Grogan, S. P., Patil, S., Otsuki, S., Hasegawa, A., Koziol, J., Lotz, M. K., and D’Lima, D. D., 2011, “Macroscopic And Histopathologic Analysis Of Human Knee Menisci In Aging And Osteoarthritis,” Osteoarthr. Cartil., 19(9), pp. 1132–1141.

[51] Kalpakci, K. N., Willard, V. P., Wong, M. E., and Athanasiou, K. A., 2011, “An Interspecies Comparison of the Temporomandibular Joint Disc,” J. Dent. Res., 90(2), pp. 193–198.

[52] Murphy, M. K., Arzi, B., Vapniarsky-Arzi, N., and Athanasiou, K. A., 2013, “Characterization of Degenerative Changes in the Temporomandibular Joint of the Bengal Tiger (Panthera Tigris Tigris) and Siberian Tiger (Panthera Tigris Altaica),” J. Comp. Pathol., 149, pp. 495–502.

[53] Huey, D. J., and Athanasiou, K. A., 2011, “Tension-Compression Loading with Chemical Stimulation Results in Additive Increases to Functional Properties of Anatomic Meniscal Constructs,” PLoS One, 6(11), pp. 1–9.

[54] Makris, E. A., MacBarb, R. F., Paschos, N. K., Hu, J. C., and Athanasiou, K. A., 2014, “Combined Use of Chondroitinase-ABC, TGF-B1, and Collagen Crosslinking Agent Lysyl Oxidase to Engineer Functional Neotissues for Fibrocartilage Repair,” Biomaterials, 35(25), pp. 6787–6796.

[55] Mardhiyah, A., Sha’Ban, M., and Azhim, A., 2017, “Evaluation of Histological and Biomechanical Properties on Engineered Meniscus Tissues Using Sonication

Decellularization," Proceedings of the Annual International Conference of the IEEE Engineering in Medicine and Biology Society, EMBS, IEEE, pp. 2064–2067.

[56] Detamore, M. S., Orfanos, J. G., Almarza, A. J., French, M. M., Wong, M. E., and Athanasiou, K. A., 2005, "Quantitative Analysis and Comparative Regional Investigation of the Extracellular Matrix of the Porcine Temporomandibular Joint Disc," Matrix Biol., 24(1), pp. 45–57.

[57] Milam, S. B., Klebe, R. J., Triplett, R. G., and Herbert, D., 1991, "Characterization of the Extracellular Matrix of the Primate Temporomandibular Joint," J. Oral Maxillofac. Surg., 49(4), pp. 381–91.

[58] Melrose, J., Smith, S., Cake, M., Read, R., and Whitelock, J., 2005, "Comparative Spatial and Temporal Localisation of Perlecan, Aggrecan and Type I, II and IV Collagen in the Ovine Meniscus: An Ageing Study," Histochem. Cell Biol., 124(3–4), pp. 225–235.

[59] Sanchez-Adams, J., and Athanasiou, K. A., 2009, "The Knee Meniscus: A Complex Tissue of Diverse Cells," Cell. Mol. Bioeng., 2(3), pp. 332–340.

[60] Ribitsch, I., Peham, C., Ade, N., Dürr, J., Handschuh, S., Schramel, J. P., Vogl, C., Walles, H., Egerbacher, M., and Jenner, F., 2018, "Structure-Function Relationships of Equine Menisci," PLoS One, 13(3), pp. 1–17.

[61] Sweigart, M. A., and Athanasiou, K. A., 2005, "Tensile and Compressive Properties of the Medial Rabbit Meniscus," Proc. Inst. Mech. Eng. Part H J. Eng. Med., 219(5), pp. 337–347.

[62] Gutman, S., Kim, D., Tarafder, S., Velez, S., Jeong, J., and Lee, C. H., 2018, "Regionally Variant Collagen Alignment Correlates with Viscoelastic Properties of the Disc of the Human Temporomandibular Joint," Arch. Oral Biol., 86, pp. 1–6.

[63] Hadidi, P., and Athanasiou, K. A., 2013, “Enhancing the Mechanical Properties of Engineered Tissue through Matrix Remodeling via the Signaling Phospholipid Lysophosphatidic Acid,” Biochem. Biophys. Res. Commun., 433(1), pp. 133–138.

[64] Cissell, D. D., Link, J. M., Hu, J. C., and Athanasiou, K. A., 2017, “A Modified Hydroxyproline Assay Based on Hydrochloric Acid in Ehrlich’s Solution Accurately Measures Tissue Collagen Content,” Tissue Eng. Part C Methods, 23(4), pp. 243–250.

[65] Bank, R. A., Beekman, B., Verzijl, N., De Roos, J. A. D. M., Nico Sakkee, A., and Tekoppele, J. M., 1997, “Sensitive Fluorimetric Quantitation of Pyridinium and Pentosidine Crosslinks in Biological Samples in a Single High-Performance Liquid Chromatographic Run,” J. Chromatogr. B Biomed. Appl., 703(1–2), pp. 37–44.

[66] Herwig, J., Egner, E., and Buddecke, E., 1984, “Chemical Changes of Human Knee Joint Menisci in Various Stages of Degeneration,” Ann. Rheum. Dis., 43(4), pp. 635–40.

[67] McDevitt, C. A., and Webber, R. J., 1990, “The Ultrastructure and Biochemistry of Meniscal Cartilage,” Clin. Orthop. Relat. Res., (252), pp. 8–18.

[68] Eyre, D. R., and Wu, J. J., 1983, “Collagen of Fibrocartilage: A Distinctive Molecular Phenotype in Bovine Meniscus,” FEBS Lett., 158(2), pp. 265–270.

[69] Cheung, H. S., 1987, “Distribution of Type I, II, III and v in the Pepsin Solubilized Collagens in Bovine Menisci,” Connect. Tissue Res., 16(4), pp. 343–356.

[70] Nakano, T., Thompson, J. R., and Aherne, F. X., 1986, “Distribution of Glycosaminoglycans and the Nonreducible Collagen Crosslink, Pyridinoline in Porcine Menisci,” Can. J. Vet. Res., 50(4), pp. 532–536.

[71] Almarza, A. J., Bean, A. C., Baggett, L. S., and Athanasiou, K. A., 2006, “Biochemical Analysis of the Porcine Temporomandibular Joint Disc,” Br. J. Oral Maxillofac. Surg., 44(2), pp. 124–128.

[72] Tissakht, M., and Ahmed, A. M., 1995, “Tensile Stress-Strain Characteristics of the Human Meniscal Material,” J. Biomech., 28(4), pp. 411–422.

[73] Kim, K. W., Wong, M. E., Helfrick, J. F., Thomas, J. B., and Athanasiou, K. A., 2003, “Biomechanical Tissue Characterization of the Superior Joint Space of the Porcine Temporomandibular Joint,” Ann. Biomed. Eng., 31(8), pp. 924–930.

[74] Sweigart, M. A., Zhu, C. F., and Agrawal, C. M., 2002, “Biomechanical Properties of the Medial Meniscus in Experimental Animal Models,” Proceedings of the Second Joint EMBS/BMES Conference, IEEE, pp. 442–443.

[75] Sweigart, M. A., Zhu, C. F., Burt, D. M., Deholl, P. D., Agrawal, C. M., Clanton, T. O., and Athanasiou, K. A., 2004, “Intraspecies and Interspecies Comparison of the Compressive Properties of the Medial Meniscus,” Ann. Biomed. Eng., 32(11), pp. 1569–1579.

[76] Huey, D. J., and Athanasiou, K. A., 2011, “Maturational Growth of Self-Assembled, Functional Menisci as a Result of TGF-B1 and Enzymatic Chondroitinase-ABC Stimulation,” Biomaterials, 32(8), pp. 2052–2058.

[77] Sweigart, M. A., and Athanasiou, K. A., 2005, “Biomechanical Characteristics of the Normal Medial and Lateral Porcine Knee Menisci,” Proc. Inst. Mech. Eng. Part H J. Eng. Med., 219(1), pp. 53–62.

[78] Mak, A. F., Lai, W. M., and Mow, V. C., 1987, “Biphasic Indentation of Articular Cartilage-I. Theoretical Analysis,” J. Biomech., 20(7), pp. 703–714.

[79] Mow, V. C., Gibbs, M. C., Lai, W. M., Zhu, W. B., and Athanasiou, K. A., 1989, “Biphasic Indentation of Articular Cartilage-II. A Numerical Algorithm and an Experimental Study,” J. Biomech., 22(8–9), pp. 853–861.

[80] Mow, V. C., Kuei, S. C., Lai, W. M., and Armstrong, C. G., 1980, “Biphasic Creep and Stress Relaxation of Articular Cartilage in Compression: Theory and Experiments,” J. Biomech. Eng., 102(1), pp. 73–84.

[81] Simon, B. R., Wu, J. S. S., and Evans, J. H., 1983, “Poroelastic Mechanical Models for the Intervertebral Disc,” Proceedings of Advances in Bioengineering: ASME Winter Annual Meeting, D.L. Bartel, ed., Boston, MA, USA, pp. 106–107.

[82] Athanasiou, K. A., and Natoli, R. M., 2008, Introduction to Continuum Biomechanics, Morgan & Claypool Publishers.

[83] Lakes, E. H., Kline, C. L., McFetridge, P. S., and Allen, K. D., 2015, “Comparing the Mechanical Properties of the Porcine Knee Meniscus When Hydrated in Saline versus Synovial Fluid,” J. Biomech., 48(16), pp. 4333–4338.

[84] Joshi, M. D., Suh, J. -K, Marui, T., and Woo, S. L.-Y., 1995, “Interspecies Variation of Compressive Biomechanical Properties of the Meniscus,” J. Biomed. Mater. Res., 29(7), pp. 823–828.

[85] Hadidi, P., Yeh, T. C., Hu, J. C., and Athanasiou, K. A., 2015, “Critical Seeding Density Improves the Properties and Translatability of Self-Assembling Anatomically Shaped Knee Menisci,” Acta Biomater., 11(1), pp. 173–182.

[86] Almarza, A. J., and Athanasiou, K. A., 2004, “Seeding Techniques and Scaffolding Choice for Tissue Engineering of the Temporomandibular Joint Disk,” Tissue Eng., 10(11–12), pp. 1787–1795.

[87] Springer, I. N. G., Fleiner, B., Jepsen, S., and Açil, Y., 2001, “Culture of Cells Gained from Temporomandibular Joint Cartilage on Non-Absorbable Scaffolds,” Biomaterials, 22(18), pp. 2569–2577.

[88] Allen, K. D., and Athanasiou, K. A., 2008, “Scaffold and Growth Factor Selection in Temporomandibular Joint Disc Engineering,” J. Dent. Res., 87(2), pp. 180–185.

[89] Johns, D. E., Wong, M. E., and Athanasiou, K. A., 2008, “Clinically Relevant Cell Sources for TMJ Disc Engineering,” J. Dent. Res., 87(6), pp. 548–552.

[90] Wang, C.-H., Wang, S., Zhang, B., Zhang, X.-Y., Tong, X.-J., Peng, H.-M., Han, X.-Z., and Liu, C., 2018, “Layering Poly (Lactic-Co-Glycolic Acid)-Based Electrospun Membranes and Co-Culture Cell Sheets for Engineering Temporomandibular Joint Disc,” J. Biol. Regul. Homeost. Agents, 32(1), pp. 55–61.

[91] Thomas, M., Grande, D., and Haug, R. H., 1991, “Development of an in Vitro Temporomandibular Joint Cartilage Analog,” J. Oral Maxillofac. Surg., 49(8), pp. 854–856.

[92] Detamore, M. S., and Athanasiou, K. A., 2004, “Effects of Growth Factors on Temporomandibular Joint Disc Cells,” Arch. Oral Biol., 49(7), pp. 577–583.

[93] Detamore, M. S., and Athanasiou, K. A., 2005, “Evaluation of Three Growth Factors for TMJ Disc Tissue Engineering,” Ann. Biomed. Eng., 33(3), pp. 383–390.

[94] Almarza, A. J., and Athanasiou, K. A., 2006, “Evaluation of Three Growth Factors in Combinations of Two for Temporomandibular Joint Disc Tissue Engineering,” Arch. Oral Biol., 51(3), pp. 215–221.

[95] Bean, A. C., Almarza, A. J., and Athanasiou, K. A., 2006, “Effects of Ascorbic Acid Concentration on the Tissue Engineering of the Temporomandibular Joint Disc,” Proc. Inst. Mech. Eng. Part H J. Eng. Med., 220(3), pp. 439–447.

[96] Almarza, A. J., and Athanasiou, K. A., 2005, “Effects of Initial Cell Seeding Density for the Tissue Engineering of the Temporomandibular Joint Disc,” Ann. Biomed. Eng., 33(7), pp. 943–950.

[97] Detamore, M. S., and Athanasiou, K. A., 2005, “Use of a Rotating Bioreactor toward Tissue Engineering the Temporomandibular Joint Disc,” Tissue Eng., 11(7–8), pp. 1188–1197.

[98] Almarza, A. J., and Athanasiou, K. A., 2006, “Effects of Hydrostatic Pressure on TMJ Disc Cells,” Tissue Eng., 12(5), pp. 1285–1294.

[99] Girdler, N. M., 1998, “In Vitro Synthesis and Characterization of a Cartilaginous Meniscus Grown from Isolated Temporomandibular Chondroprogenitor Cells,” Scand. J. Rheumatol., 27(6), pp. 446–453.

[100] Hagandora, C. K., Gao, J., Wang, Y., and Almarza, A. J., 2013, “Poly (Glycerol Sebacate): A Novel Scaffold Material for Temporomandibular Joint Disc Engineering,” Tissue Eng. Part A, 19(5–6), pp. 729–737.

[101] Anderson, D. E. J., and Athanasiou, K. A., 2008, “Passaged Goat Costal Chondrocytes Provide a Feasible Cell Source for Temporomandibular Joint Tissue Engineering,” Ann. Biomed. Eng., 36(12), pp. 1992–2001.

[102] Anderson, D. E. J., and Athanasiou, K. A., 2009, “A Comparison of Primary and Passaged Chondrocytes for Use in Engineering the Temporomandibular Joint,” Arch. Oral Biol., 54(2), pp. 138–145.

[103] Murphy, M. K., Arzi, B., Prouty, S. M., Hu, J. C., and Athanasiou, K. A., 2015, “Neocartilage Integration in Temporomandibular Joint Discs: Physical and Enzymatic Methods,” J. R. Soc. Interface, 12(103).

[104] Vapniarsky, N., Huwe, L. W., Arzi, B., Houghton, M. K., Wong, M. E., Wilson, J. W., Hatcher, D. C., Hu, J. C., and Athanasiou, K. A., 2018, “Tissue Engineering toward Temporomandibular Joint Disc Regeneration,” Sci. Transl. Med., 10(446), pp. 1–10.

[105] Puelacher, W. C., Wisser, J., Vacanti, C. A., Ferraro, N. F., Jaramillo, D., and Vacanti, J. P., 1994, “Temporomandibular Joint Disc Replacement Made by Tissue-Engineered Growth of Cartilage,” J. Oral Maxillofac. Surg., 52(11), pp. 1172–1177.

[106] Kalpakci, K. N., Kim, E. J., and Athanasiou, K. A., 2011, “Assessment of Growth Factor Treatment on Fibrochondrocyte and Chondrocyte Co-Cultures for TMJ Fibrocartilage Engineering,” Acta Biomater., 7(4), pp. 1710–1718.

[107] MacBarb, R. F., Chen, A. L., Hu, J. C., and Athanasiou, K. A., 2013, “Engineering Functional Anisotropy in Fibrocartilage Neotissues,” Biomaterials, 34(38), pp. 9980–9989.

[108] Hadidi, P., Paschos, N. K., Huang, B. J., Aryaei, A., Hu, J. C., and Athanasiou, K. A., 2016, “Tendon and Ligament as Novel Cell Sources for Engineering the Knee Meniscus,” Osteoarthr. Cartil., 24(12), pp. 2126–2134.

[109] Aufderheide, A. C., and Athanasiou, K. A., 2007, “Assessment of a Bovine Co-Culture, Scaffold-Free Method for Growing Meniscus-Shaped Constructs,” Tissue Eng., 13(9), pp. 2195–2205.

[110] Higashioka, M. M., Chen, J. A., Hu, J. C., and Athanasiou, K. A., 2014, “Building an Anisotropic Meniscus with Zonal Variations,” Tissue Eng. Part A, 20(1–2), pp. 294–302.

[111] Murphy, M. K., Huey, D. J., Reimer, A. J., Hu, J. C., and Athanasiou, K. A., 2013, “Enhancing Post-Expansion Chondrogenic Potential of Costochondral Cells in Self-Assembled Neocartilage,” PLoS One, 8(2), pp. 1–10.

[112] Murphy, M. K., Masters, T. E., Hu, J. C., and Athanasiou, K. A., 2015, “Engineering a Fibrocartilage Spectrum through Modulation of Aggregate Redifferentiation,” Cell Transplant., 24(2), pp. 235–245.

[113] Murphy, M. K., Huey, D. J., Hu, J. C., and Athanasiou, K. A., 2015, “TGF-B1, GDF-5, and BMP-2 Stimulation Induces Chondrogenesis in Expanded Human Articular Chondrocytes and Marrow-Derived Stromal Cells,” Stem Cells, 33(3), pp. 762–773.

[114] Moriguchi, Y., Tateishi, K., Ando, W., Shimomura, K., Yonetani, Y., Tanaka, Y., Kita, K., Hart, D. A., Gobbi, A., Shino, K., Yoshikawa, H., and Nakamura, N., 2013, “Repair of Meniscal Lesions Using a Scaffold-Free Tissue-Engineered Construct Derived from Allogenic Synovial MSCs in a Miniature Swine Model,” Biomaterials, 34(9), pp. 2185–2193.

[115] Nakagawa, Y., Muneta, T., Kondo, S., Mizuno, M., Takakuda, K., Ichinose, S., Tabuchi, T., Koga, H., Tsuji, K., and Sekiya, I., 2015, “Synovial Mesenchymal Stem Cells Promote Healing after Meniscal Repair in Microminipigs,” Osteoarthr. Cartil., 23(6), pp. 1007–1017.

[116] Hatsushika, D., Muneta, T., Nakamura, T., Horie, M., Koga, H., Nakagawa, Y., Tsuji, K., Hishikawa, S., Kobayashi, E., and Sekiya, I., 2014, “Repetitive Allogeneic

Intraarticular Injections of Synovial Mesenchymal Stem Cells Promote Meniscus Regeneration in a Porcine Massive Meniscus Defect Model," Osteoarthr. Cartil., 22(7), pp. 941–950.

[117] Legemate, K., Tarafder, S., Jun, Y., and Lee, C. H., 2016, "Engineering Human TMJ Discs with Protein-Releasing 3D-Printed Scaffolds," J. Dent. Res., 95(7), pp. 800–807.

[118] Ahtiainen, K., Mauno, J., Ella, V., Hagstrom, J., Lindqvist, C., Miettinen, S., Ylikomi, T., Kellomaki, M., and Seppanen, R., 2013, "Autologous Adipose Stem Cells and Polylactide Discs in the Replacement of the Rabbit Temporomandibular Joint Disc," J. R. Soc. Interface, 10(85), pp. 1–9.

[119] Suchorska, W. M., Augustyniak, E., Richter, M., and Trzeciak, T., 2017, "Comparison of Four Protocols to Generate Chondrocyte-Like Cells from Human Induced Pluripotent Stem Cells (HiPSCs)," Stem Cell Rev. Reports, 13(2), pp. 299–308.

[120] Brown, B. N., Chung, W. L., Almarza, A. J., Pavlick, M. D., Reppas, S. N., Ochs, M. W., Russell, A. J., and Badylak, S. F., 2012, "An Inductive, Scaffold-Based, Regenerative Medicine Approach to Reconstruction of the Temporomandibular Joint Disk," J. Oral Maxillofac. Surg., 70(11), pp. 2656–2668.

[121] Warren, P. B., Huebner, P., Spang, J. T., Shirwaiker, R. A., and Fisher, M. B., 2017, "Engineering 3D-Bioplotted Scaffolds to Induce Aligned Extracellular Matrix Deposition for Musculoskeletal Soft Tissue Replacement," Connect. Tissue Res., 58(3–4), pp. 342–354.

[122] Lowe, J., and Almarza, A. J., 2017, “A Review of In-Vitro Fibrocartilage Tissue Engineered Therapies with a Focus on the Temporomandibular Joint,” Arch. Oral Biol., 83, pp. 193–201.

[123] Athanasiou, K. A., Eswaramoorthy, R., Hadidi, P., and Hu, J. C., 2013, “Self-Organization and the Self-Assembling Process in Tissue Engineering,” Annu. Rev. Biomed. Eng., 15(1), pp. 115–136.

[124] MacBarb, R. F., Makris, E. A., Hu, J. C., and Athanasiou, K. A., 2013, “A Chondroitinase-ABC and TGF-B1 Treatment Regimen for Enhancing the Mechanical Properties of Tissue-Engineered Fibrocartilage,” Acta Biomater., 9(1), pp. 4626–4634.

[125] Gunja, N. J., Uthamanthil, R. K., and Athanasiou, K. A., 2009, “Effects of TGF-B1 and Hydrostatic Pressure on Meniscus Cell-Seeded Scaffolds,” Biomaterials, 30(4), pp. 565–573.

[126] Johns, D. E., and Athanasiou, K. A., 2008, “Growth Factor Effects on Costal Chondrocytes for Tissue Engineering Fibrocartilage,” Cell Tissue Res., 333(3), pp. 439–447.

[127] Kasemkijwattana, C., Menetrey, J., Goto, H., Niyibizi, C., Fu, F. H., and Huard, J., 2000, “The Use of Growth Factors, Gene Therapy and Tissue Engineering to Improve Meniscal Healing,” Mater. Sci. Eng. C, 13(1–2), pp. 19–28.

[128] Bhargava, M. M., Attia, E. T., Murrell, G. A. C., Dolan, M. M., Warren, R. F., and Hannafin, J. A., 1999, “The Effect of Cytokines on the Proliferation and Migration of Bovine Meniscal Cells,” Am. J. Sports Med., 27(5), pp. 636–643.

[129] Responte, D. J., Arzi, B., Natoli, R. M., Hu, J. C., and Athanasiou, K. A., 2012, “Mechanisms Underlying the Synergistic Enhancement of Self-Assembled Neocartilage Treated with Chondroitinase-ABC and TGF-B1,” Biomaterials, 33(11), pp. 3187–3194.

[130] Natoli, R. M., Revell, C. M., and Athanasiou, K. A., 2009, “Chondroitinase ABC Treatment Results in Greater Tensile Properties of Self-Assembled Tissue-Engineered Articular Cartilage,” Tissue Eng. Part A, 15(10), pp. 3119–3128.

[131] Makris, E. A., Responte, D. J., Paschos, N. K., Hu, J. C., and Athanasiou, K. A., 2014, “Developing Functional Musculoskeletal Tissues through Hypoxia and Lysyl Oxidase-Induced Collagen Cross-Linking,” Proc. Natl. Acad. Sci., 111(45), pp. E4832–E4841.

[132] Chen, M., Guo, W., Gao, S., Hao, C., Shen, S., Zhang, Z., Wang, Z., Wang, Z., Li, X., Jing, X., Zhang, X., Yuan, Z., Wang, M., Zhang, Y., Peng, J., Wang, A., Wang, Y., Sui, X., Liu, S., and Guo, Q., 2018, “Biochemical Stimulus-Based Strategies for Meniscus Tissue Engineering and Regeneration,” Biomed Res. Int., 2018, pp. 1–15.

[133] Shu, W., Liu, L., Bao, G., and Kang, H., 2015, “Tissue Engineering of the Temporomandibular Joint Disc: Current Status and Future Trends,” Int. J. Artif. Organs, 38(2), pp. 55–68.

[134] Baker, B. M., Shah, R. P., Huang, A. H., and Mauck, R. L., 2011, “Dynamic Tensile Loading Improves the Functional Properties of Mesenchymal Stem Cell-Laden Nanofiber-Based Fibrocartilage,” Tissue Eng. Part A, 17(9–10), pp. 1445–1455.

[135] MacBarb, R. F., Paschos, N. K., Abeug, R., Makris, E. A., Hu, J. C., and Athanasiou, K. A., 2014, “Passive Strain-Induced Matrix Synthesis and Organization in

Shape-Specific, Cartilaginous Neotissues," Tissue Eng. Part A, 20(23–24), pp. 3290–3302.

[136] Eifler, R. L., Blough, E. R., Dehlin, J. M., and Haut Donahue, T. L., 2006, "Oscillatory Fluid Flow Regulates Glycosaminoglycan Production via an Intracellular Calcium Pathway in Meniscal Cells," J. Orthop. Res., 24(3), pp. 375–384.

[137] Salinas, E. Y., Hu, J. C., and Athanasiou, K. A., 2018, "A Guide for Using Mechanical Stimulation to Enhance Tissue-Engineered Articular Cartilage Properties," Tissue Eng. Part B Rev., 24(5), pp. 345–358.

[138] White, J. L., Walker, N. J., Hu, J. C., Borjesson, D., and Athanasiou, K. A., 2018, "A Comparison of Bone Marrow and Cord Blood Mesenchymal Stem Cells for Cartilage Self-Assembly," Tissue Eng. Part A, 24(15–16), pp. 1262–1272.

[139] Bansal, S., Keah, N. M., Neuwirth, A. L., O'Reilly, O., Qu, F., Seiber, B., Mandalapu, S., Mauck, R. L., and Zgonis, M., 2017, "Large Animal Models of Meniscus Repair and Regeneration: A Systematic Review of the State of the Field," Tissue Eng. Part C Methods, 23(11), pp. 661–672.

[140] Lu, L., Arbit, H. M., Herrick, J. L., Segovis, S. G., Maran, A., and Yaszemski, M. J., 2015, "Tissue Engineered Constructs: Perspectives on Clinical Translation," Ann. Biomed. Eng., 43(3), pp. 796–804.

[141] Diehl, R., Ferrara, F., Müller, C., Dreyer, A. Y., McLeod, D. D., Fricke, S., and Boltze, J., 2017, "Immunosuppression for in Vivo Research: State-of-The-Art Protocols and Experimental Approaches," Cell. Mol. Immunol., 14(2), pp. 146–179.

[142] Brzezinski, A., Ghodbane, S. A., Patel, J. M., Perry, B. A., Gatt, C. J., and Dunn, M. G., 2017, "The Ovine Model for Meniscus Tissue Engineering: Considerations of

Anatomy, Function, Implantation, and Evaluation," Tissue Eng. Part C Methods, 23(12), pp. 829–841.

Chapter 2: Clinical Replacement Strategies for Meniscus Tissue Deficiency

Abstract

Meniscus tissue deficiency resulting from primary meniscectomy or meniscectomy after failed repair is a clinical challenge since the meniscus has little to no capacity for regeneration. Loss of meniscus tissue has been associated with early onset knee osteoarthritis due to an increase in joint contact pressures in meniscectomized knees. Clinically available replacement strategies range from allograft transplantation to synthetic implants, including the collagen meniscus implant (CMI), ACTIfit, and NuSurface. Although short-term efficacy has been demonstrated with some of these treatments, factors such as long-term durability, chondroprotective efficacy, and return to sport activities in young patients remain unpredictable. Investigations of cell-based and tissue-engineered strategies to treat meniscus tissue deficiency are ongoing.

Published as: Wang, D, Gonzalez-Leon, EA, Rodeo, SA, & Athanasiou, KA. *Clinical Replacement Strategies for Meniscus Tissue Deficiency.* Cartilage (2021)

2.1. Introduction

The meniscus plays a vital role in optimizing force transmission and providing stability in the knee. These fibrocartilaginous tissues are semilunar in shape and consist of a sparse distribution of cells surrounded by an abundant extracellular matrix that imparts the tissue's mechanical function. Meniscal tears are common, and primary surgical options include partial meniscectomy or meniscal repair. As arthroscopic techniques have advanced and biologic augmentation strategies are being investigated, meniscal repairs are now being performed for all tear types, including those in the avascular (white-white) zone that have traditionally been treated with partial meniscectomy (e.g., radial and horizontal cleavage tears).

When meniscal repair fails or is not a valid option resulting in surgical meniscectomy, the loss of meniscal tissue results in a difficult challenge. The meniscus has little capacity for tissue regeneration, and meniscus tissue deficiency has been associated with early onset knee osteoarthritis due to a decrease in tibiofemoral contact area and an increase in joint contact pressures, particularly among the active population [1]. Several treatment options exist for restoring the deficient meniscus, from allograft transplantation to artificial implants. Indications and contraindications for these treatment options are listed in Table 2.1. Despite the improvement in clinical symptoms, the long-term chondroprotective effects from meniscal transplantation or synthetic implants is unclear. A few cell-based meniscal tissue replacement options are being investigated under clinical trials, but none are currently available to date.

Table 2.1. Meniscus allograft preservation methods

Preservation Method	Technique	Cell Viability	Immunogenicity	Advantages	Disadvantages

Fresh	Storage at 4°C	Yes	Yes	Native microarchitecture and material properties	Risk of disease transmission, short storage time and logistical planning
Fresh-frozen	Deep freezing to -80°C	No	Reduced	Prolonged storage, cost-effective	Altered collagen fiber architecture
Cryopreserved	Slow-freezing to -196°C in an anhydrous environment to prevent intracellular water crystallization	Yes (4-54%)	Yes	Preservation of collagen fiber architecture, prolonged storage	Expensive, decreased viability and changes to cell metabolism
Lyophilized	Freeze-drying and storage at room temperature	No	No	Unlimited storage	Deleterious effects on mechanical properties, graft shrinkage

2.2. Meniscus Allograft Transplantation

Meniscus allograft transplantation (MAT) has proven to be an effective solution for young and active symptomatic patients who have undergone meniscectomy (Fig. 2.1) [2–6]. Ideally, MAT should be performed when there is absent or only mild preexisting arthrosis due to the graft's capacity to reduce peak tibiofemoral contact pressures and potentially slow the rate of articular cartilage degeneration. Focal articular cartilage lesions in the same compartment, limb alignment, and ligamentous stability are all necessary clinical considerations that can be concurrently addressed to preserve the longevity of the meniscal allograft and optimize patient outcomes.

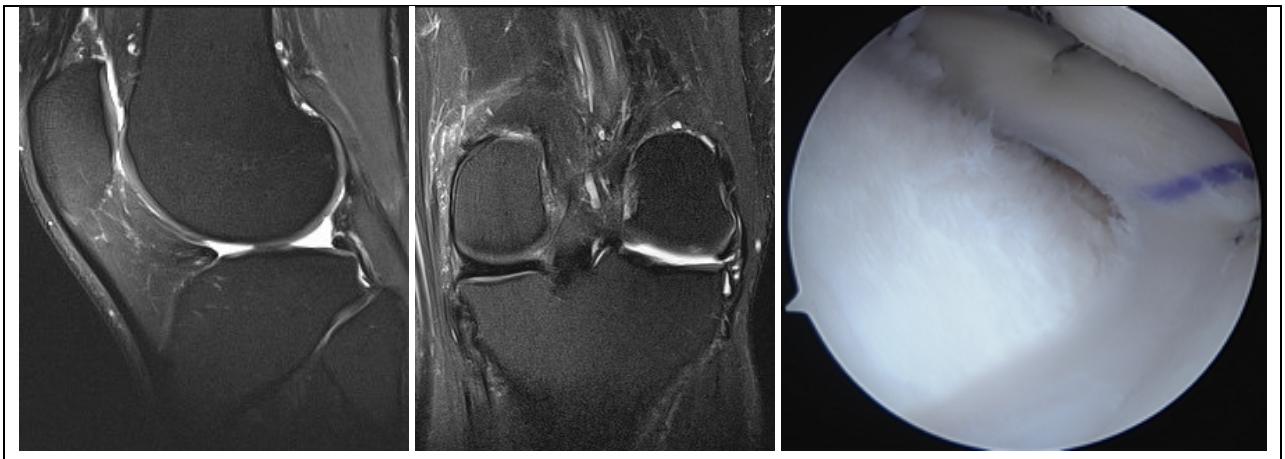

Figure 2.1. Sagittal (left) and coronal (middle) magnetic resonance imaging of the left knee shows absent lateral meniscus after previous subtotal lateral meniscectomy. The patient was treated with lateral meniscus allograft transplantation (right) using bone plug fixation.

2.2.1 Graft Processing

In the United States, meniscus allograft tissue is most commonly distributed in fresh and fresh-frozen forms, while cryopreserved allografts are infrequently offered but remain an option in other countries (Table 2.2). Lyophilization (freeze-drying) has fallen out of favor because of its deleterious effects on the mechanical properties of the allograft and graft shrinkage. Although some believe that preservation methods that maintain cell viability (i.e., fresh and cryopreserved) enhance graft survival and function, there has been no evidence to date demonstrating this supposed benefit. Data from animal models have shown a relatively rapid repopulation of donor graft tissue with recipient cells within a few weeks after transplantation [7], thereby raising questions about the necessity of cell viability in optimizing graft survival and clinical outcomes. However, fresh-frozen grafts seem to have diminished collagen fiber architecture and biomechanics compared to fresh

and cryopreserved grafts [8]. The lower cost and logistical benefits of fresh-frozen grafts account for their greater popularity at most centers.

Treatment of meniscus allografts with gamma irradiation or chemical processes can be performed in order to reduce the risk of bacterial, fungal, and viral transmission. Sterilization typically results in killing of viable cells and is thus not performed on fresh and cryopreserved grafts. Dosages of radiation required to kill viruses (i.e., 1.5 to 2.0 Mrad) can cause deleterious changes to the meniscus tissue biomechanical properties [8], and therefore, use of nonirradiated grafts is preferable. Ethylene oxide gas sterilization, which is commonly used to sterilize medical devices, produces a metabolic byproduct (ethylene chlorohydrin) that causes significant synovitis and is therefore not recommended as a sterilization agent [9]. Other sterilization techniques such as supercritical CO2, which are purported to better preserve tissue properties over gamma irradiation, are being investigated. These emerging and proprietary sterilization techniques may be more appropriate for synthetic materials rather than biologic tissue grafts.

Table 2.2. Published Success Rates and Survivorship Following MAT with Fresh-Frozen Grafts

Study	No. of Patients	Mean Follow-up (yrs)	Clinical Success Rates (%)	Graft Survivorship
Grassi *et al.* [4]	46	10.8	60-82	86% at 10 yrs
Searle *et al.* [6]	43	3.4	79	91%
Zaffagnini *et al.* [21]	147	4.0	84	95% at 6 yrs
Lee et al [5]	222	3.7	91	83.5% at 5 yrs
Bloch et al [3]	240	3.4	-	87.4% at 5 yrs

McCormick *et al.* [22]	172	4.9	-	95% at 5 yrs

2.2.2 Graft Fixation

Peripheral fixation of meniscal allografts is traditionally performed using vertical-mattress sutures along with accurate reestablishment of the meniscal horns and roots. Both inside-out mattress sutures tied over the joint capsule and all-inside sutures are widely utilized. Some native peripheral rim tissue should be retained in order to decrease peripheral extrusion and provide a firm base to which the allograft is secured. Secure fixation of the horns and roots are crucial for permitting optimal distribution of hoop stresses throughout the meniscus allograft. Three main fixation methods for securing the graft horns and roots include: 1) soft tissue only, 2) bone plugs, and 3) bone bridge. The optimal method for horn fixation continues to be debated. Recent cadaveric studies have suggested that bone plug fixation more closely reproduces the normal function of the meniscus compared to soft-tissue fixation for medial meniscal allografts [10,11]. For lateral meniscal allografts, Brial *et al.* [12] showed that although both bridge and bone plug fixation methods improved lateral tibiofemoral compartment contact mechanics compared to the meniscectomized state, bone bridge fixation better restored contact mechanics to that of the intact knee. Conversely, Novaretti *et al*. [13] found no differences between bone bridge and soft tissue fixation methods for lateral meniscal allografts with regards to kinematics and forces experienced during applied loads. Clinical studies have yet to demonstrate superiority of bone fixation techniques, which are technically more demanding, over soft-tissue fixation [14]. In a meta-analysis, Jauregui et al [14] did not find significant differences in meniscal allograft tear rates, failure rates, or patient-reported outcomes between soft tissue suture and bone fixation methods. However, several of the

studies included historical data that used lyophilized and/or irradiated grafts and older surgical techniques. Further studies are needed to determine the optimal fixation technique for MAT.

2.2.3 Clinical Outcomes

Many studies reporting on the outcomes of MAT are limited by low level of evidence, heterogeneity of data including patients, graft types, and techniques, inconsistent exclusion criteria for transplantation, and concomitant procedures that may confound results. As graft preparation and fixation techniques continue to advance, the clinical outcomes of MAT may be further optimized.

In studies evaluating the clinical outcomes of MAT, clinically significant improvements in patient-reported outcome scores, including the Lysholm, Knee Injury and Osteoarthritis Outcome Score (KOOS), and International Knee Documentation Committee (IKDC) scores, are noted at mid-term follow-up [2–5]. Although functional improvement can be maintained up to 10 years, activity and sport-specific scores seem to decline during the interval between short-/mid-term and long-term follow-up [3,15]. For fresh-frozen grafts, 5-year graft survivorship is high, ranging from 84-95% (Table 2.3). For cryopreserved grafts, 10+-year graft survivorship is reported to range from 45-71% [16–18]. The presence of grade 4 articular cartilage loss or bipolar lesions at the time of MAT seems to portend worse graft survival [2,4], suggesting that earlier treatment of symptomatic patients may be optimal before significant chondrosis is sustained. Post-operatively, the incidence of graft tears ranges from 11-16%, although the majority of these cases do not necessitate full graft removal [3]. The wide variability in rate of graft tears reported is likely due to use of different outcome measures for graft assessment,

including MRI scan and second look arthroscopy. When comparing medial MAT to lateral MAT, the functional outcomes and long-term survival rates appear to be similar [19].

Probability of returning to work after MAT can be high (>85%) [20], although this is likely dependent on the intensity of loading required on the knee for the specific occupation. In a cohort of active-duty military patients, only 20% were able to return to full duty, and 46% had permanent profile activity restrictions [21]. Although MAT is generally considered a salvage procedure with return to repetitive impact activities such as running and jumping generally being discouraged, recent studies suggest that return to modest sports activities in the short-term is a reasonable goal. In a meta-analysis, the majority of athletes and physically active patients (77%) were able to return to sport after MAT at a mean of 9.2 months postoperatively, and two-thirds of athletes were able to return to preinjury levels [22]. Graft-related reoperations, which were mostly partial meniscectomies, were reported in 13% of patients [22].

While MAT appears to decrease tibiofemoral pain in the short-term, the long-term chondroprotective effects of the procedure remain unclear. In sheep and rabbits, MAT has been shown to protect the articular cartilage from degeneration [23]. While human cadaveric studies demonstrate the biomechanical benefits of MAT with reduced peak contact pressures compared to meniscectomized knees, MAT does not fully restore contact mechanics and kinematics to that of the intact knee [13,24]. Articular cartilage benefits in animals and human biomechanical studies seem to agree with some clinical studies, but other clinical studies in humans have not found clear chondroprotective benefits. At a mean of 12 years, Verdonk *et al.* [25] found that 52% of patients did not show any change in joint space width, whereas all failure cases that were converted to

total knee arthroplasty (TKA) were characterized by an increase in joint space narrowing. A systematic review evaluating the chondroprotective effects of MAT reported a weighted mean joint space loss of 0.032 mm at 4.5 years across 11 studies [26]. Although there is evidence to support the theory that MAT reduces the progression of osteoarthritis, the current data suggest that it is unlikely to be as effective as the native meniscus.

2.3. Synthetic Options

Two synthetic, scaffold-based meniscal substitutes for partial meniscus replacement are currently commercially available for clinical use: collagen meniscus implant (CMI, Stryker Corporation, Kalamazoo, MI, USA) and ACTIfit (Orteq Sports Medicine Ltd., London, United Kingdom). Both have demonstrated promising results in early clinical trials [27–29]. In contrast to MAT, both can replace segmental meniscal defects, thereby preserving intact native meniscus tissue, and the off-the-shelf nature of synthetic grafts make surgical planning easier. However, lack of cell migration, stress shielding, and degradation products causing chronic synovitis remain a concern with any scaffold-based treatment options. Another synthetic option, the NuSurface Meniscus Implant (Active Implants LLC, Memphis, TN, USA), is a non-anchored, non-absorbable meniscal prosthesis designed for total replacement of the medial meniscus. Although these options may be clinically available, lack of third-party insurance reimbursement has limited their clinical utilization.

2.3.1 Collagen Meniscus Implant (CMI)

The CMI, which consists of type-I collagen fibers derived from bovine Achilles tendons, has gained attention since the first clinical trial was published in 1997. It received U.S. Food and Drug Administration (FDA) 510(k) clearance in 2008. Designed for segmental

meniscal replacement, the implant is sized to match the prepared meniscal defect and sutured to the surrounding intact meniscus tissue (Fig. 2.2). The bioresorbable scaffold is very porous, facilitating tissue ingrowth via proliferation of both fibroblasts and fibrochondrocytes as well as production of extracellular matrix. Second-look arthroscopy after CMI implantation has demonstrated formation of meniscus-like tissue grossly with variable degrees of maturity and integration to the host rim [27]. On MRI follow-up, remodeling of the CMI occurs up to 5 years after implantation as indicated by decreasing signal intensity and size; however, the majority of knees show persistent hyperintense signal compatible with myxoid degeneration [30].

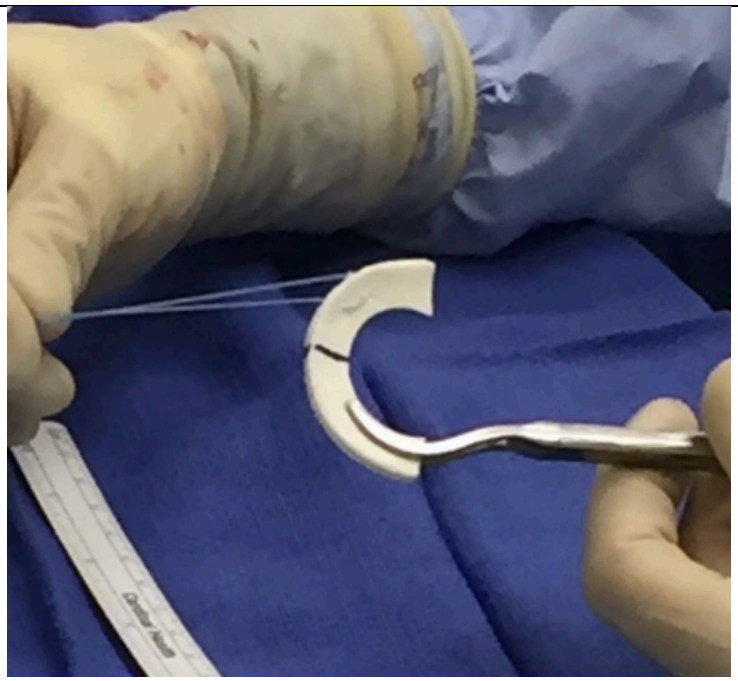

Figure 2.2. Photograph of collagen meniscal implant (CMI).

The majority of published clinical outcomes on the CMI are limited to treatment of medial meniscal defects, although short-term results after CMI treatment for lateral meniscal defects are available [31]. Ten-year data demonstrates significant clinical improvements after CMI [32], but comparative studies are scarce. In a systematic review

of 311 patients treated with CMI, the failure rate was 6.7% at a mean follow-up of 44 months [28]. VAS pain, Lysholm, and Tegner scores were significantly improved at final follow-up, with most studies demonstrating improvement in Lysholm scores above minimal clinically important difference (MCID) and patient acceptable symptom state (PASS) thresholds [28]. A randomized, controlled, multicenter clinical trial showed that in patients with prior medial meniscal procedures, those treated with CMI regained significantly higher activity (Tegner Activity Scale) and were more satisfied compared to patients treated with repeat partial medial meniscectomy. However, in patients who had no prior meniscal surgery, no difference could be observed between CMI and partial meniscectomy treatment groups [27]. In another comparative study with a minimum of 10 years follow-up, CMI-treated patients had better pain, activity level, and radiographic outcomes (less medial joint space narrowing) compared to patients treated with partial meniscectomy [32].

2.3.2 ACTIfit

The ACTIfit (Fig. 2.3), composed of a synthetic hybrid of polycaprolactone (80%) and polyurethane (20%), was first described in a clinical trial in 2011 [33] and was granted FDA Breakthrough Designation in 2020. Similar to the CMI, it was designed for segmental meniscal replacement. The ACTIfit scaffold degrades slowly over a 5-year period, starting with hydrolysis of the softer polycaprolactone segments, while the more rigid polyurethane is slowly removed by macrophages and giant cells [34]. At time zero, both the CMI and ACTIfit demonstrate significantly lower stiffness compared to native meniscus specimens and are absent of viscoelastic properties, with no notable biomechanical differences between the two artificial implants [35]. Tissue ingrowth and

formation of meniscus-like fibrocartilage tissue is evident according to histological analysis and second-look arthroscopy [33]. At long-term follow-up, viability remains low in the resultant repair tissue, and the biomechanical properties of the remodeled implants do not approach that of the native meniscus [36].

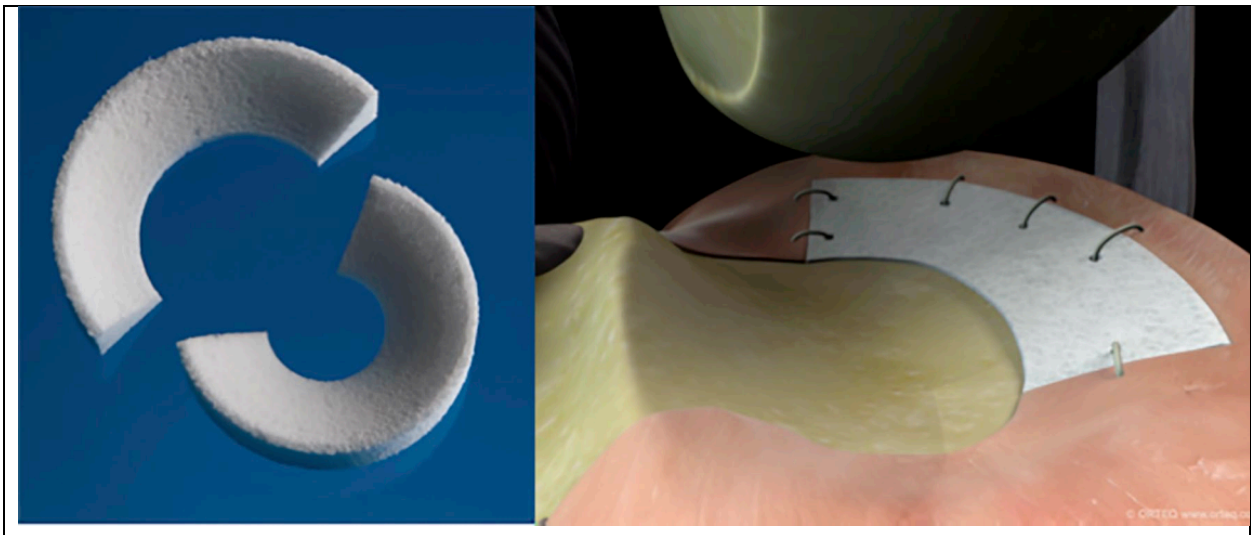

Figure 2.3. Photograph and in vivo illustration of ACTIfit implant (Courtesy of Orteq Sports Medicine, London, UK).

To date, clinical studies on the ACTIfit are limited to short- and mid-term case series. In the largest available series consisting of 155 patients, pain and knee scores improved postoperatively at 2 years and were stable out to 5 years follow-up [29]. Postoperative MRI demonstrated a smaller-sized implant with an irregular surface in the majority of cases. The overall surgical failure rate was 12.4% at 5 years, with no difference in failure rates between medial and lateral implants [29]. A few studies have attempted to compare the clinical outcomes of CMI versus ACTIfit and have demonstrated no differences in failure rate or improvement in patient-reported outcomes between groups [28,37].

2.3.3 NUSurface

The NUSurface Meniscus Implant is a non-anatomic, discoid-shaped, free floating meniscal substitute designed for total replacement of the medial meniscus. It is made of polycarbonate-urethane, a medical grade plastic. A biomechanical study showed that implantation of the NUSurface Meniscus Implant restores the average and peak tibiofemoral contact pressures to 93% and 92%, respectively, compared to the native medial meniscus [38]. The NUSurface was granted FDA Breakthrough Designation in 2019, and two Investigational Device Exemption (IDE) clinical trials are currently ongoing in the U.S. In Europe and Israel, clinical use of the NUSurface has been ongoing since 2008 but there is minimal published outcomes data available. Preliminary results have demonstrated significant improvements in pain and KOOS scores at 12 months for the NUSurface compared to non-surgical therapy and a similar adverse event rate [39,40].

2.4. Cell-Based Options

Several cell-based meniscal replacement options are being developed and tested in clinical trials. While the following cell-based options are not currently approved by the FDA, orthopedic surgeons could benefit from knowledge of these options that may be commercially available in the future.

2.4.1 Cell Bandage (Azellon):

The Cell Bandage consists of expanded (passage 1) autologous bone marrow-derived mesenchymal stromal cells (MSCs) embedded in a collagen matrix. It is a two-stage procedure, with the first stage involving harvesting of cells from host bone marrow, isolation, culture, and seeding onto the collagen matrix, followed by the second stage implantation. This treatment was designed for repair of meniscus tears in the avascular

(white-white) zone that would otherwise be an indication for meniscectomy; the seeded scaffold is placed between torn edges of the meniscus, and the tissue is reapproximated using sutures [41].

Preclinical studies for the Cell Bandage used an ovine model, in which autologous bone marrow-derived MSCs were employed [41]. Three out of five sheep showed successful healing in the white-white region of the meniscus at 13 weeks; however, no animals showed healed lesions after 6 months. In comparison, no animals in the collagen sponge- and suture-only control groups showed signs of healing at either time point.

In a first in-human study (Phase I clinical trial in the United Kingdom), implantation of the Cell Bandage appeared to be safe as no adverse local or systemic immune responses were reported [41]. The implant survived in three out of five patients at 24-month follow-up as indicated on MRI without any further treatments. Clinically significant improvement in IKDC and Tegner-Lysholm scores were observed at 12 months and maintained at 24 months. The two other patients developed recurrent symptoms due to retear or nonhealing of the meniscus before ultimately receiving subsequent meniscectomy. As the Phase I clinical trial is still ongoing (EU Clinical Trials Register, 2010-024162-22), no results with longer follow-up have been published.

2.4.2 Chondrogen (Mesoblast):

Chondrogen consists of expanded (passage 2) allogeneic adult bone marrow-derived MSCs suspended in a sodium hyaluronate solution that is injected intra-articularly following partial meniscectomy [42]. As opposed to being a meniscus tissue substitute, Chondrogen is an augmentation biologic injectable therapy that attempts to enhance meniscus regeneration and tissue volume after meniscectomy. Human MSCs are derived

from bone marrow aspirates collected from unrelated donors (18-30 years of age) and are not human leukocyte antigen (HLA)-matched to recipients.

A phase I/II, randomized, double-blind, controlled study on Chondrogen consisting of 55 patients has been reported [42]. After partial meniscectomy, patients received a single intra-articular injection of either 50 million MSCs, 150 million MSCs, or a vehicle control. No patients in any of the treatment groups exhibited abnormal immune or hematologic responses. At 24 months, three patients (18%) from the 50 million MSC group exhibited a >15% increase in meniscus volume as found on MRI, while this was not observed in patients in the 150 million and control groups. Decreased visual analogue scale (VAS) pain and increased Lysholm scores were seen at 24 months in all treatment groups with respect to baseline. This phase I/II study in the United States has been completed (ClinicalTrials.gov Identifier NCT00702741), though results have not yet been published.

2.5. Future Directions

While MAT and synthetic meniscus replacement options may be effective in alleviating knee joint pain in the short-term, their long-term durability and chondroprotective effects are questionable. Inferior mechanical properties of these grafts presumably leads to their eventual failure over time. This motivates the development of tissue-engineered meniscus replacement and regeneration options that recapitulate the mechanical, structural, and compositional properties of native meniscus tissue. Tissue engineering researchers have proposed both scaffold-based and scaffold-free meniscus replacement options. Scaffold-based technologies, including three-dimensional (3D)-printed biomimetic constructs, have been utilized in vivo to successfully replace the knee meniscus in a rabbit model

after a total meniscectomy [43]. The unique advantage of 3D-printed biomimetic constructs is that it can be personalized to the patient anatomy with use of MRI [44]. Furthermore, 3D-printed meniscus constructs can be fabricated with a variety of materials that may prevent immunorejection upon implantation, including bio-ink containing collagen and cells such as MSCs or meniscus fibrochondrocytes from autologous sources [44,45].

Scaffold-free neomenisci (Fig. 2.4) can be engineered using a self-assembling process using an abundant cell source and combined with external biochemical and biomechanical stimuli to enhance its mechanical and microstructural properties to approach those of native tissue [46]. The addition of mechanical and chemical stimuli during culture, alone or in combination, have been utilized to augment the mechanical and biochemical properties of self-assembled, tissue-engineered constructs [43,47]. For example, using a combination of TGF-ß1, chondroitinase ABC, lysyl oxidase-like protein 2, and lysophosphatidic acid induced matrix augmentation and directional remodeling in self-assembled neomenisci constructs, with synergistic increases in mechanical properties, biochemical content, and mechanical anisotropy [46]. Following the FDA paradigm for the translation of engineered tissues, large animal preclinical studies will have to be conducted in order to show the safety and efficacy of these meniscus replacement options before their implantation in human patients.

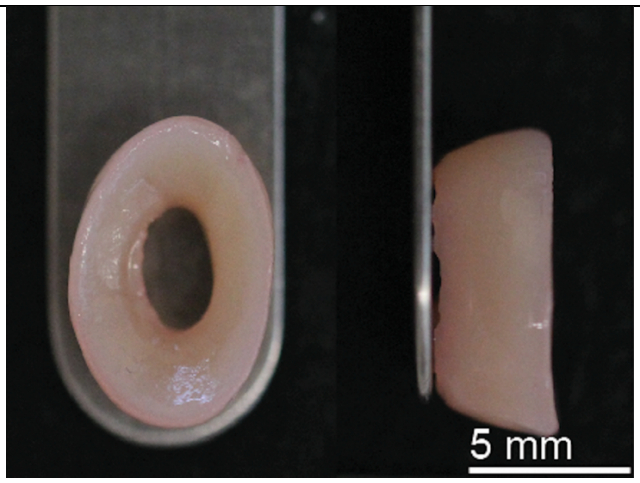

Figure 2.4. Tissue engineered neomenisci using the scaffold-free, self-assembly process.

2.6 Summary

The meniscus plays an important role in protecting the health of the knee joint. Once meniscus tissue has been torn and removed from the joint, there is little to no capacity for the meniscus to regenerate lost tissue. MAT can be an effective treatment option, with proof of short- and mid-term clinical functional improvement, although graft durability and return to sport activities remains a challenge. Artificial options, including the CMI, ACTIfit, and NuSurface are being increasingly utilized, particularly for segmental defects, although implant durability and third-party insurance reimbursement remain challenges. Investigations of cell-based meniscal tissue replacement options are ongoing. Finally, tissue-engineered options that can generate biomimetic neomeniscus tissue may further optimize patient outcomes after treatment for meniscal tissue deficiency. Even with these advances, surgeons should continue to attempt meniscal repair whenever feasible and resect as little meniscal tissue as possible in tears that are deemed irreparable.

References

[1] Koh, J. L., Zimmerman, T. A., Patel, S., Ren, Y., Xu, D., and Zhang, L. Q., 2018, “Tibiofemoral Contact Mechanics With Horizontal Cleavage Tears and Treatment of the Lateral Meniscus in the Human Knee: An In Vitro Cadaver Study,” Clin. Orthop. Relat. Res., 476(11), pp. 2262–2270.

[2] Bloch, B., Asplin, L., Smith, N., Thompson, P., and Spalding, T., 2019, “Higher Survivorship Following Meniscal Allograft Transplantation in Less Worn Knees Justifies Earlier Referral for Symptomatic Patients: Experience from 240 Patients,” Knee Surg. Sports Traumatol. Arthrosc., 27(6).

[3] Grassi, A., Macchiarola, L., Lucidi, G. A., Coco, V., Romandini, I., Filardo, G., Neri, M. P., Marcacci, M., and Zaffagnini, S., 2020, “Long-Term Outcomes and Survivorship of Fresh-Frozen Meniscal Allograft Transplant With Soft Tissue Fixation: Minimum 10-Year Follow-up Study,” Am. J. Sports Med., 48(10), pp. 2360–2369.

[4] Lee, B. S., Bin, S. Il, Kim, J. M., Kim, W. K., and Choi, J. W., 2017, “Survivorship After Meniscal Allograft Transplantation According to Articular Cartilage Status,” Am. J. Sports Med., 45(5), pp. 1095–1101.

[5] Searle, H., Asopa, V., Coleman, S., and McDermott, I., 2020, “The Results of Meniscal Allograft Transplantation Surgery: What Is Success?,” BMC Musculoskelet. Disord., 21(1).

[6] Zaffagnini, S., Grassi, A., Marcheggiani Muccioli, G. M., Benzi, A., Serra, M., Rotini, M., Bragonzoni, L., and Marcacci, M., 2016, “Survivorship and Clinical Outcomes of 147 Consecutive Isolated or Combined Arthroscopic Bone Plug Free Meniscal Allograft Transplantation,” Knee Surg. Sports Traumatol. Arthrosc., 24(5), pp. 1432–1439.

[7] Arnoczky, S. P., DiCarlo, E. F., O'Brien, S. J., and Warren, R. F., 1992, "Cellular Repopulation of Deep-Frozen Meniscal Autografts: An Experimental Study in the Dog," Arthroscopy, 8(4), pp. 428–436.

[8] Jacquet, C., Erivan, R., Sharma, A., Pithioux, M., Parratte, S., Argenson, J. N., and Ollivier, M., 2019, "Preservation Methods Influence the Biomechanical Properties of Human Lateral Menisci: An Ex Vivo Comparative Study of 3 Methods," Orthop. J. Sport. Med., 7(4).

[9] Binnet, M. S., Akan, B., and Kaya, A., 2012, "Lyophilised Medial Meniscus Transplantations in ACL-Deficient Knees: A 19-Year Follow-Up," Knee Surg. Sports Traumatol. Arthrosc., 20(1), pp. 109–113.

[10] Wang, H., Gee, A. O., Hutchinson, I. D., Stoner, K., Warren, R. F., Chen, T. O., and Maher, S. A., 2014, "Bone Plug Versus Suture-Only Fixation of Meniscal Grafts: Effect on Joint Contact Mechanics During Simulated Gait," Am. J. Sports Med., 42(7), pp. 1682–1689.

[11] Ambra, L. F., Mestriner, A. B., Ackermann, J., Phan, A. T., Farr, J., and Gomoll, A. H., 2019, "Bone-Plug Versus Soft Tissue Fixation of Medial Meniscal Allograft Transplants: A Biomechanical Study," Am. J. Sports Med., 47(12), pp. 2960–2965.

[12] Brial, C., McCarthy, M., Adebayo, O., Wang, H., Chen, T., Warren, R., and Maher, S., 2019, "Lateral Meniscal Graft Transplantation: Effect of Fixation Method on Joint Contact Mechanics During Simulated Gait," Am. J. Sports Med., 47(10), pp. 2437–2443.

[13] Novaretti, J. V., Lian, J., Sheean, A. J., Chan, C. K., Wang, J. H., Cohen, M., Debski, R. E., and Musahl, V., 2019, "Lateral Meniscal Allograft Transplantation With

Bone Block and Suture-Only Techniques Partially Restores Knee Kinematics and Forces," Am. J. Sports Med., 47(10), pp. 2427–2436.

[14] Jauregui, J. J., Wu, Z. D., Meredith, S., Griffith, C., Packer, J. D., and Henn, R. F., 2018, "How Should We Secure Our Transplanted Meniscus? A Meta-Analysis," Am. J. Sports Med., 46(9), pp. 2285–2290.

[15] Saltzman, B. M., Meyer, M. A., Leroux, T. S., Gilelis, M. E., Debot, M., Yanke, A. B., and Cole, B. J., 2018, "The Influence of Full-Thickness Chondral Defects on Outcomes Following Meniscal Allograft Transplantation: A Comparative Study," Arthroscopy, 34(2), pp. 519–529.

[16] Hommen, J. P., Applegate, G. R., and Del Pizzo, W., 2007, "Meniscus Allograft Transplantation: Ten-Year Results of Cryopreserved Allografts," Arthroscopy, 23(4).

[17] Van Der Wal, R. J. P., Thomassen, B. J. W., and Van Arkel, E. R. A., 2009, "Long-Term Clinical Outcome of Open Meniscal Allograft Transplantation," Am. J. Sports Med., 37(11), pp. 2134–2139.

[18] Carter, T. R., and Brown, M. J., 2020, "Meniscal Allograft Survivorship and Outcomes 20 Years After Implantation," Arthroscopy, 36(8), pp. 2268–2274.

[19] van der Wal, R. J. P., Nieuwenhuijse, M. J., Spek, R. W. A., Thomassen, B. J. W., van Arkel, E. R. A., and Nelissen, R. G. H. H., 2020, "Meniscal Allograft Transplantation in The Netherlands: Long-Term Survival, Patient-Reported Outcomes, and Their Association with Preoperative Complaints and Interventions," Knee Surg. Sports Traumatol. Arthrosc., 28(11), pp. 3551–3560.

[20] Agarwalla, A., Liu, J. N., Christian, D. R., Garcia, G. H., Cvetanovich, G. L., Gowd, A. K., Yanke, A. B., and Cole, B. J., 2021, "Return to Work Following

Arthroscopic Meniscal Allograft Transplantation," Cartilage, 13(1_suppl), pp. 249S-255S.

[21] Antosh, I. J., Cameron, K. L., Marsh, N. A., Posner, M. A., Deberardino, T. M., Svoboda, S. J., and Owens, B. D., 2020, "Likelihood of Return to Duty Is Low After Meniscal Allograft Transplantation in an Active-Duty Military Population," Clin. Orthop. Relat. Res., 478(4), pp. 722–730.

[22] Grassi, A., Bailey, J. R., Filardo, G., Samuelsson, K., Zaffagnini, S., and Amendola, A., 2019, "Return to Sport Activity After Meniscal Allograft Transplantation: At What Level and at What Cost? A Systematic Review and Meta-Analysis," Sports Health, 11(2), pp. 123–133.

[23] Kelly, B. T., Potter, H. G., Deng, X. H., Pearle, A. D., Turner, A. S., Warren, R. F., and Rodeo, S. A., 2006, "Meniscal Allograft Transplantation in the Sheep Knee: Evaluation of Chondroprotective Effects," Am. J. Sports Med., 34(9), pp. 1464–1477.

[24] Kim, J. G., Lee, Y. S., Bae, T. S., Ha, J. K., Lee, D. H., Kim, Y. J., and Ra, H. J., 2013, "Tibiofemoral Contact Mechanics Following Posterior Root of Medial Meniscus Tear, Repair, Meniscectomy, and Allograft Transplantation," Knee Surg. Sports Traumatol. Arthrosc., 21(9), pp. 2121–2125.

[25] Verdonk, P. C. M., Verstraete, K. L., Almqvist, K. F., De Cuyper, K., Veys, E. M., Verbruggen, G., and Verdonk, R., 2006, "Meniscal Allograft Transplantation: Long-Term Clinical Results with Radiological and Magnetic Resonance Imaging Correlations," Knee Surg. Sports Traumatol. Arthrosc., 14(8), pp. 694–706.

[26] Smith, N. A., Parkinson, B., Hutchinson, C. E., Costa, M. L., and Spalding, T., 2016, "Is Meniscal Allograft Transplantation Chondroprotective? A Systematic Review

of Radiological Outcomes," Knee Surg. Sports Traumatol. Arthrosc., 24(9), pp. 2923–2935.

[27] Rodkey, W. G., DeHaven, K. E., Montgomery, W. H., Baker, C. L., Beck, C. L., Hormel, S. E., Steadman, J. R., Cole, B. J., and Briggs, K. K., 2008, "Comparison of the Collagen Meniscus Implant with Partial Meniscectomy. A Prospective Randomized Trial," J. Bone Joint Surg. Am., 90(7), pp. 1413–1426.

[28] Houck, D. A., Kraeutler, M. J., Belk, J. W., McCarty, E. C., and Bravman, J. T., 2018, "Similar Clinical Outcomes Following Collagen or Polyurethane Meniscal Scaffold Implantation: A Systematic Review," Knee Surgery, Sport. Traumatol. Arthrosc., 26(8), pp. 2259–2269.

[29] Toanen, C., Dhollander, A., Bulgheroni, P., Filardo, G., Zaffagnini, S., Spalding, T., Monllau, J. C., Gelber, P., Verdonk, R., Beaufils, P., Pujol, N., Bulgheroni, E., Asplin, L., and Verdonk, P., 2020, "Polyurethane Meniscal Scaffold for the Treatment of Partial Meniscal Deficiency: 5-Year Follow-up Outcomes: A European Multicentric Study," Am. J. Sports Med., 48(6), pp. 1347–1355.

[30] Schenk, L., Bethge, L., Hirschmann, A., Berbig, R., Lüthi, U., Arnold, M. P., and Hirschmann, M. T., 2020, "Ongoing MRI Remodeling 3-7 Years after Collagen Meniscus Implantation in Stable Knees," Knee Surg. Sports Traumatol. Arthrosc., 28(4), pp. 1099–1104.

[31] Zaffagnini, S., Grassi, A., Marcheggiani Muccioli, G. M., Holsten, D., Bulgheroni, P., Monllau, J. C., Berbig, R., Lagae, K., Crespo, R., and Marcacci, M., 2015, "Two-Year Clinical Results of Lateral Collagen Meniscus Implant: A Multicenter Study," Arthroscopy, 31(7), pp. 1269–1278.

[32] Zaffagnini, S., Marcheggiani Muccioli, G. M., Lopomo, N., Bruni, D., Giordano, G., Ravazzolo, G., Molinari, M., and Marcacci, M., 2011, “Prospective Long-Term Outcomes of the Medial Collagen Meniscus Implant versus Partial Medial Meniscectomy: A Minimum 10-Year Follow-up Study,” Am. J. Sports Med., 39(5), pp. 977–985.

[33] Verdonk, R., Verdonk, P., Huysse, W., Forsyth, R., and Heinrichs, E. L., 2011, “Tissue Ingrowth after Implantation of a Novel, Biodegradable Polyurethane Scaffold for Treatment of Partial Meniscal Lesions,” Am. J. Sports Med., 39(4), pp. 774–782.

[34] Van Minnen, B., Van Leeuwen, M. B. M., Kors, G., Zuidema, J., Van Kooten, T. G., and Bos, R. R. M., 2008, “In Vivo Resorption of a Biodegradable Polyurethane Foam, Based on 1,4-Butanediisocyanate: A Three-Year Subcutaneous Implantation Study,” J. Biomed. Mater. Res. A, 85(4), pp. 972–982.

[35] Sandmann, G. H., Adamczyk, C., Grande Garcia, E., Doebele, S., Buettner, A., Milz, S., Imhoff, A. B., Vogt, S., Burgkart, R., and Tischer, T., 2013, “Biomechanical Comparison of Menisci from Different Species and Artificial Constructs,” BMC Musculoskelet. Disord., 14.

[36] Welsing, R. T. C., Van Tienen, T. G., Ramrattan, N., Heijkants, R., Schouten, A. J., Veth, R. P. H., and Buma, P., 2008, “Effect on Tissue Differentiation and Articular Cartilage Degradation of a Polymer Meniscus Implant: A 2-Year Follow-up Study in Dogs,” Am. J. Sports Med., 36(10), pp. 1978–1989.

[37] Reale, D., Previtali, D., Andriolo, L., Grassi, A., Candrian, C., Zaffagnini, S., and Filardo, G., 2022, “No Differences in Clinical Outcome between CMI and Actifit Meniscal

Scaffolds: A Systematic Review and Meta-Analysis," Knee Surg. Sports Traumatol. Arthrosc., 30(1), pp. 328–348.

[38] Shemesh, M., Shefy-Peleg, A., Levy, A., Shabshin, N., Condello, V., Arbel, R., and Gefen, A., 2020, "Effects of a Novel Medial Meniscus Implant on the Knee Compartments: Imaging and Biomechanical Aspects," Biomech. Model. Mechanobiol., 19(6), pp. 2049–2059.

[39] McKeon, B. P., Zaslav, K. R., Alfred, R. H., Alley, R. M., Edelson, R. H., Gersoff, W. K., Greenleaf, J. E., and Kaeding, C. C., 2020, "Preliminary Results From a US Clinical Trial of a Novel Synthetic Meniscal Implant," Orthop. J. Sport. Med., 8(9).

[40] Zaslav, K. R., Farr, J., Alfred, R., Alley, R. M., Dyle, M., Gomoll, A. H., Lattermann, C., McKeon, B. P., Kaeding, C. C., Giel, T., and Hershman, E. B., 2021, "Treatment of Post-Meniscectomy Knee Symptoms with Medial Meniscus Replacement Results in Greater Pain Reduction and Functional Improvement than Non-Surgical Care," Knee Surg. Sports Traumatol. Arthrosc.

[41] Whitehouse, M. R., Howells, N. R., Parry, M. C., Austin, E., Kafienah, W., Brady, K., Goodship, A. E., Eldridge, J. D., Blom, A. W., and Hollander, A. P., 2017, "Repair of Torn Avascular Meniscal Cartilage Using Undifferentiated Autologous Mesenchymal Stem Cells: From In Vitro Optimization to a First-in-Human Study," Stem Cells Transl. Med., 6(4), pp. 1237–1248.

[42] Vangsness, C. T., Farr, J., Boyd, J., Dellaero, D. T., Mills, C. R., and LeRoux-Williams, M., 2014, "Adult Human Mesenchymal Stem Cells Delivered via Intra-Articular

Injection to the Knee Following Partial Medial Meniscectomy," J. Bone Jt. Surgery-American Vol., 96(2), pp. 90–98.

[43] Zhang, Z. Z., Chen, Y. R., Wang, S. J., Zhao, F., Wang, X. G., Yang, F., Shi, J. J., Ge, Z. G., Ding, W. Y., Yang, Y. C., Zou, T. Q., Zhang, J. Y., Yu, J. K., and Jiang, D., 2019, "Orchestrated Biomechanical, Structural, and Biochemical Stimuli for Engineering Anisotropic Meniscus," Sci. Transl. Med., 11(487).

[44] Filardo, G., Petretta, M., Cavallo, C., Roseti, L., Durante, S., Albisinni, U., and Grigolo, B., 2019, "Patient-Specific Meniscus Prototype Based on 3D Bioprinting of Human Cell-Laden Scaffold," Bone Joint Res., 8(2), p. 101.

[45] Bandyopadhyay, A., and Mandal, B. B., 2019, "A Three-Dimensional Printed Silk-Based Biomimetic Tri-Layered Meniscus for Potential Patient-Specific Implantation," Biofabrication, 12(1).

[46] Gonzalez-Leon, E. A., Bielajew, B. J., Hu, J. C., and Athanasiou, K. A., 2020, "Engineering Self-Assembled Neomenisci through Combination of Matrix Augmentation and Directional Remodeling," Acta Biomater., 109, pp. 73–81.

[47] Huey, D. J., and Athanasiou, K. A., 2011, "Tension-Compression Loading with Chemical Stimulation Results in Additive Increases to Functional Properties of Anatomic Meniscal Constructs," PLoS One, 6(11), pp. 1–9.

Chapter 3: Engineering self-assembled neomenisci through combination of matrix augmentation and directional remodeling

Abstract

Knee meniscus injury is frequent, resulting in over 1 million surgeries annually in the United States and Europe. Because of the near-avascularity of this fibrocartilaginous tissue and its intrinsic lack of healing, tissue engineering has been proposed as a solution for meniscus repair and replacement. This study describes an approach employing bioactive stimuli to enhance both extracellular matrix content and organization of neomenisci toward augmenting their mechanical properties. Self-assembled fibrocartilages were treated with TGF-β1, chondroitinase ABC, and lysyl oxidase-like 2 (collectively termed TCL) in addition to lysophosphatidic acid (LPA). TCL+LPA treatment synergistically improved circumferential tensile stiffness and strength, significantly enhanced collagen and pyridinoline crosslink content per dry weight, and achieved tensile anisotropy (circumferential/radial) values of neomenisci close to 4. This study utilizes a combination of bioactive stimuli for use in tissue engineering studies, providing a promising path toward deploying these neomenisci as functional repair and replacement tissues.

Published as: Gonzalez-Leon, EA, Bielajew, BJ, Hu, JC, & Athanasiou, KA. *Engineering self-assembled neomenisci through combination of matrix augmentation and directional remodeling.* Acta Biomaterialia (2020)

3.1. Introduction

Fibrocartilage is found in the knee meniscus, temporomandibular joint disc, pubic symphysis, annulus fibrosus of intervertebral discs, tendons, and ligaments. Damage to these tissues is common and can result in persistent pain while impeding daily activity. The knee meniscus is a wedge-shaped, semi-circular fibrocartilaginous tissue that is situated between the distal femur and tibial plateau; the meniscus protects articular cartilage via load distribution. Injury to the meniscus is responsible for approximately 1 million surgeries annually in the U.S. and Europe, making it the most common orthopedic surgical procedure [1].

Meniscal function arises from collagen content, crosslinks, and organization. Under compressive load, menisci function by using their wedge shape to develop tension, which is resisted by circumferentially aligned collagen. The surface of the meniscus tissue exhibits random collagen alignment, while its middle depths show circumferentially aligned collagen fibers supported by tie fibers in the radial direction [2,3]. Pyridinoline, a trivalent crosslink of collagen fibrils, contributes to mechanical properties of the knee meniscus [4] and has been shown to strongly correlate with tensile properties of various collagenous tissues [5,6]. Collagen content, crosslinking, and organization are, thus, critical to the tensile properties of menisci and their function.

The knee meniscus exhibits a gradient of healing capacity which decreases from its outer, fibrous portion toward the inner portion, which is more akin to hyaline articular cartilage and lacks vascularization [7]. Injuries may lead to surgery such as meniscectomy, i.e., tissue resection, especially if the injury is in the inner portion of the tissue, which can temporarily alleviate pain symptoms but is virtually guaranteed to result in osteoarthritis of the knee joint [8]. This lack of intrinsic healing properties makes the

knee meniscus a prime candidate for repair or replacement via tissue engineering methods.

Both scaffold and scaffold-free strategies for tissue engineering the knee meniscus have been investigated. A scaffold-free method known as the self-assembling process has emerged for forming neotissue rings [9–14] while resolving issues that may result from scaffold use such as stress shielding and scaffold degradation byproducts [15]. The self-assembling process depends on both integrin-matrix binding and cell-to-cell communication via cadherin binding [16], resulting in a sequence of extracellular matrix (ECM) accumulation that is reminiscent to the sequence seen for native cartilage [17]. The neotissue rings are then cut into two meniscus-shaped constructs (termed "neomenisci") that resemble the morphology of the native leporine knee meniscus. Mechanical properties are directly related to ECM content and organization and, as such, our group has utilized bioactive agents during culture to enhance these biochemical features and create self-assembled fibrocartilage with compressive properties that reach levels seen in native tissue [18]. However, tensile mechanical properties of neomenisci are still lacking, especially in the circumferential direction. Tensile properties still require improvement before these engineered tissues can be deployed as functional repair or replacement alternatives; as such, this study aims to improve tensile properties of engineered neomenisci through the addition of bioactive stimuli during *in vitro* culture.

Bioactive stimuli have frequently been used to augment ECM content, leading to enhanced mechanical properties. Growth factors such as TGF-β1 [14,18–20], TGF-β3 [21–23], CTGF [23], PDGF [24–26], bFGF [24,27,28], IGF-1 [24,25,27–30], and EGF [25,26] have shown efficacy toward enhancing tissue engineered fibrocartilage formation.

In addition, our group has previously used anabolic growth factor TGF-β1 to enhance ECM production, glycosaminoglycan (GAG)-cleaving enzyme chondroitinase ABC (C-ABC) to temporarily remove GAG, and collagen crosslinking enzyme lysyl oxidase-like 2 (LOXL2) to increase collagen crosslinking. These bioactive agents have been used alone or in combination to enhance mechanical properties of cartilaginous and fibrocartilaginous tissues [13,18,19,31,32]. A treatment based on this cocktail of bioactive agents (collectively termed TCL) results in matrix augmentation contributing to more robust engineered tissues.

Less frequent than the use of bioactive stimuli are strategies to induce or to accentuate ECM organization of engineered neomenisci, resulting in anisotropy. An example is lysophosphatidic acid (LPA), a phospholipid mediator that induces contractions in fibroblasts [33], which has been used to induce contraction of collagen matrices seeded with fibroblasts or myofibroblasts [34–36]. In addition to inducing contraction in fibroblasts, LPA has also been shown to be an anti-apoptotic and pro-survival factor in both fibroblasts [37] and chondrocytes [38]. Because we have observed that meniscal fibrochondrocytes seeded in a ring-shaped mold create circumferential hoop stress [9], we have used LPA in the past to enhance this hoop stress and, thus, circumferential ECM organization, by accentuating cellular traction forces that give rise to hoop stresses [10]. Thus, while self-assembled neomenisci already exhibit anisotropic tensile properties, indicating a certain degree of collagen alignment, cytoskeletal contraction induced by LPA enhances this anisotropy by increasing collagen organization.

Because TCL and LPA do not have overlapping functions, their use in combination may act synergistically toward bolstering tissue properties. Matrix augmentation has been

observed in self-assembled cartilaginous tissues when applying TCL treatment, while LPA has induced directional remodeling in self-assembled neomenisci to enhance organization and anisotropy. The objective of this study was to increase the tensile properties of self-assembled neomeniscus constructs in an anisotropic fashion by combining TCL with LPA to increase and to remodel ECM content. Neomenisci were cultured for 5 weeks and treated with TCL and LPA alone or in combination. Unstimulated neomenisci served as controls. It was hypothesized that 1) treatment of constructs with TCL and LPA would lead to a synergistic increase in tensile properties, 2) an increase in tensile properties would be accompanied by an increase in the amount of pyridinoline collagen crosslinks, and 3) TCL+LPA treatment would produce neomenisci with anisotropic tensile mechanical properties.

3.2. Materials and methods

3.2.1 Chondrocyte and meniscus cell isolation

Primary bovine articular chondrocytes and meniscus cells were isolated from juvenile bovine knee joints (Research 87). Articular cartilage resected from the distal femur was minced and digested in 0.2% collagenase type II (Worthington) for 18 hours at 37°C. Meniscus tissue was isolated from the knee joint and digested as previously described [10]. Briefly, the outer rim was removed, and remaining meniscus tissue was minced and digested in 0.25% pronase (Sigma-Aldrich) for 2 hours followed by 0.2% collagenase type II for 18 hours. After isolation, cells were frozen at -80°C for 24 hours in Dulbecco's modified Eagle's medium (DMEM) supplemented with 20% fetal bovine serum and 10% dimethyl sulfoxide medium at 30 million cells per milliliter and stored in liquid nitrogen until seeding.

3.2.2 Self-assembly and culture of constructs

Non-adherent agarose wells in the shape of the native leporine meniscus were prepared as previously described [10–12]. Wells were saturated for five days prior to seeding with serum-free chondrogenic medium and throughout culture. Chondrogenic medium consists of: DMEM with GlutaMAX (Gibco, Grand Island, NY, USA); 1% nonessential amino acids (Gibco); 1% insulin, human transferrin, and selenous acid (ITS+; BD Biosciences, San Jose, CA, USA); 1% penicillin-streptomycin-fungizone (Lonza BioWhittaker, Walkersville, MD, USA); 3.5 nM dexamethasone (Sigma-Aldrich, St. Louis, MO, USA); 50 µg/mL ascorbate-2-phosphate (Sigma-Aldrich); 100 µg/mL sodium pyruvate (Sigma-Aldrich) and 40 µg/mL L-proline (Sigma-Aldrich). A 1:1 co-culture of primary articular chondrocytes and meniscal cells was seeded at a density of 20 million total cells per 180 µL as previously described [39]. An additional 2 mL of media was added 4 hours after construct seeding, and all medium was changed daily. Constructs were removed from the agarose wells after 7 days and kept in culture, during which medium was changed every other day (5 mL).

3.2.3 Treatments

Neomenisci treatment groups were as follows: 1) unstimulated controls, 2) LPA only, 3) TCL only, 4) TCL+LPA. TCL groups were treated with the combination of 1) TGF-β1 continuously throughout culture at 10 ng/mL, 2) a one-time C-ABC treatment, added to medium with a 0.05 M sodium acetate activator, at day 7 of culture at 2 U/mL for a duration of 4 hours, and 3) LOXL2 applied continuously from days 7-21 (weeks 2-3) at 0.15 ng/mL as previously described [19,32,40]. Neomenisci that were treated with LPA (Enzo Life Sciences) were stimulated during days 21-28 (week 4) at a final concentration of 10 µM

as previously described [10]. All constructs were cultured for 5 weeks at 37°C and 5% CO_2.

3.2.4 Tissue gross morphology, histology, and macroscopic characterization

At day 35, neomenisci were removed from culture, photographed, and measured using ImageJ (NIH). Wet weights were measured before resecting pieces for mechanical testing, biochemical analysis, and histology. For histology, construct samples were fixed in 10% neutral buffered formalin then embedded in paraffin and sectioned at 5μm. Safranin O/Fast Green, Picrosirius Red, and hematoxylin and eosin (H&E) stains were conducted to visualize GAG, collagen, and cell distributions, respectively. Collagen fiber alignment of samples was examined using second-harmonic generation (SHG) imaging microscopy (Zeiss, Jena, Germany). The acquisition of SHG images was conducted using an excitation wavelength of 800 nm and a 20x objective.

3.2.5 Tensile and compressive testing

Tensile properties were assessed using uniaxial, strain-to-failure testing. Using custom-made jigs, samples were cut to a depth of 1.0 mm and gauge length of 0.95 mm and 0.40 mm for circumferential and radial tensile samples, respectively. Samples were then photographed, cut into dog-bone shapes, measured with ImageJ, and adhered to paper strips with cyanoacrylate glue at their ends to ensure that a glue bridge would not form across the gauge length. Samples were then clamped within a uniaxial testing machine (Instron model 5565) and subjected to a 1% s^{-1} strain rate until failure. Young's modulus (E_Y) was calculated from the linear portion of the stress-strain curve, and ultimate tensile strength (UTS) was calculated from the maximum stress (Supplementary Figure 1.1).

Compressive properties were assessed using unconfined stress-relaxation testing, with a non-porous, stainless steel platen larger in diameter than the tissue sample. Punches measuring 2-3 mm in diameter were resected from neomenisci. Sample thickness was determined via a custom program on the testing machine (Instron model 5565). Samples were subjected to stress relaxation via a 20% step-strain while submerged in a PBS bath. Viscoelastic properties such as instantaneous modulus (E_I), relaxation modulus (E_R), and coefficient of viscosity (μ) were calculated by fitting data curves to a standard Kelvin solid model [41].

3.2.6 Analysis of tissue biochemical content

Biochemistry samples were weighed wet, then frozen and lyophilized to acquire dry weights. DNA content was calculated with the use of PicoGreen dsDNA reagent (Invitrogen), assuming a conversion factor of 7.7 pg DNA/cell. Collagen content was measured with the use of a Sircol standard (Biocolor) and a Chloramine-T colorimetric hydroxyproline assay [42]. GAG content was quantified using the Blyscan assay kit (Invitrogen). All quantification measurements for DNA, GAG, and collagen content were performed with a GENios spectrophotometer/spectrofluorometer (TECAN).

Quantification of pyridinoline crosslink content was performed via a liquid chromatography mass spectrometry (LC-MS) assay [43]. Lyophilized samples were hydrolyzed in 6N HCl at 105°C for 18 hours, then acid was evaporated by SpeedVac (Labconco). Dried hydrolysates were resuspended in 25% (v/v) acetonitrile and 0.1% (v/v) formic acid in water, centrifuged at 15,000g for 5 min, and the supernatant was transferred to a LCMS autosampler vial. Liquid chromatography was carried out on a Cogent Diagmond Hydride HPLC Column (2.1 mm x 150 mm, particle size 2.2 μm, pore size 120

Å, MicroSolv). The elution gradient used 0.1% (v/v) formic acid in water as solvent A, and 100% acetonitrile as solvent B. The 5-minute elution gradient ran at 300 µL/min as follows: 0 min 25% B, 2 min 25% B, 2.2 min 5% B, 3 min 25% B. Mass spectrometry was performed on a Quadrupole Mass Detector (ACQUITY QDa, Waters) in ESI+ MS scan mode. The quadrupole range was set to 150 - 450 m/z with cone voltage 12.5 V. MassLynx software version 4.1 with TargetLynx was used to quantify pyridinoline in 10 µL injections of neomeniscus hydrolysate by integrating the extracted ion chromatogram of double-charged pyridinoline (m/z=215.1) into a standard curve of serially diluted pyridinoline standard (BOC Sciences). The standard curve contained 6 standards and was linear with $R^2 > 0.999$ on a range of 1,000 to 4.115 pg/µL pyridinoline.

3.2.7 Statistical analysis

For each biomechanical and biochemical test, n=6-7 samples were used. Results were analyzed with single-factor analysis of variance (ANOVA) followed by a Tukey's HSD post hoc test when merited ($p<0.05$). TCL and LPA effect on anisotropy was analyzed with two-factor ANOVA followed by a Tukey's HSD post hoc test when merited ($p<0.05$). All data are presented as means ± standard deviations. For all figures, statistical significance is indicated by groups not sharing the same letters.

3.3. Results

3.3.1 Gross morphology, histology, and immunohistochemistry

Neomenisci resembled native meniscus fibrocartilage [44,45] in terms of gross appearance (Figure 3.1) [45–47]. The characteristic wedge-shaped profile was maintained after 5 weeks of culture (Supplementary Figure 3.2). Morphologically, TCL and TCL+LPA treated groups were significantly smaller ($p<0.0005$) than controls and

constructs treated with LPA alone in terms of outer major and minor diameters, inner minor diameter, and height (Table 3.1). TCL+LPA was significantly smaller in terms of inner major diameter when compared to all other groups (p=0.03). Both outer (p=0.04) and inner (p=0.007) aspect ratios (defined as major diameter/minor diameter) were also significantly higher in TCL+LPA treated neomenisci when compared to controls. Wet weights were significantly different among groups, with TCL and TCL+LPA groups both weighing significantly less (p<0.0001) than controls and LPA treated groups (Table 3.1). Hydration percentages were also significantly lower (p<0.0001) in TCL and TCL+LPA treated groups when compared to control and LPA-only groups (Table 3.1). Dry weights for TCL and TCL+LPA groups, in turn, were significantly lower than control and LPA-treated constructs.

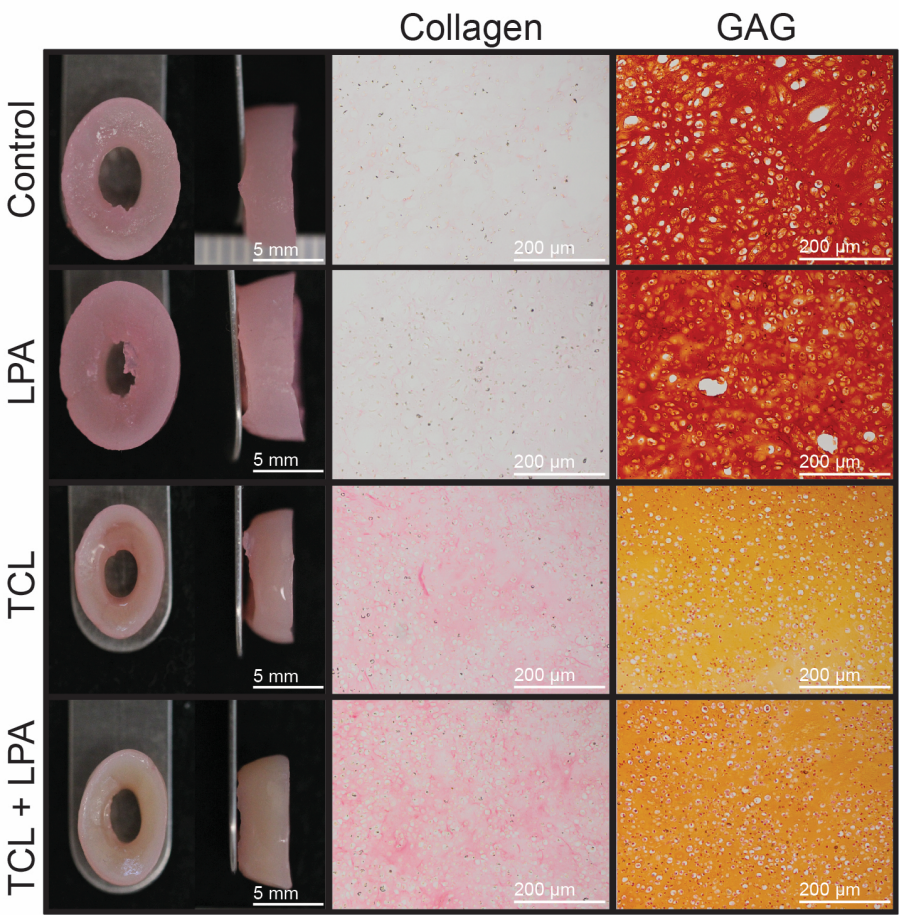

Figure 3.1: Gross morphology and histological staining of self-assembled neomenisci. Tissue engineered constructs retained the characteristic wedge-shape of the native knee meniscus during and after culture. Slight contraction occurred in TCL+LPA groups when compared to controls. Collagen staining of TCL+LPA treated constructs appeared more intense than that of control constructs, while GAG staining in the TCL and TCL+LPA groups was less intense than controls.

Table 3.1: Morphological properties of neomenisci. Values marked with different letters within each category are significantly different ($p<0.05$), n=7 per group.

Group	Wet Weight (mg)	Dry Weight (mg)	Hydration (%)	Cells/ construct (millions)	Outer Major Diameter (mm)	Outer Minor Diameter (mm)	Inner Major Diameter (mm)	Inner Minor Diameter (mm)	Outer Aspect Ratio	Inner Aspect Ratio	Height (mm)
Control	207 ± 8^{C}	25 ± 1^{B}	88 ± 0^{B}	13 ± 4	11 ± 0^{B}	8 ± 0^{B}	4 ± 0^{B}	3 ± 0^{B}	1 ± 0^{B}	1 ± 0^{B}	4 ± 0^{B}
LPA	224 ± 10^{B}	25 ± 2^{B}	89 ± 1^{B}	15 ± 4	11 ± 0^{B}	8 ± 0^{B}	4 ± 0^{B}	2 ± 0^{B}	1 ± 0^{B}	2 ± 0^{AB}	4 ± 0^{B}
TCL	89 ± 5^{A}	15 ± 1^{A}	83 ± 1^{A}	15 ± 1	9 ± 1^{A}	6 ± 0^{A}	3 ± 0^{B}	2 ± 0^{A}	1 ± 0^{AB}	2 ± 0^{AB}	3 ± 0^{A}
TCL+LPA	91 ± 5^{A}	15 ± 1^{A}	83 ± 1^{A}	16 ± 1	9 ± 0^{A}	6 ± 1^{A}	3 ± 0^{A}	2 ± 0^{A}	2 ± 0^{A}	2 ± 0^{A}	3 ± 0^{A}

3.3.2 Tissue biomechanics

Biomechanical data revealed a significant difference among control and treated constructs, especially those that were treated with TCL+LPA (Figure 3.2). Application of TCL+LPA resulted in increased tensile properties over both unstimulated control and LPA treatment groups. Circumferential Young's modulus and ultimate tensile strength (UTS) were highest ($p<0.0001$) in TCL+LPA treated groups (Figure 3.2A, 3.2B). TCL+LPA

treated constructs increased circumferential Young's modulus and UTS to 221% and 218% higher than control values, respectively. In addition, TCL+LPA treated constructs displayed increases to the radial Young's modulus (p=0.03) and UTS (p=0.001) of 152% and 239% over controls, respectively (Figure 3.2C, 3.2D).

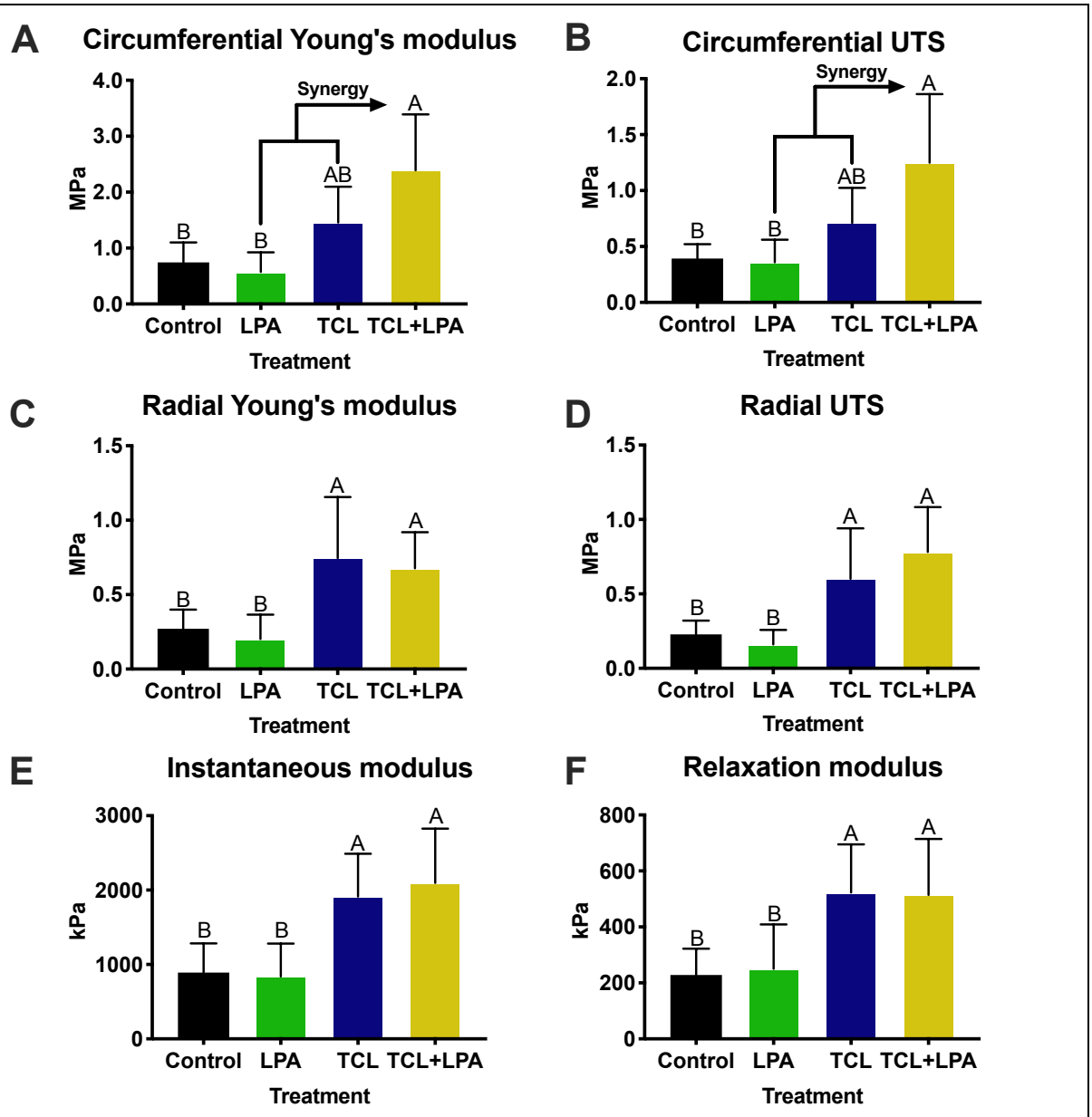

Figure 2: Mechanical properties of neomenisci. TCL+LPA synergistically increased circumferential tensile properties over controls. TCL+LPA and TCL treatments both

increased radial tensile properties and compressive properties over controls and LPA only groups. All data are presented as means ± standard deviations. For all figures, statistical significance is indicated by bars not sharing the same letters.

In addition to increases in tensile properties, compressive properties also were significantly higher in constructs treated with TCL+LPA when compared to non-treated controls. When quantifying compressive properties, TCL+LPA stimulated constructs yielded increases over controls in the instantaneous modulus (p=0.003) and relaxation modulus (p=0.02), by 135% and 125%, respectively (Figure 3.2E, 3.2F). TCL treatment also significantly increased (p=0.01) compressive properties over controls. No significant differences in coefficient of viscosity were seen among treatment groups (Supplementary Figure 3.3).

3.3.3 Tissue biochemistry

Biochemical treatment led to significant increases in collagen content and pyridinoline crosslink content (Figure 3.3A, 3.3C). TCL+LPA treatment enhanced (p<0.0001) collagen and pyridinoline content per wet weight by 125% and 185% over control values, respectively (Supplementary Figure 3.4A, 3.4B). There were no significant differences in GAG content per wet weight among treatment groups (Supplementary Figure 3.4C). Collagen and pyridinoline content normalized by dry weight also showed increases (p<0.003) over controls when treating with TCL+LPA, by 61% and 81% of control values, respectively. However, there were no significant differences among groups in terms of pyridinoline normalized to collagen content (Figure 3.3D). GAG content normalized to dry weight was significantly lower (p<0.0001) for TCL+LPA treated constructs (by 39% of controls). TCL treatment also significantly decreased (p<0.0001) GAG content per dry

weight when compared to control groups (Figure 3.3B). There were no significant differences in DNA content among groups (Table 3.1).

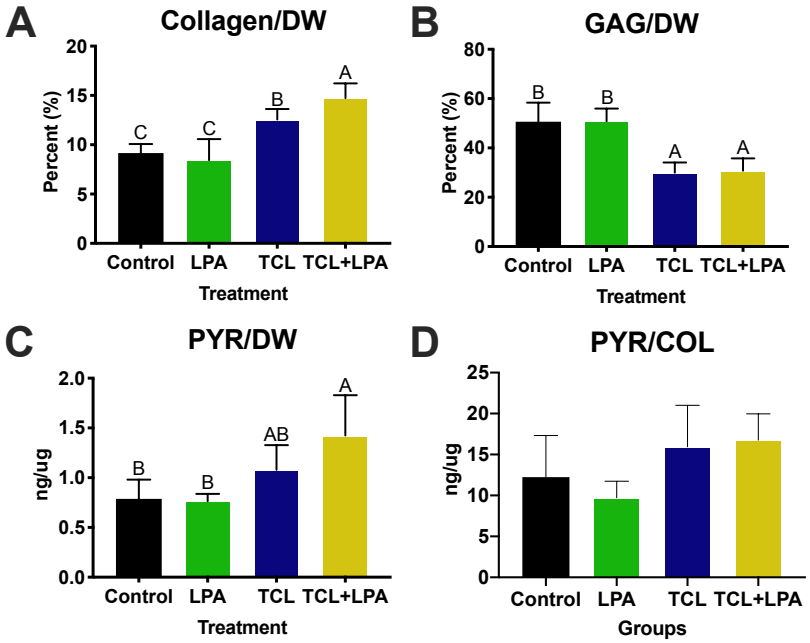

Figure 3.3: Biochemical properties of self-assembled neomenisci. TCL+LPA treatment enhanced collagen content over all other groups. GAG content was lowered closer to native tissue values in TCL+LPA and TCL groups. Pyridinoline crosslink content in TCL+LPA treated constructs increased over controls, while there were no differences among groups in pyridinoline crosslink content normalized to collagen content.

3.3.4 Tissue organization

Two-way ANOVA tests were conducted to examine the effect of TCL and LPA treatments on anisotropy of tensile properties, namely, tensile Young's modulus and UTS (Figure 3.4A, 3.4B). These tests showed that LPA treatment significantly increased (p=0.02) anisotropy, as indicated by differences of the Young's modulus values in the circumferential versus the radial directions, while TCL significantly decreased (p=0.02)

UTS anisotropy. Anisotropy ratios of tensile properties (circumferential/radial values) reached as high as 4-fold with TCL+LPA treatment. In addition, SHG signals in LPA (Supplementary Figure 3.5B) and TCL+LPA (Supplementary Figure 3.5D) treated groups appeared more intense than those of control and TCL treatment groups.

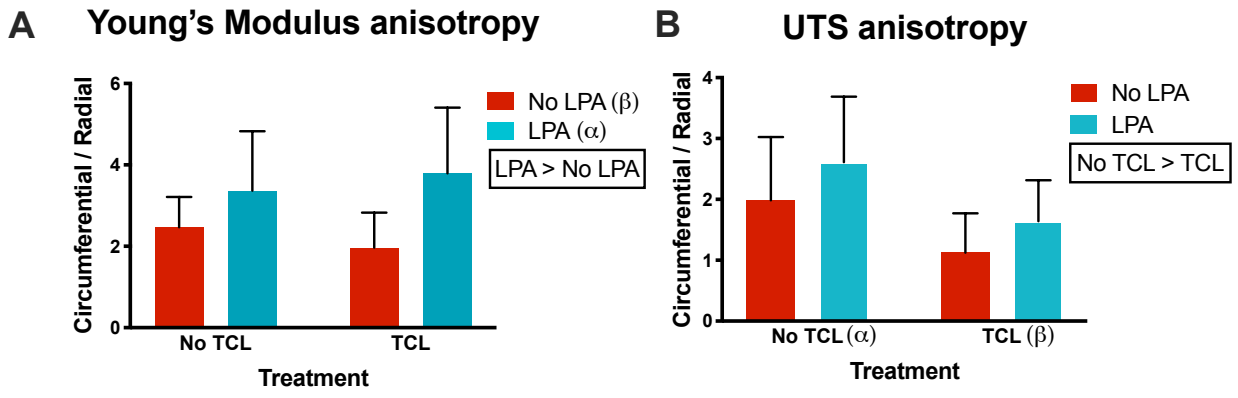

Figure 3.4: TCL+LPA treatment enhances anisotropy. Two-way analysis of variance shows LPA treatment significantly contributed to increases in Young's modulus anisotropy, while TCL significantly contributed to decreases in UTS anisotropy. Tukey's post hoc showed that none of the groups differed from one another (i.e., there were no statistical differences among the bars). Control groups are represented by the "No TCL" and "No LPA" bar. The alpha and beta represent statistical significance between treatment levels; treatments without these symbols indicate no significant differences between levels.

3.4. Discussion

Building upon prior work that showed increases in mechanical properties of self-assembled fibrocartilage treated with TCL [18] and directionality imparted by LPA in neomenisci [10], this study sought to promote matrix augmentation and directional remodeling in order to enhance tensile properties. Experimental results supported the

three hypotheses underlying this study, namely: 1) TCL+LPA treatment would enhance the tensile properties of self-assembling neomenisci, 2) these increases in tensile properties would be accompanied by an increase in the amount of pyridinoline collagen crosslinks, and 3) TCL+LPA treatment would produce neomenisci with anisotropic tensile mechanical properties. To the best of our knowledge, this is the first study to use a treatment that both augments matrix content of engineered neomenisci and utilizes a soluble factor to enhance matrix organization and anisotropy. This study demonstrates the combination of matrix augmentation and directional remodeling as a beneficial strategy in tissue engineering of the knee meniscus.

The knee meniscus functions by developing tension when under compressive load, highlighting the importance of attaining tensile properties akin to native tissue in engineered neomenisci. It was found that TCL+LPA treatment resulted in synergistic enhancements to tensile properties of engineered neomenisci, increasing circumferential stiffness and strength by more than 2-fold. In addition, radial stiffness and strength were also increased by more than 1.5- and 2-fold, respectively. Values for tensile strength and stiffness in the circumferential direction were approximately 4-fold higher when compared to values from neomenisci in a study by our group that were treated with only LPA [10]. Also, tissue circumferential tensile properties were on par with those of self-assembled neomenisci that used both biochemical and mechanical stimulation to enhance matrix content organization [13]. However, circumferential tensile modulus values in neomenisci treated with TCL+LPA still fall short of native tissue values (100-300 MPa) [48], denoting the importance of research that aims to enhance this mechanical property that is crucial to meniscus function. In the radial direction, tensile strength and stiffness were

approximately one-tenth of values derived from native tissue (10-30 MPa) [48,49], respectively. Increasing tensile properties of engineered neomenisci is a critical step toward deploying them as functional tissues *in vivo*; ultimately, TCL+LPA treatment was effective in elevating tissue tensile properties, which results from its positive effects on matrix content and organization.

In addition to TCL+LPA treatment having beneficial increases to tensile properties, an accompanying increase in collagen content was also seen over all other groups (Figure 3.3). The significant difference in collagen content between TCL+LPA and TCL groups likely stems from the addition of LPA, which has been shown to increase collagen deposition in engineered tissue [50]. Overall, collagen per dry weight in TCL+LPA groups reached values approximately 2-fold greater than those reported for self-assembled neomenisci treated with only LPA [10]. After being able to increase collagen content, it would be important to increase the degree of crosslinking and fiber organization to improve tensile properties. The TCL+LPA treatment used by this study provides a firm foundation for crosslinks by increasing collagen content closer to that of the native meniscus, in agreement with increases in tensile properties. The native meniscus contains mostly collagen types I and II, with some minor collagens such as types III, IV, VI, and XVIII [44]. While the hydroxyproline assay only measures overall collagen, without discriminating individual collagen types, self-assembled neomenisci have been shown to contain both collagens I and II via IHC [9]. Other self-assembled fibrocartilages have also been shown to contain different ratios of collagen types I and II [51], and future work on self-assembled neomenisci may include methods to better determine the similarities and

differences between different collagen types of native menisci and self-assembled neomenisci.

A significant increase to pyridinoline crosslink content over controls was seen in TCL+LPA treated constructs, which follows previous results seen when applying LOXL2 in self-assembled fibrocartilage [18]. This significant increase in crosslinking was observed in conjunction with significant increases in collagen content, indicating that collagen maturation and crosslinking are occurring at the same rate. The TCL+LPA group contained 1.42 ng/μg pyridinoline per dry weight on average, which is on par with historical values for pyridinoline content of native fibrocartilages. For example, calculation using the pyridinoline per hydroxyproline and hydroxyproline per dry weight measurements of prior work [52] shows that human menisci have 1.16 ng/μg pyridinoline per dry weight. Similarly, human intervertebral discs have been reported to contain 1.10 ng/μg pyridinoline per dry weight [53]. It is worth noting that these prior studies used an HPLC fluorescence detection assay for pyridinoline quantification as opposed to the LC-MS technique used in this paper. Because LC-MS methods have repeatedly been shown to be more precise and accurate than HPLC fluorescence detection methods [54–56], future characterization studies on native fibrocartilage crosslinks using LC-MS would yield more comparable data to those collected by our study. Overall, TCL+LPA treated neomenisci exhibited crosslink content that appears to meet or exceed values reported in the literature, though characterization of native tissue via LC-MS methods is warranted.

The anisotropic organization of ECM within the meniscus, with circumferential tensile stiffness being approximately 10-fold that of the radial direction [49], is crucial to the tissue's function. In this study, we showed that LPA was significant toward enhancing

anisotropy, while TCL's robust matrix augmentation effect brought anisotropy ratios (circumferential/radial) closer to 1 (Figure 3.4). In addition, the SHG signal of TCL+LPA treated constructs appeared more intense than controls, indicating a higher degree of circumferentially aligned collagen fibers (Supplementary Figure 3.5). While this study utilized soluble bioactive agents to induce or enhance anisotropy, other methods to induce or enhance anisotropy within engineered menisci include mechanical stimuli via a bioreactor [13], scaffolds [57,58], or their use in combination [59]. While these methods have proven to be effective toward inducing anisotropy, LPA can be seen as a chemical analogue to these techniques that simplifies the tissue engineering process. For example, bioreactor manufacturing can become expensive and time-consuming; in addition, the use of scaffolds can result in harmful effects such as degradation byproducts or stress shielding of cells, further highlighting the benefits of using chemical analogues to achieve proper matrix organization in engineered tissues. Despite financial and temporal considerations, bioreactors that apply mechanical stimulation may further enhance matrix organization, and have previously led to increased tensile properties of self-assembled cartilage [32]. Without proper collagen fiber alignment, augmenting ECM content would likely not improve mechanical properties substantially, rendering the tissue unable to behave as it would in its native environment. Tissue engineering of the meniscus should focus on enhancing both mechanical and anisotropic properties to levels of native tissue. Thus, future work may examine the use of TCL+LPA treatment, in conjunction with additional bioactive factors or mechanical stimuli to increase ECM alignment and, consequently, tensile properties.

Interestingly, while the combination of TCL+LPA induced improvements of neomenisci tensile properties, the LPA only group did not differ mechanically or morphologically from the control group. This contradicts previous results shown when using LPA in the tissue engineering of self-assembled neomenisci [10]. No increases in tensile properties over controls in the LPA treatment group may have resulted due to the higher amounts of GAG in non-TCL treated tissues, which may have induced more swelling pressure and caused resistance to contraction by the collagen network. The use of C-ABC, which temporarily depletes GAG within the ECM and allows for more dense organization of collagen fibers [19], could have relieved this swelling pressure and allowed cell traction forces to align collagen fibers. In addition, this depletion of GAG due to C-ABC treatment likely contributed to lower wet weights and hydration percentages in TCL-treated groups, as negatively charged GAG attract water into the ECM [14]. Lower dry weights in groups treated with TCL may also likely stem from decreased GAG content as a result of C-ABC treatment. Also, despite morphological differences, a significant difference in circumferential tensile properties was not seen between TCL+LPA and TCL groups (p=0.06), although neomenisci treated with TCL+LPA trended higher. This trend may result from a significantly higher amount of collagen in the TCL+LPA group over TCL treated neomenisci, in addition to morphological differences that imply a degree of difference in organization.

Due to the prevalence and economic impact of meniscal injuries, creating engineered meniscal tissue that recapitulates native tissue properties is crucial for its successful translation from the benchtop to the clinic. Enhancements to mechanical, biochemical, and anisotropic tensile properties of neomenisci, induced by TCL+LPA

treatment, narrow the gap between native and engineered tissue properties and provide a promising path toward translation. While this study utilized bioactive agents to induce anisotropic tensile properties in neomenisci, other groups have utilized techniques such as 3D-printed scaffolds to replicate this property with the consideration of translation as the end goal [59]. In addition, as the native knee meniscus is zonally inhomogeneous, anisotropic engineered neomenisci with zonal variations have been created using the self-assembling process [60]. Since an entire neomeniscus might not be required for a repair procedure, a portion may be cut out to interface with native tissue to achieve a healing response. Investigation for this sort of engineered-native tissue interaction would require visualization of cell migration, likely through fluorescent tagging of chondrocytes and meniscal cells used to engineer self-assembled neomenisci. A previous study in which our group implanted tissue engineered constructs into fibrocartilage of the temporomandibular joint (TMJ) disc showed host cells infiltrating the implant [61]; due to the fibrocartilaginous nature and similarities between the knee meniscus and TMJ discs, we expect that a similar *in vivo* response may be seen when implanting neomenisci. Further *in vivo* work showing the safety and efficacy of engineered neomenisci toward repairing or replacing injured meniscal tissue, especially in large animal models, is required to navigate the Food and Drug Administration paradigm [62] and translate these tissues to the clinic.

3.5. Conclusions

This work demonstrates that treatment with TCL+LPA can augment and align the mechanical properties of engineered fibrocartilaginous tissues. Higher collagen and pyridinoline crosslink content accompanied a synergistic increase in tensile properties,

and anisotropic mechanical properties were observed in treated tissues. This work highlights the use of a combination of bioactive stimuli to achieve synergistic improvements in properties of engineered knee meniscus tissue. Future studies combining TCL+LPA with mechanical stimuli or additional bioactive agents to further enhance tensile properties of neomenisci are warranted to ensure functionality of these tissues *in vivo*.

References

[1] Salata, M. J., Gibbs, A. E., and Sekiya, J. K., 2010, "A Systematic Review of Clinical Outcomes in Patients Undergoing Meniscectomy," Am. J. Sports Med., 38(9), pp. 1907–1916.

[2] Petersen, W., and Tillmann, B., 1998, "Collagenous Fibril Texture of the Human Knee Joint Menisci," Anat. Embryol. (Berl)., 197(4), pp. 317–324.

[3] Andrews, S. H. J., Rattner, J. B., Abusara, Z., Adesida, A., Shrive, N. G., and Ronsky, J. L., 2014, "Tie-Fibre Structure and Organization in the Knee Menisci," J. Anat., 224(5), pp. 531–537.

[4] Eleswarapu, S. V., Responte, D. J., and Athanasiou, K. A., 2011, "Tensile Properties, Collagen Content, and Crosslinks in Connective Tissues of the Immature Knee Joint," PLoS One, 6(10), p. e26178.

[5] Williamson, A. K., Chen, A. C., Masuda, K., Thonar, E. J. M. A., and Sah, R. L., 2003, "Tensile Mechanical Properties of Bovine Articular Cartilage: Variations with Growth and Relationships to Collagen Network Components," J. Orthop. Res., 21(5), pp. 872–880.

[6] Chan, B. P., Fu, S. C., Qin, L., Rolf, C., and Chan, K. M., 1998, “Pyridinoline in Relation to Ultimate Stress of the Patellar Tendon during Healing: An Animal Study,” J. Orthop. Res., 16(5), pp. 597–603.

[7] Arnoczky, S. P., and Warren, R. F., 1982, “Microvasculature of the Human Meniscus,” Am. J. Sports Med., 10(2), pp. 90–95.

[8] Rangger, C., Kathrein, A., Klestil, T., and Glötzer, W., 1997, “Partial Meniscectomy and Osteoarthritis. Implications for Treatment of Athletes.,” Sports Med., 23(1), pp. 61–68.

[9] Aufderheide, A. C., and Athanasiou, K. A., 2007, “Assessment of a Bovine Co-Culture, Scaffold-Free Method for Growing Meniscus-Shaped Constructs,” Tissue Eng., 13(9), pp. 2195–2205.

[10] Hadidi, P., and Athanasiou, K. A., 2013, “Enhancing the Mechanical Properties of Engineered Tissue through Matrix Remodeling via the Signaling Phospholipid Lysophosphatidic Acid,” Biochem. Biophys. Res. Commun., 433(1), pp. 133–138.

[11] Hadidi, P., Yeh, T. C., Hu, J. C., and Athanasiou, K. A., 2015, “Critical Seeding Density Improves the Properties and Translatability of Self-Assembling Anatomically Shaped Knee Menisci,” Acta Biomater., 11(1), pp. 173–182.

[12] Hadidi, P., Paschos, N. K., Huang, B. J., Aryaei, A., Hu, J. C., and Athanasiou, K. A., 2016, “Tendon and Ligament as Novel Cell Sources for Engineering the Knee Meniscus,” Osteoarthr. Cartil., 24(12), pp. 2126–2134.

[13] Huey, D. J., and Athanasiou, K. A., 2011, “Tension-Compression Loading with Chemical Stimulation Results in Additive Increases to Functional Properties of Anatomic Meniscal Constructs,” PLoS One, 6(11), pp. 1–9.

[14] Huey, D. J., and Athanasiou, K. A., 2011, “Maturational Growth of Self-Assembled, Functional Menisci as a Result of TGF-B1 and Enzymatic Chondroitinase-ABC Stimulation,” Biomaterials, 32(8), pp. 2052–2058.

[15] Hu, J. C., and Athanasiou, K. A., 2006, “A Self-Assembling Process in Articular Cartilage Tissue Engineering,” Tissue Eng., 12(4), pp. 969–979.

[16] Lee, J. K., Hu, J. C. Y., Yamada, S., and Athanasiou, K. A., 2016, “Initiation of Chondrocyte Self-Assembly Requires an Intact Cytoskeletal Network,” Tissue Eng. Part A, 22(3–4), pp. 318–325.

[17] Ofek, G., Revell, C. M., Hu, J. C., Allison, D. D., Grande-Allen, K. J., and Athanasiou, K. A., 2008, “Matrix Development in Self-Assembly of Articular Cartilage,” PLoS One, 3(7).

[18] Makris, E. A., MacBarb, R. F., Paschos, N. K., Hu, J. C., and Athanasiou, K. A., 2014, “Combined Use of Chondroitinase-ABC, TGF-B1, and Collagen Crosslinking Agent Lysyl Oxidase to Engineer Functional Neotissues for Fibrocartilage Repair,” Biomaterials, 35(25), pp. 6787–6796.

[19] MacBarb, R. F., Makris, E. A., Hu, J. C., and Athanasiou, K. A., 2013, “A Chondroitinase-ABC and TGF-B1 Treatment Regimen for Enhancing the Mechanical Properties of Tissue-Engineered Fibrocartilage,” Acta Biomater., 9(1), pp. 4626–4634.

[20] Gunja, N. J., Uthamanthil, R. K., and Athanasiou, K. A., 2009, “Effects of TGF-B1 and Hydrostatic Pressure on Meniscus Cell-Seeded Scaffolds,” Biomaterials, 30(4), pp. 565–573.

[21] Allen, K. D., and Athanasiou, K. A., 2008, “Scaffold and Growth Factor Selection in Temporomandibular Joint Disc Engineering,” J. Dent. Res., 87(2), pp. 180–185.

[22] Wang, C.-H., Wang, S., Zhang, B., Zhang, X.-Y., Tong, X.-J., Peng, H.-M., Han, X.-Z., and Liu, C., 2018, “Layering Poly (Lactic-Co-Glycolic Acid)-Based Electrospun Membranes and Co-Culture Cell Sheets for Engineering Temporomandibular Joint Disc,” J. Biol. Regul. Homeost. Agents, 32(1), pp. 55–61.

[23] Legemate, K., Tarafder, S., Jun, Y., and Lee, C. H., 2016, “Engineering Human TMJ Discs with Protein-Releasing 3D-Printed Scaffolds,” J. Dent. Res., 95(7), pp. 800–807.

[24] Detamore, M. S., and Athanasiou, K. A., 2004, “Effects of Growth Factors on Temporomandibular Joint Disc Cells,” Arch. Oral Biol., 49(7), pp. 577–583.

[25] Johns, D. E., and Athanasiou, K. A., 2008, “Growth Factor Effects on Costal Chondrocytes for Tissue Engineering Fibrocartilage,” Cell Tissue Res., 333(3), pp. 439–447.

[26] Kasemkijwattana, C., Menetrey, J., Goto, H., Niyibizi, C., Fu, F. H., and Huard, J., 2000, “The Use of Growth Factors, Gene Therapy and Tissue Engineering to Improve Meniscal Healing,” Mater. Sci. Eng. C, 13(1–2), pp. 19–28.

[27] Detamore, M. S., and Athanasiou, K. A., 2005, “Evaluation of Three Growth Factors for TMJ Disc Tissue Engineering,” Ann. Biomed. Eng., 33(3), pp. 383–390.

[28] Almarza, A. J., and Athanasiou, K. A., 2006, “Evaluation of Three Growth Factors in Combinations of Two for Temporomandibular Joint Disc Tissue Engineering,” Arch. Oral Biol., 51(3), pp. 215–221.

[29] Kalpakci, K. N., Kim, E. J., and Athanasiou, K. A., 2011, “Assessment of Growth Factor Treatment on Fibrochondrocyte and Chondrocyte Co-Cultures for TMJ Fibrocartilage Engineering,” Acta Biomater., 7(4), pp. 1710–1718.

[30] Bhargava, M. M., Attia, E. T., Murrell, G. A. C., Dolan, M. M., Warren, R. F., and Hannafin, J. A., 1999, “The Effect of Cytokines on the Proliferation and Migration of Bovine Meniscal Cells,” Am. J. Sports Med., 27(5), pp. 636–643.

[31] Makris, E. A., MacBarb, R. F., Responte, D. J., Hu, J. C., and Athanasiou, K. A., 2013, “A Copper Sulfate and Hydroxylysine Treatment Regimen for Enhancing Collagen Cross-Linking and Biomechanical Properties in Engineered Neocartilage.,” FASEB J., 27(6), pp. 2421–30.

[32] Lee, J. K., Huwe, L. W., Paschos, N., Aryaei, A., Gegg, C. A., Hu, J. C., and Athanasiou, K. A., 2017, “Tension Stimulation Drives Tissue Formation in Scaffold-Free Systems,” Nat. Mater., 16(8), pp. 864–873.

[33] Grinnell, F., 2003, “Fibroblast Biology in Three-Dimensional Collagen Matrices,” Trends Cell Biol., 13(5), pp. 264–269.

[34] Abe, M., Ho, C. H., Kamm, K. E., and Grinnell, F., 2003, “Different Molecular Motors Mediate Platelet-Derived Growth Factor and Lysophosphatidic Acid-Stimulated Floating Collagen Matrix Contraction,” J. Biol. Chem., 278(48), pp. 47707–47712.

[35] Abe, M., Sogabe, Y., Syuto, T., Yokoyama, Y., and Ishikawa, O., 2007, “Evidence That PI3K, Rac, Rho, and Rho Kinase Are Involved in Basic Fibroblast Growth Factor-Stimulated Fibroblast-Collagen Matrix Contraction,” J. Cell. Biochem., 102(5), pp. 1290–1299.

[36] Parizi, M., Howard, E. W., and Tomasek, J. J., 2000, “Regulation of LPA-Promoted Myofibroblast Contraction: Role of Rho, Myosin Light Chain Kinase, and Myosin Light Chain Phosphatase,” Exp. Cell Res., 254(2), pp. 210–220.

[37] Tigyi, G., Dyer, D. L., and Miledi, R., 1994, “Lysophosphatidic Acid Possesses Dual Action in Cell Proliferation.,” Proc. Natl. Acad. Sci., 91(5), pp. 1908–1912.

[38] Hurst-Kennedy, J., Boyan, B. D., and Schwartz, Z., 2009, “Lysophosphatidic Acid Signaling Promotes Proliferation, Differentiation, and Cell Survival in Rat Growth Plate Chondrocytes,” Biochim. Biophys. Acta - Mol. Cell Res., 1793(5), pp. 836–846.

[39] Aufderheide, A. C., and Athanasiou, K. A., 2007, “Assessment of a Bovine Co-Culture, Scaffold-Free Method for Growing Meniscus-Shaped Constructs,” Tissue Eng., 13(9), pp. 2195–2205.

[40] Makris, E. A., Responte, D. J., Paschos, N. K., Hu, J. C., and Athanasiou, K. A., 2014, “Developing Functional Musculoskeletal Tissues through Hypoxia and Lysyl Oxidase-Induced Collagen Cross-Linking,” Proc. Natl. Acad. Sci., 111(45), pp. E4832–E4841.

[41] Allen, K. D., and Athanasiou, K. A., 2006, “Viscoelastic Characterization of the Porcine Temporomandibular Joint Disc under Unconfined Compression,” J. Biomech., 39(2), pp. 312–322.

[42] Cissell, D. D., Link, J. M., Hu, J. C., and Athanasiou, K. A., 2017, “A Modified Hydroxyproline Assay Based on Hydrochloric Acid in Ehrlich’s Solution Accurately Measures Tissue Collagen Content,” Tissue Eng. Part C Methods, 23(4), pp. 243–250.

[43] Naffa, R., Watanabe, S., Zhang, W., Maidment, C., Singh, P., Chamber, P., Matyska, M. T., and Pesek, J. J., 2019, “Rapid Analysis of Pyridinoline and Deoxypyridinoline in Biological Samples by Liquid Chromatography with Mass Spectrometry and a Silica Hydride Column,” J. Sep. Sci., 42(8), pp. 1482–1488.

[44] Makris, E. A., Hadidi, P., and Athanasiou, K. A., 2011, “The Knee Meniscus: Structure-Function, Pathophysiology, Current Repair Techniques, and Prospects for Regeneration,” Biomaterials, 32(30), pp. 7411–7431.

[45] Pauli, C., Grogan, S. P., Patil, S., Otsuki, S., Hasegawa, A., Koziol, J., Lotz, M. K., and D’Lima, D. D., 2011, “Macroscopic And Histopathologic Analysis Of Human Knee Menisci In Aging And Osteoarthritis,” Osteoarthr. Cartil., 19(9), pp. 1132–1141.

[46] Ribitsch, I., Peham, C., Ade, N., Dürr, J., Handschuh, S., Schramel, J. P., Vogl, C., Walles, H., Egerbacher, M., and Jenner, F., 2018, “Structure-Function Relationships of Equine Menisci,” PLoS One, 13(3), pp. 1–17.

[47] Nakagawa, K., Otsuki, S., Murakami, T., Okamoto, Y., Okuno, N., Wakama, H., Sezaki, S., Ikeda, K., Okayoshi, T., and Neo, M., 2019, “Histological Analysis of the Wrapping Treatment for Meniscal Horizontal Tears in Rabbits,” Cartilage.

[48] Fithian, D. C., Kelly, M. A., and Mow, V. C., 1990, “Material Properties and Structure-Function Relationships in the Menisci.,” Clin. Orthop. Relat. Res., (252), pp. 19–31.

[49] Tissakht, M., and Ahmed, A. M., 1995, “Tensile Stress-Strain Characteristics of the Human Meniscal Material,” J. Biomech., 28(4), pp. 411–422.

[50] Chabaud, S., Marcoux, T. L., Deschênes-Rompré, M. P., Rousseau, A., Morissette, A., Bouhout, S., Bernard, G., and Bolduc, S., 2015, “Lysophosphatidic Acid Enhances Collagen Deposition and Matrix Thickening in Engineered Tissue,” J. Tissue Eng. Regen. Med., 9(11), pp. E65–E75.

[51] Murphy, M. K., Masters, T. E., Hu, J. C., and Athanasiou, K. A., 2015, “Engineering a Fibrocartilage Spectrum through Modulation of Aggregate Redifferentiation,” Cell Transplant., 24(2), pp. 235–245.

[52] Takahashi, M., Suzuki, M., Kushida, K., Hoshino, H., and Inoue, T., 1998, “The Effect of Aging and Osteoarthritis on the Mature and Senescent Cross-Links of Collagen in Human Meniscus,” Arthrosc. - J. Arthrosc. Relat. Surg., 14(4), pp. 366–372.

[53] Tan, C. I., Neil Kent, G., Randall, A. G., Edmondston, S. J., and Singer, K. P., 2003, “Age-Related Changes in Collagen, Pyridinoline, and Deoxypyridinoline in Normal Human Thoracic Intervertebral Discs,” Journals Gerontol. Ser. A Biol. Sci. Med. Sci., 58(5), pp. B387–B393.

[54] Bandeira, R. D. da C. C., Uekane, T. M., da Cunha, C. P., Rodrigues, J. M., de la Cruz, M. H. C., de Oliveira Godoy, R. L., and Fioravante, A. de L., 2013, “Comparison of High Performance Liquid Chromatography with Fluorescence Detector and with Tandem Mass Spectrometry Methods for Detection and Quantification of Ochratoxin A in Green and Roasted Coffee Beans,” Brazilian Arch. Biol. Technol., 56(6), pp. 911–920.

[55] Wang, H., Walaszczyk, E. J., Li, K., Chung-Davidson, Y. W., and Li, W., 2012, “High-Performance Liquid Chromatography with Fluorescence Detection and Ultra-Performance Liquid Chromatography with Electrospray Tandem Mass Spectrometry Method for the Determination of Indoleamine Neurotransmitters and Their Metabolites in Sea Lamprey Pl,” Anal. Chim. Acta, 721, pp. 147–153.

[56] Milićević, D., Jurić, V., Stefanović, S., Baltić, T., and Janković, S., 2010, “Evaluation and Validation of Two Chromatographic Methods (HPLC-Fluorescence and

LC-MS/MS) for the Determination and Confirmation of Ochratoxin A in Pig Tissues," Arch. Environ. Contam. Toxicol., 58(4), pp. 1074–1081.

[57] Zhang, Z. Z., Jiang, D., Ding, J. X., Wang, S. J., Zhang, L., Zhang, J. Y., Qi, Y. S., Chen, X. S., and Yu, J. K., 2016, "Role of Scaffold Mean Pore Size in Meniscus Regeneration," Acta Biomater., 43, pp. 314–326.

[58] Baek, J., Sovani, S., Glembotski, N. E., Du, J., Jin, S., Grogan, S. P., and D'Lima, D. D., 2016, "Repair of Avascular Meniscus Tears with Electrospun Collagen Scaffolds Seeded with Human Cells," Tissue Eng. Part A, 22(5–6), pp. 436–448.

[59] Zhang, Z. Z., Chen, Y. R., Wang, S. J., Zhao, F., Wang, X. G., Yang, F., Shi, J. J., Ge, Z. G., Ding, W. Y., Yang, Y. C., Zou, T. Q., Zhang, J. Y., Yu, J. K., and Jiang, D., 2019, "Orchestrated Biomechanical, Structural, and Biochemical Stimuli for Engineering Anisotropic Meniscus," Sci. Transl. Med., 11(487).

[60] Higashioka, M. M., Chen, J. A., Hu, J. C., and Athanasiou, K. A., 2014, "Building an Anisotropic Meniscus with Zonal Variations," Tissue Eng. Part A, 20(1–2), pp. 294–302.

[61] Vapniarsky, N., Huwe, L. W., Arzi, B., Houghton, M. K., Wong, M. E., Wilson, J. W., Hatcher, D. C., Hu, J. C., and Athanasiou, K. A., 2018, "Tissue Engineering toward Temporomandibular Joint Disc Regeneration," Sci. Transl. Med., 10(446), pp. 1–10.

[62] Donahue, R. P., Gonzalez-Leon, E. A., Hu, J. C., and Athanasiou, K. A., 2019, "Considerations for Translation of Tissue Engineered Fibrocartilage from Bench to Bedside," J. Biomech. Eng., 141(7).

Supplementary Materials

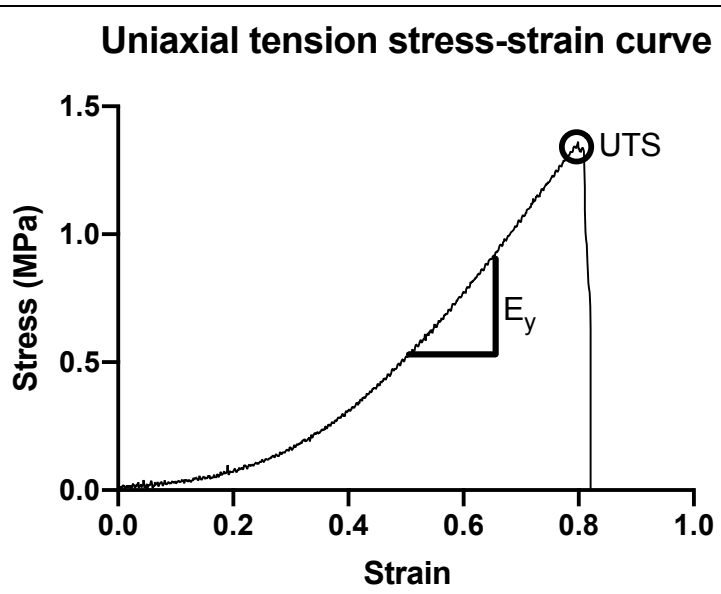

Supplementary Figure 3.1: A typical uniaxial tensile stress-strain curve for self-assembled neomeniscus. A uniaxial tension test was used to determine tensile Young's modulus and ultimate tensile strength. Strain is depicted in relation to gauge length. The example shown is from a neomeniscus treated with TCL+LPA.

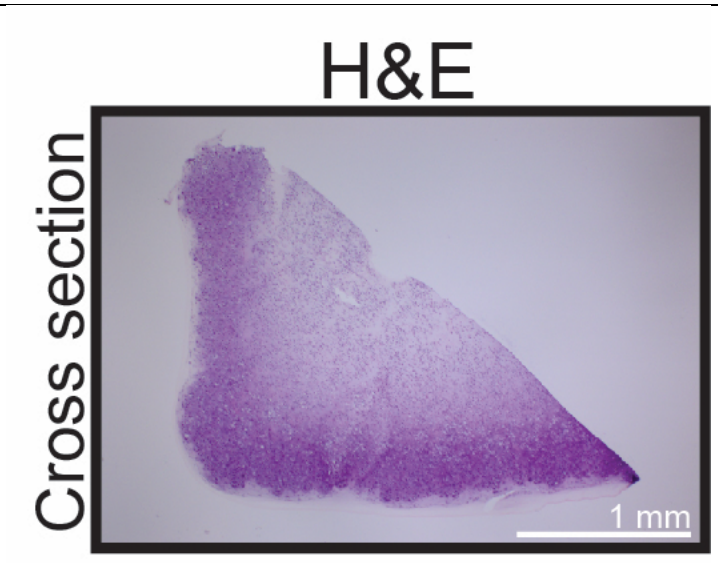

Supplementary Figure 3.2: Self-assembled neomenisci maintained native tissue morphology. H&E staining of a cross-section of a self-assembled neomeniscus

illustrating that engineered neomenisci maintain the characteristic wedge-shaped profile of the native knee meniscus. A neomeniscus from the TCL treatment group is shown.

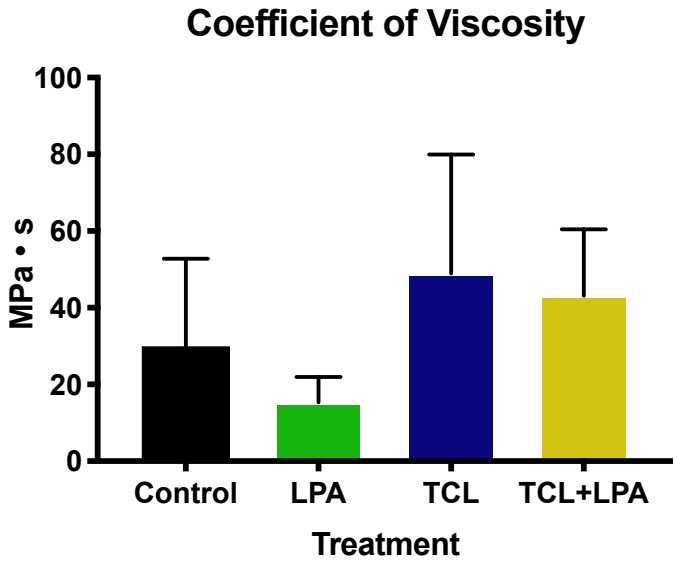

Supplementary Figure 3.3: Self-assembled neomenisci coefficients of viscosity. Stress relaxation compressive testing showed no significant differences in coefficient of viscosity among treatment groups.

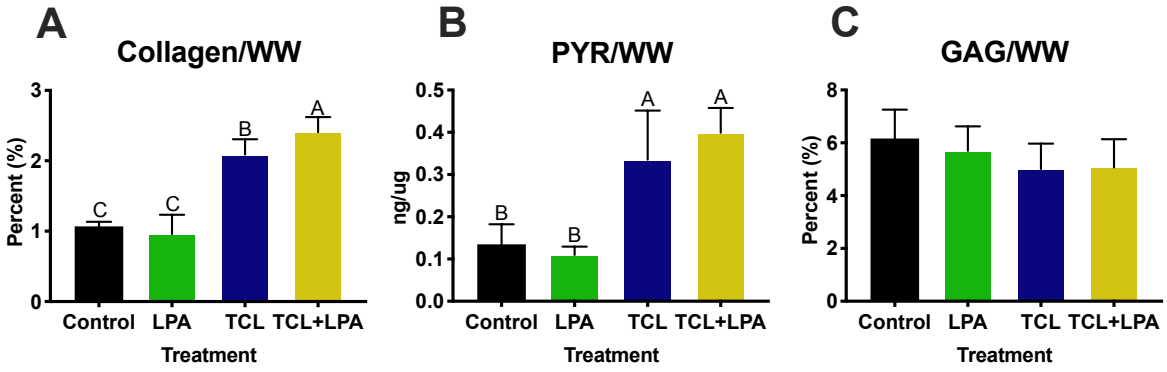

Supplementary Figure 3.4: Biochemical properties of self-assembled neomenisci normalized to wet weight. TCL+LPA treatment enhanced collagen content over all

other groups. Pyridinoline crosslink content in TCL and TCL+LPA treated constructs increased over controls and LPA treated groups. No significant difference in GAG content was seen among groups.

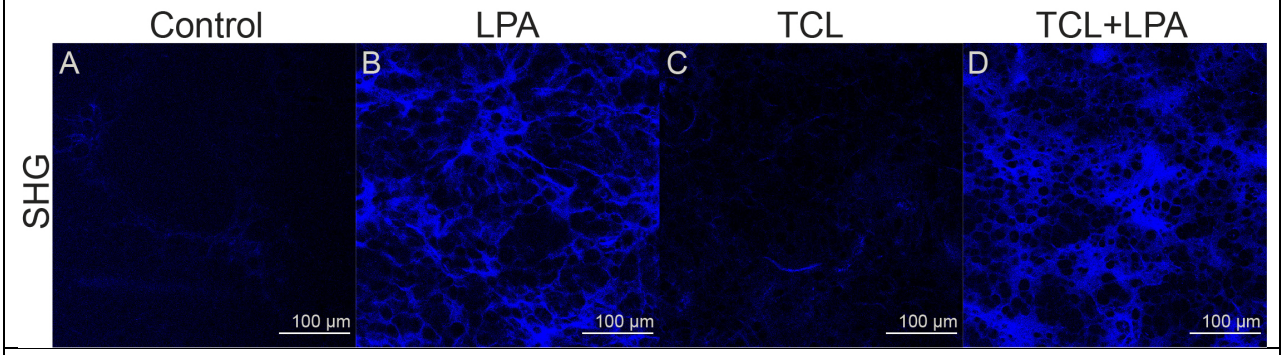

Supplementary Figure 3.5: Second-harmonic generation (SHG) imaging of self-assembled neomenisci. Second-harmonic imaging signal of LPA and TCL+LPA treated constructs appeared more intense than controls, indicating a higher degree of circumferentially aligned collagen fibers.

Chapter 4: Hyperelastic mechanical properties correlate to biochemical composition of native and tissue-engineered knee menisci

Abstract

Surgery to repair injuries to the knee meniscus, which represent the most common cause of orthopaedic surgery, do not prevent the onset of degenerative changes. Neomenisci with biomimetic features offer an alternative treatment strategy that may slow or prevent the onset of osteoarthritis following events that lead to injury. To achieve this goal, it is crucial for neomenisci to exhibit the functional behavior of the knee meniscus in the native knee joint. Small-strain analysis is largely phenomenological and is typically used to model the meniscus; however, the meniscus experiences large strains (~40%) under normal loading conditions. This study aimed to identify a hyperelastic model that could capture native and engineered meniscus function to better inform meniscus tissue engineering strategies. To investigate how changes in matrix structure affect function, native tissue extracellular matrices were perturbed with collagenase, leading to significant decreases in tensile properties and collagen content; data from a previously published study in which engineered neomenisci were treated with bioactive factors that were also used. Three hyperelasticity models were examined, namely Neo-Hookean, Yeoh, and fiber-reinforced neo-Hookean models. Out of the three, the fiber-reinforced Neo-Hookean model, which incorporates tissue microstructural properties, was found to be the best

In preparation for submission as: Espinosa, MG, Gonzalez-Leon, EA, Hu, JC, & Athanasiou, KA. *Hyperelastic mechanical properties correlate to biochemical composition of native and tissue-engineered knee menisci*.

model based on goodness-of-fit. We identified moderate positive correlations between both collagen content (ρ=0.81) and pyridinoline crosslinking (ρ=0.69) and the fiber modulus (γ), a stress-like material property determined from mechanical tests of the tissue. Interestingly, the strongest correlation exists between the collagen to GAG ratio (ρ=0.84) and the nonlinearity parameter (α); a higher α value indicates a higher degree of nonlinearity. This suggests that the nonlinear response of engineered menisci is due to the interaction between collagen fibers and the surrounding GAG matrix. Together, these data provide a hyperelastic model that allows for deeper understanding of meniscal function with regard to its structural properties, and aids tissue engineers in the design of functional neomenisci toward their use in repair and replacement technologies.

4.1. Introduction

Knee meniscus lesions are the most common intra-articular knee injury [1], which leads to these injuries accounting for up to 20% of orthopedic procedures; in total, approximately 850,000 patients per year receive surgery involving the meniscus, and meniscal injuries are the most frequent cause of orthopedic surgical procedures in the U.S. [2] However, surgical interventions, such as partial or full meniscectomy, have been reported to relieve pain but lead to the emergence of osteoarthritis [3]. Novel regenerative solutions, such as biomimetic tissue-engineered menisci created with the self-assembling process [4–7], offer alternative therapy options that may slow or halt the progression of OA following injury.

To achieve this goal, it is imperative that engineered neomenisci recapitulate the mechanical behavior of the knee meniscus in its native, physiological environment. Although it has been reported that the meniscus undergoes 40% strain under normal

loading conditions [8]; current tissue-engineering approaches model the tissue using small-strain approximations. For example, linear biphasic finite element models have previously predicted that meniscus strains vary from 1-10% [9]. Hyperelastic modeling provides the means to characterize tissue mechanical properties at finite deformations. While parameters in hyperelastic models of native hyaline cartilage are increasingly structurally motivated [10], modeling of the meniscus is still largely phenomenological with little insight into the structure-function relationship of the meniscus at large deformations.

The knee meniscus, a fibrocartilaginous tissue with anisotropic mechanical properties, derives its functional attributes from its extracellular matrix (ECM) and structural organization [11]. Its wedge shape allows for compressive loads to be resisted by tensile hoop stresses developed by circumferentially aligned collagen fibers. Radial tie fibers also support circumferentially aligned fibers in the deep zone of the tissue and have been postulated to resist longitudinal tears [12–14]. Crosslinks, such as pyridinoline, contribute to mechanical properties of the knee meniscus and correlate with tensile properties of several collagenous tissues [15–17]. Self-assembled neomenisci, meanwhile, have been able to recapitulate anisotropy in tensile properties with the addition of mechanical or biochemical stimuli; pyridinoline crosslink content of neomenisci has also reached levels on par with those of native human fibrocartilages [4,6,18]. However, tensile properties still fall short of native values by at least one order of magnitude [4–6]. Additionally, glycosaminoglycan (GAG) content, which has been correlated with compressive properties of native and engineered cartilaginous tissues, is higher in engineered neomenisci compared to native tissue [4]. Together, these ECM

components and their structure allow the knee meniscus to function within the joint and provide a physiological benchmark for tissue engineers.

To better understand how ECM components such as collagen, GAG, and crosslinks interact and contribute to functional mechanical properties of the knee meniscus, computational models with physiologically relevant strain assumptions are needed. The mechanical characterization of the native knee meniscus typically relies on small-strain approximations; however, due to the large deformation that the tissue undergoes (>40% strain), linear small-strain models may not fully capture its functionality. Hyperelastic models, such as the Neo-Hookean model, have been used in an attempt to understand meniscus functionality when experiencing large strains [19]. Other models, such as the Yeoh model, includes more parameters that may increase fidelity of experimental data to the model. However, many of these models are largely phenomenological and provide little insight into how structural properties of the native knee meniscus contribute to the tissue's functionality. A model of interest for hyperelastic analysis of the meniscus is the fiber-reinforced Neo-Hookean, which takes tissue microstructural components into account. Ideally, structure-function relationships of native menisci, using assumptions from native loading conditions, should be incorporated into hyperelastic descriptions of the knee meniscus and engineered meniscus replacements.

To better understand structure-function relationships of native tissues, and subsequently compare them to those of engineered tissues, it is pertinent to investigate how altering ECM content and structure contributes to changes in meniscus functionality. For example, differences in ECM content and structure resulting from the application of

different mechanical or bioactive stimuli ultimately affect the functional properties of the engineered neocartilage and neomenisci tissues [4,6,20]. Comparing native meniscal tissue treated with and without exogenous factors that perturb its ECM and alters biochemical content could elucidate how knee menisci function mechanically under different structural conditions and provide a better template for how engineered neomenisci should be designed; native menisci explants treated with an exogenous crosslinking agent, for example, exhibited tensile properties that were 1.9-fold higher compared to nonstimulated controls [21]. Thus, a comparison of mechanical and biochemical properties of native and engineered menisci with varying ECM compositions and structures will both inform the selection of an appropriate hyperelastic model and provide crucial insight into where engineered neomenisci fall short of native tissue structure-function characteristics.

This work aimed to examine structure-function properties of native knee meniscus and engineered neomenisci using hyperelasticity. This was pursued with the intention of identifying a model with large-strain assumptions that 1) has parameters that correlate to tissue microstructural properties and 2) is applicable to both native and engineered meniscus tissues. In this study, we conducted hyperelastic analyses on native bovine menisci in addition to data from self-assembled, scaffoldless tissue constructs in the shape of the meniscus that were reported in a previous study [4]. Mechanical and biochemical properties were modulated with either collagenase or previously used bioactive agents for native and engineered menisci, respectively [4,5,22,23]. The menisci underwent a series of mechanical and biochemical assays to quantify the effects of the changes to the ECM. We hypothesized that a microstructural, hyperelastic model would

better describe the experimental data and provide model parameters that would correlate with the biochemical content of both native and engineered tissues.

4.2. Materials and methods

4.2.1 Collection of native tissue samples and treatments

For native tissue samples, medial menisci were excised from 6 juvenile bovine knee joints. Native tissue tensile samples were digested in 0.02%collagenase type II (Worthington) for 18 hours at 37°C. Menisci were photographed and measured using ImageJ (NIH) before resecting pieces for mechanical testing and biochemical analysis (Figure 4.1).

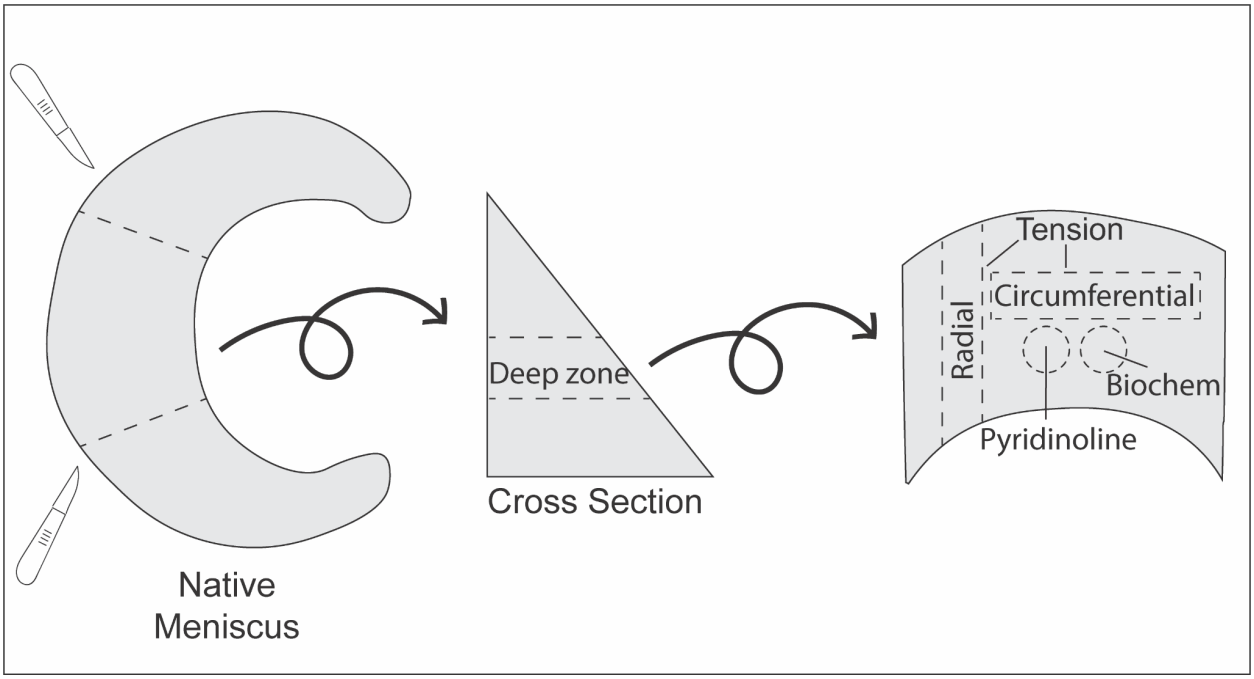

Figure 4.1: Division of bovine knee menisci for mechanical and biochemical analyses. The central region of each meniscus was first isolated. Subsequently, each central region was cut into layers; tensile (circumferential and radial directions),

biochemistry, and mass spectrometry samples were collected from the deep zone of the meniscus.

4.2.2 The tissue engineering of neomenisci and treatment groups [4]

As described previously [4], ring-shaped neomenisci constructs were produced using the self-assembling process with a 50:50 mix of native bovine articular chondrocytes and meniscus cells, at a total seeding density of 20 million cells per construct. TGF-β1, glycosaminoglycan-cleaving enzyme chondroitinase ABC (C-ABC), and crosslinking agent lysyl oxidase-like 2 (LOXL2) treatments (together termed “TCL”) were applied to neomenisci in addition to lysophosphatidic acid treatment (LPA) during culture. These bioactive factors were selected due to their previous efficacy toward increasing neomenisci tensile properties [5,22,23].

Treatment groups for neomenisci constructs were previously described [4]. Briefly, neomenisci treatment groups consisted of 1) unstimulated controls, 2) LPA only, 3) TCL only, 4) TCL+LPA. TCL groups were treated with the combination of 1) TGF-β1 continuously throughout culture at 10 ng/mL, 2) a one-time C-ABC treatment, added to medium with a 0.05 M sodium acetate activator, at day 7 of culture at 2 U/mL for a duration of 4 hours, and 3) LOXL2 applied continuously from days 7-21 (weeks 2-3) at 0.15 ng/mL as previously described [20,21,24]. Neomenisci that were treated with LPA (Enzo Life Sciences) were stimulated during days 21-28 (week 4) at a final concentration of 10 mM as previously described [4,5]. The total culture time was 35 days, and all constructs were cultured for 5 weeks at 37°C and 5% CO2.

4.2.3 Tensile testing

Tensile properties were assessed using uniaxial, strain-to-failure testing. Samples were photographed, cut into rectangular strips, and measured with ImageJ. Samples were then clamped within a uniaxial testing machine (Instron model 5565) and subjected to a 1% s-1 strain rate until failure. Young's modulus (EY) was calculated from the linear portion of the stress-strain curve, and ultimate tensile strength (UTS) was calculated from the maximum stress. The corresponding strain at failure was also recorded.

4.2.4 Analysis of tissue biochemical content

Biochemistry samples were weighed wet, then frozen and lyophilized to acquire dry weights. Collagen content was measured with the use of a Sircol standard (Biocolor) and a Chloramine-T colorimetric hydroxyproline assay [25]. GAG content was quantified using the Blyscan assay kit (Invitrogen). All quantification measurements for DNA, GAG, and collagen content were performed with a GENios spectrophotometer/spectrofluorometer (TECAN).

Quantification of pyridinoline crosslink content was performed via a liquid chromatography mass spectrometry (LC-MS) assay. Lyophilized samples were hydrolyzed in 6N HCl at 105°C for 18 hours. After evaporation, dried hydrolysates were resuspended in 25% (v/v) acetonitrile and 0.1% (v/v) formic acid in water, centrifuged at 15,000g for 5 min, and the supernatant was transferred to a LCMS autosampler vial. Liquid chromatography was carried out on a Cogent Diamond Hydride HPLC Column (2.1 mm x 150 mm, particle size 2.2 µm, pore size 120 Å, MicroSolv) and a pyridinoline standard (BOC Sciences) as previously described [4,26].

4.2.5 Modeling

Three hyperelastic models were fit to the tensile stress-strain curves from control native tissue. The strain energy density functions (W) for the Neo-Hookean (Eq. 1), Yeoh (Eq. 2), and fiber-reinforced Neo-Hookean (Eq.3) models are given below:

$$W = \frac{\mu_{nh}}{2}(I_1 - 3), \quad (1)$$

$$W = \sum_{i=1}^{2} \frac{\mu_{yi}}{2}(I_1 - 3)^i, \text{ and} \quad (2)$$

$$W = \frac{\mu_f}{2}(I_1 - 3) + \frac{\gamma}{4\alpha}\left(e^{\alpha(I_4-1)^2} - 1\right). \quad (3)$$

For these strain energy density functions (Eq. 1-3), μ, γ, and α are material parameters and I_n is the nth invariant. To reduce the number of free parameters in the fiber-reinforced Neo-Hookean, μ_f was set to 0.02 MPa after performing a sensitivity analysis (Figure 4.2). The remaining parameters were determined by fitting the model to the entire experimental curve. The best model was determined by goodness-of-fit as measured by R^2 and the residual norm; the residual norm is a measure of the goodness of fit, where a smaller value indicates a better fit.

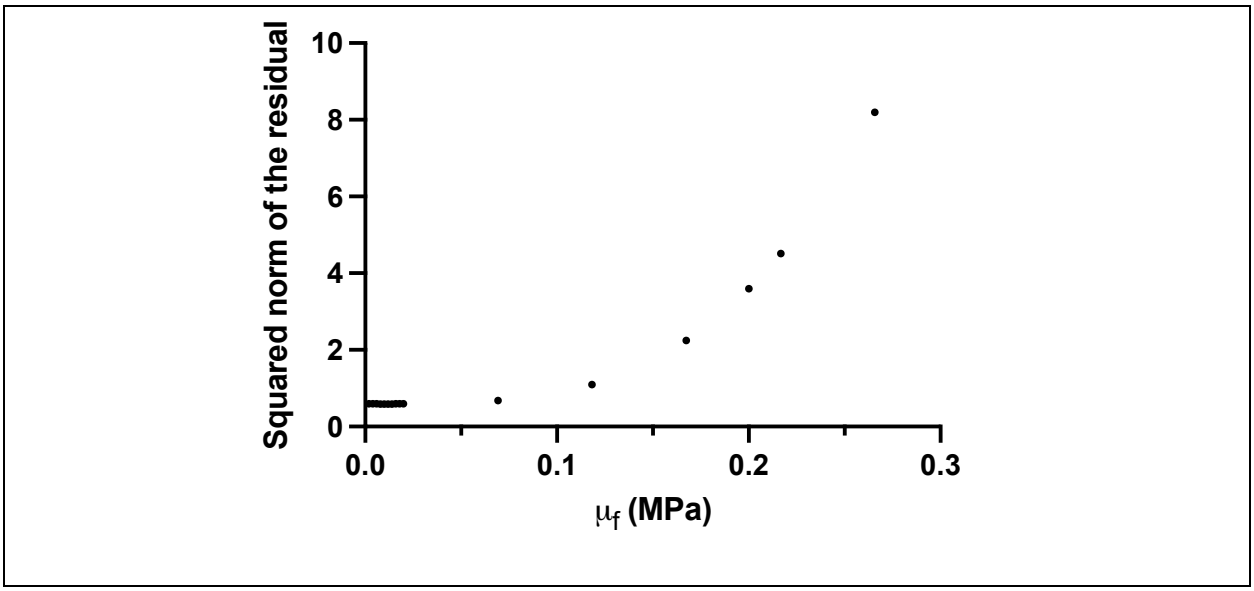

Figure 4.2: Sensitivity analysis of hyperelastic parameter, μ_f, from fiber-reinforced Neo-Hookean model. Parameter sensitivity is negligible at values <0.1 as seen by the relatively constant squared norm of the residual. This justified fixing μ_f to 0.02 MPa.

4.2.7 Statistical analysis

For each biomechanical and biochemical test, n=6 samples were used. Results were analyzed with single-factor analysis of variance (ANOVA) followed by a Tukey's HSD post hoc test when merited ($p \leq 0.05$). All data are presented as means ± standard deviations. For all figures, a connecting letters report shows statistical significance as indicated by groups not sharing the same letters. We also used Spearman's ρ test to find the strength, direction, and significance of correlations between hyperelastic parameters and each biochemical component. Correlation strength and direction are given by the coefficient of correlation (ρ), and statistical significance is defined by $p \leq 0.05$.

4.3. Results

4.3.1 Tissue linear biomechanics

Biomechanical data revealed a significant difference among control and collagenase-treated native meniscus samples. Specifically, control native tissue samples exhibited significantly higher tensile Young's modulus in the circumferential direction when compared to samples treated with collagenase; control Young's modulus values were 171% higher than the collagenase group (Figure 4.3A).

As previously reported [4], significant differences among control and treated constructs were observed, especially those that were treated with TCL+LPA. TCL+LPA

treatment led to increased tensile properties over both unstimulated control and LPA treatment groups. Circumferential Young's modulus was highest in TCL+LPA treated groups (Figure 4.3B). TCL+LPA treatment increased Young's modulus in the circumferential direction to 221% higher than control values.

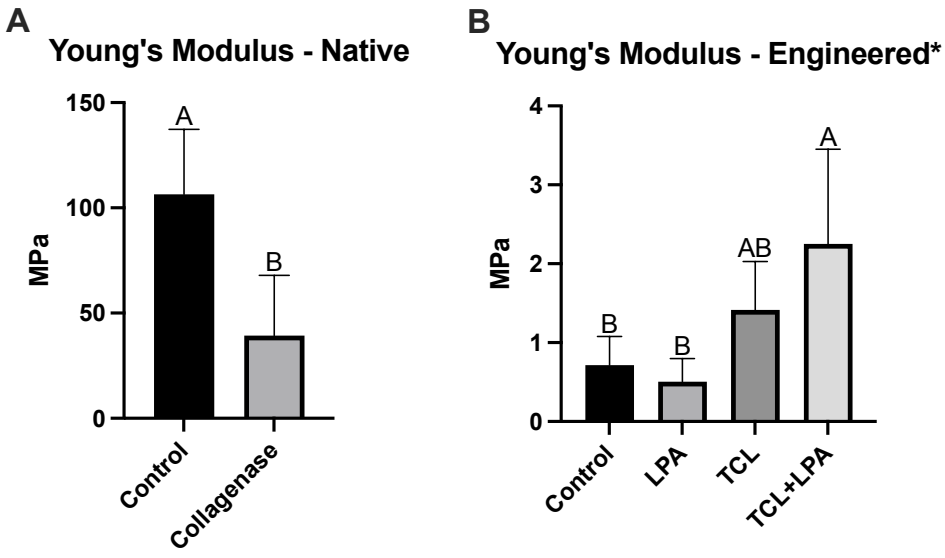

Figure 4.3: Tensile stiffness of native and engineered menisci. Young's modulus for (A) native and (B) engineered menisci are shown. *Data reported in Gonzalez-Leon *et al.* [4].

4.3.2 Failure mechanics

In terms of ultimate tensile strength (UTS), native control samples exhibited significantly higher values when compared to samples treated with collagenase (Figure 4.4); UTS was 256% higher in the control group when compared to the collagenase group. For engineered neomenisci, as previously reported [4], TCL+LPA constructs exhibited the highest UTS values and were significantly higher compared to controls; specifically, UTS was increased by 218% over controls. Additionally, no significant difference was seen among groups in terms of ultimate tensile strain.

The failure strains for both native and engineered menisci and all treatment groups were greater than 10%. The failure strain for native control tissue was 42±13% and was not significantly different compared to the values from the collagenase treatment group. The failure strains achieved in the tissue engineered menisci were all greater than that of native controls; specifically, TCL+LPA treated neomenisci previously exhibited failure strains that were 88% higher than native controls examined in this study.

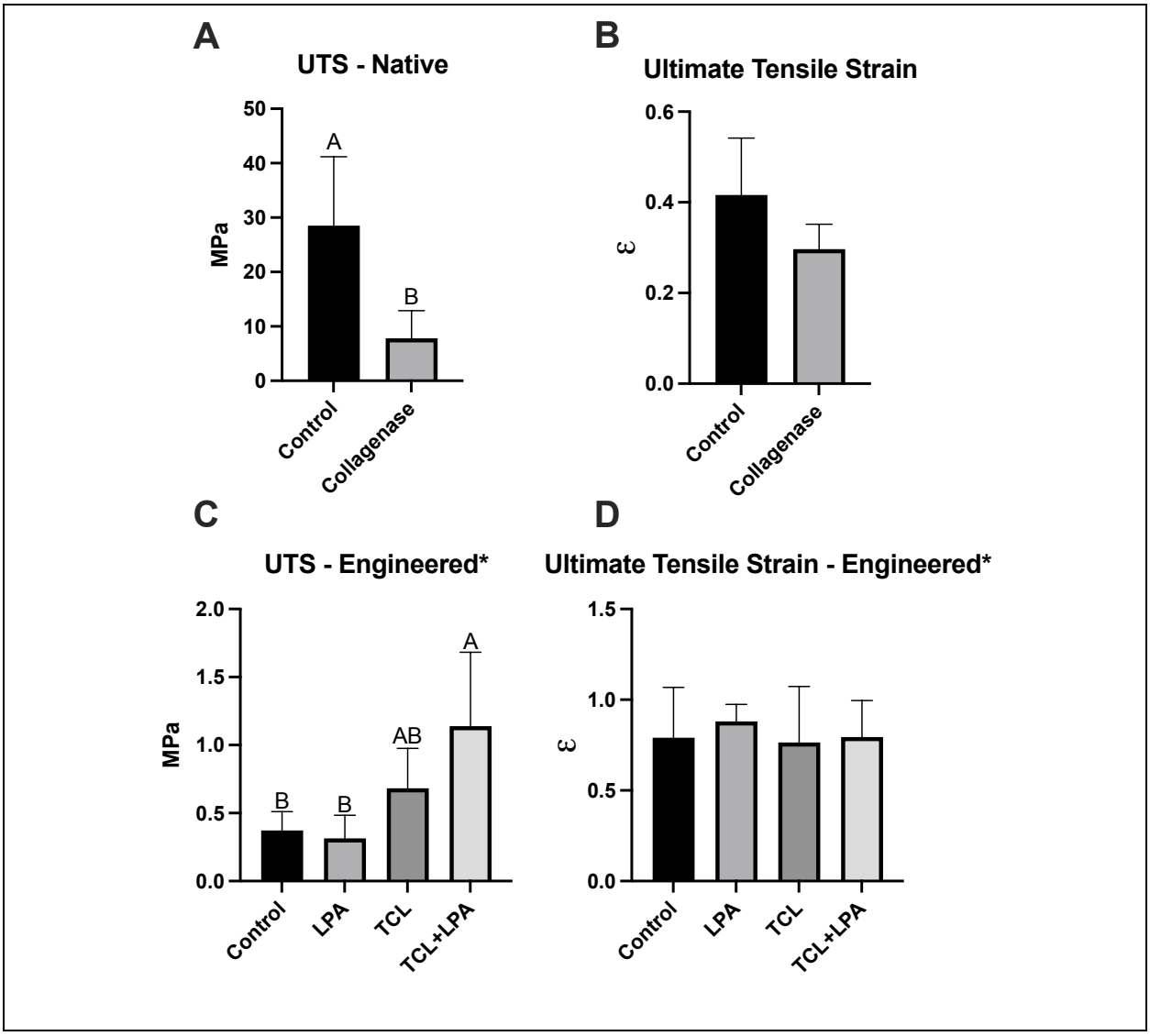

Figure 4.4: UTS and failure strain. UTS and failure strain values for native (A-B) and engineered (C-D) menisci are shown, respectively. *Data reported in Gonzalez-Leon *et al.* [4]

4.3.3 Hyperelastic modeling

All model fits were visually inspected and evaluated for goodness-of-fit. The best and worst fits for each model are shown in Figure 4.5. Although the Neo-Hookean model's R^2 value is significantly lower than that of the Yeoh and fiber-reinforced Neo-Hookean models, its residual norm is significantly higher by 1167% and 859%, respectively (Figure 4.6). This is in agreement with the plots from Figure 4.5. Each model's parameters are given in Table 4.1.

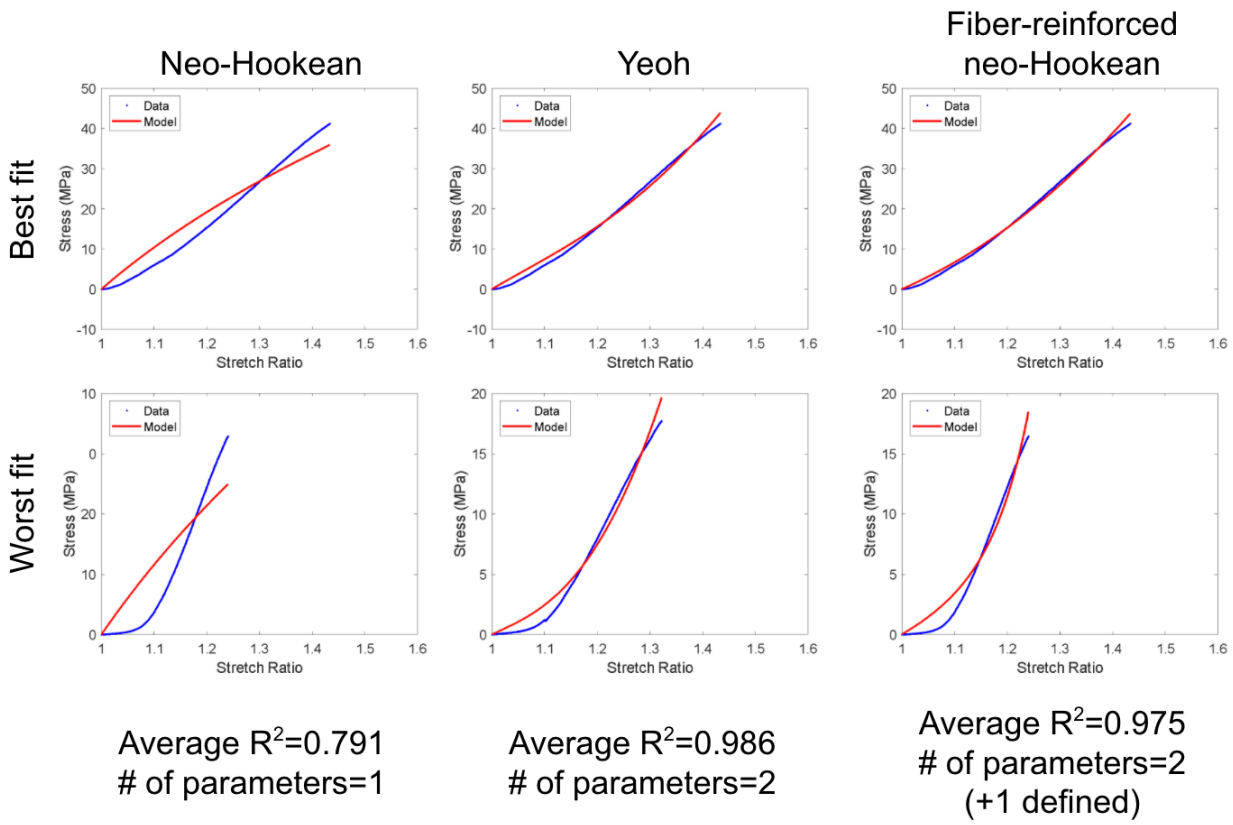

Figure 4.5: Best and worst model fits to experimental data. Fits to Neo-Hookean, Yeoh, and fiber-reinforced Neo-Hookean models are shown. The stretch ratio is defined as the ratio between the final and initial lengths of the tissue material.

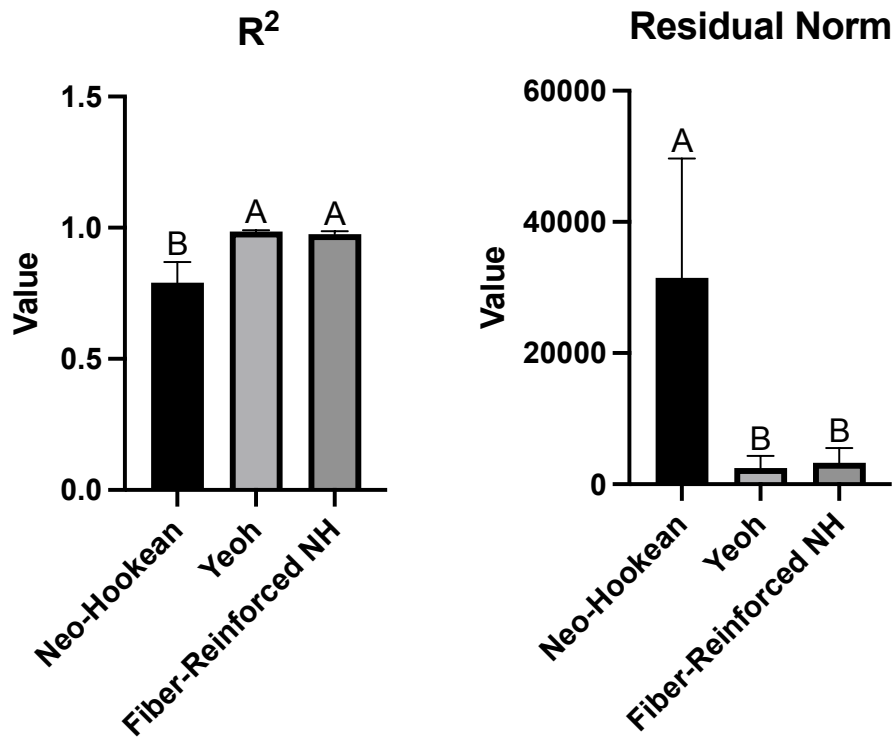

Figure 4.6: Bar graph of R^2 (A) and residual norm (B) values for all hyperelastic models. Values for Neo-Hookean, Yeoh, and fiber-reinforced models are shown.

Table 4.1: Hyperelastic parameters for Neo-Hookean, Yeoh, and fiber-reinforced Neo-Hookean models fitted to control native menisci mechanical data.

Neo-Hookean	Yeoh		Fiber-reinforced Neo-Hookean	
μ_{NH} (MPa)	μ_{y1} (MPa)	μ_{y2} (MPa)	γ (MPa)	α
37.59	25.89	0.87	28.52	9.76×10^{-11}

18.02	6.83	5.42	11.56	0.88
33.59	14.02	5.18	22.82	0.99
20.78	5.27	15.99	12.67	2.56
13.98	3.72	8.88	8.06	1.18

Hyperelastic parameters, such as γ and α, were also affected by bioactive treatments in native and engineered samples. For example, a significant difference was seen in γ values between native control and collagenase samples, respectively (Figure 4.7); native control samples exhibited γ values that were 139% higher than control samples, respectively. Additionally, while no significant difference was seen between TCL+LPA treated neomenisci and nonstimulated controls in terms of γ and α values, TCL+LPA treatment increased these parameter values by 99% and 243%, respectively (Figure 4.8).

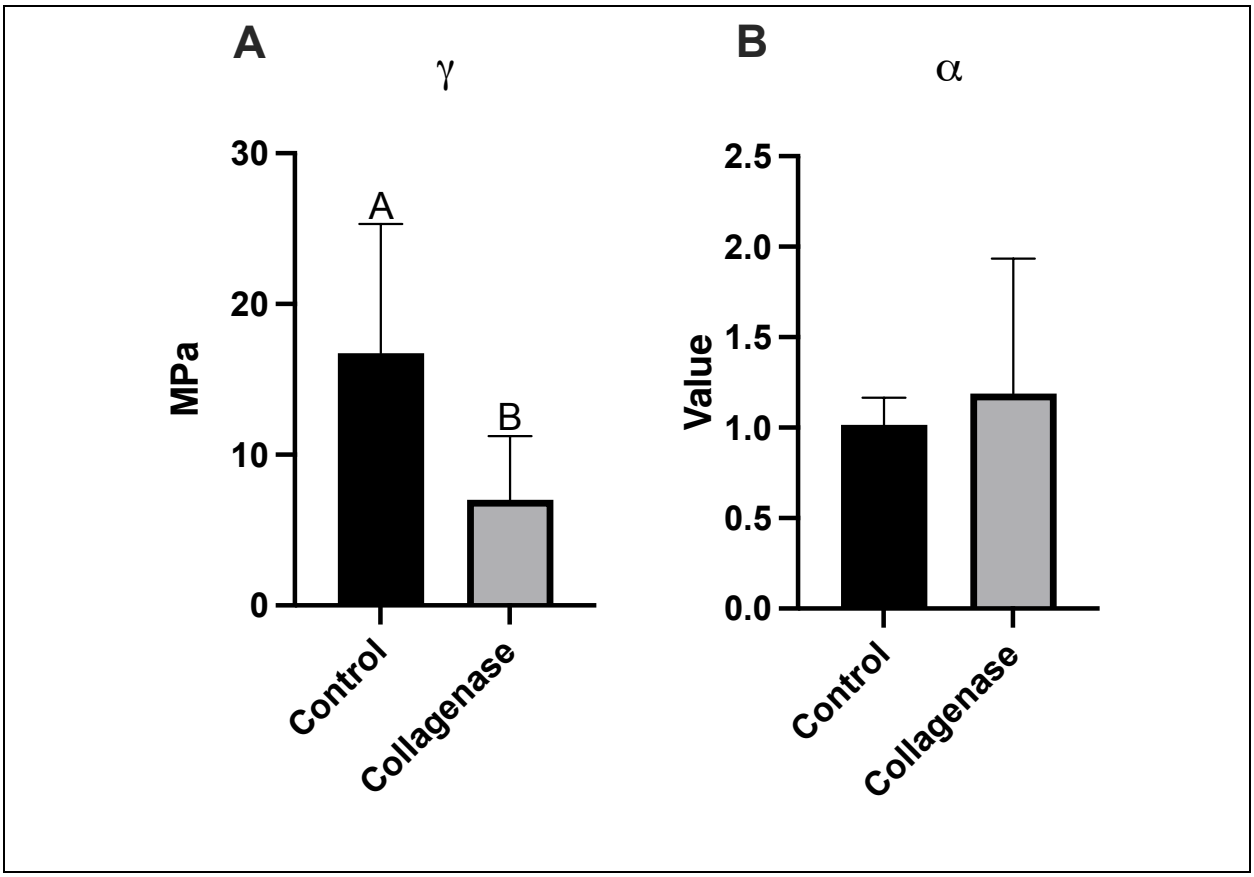

Figure 4.7: Native tissue hyperelastic parameters from fiber-reinforced Neo-Hookean model. γ (A) and α (B) from nonstimulated controls and collagenase treatment groups are shown.

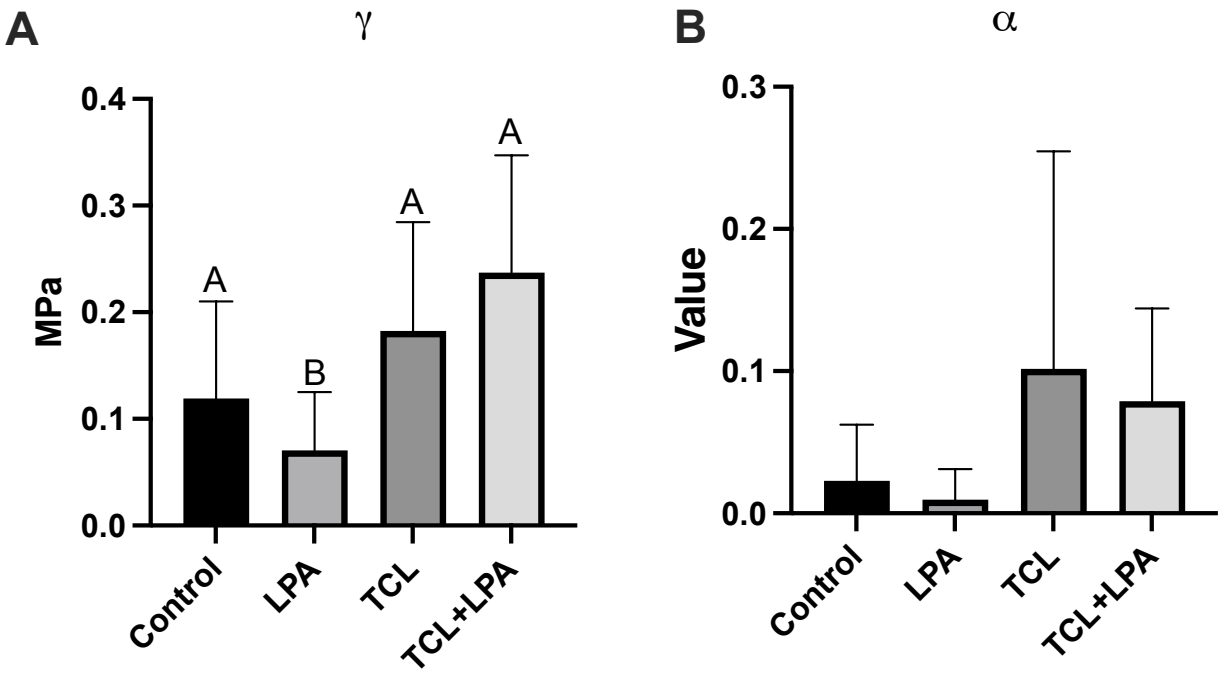

Figure 4.8: Engineered neomenisci hyperelastic parameters from fiber-reinforced neo-Hookean model. γ (A) and α (B) between treatment groups in engineered neomenisci are shown.

4.3.4 Tissue biochemistry

Treatment of native tissue samples with collagenase resulted in decreased collagen and GAG content compared to controls (Figure 4.9). Specifically, collagenase treatment significantly decreased collagen and GAG content per wet weight (WW) by 31% and 29%, respectively; additionally, collagen per dry weight (DW) was significantly decreased by 20% compared to controls. In terms of pyridinoline (PYR) crosslink content, no significant

difference was found between control and collagenase-treated samples normalized to WW and DW, respectively; native control PYR/WW and PYR/DW values were 42% and 13% higher than the collagenase group.

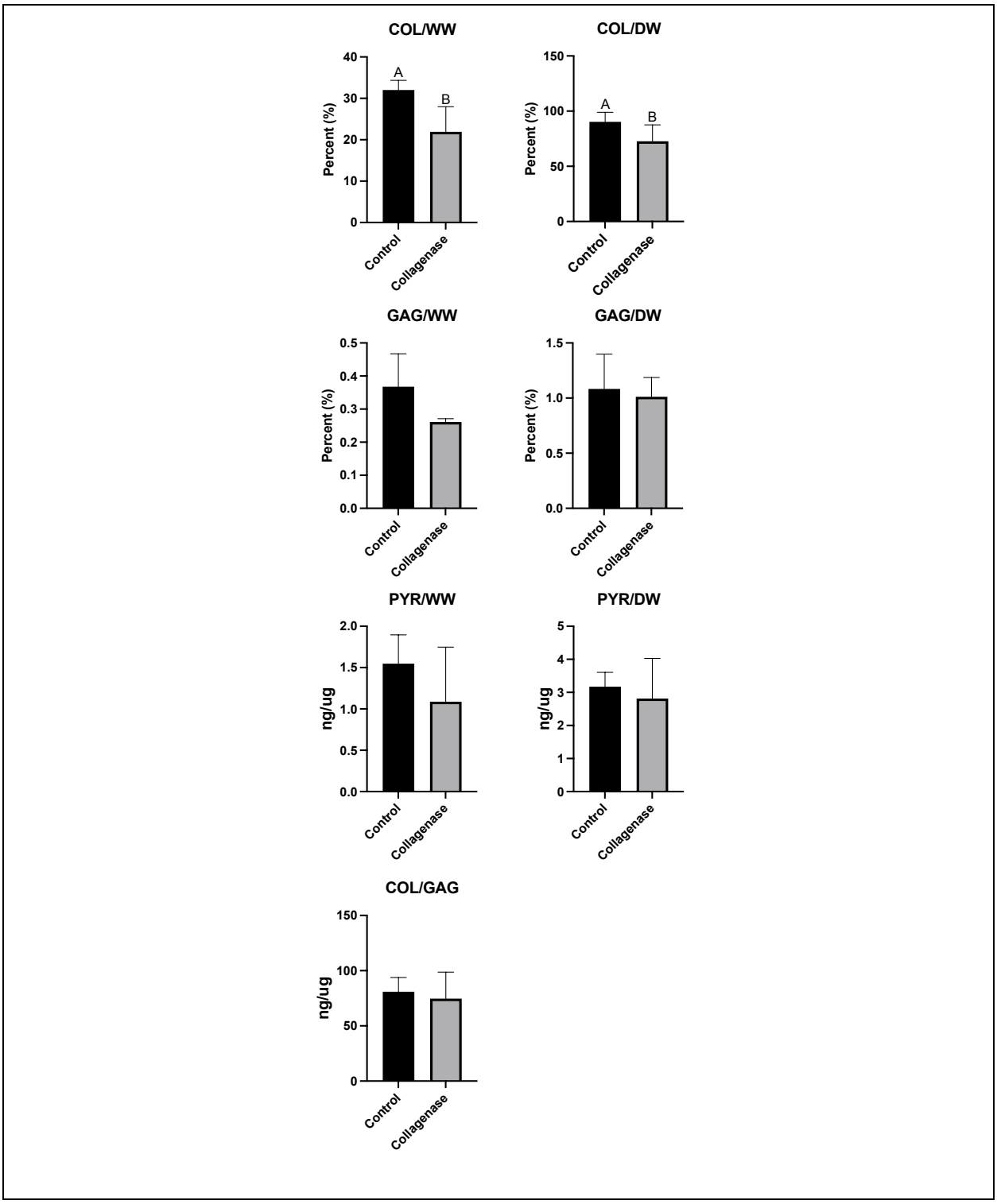

Figure 4.9: Native menisci biochemical properties. Collagen, GAG, and crosslink content of native knee menisci are shown normalized to wet and dry weights, respectively.

As previously reported [4], biochemical treatment of engineered neomenisci significantly increased collagen and pyridinoline crosslink content (Figure 4.10). TCL+LPA exhibited enhanced collagen and pyridinoline content per WW that were 125% and 185% higher than control values, respectively. No significant differences in GAG content per wet weight were observed among treatment groups. Collagen and pyridinoline content normalized by DW also showed increases over controls when treating with TCL+LPA, by 61% and 81% of control values, respectively. However, no significant differences among groups in terms of pyridinoline normalized to collagen content were observed. GAG content normalized to DW was significantly lower for TCL+LPA treated constructs, which was 39% less than control values. TCL treatment also significantly decreased ($p<0.0001$) GAG/DW compared to control groups.

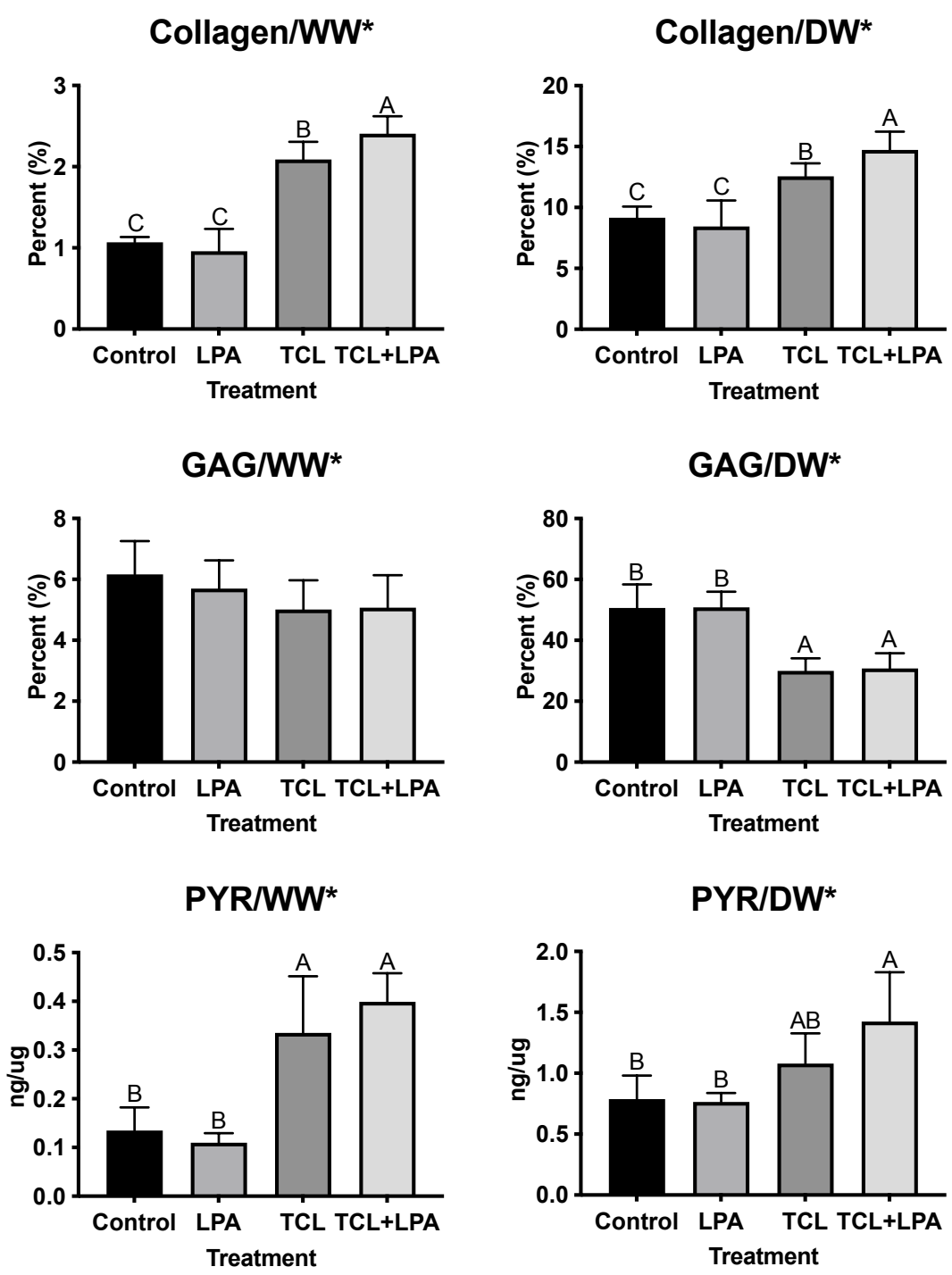

Figure 4.10: Neomenisci biochemical properties. Collagen, GAG, and pyridinoline crosslink content of self-assembled neomenisci are shown normalized to wet and dry weights, respectively. *Data reported in Gonzalez-Leon *et al.* [4].

4.3.5 Structure-function correlations

Several significant correlations between biochemical content and the fitted hyperelastic parameters were identified. The fiber modulus, γ, was most strongly correlated with collagen by WW, with a correlation coefficient of 0.81 (Figure 4.11). Pyridinoline was also moderately correlated with γ. Although the nonlinearity parameter, α, had several significant correlations to biochemical components, the strongest correlation (ρ=0.84) existed between α and the COL/GAG ratio (Figure 4.11). Both model parameters significantly correlated with Young's modulus, but the correlation was much stronger to γ γ than α (0.95 vs 0.72).

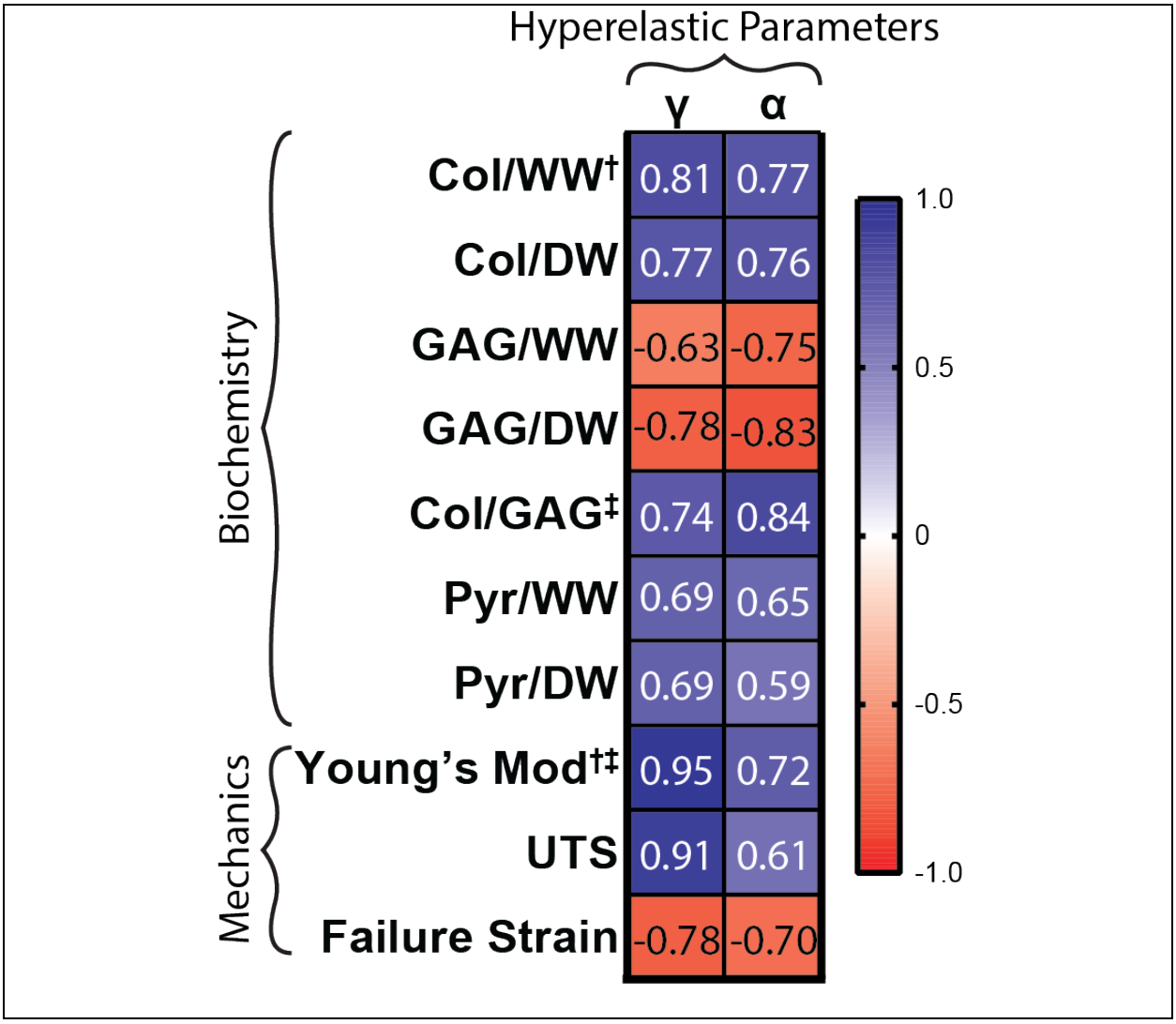

Figure 4.11: Spearman ρ values for correlations between parameters from the fiber-reinforced Neo-Hookean model and experimental measures of biochemical composition and mechanics. Each cell's number and color show the strength and direction of the correlation (blue = positive, red = negative). All correlations shown are significant, with $p<0.05$. † and ‡ point to the strongest biochemical and mechanical correlations between the experimental value and either γ or α, respectively.

4.4. Discussion

The objective of this study was to identify a hyperelastic model that was applicable to both native and engineered menisci, while accounting for their biochemical composition. This was performed by quantifying mechanical and biochemical properties of native tissue treated with and without collagenase; quantified changes to properties of self-assembled neomeniscus rings receiving bioactive treatments that were reported in a previously published study [4] were used when applying models to engineered tissue. We compared three hyperelastic models and selected a fiber-reinforced Neo-Hookean matrix model to describe our native and engineered menisci; this microstructurally inspired model has been previously used to characterize other fibrous tissue [10]. The hypothesis that the microstructurally motivated hyperelastic model would both provide a strong fit to the experimental data and yield parameters that correlate with the biochemical content of our native tissue and tissue-engineered neomenisci was supported by the data. This is significant because the data imply that modeling the meniscus using large-strain analysis provides greater model fidelity and better correlates to changes in the biochemical content and structure of these tissues.

Linear models under small-strain conditions have typically been used to model the knee meniscus, though they do not capture the high strains that the tissue undergoes when loaded; hyperelastic models are becoming more common when modeling the meniscus but choosing the correct hyperelastic model is crucial. In this study, native and engineered tissues underwent strains far exceeding the strain that small-strain models assume (Figure 4.4), showing that models that assume large strains are needed to fully capture meniscal functionality. The Neo-Hookean model is arguably the most widely used hyperelastic model in biomechanics [27–30], however our data illustrate that it is not suitable for the knee meniscus (Figures 4.5 and 4.6). Both the Neo-Hookean and Yeoh hyperelastic models assume a homogeneous matrix [30,31], which is not representative of fibrocartilage. Instead, a fiber-reinforced Neo-Hookean model depicts a composite material consisting of a matrix and fibers and can be related to tissue structural components. Therefore, it is not surprising that the Neo-Hookean displays a higher propensity for error when modeling the meniscus (Figure 4.6). Our model selection process, which does not rely solely on R^2 values, underscores the need to utilize alternative measures of goodness-of-fit (such as the residual norm) as well as a physical understanding of the tissue in question. Although the Yeoh model was comparable to the fiber-reinforced Neo-Hookean model with regards to goodness-of-fit, we opted for the latter because of its clear structure-based terms. The correlations between the fiber-reinforced Neo-Hookean parameters and collagen and GAG content elucidate the structure-function relationships of the knee meniscus.

Here, we assumed that the Neo-Hookean matrix component corresponds to GAG content, while the exponential term corresponds to the collagen fiber contribution. The

Neo-Hookean constant was fixed as it was found to be insensitive to variation, reducing the number of parameters in the fiber-reinforced model from three to two (Figure 4.2). This implies that GAGs do not significantly contribute to tensile properties; GAG content in engineered and native tissues has previously been correlated to compressive properties [32]. As expected, the fiber modulus correlated well with collagen content (Figure 4.11); interestingly, the Young's modulus also correlated strongly with the fiber modulus, showing that small-strain models are still able capture aspects of meniscal functionality. The strong correlation between the nonlinearity parameter and the COL/GAG ratio suggests that the nonlinear behavior is not solely due to a single component, but rather the interaction between matrix proteins. This observation is overlooked by small-strain analysis of the tissue mechanics, and shows the importance of including microstructural properties within a hyperelastic model of the meniscus to more accurately depict its function under normal loading conditions.

The current model is a single fiber-family formulation which assumes that collagen fibers are only circumferentially oriented. Given the importance of anisotropy in the meniscus, a better representation of the distribution of fiber orientations along the circumferential and radial directions could be included. For example, the meniscus has been shown to have tensile properties that are approximately 10-times higher in the circumferential direction compared to the radial direction, stemming from collagen fibers aligned primarily in the circumferential direction [33,34]. Radial fibers, however, are crucial to meniscus functionality and have been posited to withstand the splitting of circumferentially aligned fibers in longitudinal tears [35]. Inclusion of more robust fiber

alignment data, in concert with functional data collected in the radial direction within the meniscus, may improve the fidelity of the model to experimental results.

Although the knee meniscus withstands large deformations in vivo, the field of tissue-engineering still primarily employs small strain analysis to assess tissue mechanics. Our use of a microstructurally based hyperelastic model to characterize native and engineered menisci is both novel and critical to translation to the native environment. In this study, we show that the model captures the deleterious effect of perturbing the native meniscus matrix, which leads to losses in functionality; additionally, the positive, synergistic effects of the TCL+LPA treatment on neomenisci structural and functional properties [4] were also captured with the fiber-reinforced Neo-Hookean model. Further studies should assess the effect of mechanical stimulation, such as uniaxial tension or fluid-induced shear, on hyperelastic characteristics; mechanical stimuli have been shown to increase the functional and structural properties of engineered neomenisci [6,36]. To further guide our tissue engineering strategies that will be employed in future studies, a “gold-standard” based on native meniscus hyperelastic properties should be established.

Ultimately, three hyperelastic models were applied to experimental data obtained from native and engineered [4] knee meniscus tissues. The fiber-reinforced Neo-Hookean model was a better fit to the experimental data compared to a matrix-only Neo-Hookean model and was chosen as the ideal model over Yeoh methods due to the incorporation of microstructural properties that are crucial for meniscus functionality. These microstructural components of the meniscus matrix, such as collagen and GAG, were manipulated using collagenase treatment in native tissue or TCL+LPA treatment in

engineered neomenisci [4]; the fiber-reinforced Neo-Hookean model adequately captured these changes stemming from bioactive treatments, showing the efficacy of the model. Together, these data represent an innovative and collaborative approach to the development of a mechanically robust tissue engineered meniscus.

References

[1] Salata, M. J., Gibbs, A. E., and Sekiya, J. K., 2010, “A Systematic Review of Clinical Outcomes in Patients Undergoing Meniscectomy,” Am. J. Sports Med., 38(9), pp. 1907–1916.

[2] Logerstedt, D. S., Snyder-Mackler, L., Ritter, R. C., and Axe, M. J., 2010, “Knee Pain and Mobility Impairments: Meniscal and Articular Cartilage Lesions,” J. Orthop. Sports Phys. Ther., 40(6).

[3] Rangger, C., Kathrein, A., Klestil, T., and Glötzer, W., 1997, “Partial Meniscectomy and Osteoarthritis. Implications for Treatment of Athletes.,” Sports Med., 23(1), pp. 61–68.

[4] Gonzalez-Leon, E. A., Bielajew, B. J., Hu, J. C., and Athanasiou, K. A., 2020, “Engineering Self-Assembled Neomenisci through Combination of Matrix Augmentation and Directional Remodeling,” Acta Biomater., 109, pp. 73–81.

[5] Hadidi, P., and Athanasiou, K. A., 2013, “Enhancing the Mechanical Properties of Engineered Tissue through Matrix Remodeling via the Signaling Phospholipid Lysophosphatidic Acid,” Biochem. Biophys. Res. Commun., 433(1), pp. 133–138.

[6] Huey, D. J., and Athanasiou, K. A., 2011, “Tension-Compression Loading with Chemical Stimulation Results in Additive Increases to Functional Properties of Anatomic Meniscal Constructs,” PLoS One, 6(11), pp. 1–9.

[7] Arzi, B., Duraine, G. D., Lee, C. A., Huey, D. J., Borjesson, D. L., Murphy, B. G., Hu, J. C. Y., Baumgarth, N., and Athanasiou, K. A., 2015, “Cartilage Immunoprivilege Depends on Donor Source and Lesion Location,” Acta Biomater., 23, pp. 72–81.

[8] Netravali, N. A., Koo, S., Giori, N. J., and Andriacchi, T. P., 2011, “The Effect of Kinematic and Kinetic Changes on Meniscal Strains during Gait,” J. Biomech. Eng., 133(1).

[9] Upton, M. L., Hennerbichler, A., Fermor, B., Guilak, F., Weinberg, J. B., and Setton, L. A., 2006, “Biaxial Strain Effects on Cells from the Inner and Outer Regions of the Meniscus,” Connect. Tissue Res., 47(4), pp. 207–214.

[10] Pierce, D. M., Ricken, T., and Holzapfel, G. A., 2013, “A Hyperelastic Biphasic Fibre-Reinforced Model of Articular Cartilage Considering Distributed Collagen Fibre Orientations: Continuum Basis, Computational Aspects and Applications,” Comput. Methods Biomech. Biomed. Engin., 16(12), pp. 1344–1361.

[11] Fithian, D. C., Kelly, M. A., and Mow, V. C., 1990, “Material Properties and Structure-Function Relationships in the Menisci,” Clin. Orthop. Relat. Res., (252), pp. 19–31.

[12] Skaggs, D. L., Warden, W. H., and Mow, V. C., 1994, “Radial Tie Fibers Influence the Tensile Properties of the Bovine Medial Meniscus,” J. Orthop. Res., 12(2), pp. 176–185.

[13] Petersen, W., and Tillmann, B., 1998, “Collagenous Fibril Texture of the Human Knee Joint Menisci,” Anat. Embryol. (Berl)., 197(4), pp. 317–324.

[14] Andrews, S. H. J., Rattner, J. B., Abusara, Z., Adesida, A., Shrive, N. G., and Ronsky, J. L., 2014, “Tie-Fibre Structure and Organization in the Knee Menisci,” J. Anat., 224(5), pp. 531–537.

[15] Eleswarapu, S. V., Responte, D. J., and Athanasiou, K. A., 2011, “Tensile Properties, Collagen Content, and Crosslinks in Connective Tissues of the Immature Knee Joint,” PLoS One, 6(10).

[16] Williamson, A. K., Chen, A. C., Masuda, K., Thonar, E. J., and Sah, R. L., 2003, “Tensile Mechanical Properties of Bovine Articular Cartilage: Variations with Growth and Relationships to Collagen Network Components,” J. Orthop. Res., 21(5), pp. 872–880.

[17] Chan, B. P., Fu, S. C., Qin, L., Rolf, C., and Chan, K. M., 1998, “Pyridinoline in Relation to Ultimate Stress of the Patellar Tendon during Healing: An Animal Study,” J. Orthop. Res., 16(5), pp. 597–603.

[18] Takahashi, M., Suzuki, M., Kushida, K., Hoshino, H., and Inoue, T., 1998, “The Effect of Aging and Osteoarthritis on the Mature and Senescent Cross-Links of Collagen in Human Meniscus,” Arthrosc. J. Arthrosc. Relat. Surg., 14(4), pp. 366–372.

[19] Abraham, A. C., Moyer, J. T., Villegas, D. F., Odegard, G. M., and Haut Donahue, T. L., 2011, “Hyperelastic Properties of Human Meniscal Attachments,” J. Biomech., 44(3), pp. 413–418.

[20] Lee, J. K., Huwe, L. W., Paschos, N., Aryaei, A., Gegg, C. A., Hu, J. C., and Athanasiou, K. A., 2017, “Tension Stimulation Drives Tissue Formation in Scaffold-Free Systems,” Nat. Mater., 16(8), pp. 864–873.

[21] Makris, E. A., Responte, D. J., Paschos, N. K., Hu, J. C., and Athanasiou, K. A., 2014, “Developing Functional Musculoskeletal Tissues through Hypoxia and Lysyl

Oxidase-Induced Collagen Cross-Linking," Proc. Natl. Acad. Sci., 111(45), pp. E4832–E4841.

[22] Huey, D. J., and Athanasiou, K. A., 2011, "Maturational Growth of Self-Assembled, Functional Menisci as a Result of TGF-B1 and Enzymatic Chondroitinase-ABC Stimulation," Biomaterials, 32(8), pp. 2052–2058.

[23] Makris, E. A., MacBarb, R. F., Paschos, N. K., Hu, J. C., and Athanasiou, K. A., 2014, "Combined Use of Chondroitinase-ABC, TGF-B1, and Collagen Crosslinking Agent Lysyl Oxidase to Engineer Functional Neotissues for Fibrocartilage Repair," Biomaterials, 35(25), pp. 6787–6796.

[24] MacBarb, R. F., Makris, E. A., Hu, J. C., and Athanasiou, K. A., 2013, "A Chondroitinase-ABC and TGF-B1 Treatment Regimen for Enhancing the Mechanical Properties of Tissue-Engineered Fibrocartilage," Acta Biomater., 9(1), pp. 4626–4634.

[25] Cissell, D. D., Link, J. M., Hu, J. C., and Athanasiou, K. A., 2017, "A Modified Hydroxyproline Assay Based on Hydrochloric Acid in Ehrlich's Solution Accurately Measures Tissue Collagen Content," Tissue Eng. Part C Methods, 23(4), pp. 243–250.

[26] Bielajew, B. J., Hu, J. C., and Athanasiou, K. A., 2021, "Methodology to Quantify Collagen Subtypes and Crosslinks: Application in Minipig Cartilages," Cartilage.

[27] Kazemi, M., and Li, L. P., 2014, "A Viscoelastic Poromechanical Model of the Knee Joint in Large Compression," Med. Eng. Phys., 36(8), pp. 998–1006.

[28] Robinson, D. L., Kersh, M. E., Walsh, N. C., Ackland, D. C., de Steiger, R. N., and Pandy, M. G., 2016, "Mechanical Properties of Normal and Osteoarthritic Human Articular Cartilage," J. Mech. Behav. Biomed. Mater., 61, pp. 96–109.

[29] Lin, W. Y., Chang, Y. H., Wang, H. Y., Yang, T. C., Chiu, T. K., Huang, S. Bin, and Wu, M. H., 2014, “The Study of the Frequency Effect of Dynamic Compressive Loading on Primary Articular Chondrocyte Functions Using a Microcell Culture System,” Biomed Res. Int., 2014.

[30] Shriram, D., Praveen Kumar, G., Cui, F., Lee, Y. H. D., and Subburaj, K., 2017, “Evaluating the Effects of Material Properties of Artificial Meniscal Implant in the Human Knee Joint Using Finite Element Analysis,” Sci. Rep., 7(1).

[31] Dwivedi, K. K., Lakhani, P., Kumar, S., and Kumar, N., 2022, “A Hyperelastic Model to Capture the Mechanical Behaviour and Histological Aspects of the Soft Tissues,” J. Mech. Behav. Biomed. Mater., 126, p. 105013.

[32] Basalo, I. M., Mauck, R. L., Kelly, T. A. N., Nicoll, S. B., Chen, F. H., Hung, C. T., and Ateshian, G. A., 2004, “Cartilage Interstitial Fluid Load Support in Unconfined Compression Following Enzymatic Digestion,” J. Biomech. Eng., 126(6), pp. 779–786.

[33] Makris, E. A., Hadidi, P., and Athanasiou, K. A., 2011, “The Knee Meniscus: Structure-Function, Pathophysiology, Current Repair Techniques, and Prospects for Regeneration,” Biomaterials, 32(30), pp. 7411–7431.

[34] Gonzalez-Leon, E. A., Hu, J. C., and Athanasiou, K. A., 1AD, “Yucatan Minipig Knee Meniscus Regional Biomechanics and Biochemical Structure Support Its Suitability as a Large Animal Model for Translational Research,” Front. Bioeng. Biotechnol., 0, p. 239.

[35] Bansal, S., Mandalapu, S., Aeppli, C., Qu, F., Szczesny, S. E., Mauck, R. L., and Zgonis, M. H., 2017, “Mechanical Function near Defects in an Aligned Nanofiber

Composite Is Preserved by Inclusion of Disorganized Layers: Insight into Meniscus Structure and Function," Acta Biomater., 56, pp. 102–109.

[36] Zhang, Z. Z., Chen, Y. R., Wang, S. J., Zhao, F., Wang, X. G., Yang, F., Shi, J. J., Ge, Z. G., Ding, W. Y., Yang, Y. C., Zou, T. Q., Zhang, J. Y., Yu, J. K., and Jiang, D., 2019, "Orchestrated Biomechanical, Structural, and Biochemical Stimuli for Engineering Anisotropic Meniscus," Sci. Transl. Med., 11(487).

Chapter 5: Improving mechanical properties of neocartilage with a combination of uniaxial tension and fluid-induced shear stress during tissue culture

Abstract

The manipulation of neocartilage construct mechanical properties toward native tissue values is typically achieved with bioactive factors or, less frequently, with applied mechanical stimuli during culture. Uniaxial tension stress, for example, has been found to improve tensile stiffness and strength of bovine-derived neocartilage constructs, while fluid-induced shear improved constructs' compressive stiffness. The objectives of this two-phase study were, first, to identify whether combining two mechanical stimulation strategies, specifically uniaxial tension and fluid-induced shear, would improve multiple neocartilage mechanical properties more effectively compared to using one stimulus alone and, second, to identify which order of application would lead to the most robust neocartilage constructs. It was found that the combination of both mechanical stimuli led to synergistic improvements to tensile properties and compressive stiffness. Furthermore, combining the stimuli had additive effects on the extracellular matrix content of constructs, compared to nonstimulated controls. Finally, it was determined that applying tension before fluid-induced shear was more effective toward improving tissue mechanical properties when compared to applying fluid-induced shear before tension. Overall, the use of complementary dual mechanical stimuli synergistically increased neocartilage

In preparation for submission as: Salinas, EY*, Gonzalez-Leon, EA*, Hu, JC, & Athanasiou, KA. *Improving mechanical properties of neocartilage with a combination of uniaxial tension and fluid-induced shear stress during tissue culture*, *indicates co-first authorship.

properties and a dependence on the order of application was identified; thus, researchers should consider applying these or other forms of complementary mechanical stimuli toward engineering neocartilage with robust properties.

5.1 Introduction

As an avascular tissue, articular cartilage does not have access to circulating progenitor cells and is not amenable to self-repair [1]. For the 250,000 Americans a year that seek clinical treatment for articular cartilage damage and degradation, tissue-engineered neocartilage has the potential to provide a long-term repair option [2]. Numerous studies have shown the benefits of using mechanical stimulation such as tension, compression, fluid-induced shear (FIS), and hydrostatic pressure during tissue engineering to enhance properties of a variety of tissues, including self-assembled neocartilage [3–8]. Such approaches often attempt to replicate mechanical movement in the body that enables nutrient delivery, cellular waste disposal, and signaling in cartilage [4]. Although the knee joint's movements combine to activate multiple mechanotransduction pathways [9], typical tissue engineering studies examine only one mechanical stimulus at a time [10–16].

Stimulating neocartilage with mechanical stresses during tissue culture has shown efficacy in improving neocartilage construct mechanical properties [15,17–22]. For example, intermittent (InTenS) and continuous (CoTenS) uniaxial tensile stress applied to self-assembled neocartilage on days 10-14 and days 7-28 of culture, respectively, led to improvements in tensile stiffness and strength that neared native tissue values [15], although increases to compressive properties were not seen. Additionally, uniaxial tensile stimulation has resulted in mechanical anisotropy in neocartilage constructs through

alignment of maturing collagen fibers along the axis of applied tension [15]. Tensile stimulation has not been applied beginning later than day 10 in the self-assembling process, though effectiveness may still be seen with a later application period due to the production and maturation of collagen fibers lasting several weeks [23]. Thus, while uniaxial tension has been effective in increasing tensile properties of self-assembled neocartilage near those of native tissue, a complementary stimulus regimen might be required to bolster compressive properties.

Another form of mechanical stimulus that has shown efficacy in improving self-assembled cartilage properties is FIS. When implemented at low frequencies (<1 Hz) and low magnitudes (<0.5 Pa) from days 7-13, days 7-19, or days 15-22, FIS has been shown to improve compressive properties and fiber density of neocartilage [16,24]. For example, the compressive aggregate modulus of self-assembled neocartilage increased by 450% over controls when subjected to FIS and was on par with that of native tissue [16,25]. Because no increases in collagen or GAG content were seen when applying FIS compared to nonstimulated controls, it was postulated that compressive properties benefited from increased fiber density [16]. Additionally, despite robust increases to compressive properties, tensile stiffness values of constructs attained were only 12% of native values [16,26]. This illustrates that FIS stimulus, despite improving compressive properties, may not be sufficient on its own to bring tensile properties to native values; the FIS stimulus could benefit from another form of stimulus during culture such as uniaxial tension.

Robust mechanical properties are needed for neocartilage implants because of the demanding mechanical environment within the knee [9,27–30]; combining

complementary forms of mechanical stimuli such as uniaxial tension and FIS may aid in elevating both tensile and compressive properties of neocartilage toward those of native tissue. Practical considerations into the application of multiple mechanical stimuli would include the sequence of application, which may require modifications to previously used regimens. For example, modification of the uniaxial tension regimen from days 7-28 to days 14-28 would allow for the investigation of the effects of applying a stimulus, such as FIS, before tension. While prior work showed that CoTenS applied to self-assembled neocartilage led to more robust tensile properties when combined with bioactive factors, shorter periods of applied uniaxial tension (InTenS; applied days 10-14) have also been effective toward increasing neocartilage tensile properties [15]. Thus, while modified versions of efficacious regimens are needed to accommodate an investigation into their sequential application, modified stimulus regimens might still provide benefits to neocartilage properties.

While modified mechanical stimulus regimens might be needed to investigate their sequential application to neocartilage constructs in different bioreactors, the order of their application and the animal model used should also be considered. Direct comparison of the order in which stimuli are applied (i.e., tension before shear versus shear before tension) to nonstimulated controls in another experimental phase would better elucidate the optimal order of application. Furthermore, comparing the application of only uniaxial tension to nonstimulated controls in an initial experimental phase would also serve to elucidate the effects of this mechanical stimuli in a new model, as previous investigations into its effectiveness have primarily used bovine or human models [15,16]. Thus, proposed regimens in these two experimental phases could elucidate whether these

stimuli are more beneficial in a sequential combination than on their own and could also validate the optimal order in which to apply them.

Motivated by the benefits of mechanical stimulation via uniaxial tension and FIS, the objective of this work was to examine these stimuli in combination as well as the order of application for each stimulus, using a two-phase design. The first phase of this study compared the combination of tension in addition to FIS stimulation (T+S) on neocartilage constructs against neocartilage that was stimulated with only tension (T), only FIS (S), or nonstimulated controls in static culture to identify whether either stimulus was effective on its own and whether using two stimuli was more effective than using only one. For the first phase of the study, it was hypothesized that 1) T and S would improve tensile and compressive properties of neocartilage over nonstimulated controls, respectively, and 2) neocartilage constructs receiving T+S would display improved mechanical and biochemical properties over constructs that only received one form of mechanical stimulus or no stimulus at all. In the second phase of this study, which depended on the results from phase 1, the order of application in which stimuli were applied was investigated to identify an optimized stimulation regimen for increasing tissue properties. For phase 2, it was hypothesized that the order in which mechanical stimuli were applied would lead to differences in functional properties of neocartilage.

5.2 Materials and Methods

5.2.1 Study design

Phase 1 - Neocartilage constructs were created with expanded and rejuvenated minipig costal chondrocytes using the self-assembling process [15]. Constructs were treated according to four different experimental groups: 1) nonstimulated control, 2) uniaxial

tensile stress (T), 3) FIS stress (S), 4) combination of uniaxial tensile stress followed by FIS stress (T+S; Figure 5.1), as described under Mechanical stimulation.

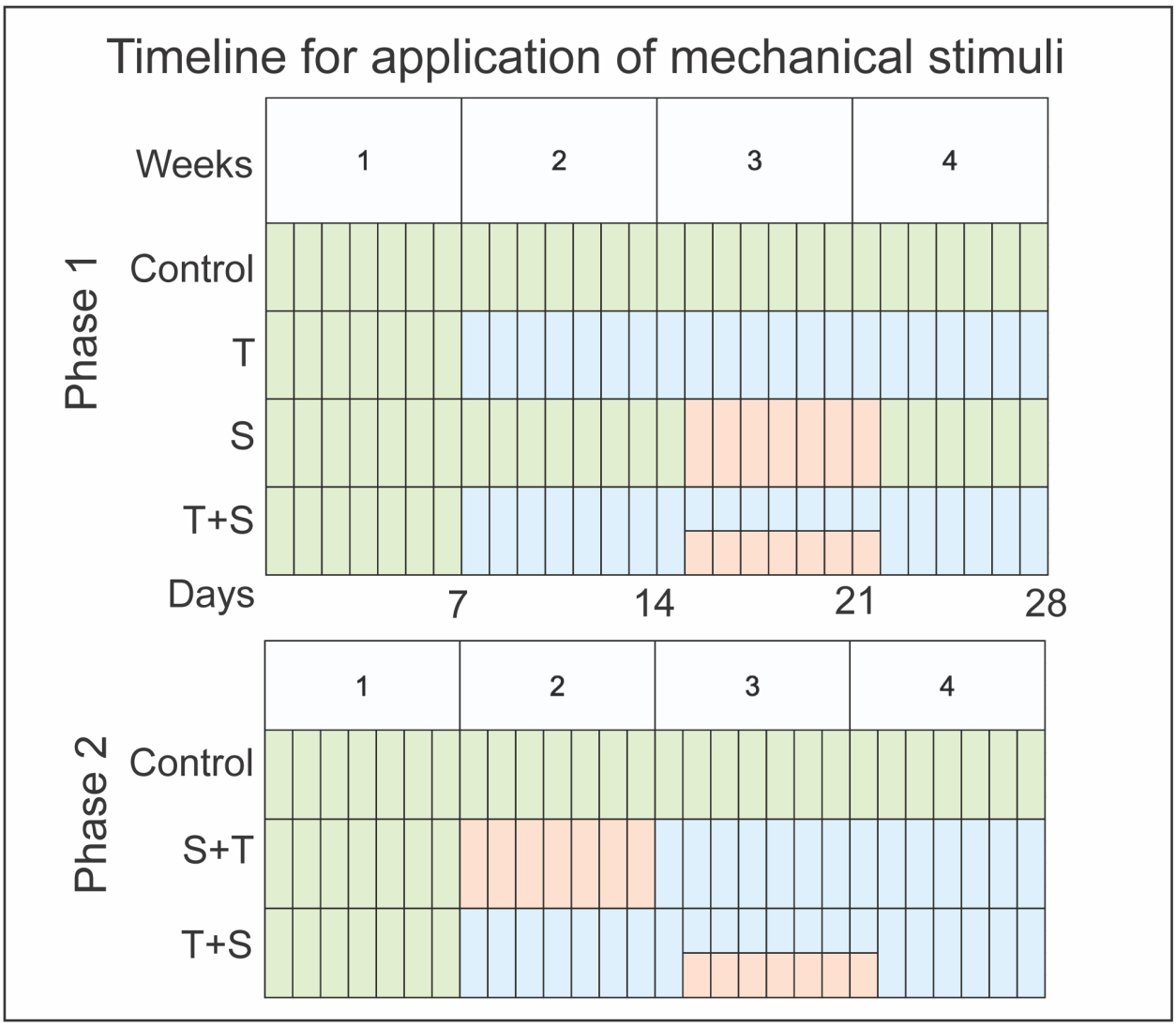

Figure 5.1: Timeline of mechanical stimulation applications. Uniaxial tension was applied to neocartilage constructs from days 7-28 in T and T+S groups, while S+T groups received tension from days 14-28. S and T+S groups were treated with fluid-induced shear stress (FIS) from days 15-22, while FIS was applied from days 7-14 for the S+T group.

Phase 2 - Neocartilage constructs were created with expanded and rejuvenated minipig costal chondrocytes using the self-assembling process. Neocartilage constructs were treated according to three different experimental groups: 1) nonstimulated control, 2) combination of FIS stress followed by uniaxial tensile stress (S+T), 3) combination of uniaxial tensile stress followed by FIS stress (T+S).

5.2.2 Mini pig costal chondrocyte harvest

Mini pig costal chondrocytes were harvested from the costal cartilage of juvenile (6-8 months) Yucatan minipigs (S&S Farms, California, USA). The perichondrium was first removed from the costal cartilage before mincing. Next, the minced cartilage was digested in a solution of 0.2% w/v collagenase and 3% fetal bovine serum (FBS) for 18 hours. After isolation, cells were frozen at -80°C for 24 hours in Dulbecco's modified Eagle's medium (DMEM) supplemented with 20% fetal bovine serum and 10% dimethyl sulfoxide medium at 5 million cells per milliliter before being stored in liquid nitrogen until seeding.

5.2.3 Expansion and aggregate rejuvenation

Minipig costal chondrocytes were thawed in a water bath at 37°C, rinsed in wash media, centrifuged at 400 x g, and resuspended in warm chondrogenic medium (CHG) with 2% FBS. The cells were counted and brought to 1e6 cells/ml in CHG+2% FBS plus growth factors (1ng/ml TGF-β1 + 5ng/ml bFGF + 10ng/ml PDGF). Finally, 2.5ml of the cell solution plus 27.5 ml of CHG+2% FBS were seeded per T225 flask, and the flasks were placed in an incubator at 10% CO2. Chondrogenic medium and growth factors were changed every 3-4 days. Cells were passaged once they reached approximately 95% confluency, as previously described [31].

Briefly, cells were lifted using 0.05% Trypsin-EDTA and then rinsed in chondrogenic medium. Cells were then resuspended in a solution of 2% collagenase and 3% FBS for 2 hours at 37°C. Cells were then seeded onto a T225 flask as specified above. Once the cells were expanded to passage 3, they were placed into aggregate rejuvenation, as described previously [32,33]. Briefly, cells were lifted from expansion and placed in a 1% agarose coated petri dish at 10e6 cell/mL of chondrogenic medium and growth factors (10ng/mL TGF-β1 + 100ng/mL GDF5 + 100ng/mL BMP-2). The petri dish was then placed on an orbital shaker at 50 RPM for the first 24 hours after seeding. Next, the petri dish was taken off the shaker and fed every 3-4 days for 11 days. The aggregates were then digested using 0.05% trypsin-EDTA solution for 45 minutes and, subsequently, 2% collagenase solution (with 3% FBS) for 1.5 hours to liberate the chondrocytes that were used to make the neocartilage.

5.2.4 Neocartilage self-assembly

First, 8x13mm agarose (2%) wells were created using an acrylic well-maker as described previously [34]. Each well was seeded with 7 million chondrocytes suspended in 250µl of CHG; after 4 hours, the cells were fed with 1 mL CHG. Medium in the wells was replaced every day for the first 2 days. On day 3, the neocartilage was removed from the wells, placed in 6-well plates, and CHG (5mL) was replaced every other day. The total culture duration time was 28 days.

5.2.5 Mechanical stimulation

Phase 1 - Continuous uniaxial tension regimen was implemented as previously described [15]. Briefly, the application of tensile strain was as follows: 12-15% on day 7, followed by approximately 4-6% additional strain applied each day from days 8-12 and then held taut

under tension until day 28 (Figure 5.1); thus, tensile strain was applied continuously from days 7-28. FIS stress was applied in a separate bioreactor (Figure 5.2) from days 15-22 at a previously identified optimal magnitude of 0.05-0.21Pa at 50 RPM [16] (Figure 5.2).

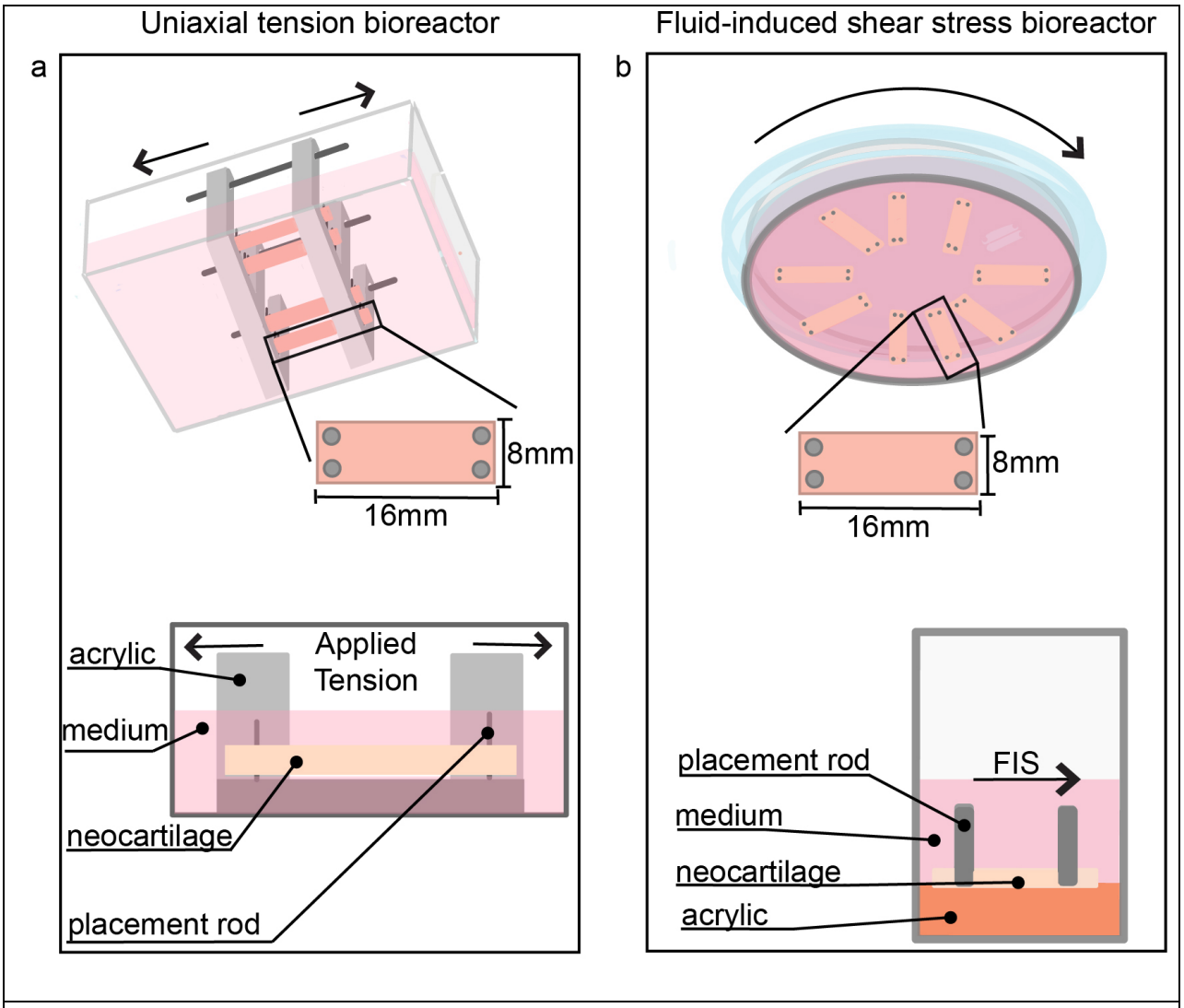

Figure 2: Bioreactor design. Bottom-up and side views of a) uniaxial tension and b) fluid-induced shear (FIS) stress bioreactors are shown not drawn to scale.

Phase 2 – The mechanical stimulation regimen for the T+S group in phase 1 was also used in phase 2. For the S+T stimulated groups, FIS stress was applied from day 7-14 as described above; in terms of uniaxial tension applied to S+T constructs, 12-15% tensile

strain was applied on day 14, followed by approximately 4-6% additional strain applied each day from days 15-19 and held taught under tension until day 28.

5.2.6 Mechanical testing

At day 28, neocartilage constructs were removed from culture, photographed, and measured using ImageJ (NIH). To determine the compressive properties, a cylindrical 2mm punch was taken from the center of the construct, and a creep indentation test was administered. The aggregate modulus was calculated as described previously [35].

Tensile testing was conducted parallel to the direction of applied tension of neocartilage constructs (i.e., along the long axis) using a uniaxial material testing machine (Instron model 5565); phase 2 of this study also investigated tensile properties in the direction perpendicular to applied tension (i.e., along the short axis). Neocartilage constructs were cut into dog bone-shaped samples and glued to paper strips with cyanoacrylate glue; the paper strips were then clamped within a uniaxial testing machine (Instron model 5565) and subjected to a strain rate of 1% of the gauge length per second strain rate until failure. ImageJ was used to measure sample thickness and width to calculate the cross-sectional area. Load–displacement curves were normalized to the cross-sectional area of each sample, and the Young's modulus and ultimate tensile strength (UTS) were calculated with MATLAB.

5.2.7 Extracellular matrix content analysis

Biochemistry samples were weighed wet, then frozen and lyophilized to acquire dry weights. Collagen content was measured with the use of a Sircol standard (Biocolor) and a modified Chloramine-T colorimetric hydroxyproline assay [36]. GAG content was quantified using the Blyscan assay kit (Invitrogen). All quantification measurements for

collagen and GAG content were performed with a GENios spectrophotometer/spectrofluorometer (TECAN).

5.2.8 Statistics

For each biomechanical and biochemical test, n=5-6 samples were used; biochemical tests for the nonstimulated control group in Phase 2 of this study used n=3 due to the loss of a sample. Results were analyzed with single-factor analysis of variance (ANOVA) followed by a Tukey's HSD post hoc test when merited ($p<0.05$). All data are presented as means ± standard deviations. For all figures, statistical significance is indicated by a connecting letters report; significance is indicated by groups not sharing the same letters. To examine synergism in Phase 1, the following equation was used:

$$(\mu_{T+S} - \mu_{control}) > (\mu_T - \mu_{control}) + (\mu_S - \mu_{control})$$

5.3 Results

5.3.1 Phase 1

Tensile Properties

Neocartilage constructs in the T+S and T groups displayed significantly higher tensile Young's modulus and UTS values compared to those in the nonstimulated control group; additionally, T+S stimulated constructs were significantly stiffer than all other groups, and significantly stronger in tension than S and nonstimulated control groups (Figure 5.3). T+S Young's modulus and UTS values were measured at 4.67±0.49 MPa and 2.06±0.46 MPa, respectively. Constructs from the S only group were not significantly different from nonstimulated controls in tensile Young's modulus or UTS.

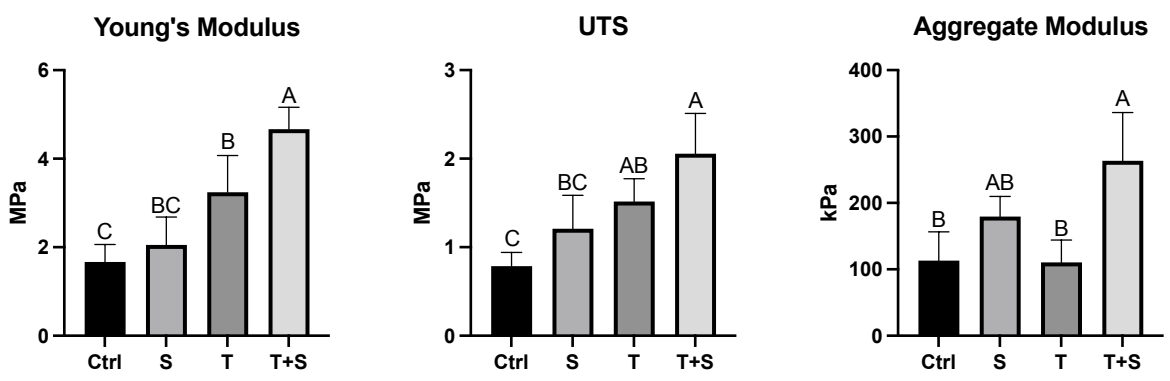

Figure 5.3: Mechanical properties of Phase 1 neocartilage constructs. Tensile Young's modulus, ultimate tensile strength (UTS), and aggregate modulus are shown. A significant difference was seen in tensile stiffness between Tension+Shear (T+S) constructs and tension only (T), FIS only (S), and nonstimulated controls (Ctrl). A significant difference was seen in tensile strength between T+S and Ctrl constructs. T+S constructs also exhibited significantly higher aggregate modulus values than Ctrl and T groups. All data are presented as means ± standard deviations. For all figures, statistical significance is indicated by bars not sharing the same letters within the same meniscus.

Compressive properties

Neocartilage constructs receiving T+S treatment exhibited significantly higher aggregate modulus values over T and nonstimulated control groups. (Figure 5.3); the combination of T+S stimulation in neocartilage tissue culture synergistically increased the aggregate modulus to 263±73 kPa. Compressive stiffness was not significantly different between the nonstimulated control group and samples stimulated with S or T only (Figure 5.3).

Biochemical properties

Neocartilage constructs treated with T+S and S stimulation contained a significantly higher amount of collagen (COL) per wet weight (WW) compared to nonstimulated controls (Figure 5.4); T+S and S groups contained 2.02±0.19% and 1.85±0.23% COL/WW, respectively. Neocartilage constructs that were stimulated with only T did not contain a significantly different amount of COL/WW than nonstimulated control or T+S groups. No significant differences were seen among groups in collagen content normalized to dry weight (DW).

Neocartilage constructs that were stimulated with T did not contain a significantly different amount of glycosaminoglycan (GAG) per wet weight than nonstimulated control or S groups. The T+S and S groups contained a significantly higher amount of GAG/WW than nonstimulated controls; the T+S group also contained significantly more GAG/WW than T only constructs. T+S and S groups contained 4.82±0.36% and 4.28±0.45% GAG/WW, respectively. T+S stimulated constructs contained 35.93±2.73% GAG/DW, which was significantly higher than nonstimulated control and T groups.

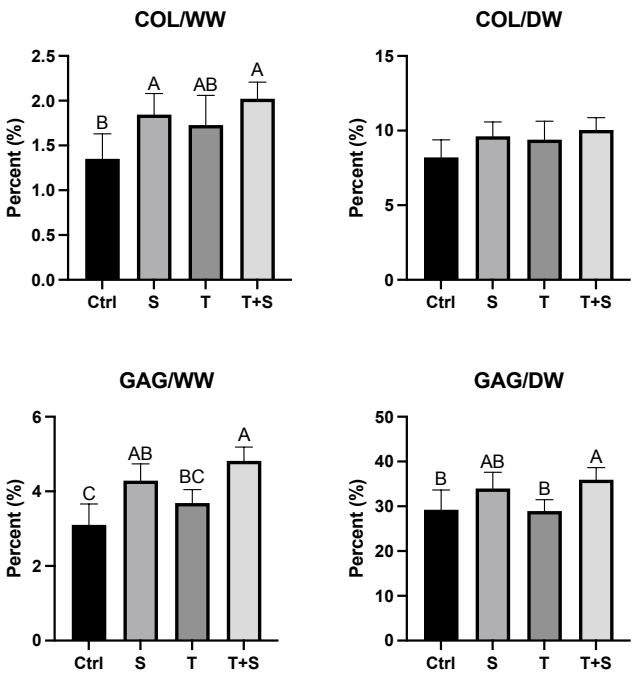

Figure 4: Biochemical properties of Phase 1 neocartilage constructs. T+S and S stimulated constructs were significantly higher in COL/WW than nonstimulated controls, while no differences were seen among groups in COL/DW. T+S stimulated constructs were significantly higher in GAG/WW and GAG/DW content over nonstimulated controls and T only groups. All data are presented as means ± standard deviations.

5.3.2 Phase 2

Tensile Properties

Neocartilage constructs stimulated with T+S were significantly stiffer and stronger in tension in the parallel direction compared to nonstimulated controls; however, no differences were seen between T+S and S+T groups (Figure 5.5). T+S stimulated constructs contained Young's modulus and UTS values of 5.70±1.91 MPa and 1.33±0.23 MPa in the parallel direction, respectively. Additionally, no significant differences were seen among all groups in tensile Young's modulus or UTS in the perpendicular direction.

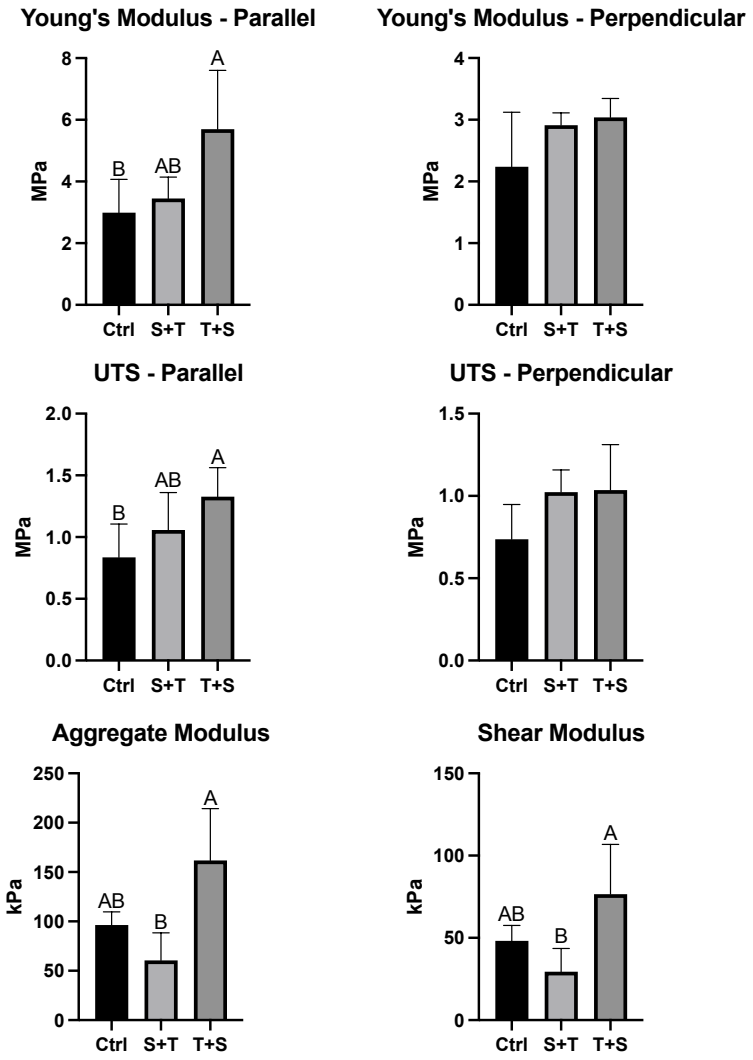

Figure 5.5: Mechanical properties of phase 2 neocartilage constructs. T+S stimulated constructs were significantly stiffer and stronger in tension in the parallel direction than non-stimulated controls; no significant differences were seen in tensile properties in the parallel direction. T+S stimulated constructs exhibited significantly higher aggregate and shear modulus values than S+T stimulated constructs but were not significantly different when compared to nonstimulated controls. All data are presented as means ± standard deviations.

Compressive properties

Neocartilage construct aggregate modulus values were significantly higher in the T+S group compared to the S+T group; however, no significant differences were seen in either the S+T or T+S groups over nonstimulated controls. T+S, S+T, and nonstimulated controls exhibited aggregate modulus values of 161±53, 61±28, and 96±13 kPa, respectively.

Biochemical properties

Neocartilage constructs that were stimulated with S+T and T+S both contained significantly more COL/WW and COL/DW than nonstimulated controls (Figure 5.6). S+T and T+S groups contained 1.36±0.1% and 1.51±0.11% COL/WW, respectively, in addition to 10.68±0.75% and 11.44±0.74% COL/DW, respectively. Additionally, no differences were found among groups in GAG/WW and GAG/DW.

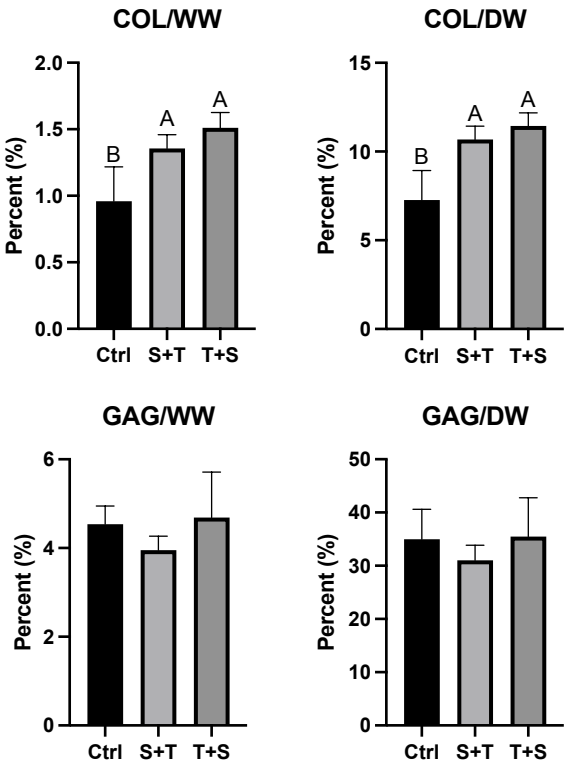

Figure 5.6: Biochemical properties of phase 2 neocartilage constructs. T+S and S+T stimulated groups both contained significantly more COL/WW and COL/DW than nonstimulated controls. No significant differences were seen among groups in GAG/WW or GAG/DW. All data are presented as means ± standard deviations.

5.4 Discussion

Previously, the application of uniaxial tension during culture was found to improve tensile stiffness and strength to near native articular cartilage values [15], while the application of FIS stress was found to improve compressive stiffness [16]. Toward reaping the benefits of both stimuli, the main objective of this work, conducted as a two-phase study, was first to determine if a combination of mechanical stimulation methods, specifically the application of uniaxial tension and FIS, could improve neocartilage construct properties over either form of stimulus alone. Secondly, the order in which the stimuli were applied was investigated to determine which regimen resulted in the most robust neocartilage constructs in terms of mechanical and biochemical properties. The hypotheses that 1) applying T and S on their own would lead to improvements in tensile and compressive properties over nonstimulated controls, respectively, and 2) applying the combination of T+S would yield improved mechanical properties over either stimulus alone and nonstimulated controls was largely supported by the data in phase 1 of this study. T significantly improved tensile stiffness and strength by 94% and 93% over nonstimulated controls, respectively; additionally, T+S stimulation synergistically improved neocartilage tensile Young's modulus, UTS, and aggregate modulus over the nonstimulated control group by 180%, 161%, and 133%, respectively. Subsequently, in phase 2 of this study, the hypothesis that the order in which mechanical stimuli were applied would lead to

differences in functional properties of neocartilage was supported; applying T+S led to significant increases of 90% and 59% to Young's modulus and UTS values over controls, respectively, whereas S+T only increased these same properties by 15% and 27%, respectively. These findings are significant because the data show that applying a combination of uniaxial tension and FIS is more effective toward increasing mechanical and biochemical properties of self-assembled neocartilage closer to values of native tissue than the use of one stimulus alone.

The results of phase 1 of this study indicated that a combination of complementary mechanical stimuli, uniaxial tension and FIS, synergistically improved mechanical and biochemical properties of neocartilage constructs. Tensile Young's modulus of T+S treated constructs reached approximately 56% of native tissue values, while aggregate modulus values of T+S constructs were on par with those of native tissue and 158% higher than those achieved with a combination of InTenS and a bioactive factor cocktail [16,25,26]; these results were not previously attainable with only one form of mechanical stimulus alone [15,16]. Phase 1 of this study also showed that COL/WW and GAG/WW levels of neocartilage constructs were significantly higher than controls by 50% and 55%, respectively, when receiving combined T+S treatment. In terms of extracellular matrix levels, the neocartilage constructs that received combined T+S treatment in phase 1 trended higher but were not significantly different from constructs in the S group. However, the significant and synergistic improvements observed in mechanical properties indicate that uniaxial tension stress may be contributing to neocartilage extracellular matrix in ways that were not investigated here. For example, previous studies have demonstrated elevated levels of pyridinoline crosslinks in neocartilage

constructs stimulated with uniaxial tension stress [15,37–39]. Furthermore, uniaxial tension has also been shown to orient extracellular matrix fibers in the direction of applied tension, leading to anisotropy and enhancements in directional tensile properties [15]. Overall, the combination of uniaxial tension stress and fluid-induced shear stress yielded improvements to mechanical and extracellular matrix properties that were not seen in neocartilage constructs stimulated with only one form of mechanical stimulus.

Phase 2 affirmed that the order in which mechanical stimuli are applied is important to the effect on neocartilage properties; from phase 1, T+S stimulation was identified as the optimal stimulus regimen, because only T+S treated constructs significantly increased tensile stiffness, tensile strength, and compressive stiffness over nonstimulated controls. In phase 2, T+S was again found to significantly increase tensile stiffness and strength over nonstimulated controls. In comparison, the S+T group did not differ significantly in mechanical properties over controls. Instead, the S+T treatment regimen led to a 37% decrease in aggregate modulus compared to controls. Additionally, the T+S and S+T groups did not differ significantly in collagen or GAG content, implying that the order of applied stimulus affects neocartilage ECM structure and, thus, their functional properties. Therefore, applying tension early in the self-assembling process when extracellular matrix is produced [23] might aid in aligning the maturing collagen network in the direction parallel to that of the applied tension, thus contributing to improved tensile properties in that direction but not in the perpendicular direction. Also, while T+S treatment in phase 2 of this study led to a strong increasing trend of 68% in aggregate modulus values over controls ($p=0.11$), statistical significance was not seen as in phase 1. This is significant because it indicates that the order in which mechanical stimulation regimens are applied

can be configured to drive a multitude of neocartilage mechanical properties toward those of native tissue.

Interestingly, benefits to neocartilage properties from application of uniaxial tension or FIS that were first identified in previous studies were also seen in the current set of experiments [15,16]. Specifically, previous studies that applied T to self-assembled neocartilage used mainly bovine and human models while this one employed costal chondrocyte from minipigs [15,16]. T treatment significantly increased tensile properties of neocartilage over nonstimulated controls as hypothesized, validating the use of uniaxial tension toward enhancing properties of minipig-derived neocartilage. S treatment also significantly increased collagen content as seen in previous studies that applied FIS to minipig-derived neocartilage [24] and exhibited an increasing trend over controls in terms of aggregate modulus values ($p=0.19$). FIS stimulation in the S+T treatment was more akin to the original regimen used in bovine and human models, where it was applied on days 7-13 (S+T applied FIS from days 7-14 in this study), yet this did not lead to improvement in mechanical properties over nonstimulated controls; a previous study in which FIS was applied during the synthesis phase of the self-assembling process (days 7-14) did not lead to improvements in mechanical or biochemical properties of minipig-derived neocartilage constructs, supporting the findings in this work [24]. Thus, the T and S regimens were largely effective toward increasing neocartilage properties when applied on their own in constructs derived from a Yucatan minipig model, which is becoming increasingly used in translational orthopedic research [40–42].

Inasmuch as different forms of mechanical stimuli, and their sequential combination, were effective toward increasing neocartilage properties, a pertinent next

step might be to develop a bioreactor that allows for their simultaneous application from the onset of the stimulus regimen; a limitation of this study is that constructs were not able to receive additional tensile strain within the FIS bioreactor, despite being able to keep constructs taut under constant tension after being moved from the uniaxial tension bioreactor. This would allow for both stimuli to begin at the same time, last for up to the duration of the entire culture period, and possibly stimulate different mechanotransduction pathways in concert to better enhance tissue properties. T+S treatment led to the most robust increases to neocartilage properties in both experimental phases and was the only regimen that had a period of overlapping stimuli (Figure 5.1), showing the benefits of simultaneous stimulus application. Thus, the data provided in this study helps establish the use of these two complementary mechanical stimuli toward benefitting self-assembled neocartilage properties and motivates the use of bioreactors that facilitate their simultaneous application.

When tissue-engineering articular cartilage, stimuli such as exogenous bioactive factors are more commonly used in tissue culture than mechanical stimulation. Previous studies have found that bioactive factors can be used in combination to improve multiple neocartilage properties [43–46]. For example, the use of TGF-β1, C-ABC, and LOXL2 (TCL) has been found to improve collagen content and tensile properties of self-assembled neocartilage [43,47]; interestingly, the use of T+S in this set of experiments without using TCL led to neocartilage that was 84% and 78% stiffer in tension and compression, respectively, compared to constructs that were treated with the TCL regimen in a previous study [15]. Although the ease of applying soluble bioactive factors, such as growth factors and enzymes, is appealing, there are several drawbacks when

translating their use to preclinical studies. For example, some bioactive factors, such as transforming growth factors, elicit pleiotropic effects that could potentially lead to mutations, unless the growth factors are sufficiently washed away before implantation; additionally, the use of enzymes increases the risk of carrying over these enzymes into the body by the implanted neocartilage [48–51]. Furthermore, biochemical stimuli can be financially burdensome, especially when used in large quantities; meanwhile, bioreactors for mechanically stimulating neocartilage constructs might, for example, be created using additive manufacturing or molds at a low cost and are readily available for re-use. Safety and financial factors of culture additives or stimuli should be considered when aiming to translate tissue engineered regenerative solutions from the bench to the clinic and, thus, mechanical stimuli should be considered during culture as they provide a safe and effective way of tailoring neocartilage properties closer to those of native tissue [52].

The prevalence and economic impact of articular cartilage injuries motivate novel regenerative solutions through tissue engineering, and investigation into stimuli that help engineered tissue properties approach those of native tissue. There is still much to be studied in terms of using mechanical stimulation in neocartilage tissue engineering, specifically those created using the self-assembling process. A study comparing the outcomes of using only bioactive factors to the use of only mechanical stimulation with uniaxial tension and fluid-induced shear, for example, could demonstrate which is more efficient in improving neocartilage properties. Alternatively, combining the use of both mechanical stimuli and bioactive factors that have been shown to not have adverse effects in vivo may be useful in enhancing engineered tissue properties. Manipulating neocartilage constructs with mechanical stimulation can provide mechanically robust and

potentially safer options for implantation in preclinical studies bringing tissue engineered articular cartilage closer to the clinic.

References

[1] Huey, D. J., Hu, J. C., and Athanasiou, K. A., 2012, “Unlike Bone, Cartilage Regeneration Remains Elusive.,” Science, 338(6109), pp. 917–21.

[2] McCormick, F., Harris, J. D., Abrams, G. D., Frank, R., Gupta, A., Hussey, K., Wilson, H., Bach, B., and Cole, B., 2014, “Trends in the Surgical Treatment of Articular Cartilage Lesions in the United States: An Analysis of a Large Private-Payer Database over a Period of 8 Years,” Arthroscopy, 30(2), pp. 222–226.

[3] Salinas, E. Y., Hu, J. C., and Athanasiou, K., 2018, “A Guide for Using Mechanical Stimulation to Enhance Tissue-Engineered Articular Cartilage Properties,” Tissue Eng. Part B. Rev., 24(5), pp. 345–358.

[4] Li, K., Zhang, C., Qiu, L., Gao, L., and Zhang, X., 2017, “Advances in Application of Mechanical Stimuli in Bioreactors for Cartilage Tissue Engineering,” Tissue Eng. Part B. Rev., 23(4), pp. 399–411.

[5] Park, S., Hung, C. T., and Ateshian, G. A., 2004, “Mechanical Response of Bovine Articular Cartilage under Dynamic Unconfined Compression Loading at Physiological Stress Levels,” Osteoarthr. Cartil., 12(1), pp. 65–73.

[6] Lin, W. Y., Chang, Y. H., Wang, H. Y., Yang, T. C., Chiu, T. K., Huang, S. Bin, and Wu, M. H., 2014, “The Study of the Frequency Effect of Dynamic Compressive Loading on Primary Articular Chondrocyte Functions Using a Microcell Culture System,” Biomed Res. Int., 2014.

[7] Natenstedt, J., Kok, A. C., Dankelman, J., and Tuijthof, G. J. M., 2015, “What Quantitative Mechanical Loading Stimulates in Vitro Cultivation Best?,” J. Exp. Orthop., 2(1), pp. 1–15.

[8] El-Ayoubi, R., Degrandpré, C., Diraddo, R., Yousefi, A. M., and Lavigne, P., 2011, “Design and Dynamic Culture of 3D-Scaffolds for Cartilage Tissue Engineering,” J. Biomater. Appl., 25(5), pp. 429–444.

[9] Athanasiou, K. A., Darling, E. M., DuRaine, G. D., Hu, J. C., and Reddi, A. H., 2017, Articular Cartilage, Second Edition, CRC Press.

[10] Park, S., Krishnan, R., Nicoll, S. B., and Ateshian, G. A., 2003, “Cartilage Interstitial Fluid Load Support in Unconfined Compression,” J. Biomech., 36(12), p. 1785.

[11] Correia, C., Pereira, A. L., Duarte, A. R. C., Frias, A. M., Pedro, A. J., Oliveira, J. T., Sousa, R. A., and Reis, R. L., 2012, “Dynamic Culturing of Cartilage Tissue: The Significance of Hydrostatic Pressure,” Tissue Eng. Part A, 18(19–20), pp. 1979‑1991.

[12] Elder, B. D., and Athanasiou, K. A., 2009, “Effects of Temporal Hydrostatic Pressure on Tissue-Engineered Bovine Articular Cartilage Constructs,” Tissue Eng. Part A, 15(5), p. 1151.

[13] Elder, B. D., and Athanasiou, K. A., 2008, “Synergistic and Additive Effects of Hydrostatic Pressure and Growth Factors on Tissue Formation,” PLoS One, 3(6).

[14] Smith, R. L., Lin, ; J, Trindade, ; M C D, Shida, ; J, Kajiyama, ; G, Vu, ; T, Hoffman, ; A R, Van Der Meulen, ; M C H, Goodman, ; S B, Schurman, ; D J, and Carter, ; D R, “Time-Dependent Effects of Intermittent Hydrostatic Pressure on Articular c on Rocyte Type II Collagen and Aggrecan MRNA Expression,” Dep. Veterans Aff. J. Rehabil. Res. Dev., 37(2), pp. 153–161.

[15] Lee, J. K., Huwe, L. W., Paschos, N., Aryaei, A., Gegg, C. A., Hu, J. C., and Athanasiou, K. A., 2017, “Tension Stimulation Drives Tissue Formation in Scaffold-Free Systems,” Nat. Mater., 16(8), pp. 864–873.

[16] Salinas, E. Y., Aryaei, A., Paschos, N., Berson, E., Kwon, H., Hu, J. C., and Athanasiou, K. A., 2020, “Shear Stress Induced by Fluid Flow Produces Improvements in Tissue-Engineered Cartilage,” Biofabrication, 12(4).

[17] Wu, S., Wang, Y., Streubel, P. N., and Duan, B., 2017, “Living Nanofiber Yarn-Based Woven Biotextiles for Tendon Tissue Engineering Using Cell Tri-Culture and Mechanical Stimulation,” Acta Biomater., 62, pp. 102–115.

[18] Wartella, K. A., and Wayne, J. S., 2009, “Bioreactor for Biaxial Mechanical Stimulation to Tissue Engineered Constructs,” J. Biomech. Eng., 131(4).

[19] Gemmiti, C. V., and Guldberg, R. E., 2009, “Shear Stress Magnitude and Duration Modulates Matrix Composition and Tensile Mechanical Properties in Engineered Cartilaginous Tissue,” Biotechnol. Bioeng., 104(4), p. 809.

[20] Gemmiti, C. V., and Guldberg, R. E., 2006, “Fluid Flow Increases Type II Collagen Deposition and Tensile Mechanical Properties in Bioreactor-Grown Tissue-Engineered Cartilage,” Tissue Eng., 12(3), pp. 469–479.

[21] Nebelung, S., Gavenis, K., Lüring, C., Zhou, B., Mueller-Rath, R., Stoffel, M., Tingart, M., and Rath, B., 2012, “Simultaneous Anabolic and Catabolic Responses of Human Chondrocytes Seeded in Collagen Hydrogels to Long-Term Continuous Dynamic Compression,” Ann. Anat., 194(4), pp. 351–358.

[22] Kisiday, J. D., Jin, M., DiMicco, M. A., Kurz, B., and Grodzinsky, A. J., 2004, “Effects of Dynamic Compressive Loading on Chondrocyte Biosynthesis in Self-Assembling Peptide Scaffolds,” J. Biomech., 37(5), pp. 595–604.

[23] Athanasiou, K. A., Eswaramoorthy, R., Hadidi, P., and Hu, J. C., 2013, “Self-Organization and the Self-Assembling Process in Tissue Engineering,” Annu. Rev. Biomed. Eng., 15(1), pp. 115–136.

[24] Salinas, E. Y., Donahue, R. P., Hu, J. C., and Athanasiou, K. A., 2022, “The Functionality and Translatability of Neocartilage Constructs Are Improved with the Combination of Fluid-Induced Shear Stress and Bioactive Factors,” FASEB J.

[25] Oyadomari, S., Brown, W. E., Kwon, H., Otarola, G., Link, J. M., Athanasiou, K. A., and Wang, D., 2021, “In Vitro Effects of Bupivacaine on the Viability and Mechanics of Native and Engineered Cartilage Grafts,” Am. J. Sports Med., 49(5), pp. 1305–1312.

[26] Eleswarapu, S. V., Responte, D. J., and Athanasiou, K. A., 2011, “Tensile Properties, Collagen Content, and Crosslinks in Connective Tissues of the Immature Knee Joint,” PLoS One, 6(10).

[27] Martinac, B., 2004, “Mechanosensitive Ion Channels: Molecules of Mechanotransduction,” J. Cell Sci., 117(Pt 12), pp. 2449–2460.

[28] Wang, N., Tytell, J. D., and Ingber, D. E., 2009, “Mechanotransduction at a Distance: Mechanically Coupling the Extracellular Matrix with the Nucleus,” Nat. Rev. Mol. Cell Biol. 2009 101, 10(1), pp. 75–82.

[29] Katsumi, A., Orr, A. W., Tzima, E., and Schwartz, M. A., 2004, “Integrins in Mechanotransduction *,” J. Biol. Chem., 279(13), pp. 12001–12004.

[30] Dahl, K. N., Ribeiro, A. J. S., and Lammerding, J., 2008, “Nuclear Shape, Mechanics, and Mechanotransduction,” Circ. Res., 102(11), pp. 1307–1318.

[31] Vapniarsky, N., Huwe, L. W., Arzi, B., Houghton, M. K., Wong, M. E., Wilson, J. W., Hatcher, D. C., Hu, J. C., and Athanasiou, K. A., 2018, “Tissue Engineering toward Temporomandibular Joint Disc Regeneration,” Sci. Transl. Med., 10(44).

[32] Murphy, M. K., Masters, T. E., Hu, J. C., and Athanasiou, K. A., 2015, “Engineering a Fibrocartilage Spectrum through Modulation of Aggregate Redifferentiation,” Cell Transplant., 24(2), pp. 235–245.

[33] Kwon, H., Brown, W. E., O’Leary, S. A., Hu, J. C., and Athanasiou, K. A., 2021, “Rejuvenation of Extensively Passaged Human Chondrocytes to Engineer Functional Articular Cartilage,” Biofabrication, 13(3).

[34] Huwe, L. W., Sullan, G. K., Hu, J. C., and Athanasiou, K. A., 2018, “Using Costal Chondrocytes to Engineer Articular Cartilage with Applications of Passive Axial Compression and Bioactive Stimuli,” Tissue Eng. Part A, 24(5–6), pp. 516–526.

[35] Mow, V. C., Gibbs, M. C., Lai, W. M., Zhu, W. B., and Athanasiou, K. A., 1989, “Biphasic Indentation of Articular Cartilage-II. A Numerical Algorithm and an Experimental Study,” J. Biomech., 22(8–9), pp. 853–861.

[36] Cissell, D. D., Link, J. M., Hu, J. C., and Athanasiou, K. A., 2017, “A Modified Hydroxyproline Assay Based on Hydrochloric Acid in Ehrlich’s Solution Accurately Measures Tissue Collagen Content,” Tissue Eng. Part C Methods, 23(4), pp. 243–250.

[37] Makris, E. A., MacBarb, R. F., Responte, D. J., Hu, J. C., and Athanasiou, K. A., 2013, “A Copper Sulfate and Hydroxylysine Treatment Regimen for Enhancing Collagen

Cross-Linking and Biomechanical Properties in Engineered Neocartilage.," FASEB J., 27(6), pp. 2421–30.

[38] Williamson, A. K., Chen, A. C., Masuda, K., Thonar, E. J., and Sah, R. L., 2003, "Tensile Mechanical Properties of Bovine Articular Cartilage: Variations with Growth and Relationships to Collagen Network Components," J. Orthop. Res., 21(5), pp. 872–880.

[39] Williamson, A. K., Masuda, K., Thonar, E. J. M. A., and Sah, R. L., 2003, "Growth of Immature Articular Cartilage in Vitro: Correlated Variation in Tensile Biomechanical and Collagen Network Properties," Tissue Eng., 9(4), pp. 625–634.

[40] Pfeifer, C. G., Fisher, M. B., Saxena, V., Kim, M., Henning, E. A., Steinberg, D. A., Dodge, G. R., and Mauck, R. L., 2017, "Age-Dependent Subchondral Bone Remodeling and Cartilage Repair in a Minipig Defect Model," Tissue Eng. Part C. Methods, 23(11), pp. 745–753.

[41] Sennett, M. L., Friedman, J. M., Ashley, B. S., Stoeckl, B. D., Patel, J. M., Alini, M., Cucchiarini, M., Eglin, D., Madry, H., Mata, A., Semino, C., Stoddart, M. J., Johnstone, B., Moutos, F. T., Estes, B. T., Guilak, F., Mauck, R. L., and Dodge, G. R., 2021, "Long Term Outcomes of Biomaterial-Mediated Repair of Focal Cartilage Defects in a Large Animal Model," Eur. Cell. Mater., 41, pp. 40–51.

[42] Nordberg, R. C., Huebner, P., Schuchard, K. G., Mellor, L. F., Shirwaiker, R. A., Loboa, E. G., and Spang, J. T., 2021, "The Evaluation of a Multiphasic 3D-Bioplotted Scaffold Seeded with Adipose Derived Stem Cells to Repair Osteochondral Defects in a Porcine Model," J. Biomed. Mater. Res. B. Appl. Biomater., 109(12), pp. 2246–2258.

[43] Makris, E. A., MacBarb, R. F., Paschos, N. K., Hu, J. C., and Athanasiou, K. A., 2014, "Combined Use of Chondroitinase-ABC, TGF-B1, and Collagen Crosslinking Agent

Lysyl Oxidase to Engineer Functional Neotissues for Fibrocartilage Repair," Biomaterials, 35(25), pp. 6787–6796.

[44] Elder, B. D., and Athanasiou, K. A., 2009, "Systematic Assessment of Growth Factor Treatment on Biochemical and Biomechanical Properties of Engineered Articular Cartilage Constructs," Osteoarthritis Cartilage, 17(1), p. 114.

[45] Huang, A. H., Stein, A., Tuan, R. S., and Mauck, R. L., 2009, "Transient Exposure to Transforming Growth Factor Beta 3 Improves the Mechanical Properties of Mesenchymal Stem Cell-Laden Cartilage Constructs in a Density-Dependent Manner," Tissue Eng. Part A, 15(11), pp. 3461–3472.

[46] Studer, R. K., Bergman, R., Stubbs, T., and Decker, K., 2003, "Chondrocyte Response to Growth Factors Is Modulated by P38 Mitogen-Activated Protein Kinase Inhibition," Arthritis Res Ther 2004 61, 6(1), pp. 1–9.

[47] Kwon, H., O'Leary, S. A., Hu, J. C., and Athanasiou, K. A., 2019, "Translating the Application of Transforming Growth Factor-B1, Chondroitinase-ABC, and Lysyl Oxidase-like 2 for Mechanically Robust Tissue-Engineered Human Neocartilage," J. Tissue Eng. Regen. Med., 13(2), pp. 283–294.

[48] Bian, L., Crivello, K. M., Ng, K. W., Xu, D., Williams, D. Y., Ateshian, G. A., and Hung, C. T., 2009, "Influence of Temporary Chondroitinase ABC-Induced Glycosaminoglycan Suppression on Maturation of Tissue-Engineered Cartilage," Tissue Eng. Part A, 15(8), pp. 2065–2072.

[49] Lin, R., Kwok, J. C. F., Crespo, D., and Fawcett, J. W., 2008, "Chondroitinase ABC Has a Long-Lasting Effect on Chondroitin Sulphate Glycosaminoglycan Content in the Injured Rat Brain," J. Neurochem., 104(2), pp. 400–408.

[50] Fleisch, M. C., Maxwell, C. A., and Barcellos-Hoff, M. H., 2006, “The Pleiotropic Roles of Transforming Growth Factor Beta in Homeostasis and Carcinogenesis of Endocrine Organs,” Endocr. Relat. Cancer, 13(2), pp. 379–400.

[51] Farhat, Y. M., Al-Maliki, A. A., Chen, T., Juneja, S. C., Schwarz, E. M., O’Keefe, R. J., and Awad, H. A., 2012, “Gene Expression Analysis of the Pleiotropic Effects of TGF-B1 in an in Vitro Model of Flexor Tendon Healing,” PLoS One, 7(12).

[52] Donahue, R. P., Gonzalez-Leon, E. A., Hu, J. C., and Athanasiou, K. A., 2019, “Considerations for Translation of Tissue Engineered Fibrocartilage from Bench to Bedside,” J. Biomech. Eng., 141(7).

Chapter 6: Yucatan minipig knee meniscus regional biomechanics structure support its suitability as a large animal model for translational research

Abstract

Knee meniscus injuries are the most frequent causes of orthopedic surgical procedures in the U.S., motivating tissue engineering attempts and the need for suitable animal models. Despite extensive use in cardiovascular research and the existence of characterization data for the menisci of farm pigs, the farm pig may not be a desirable preclinical model for the meniscus due to rapid weight gain. Minipigs are conducive to *in vivo* experiments due to their slower growth rate than farm pigs and similarity in weight to humans. However, characterization of minipig knee menisci is lacking**.** The objective of this study was to extensively characterize structural and functional properties within different regions of both medial and lateral Yucatan minipig knee menisci to inform this model's suitability as a preclinical model for meniscal therapies. Menisci measured 23.2-24.8mm in anteroposterior length (33-40mm for human), 7.7-11.4mm in width (8.3-14.8mm for human), and 6.4-8.4mm in peripheral height (5-7mm for human). Per wet weight, biochemical evaluation revealed 23.9-31.3% collagen (COL; 22% for human) and 1.20-2.57% glycosaminoglycans (GAG; 0.8% for human). Also, per dry weight, pyridinoline crosslinks (PYR) were 0.12-0.16% (0.12% for human) and, when normalized to collagen content, reached as high as 1.45-1.96ng/μg. Biomechanical testing revealed

Published as: Gonzalez-Leon, EA, Hu, JC, & Athanasiou, KA. *Yucatan minipig knee meniscus regional biomechanics and biochemical structure support its suitability as a large animal model for translational research.* Frontiers in Biomedical Engineering and Biotechnology. (2022).

circumferential Young's modulus of 78.4-116.2MPa (100-300MPa for human), circumferential ultimate tensile strength (UTS) of 18.2-25.9MPa (12-18MPa for human), radial Young's modulus of 2.5-10.9MPa (10-30MPa for human), radial UTS of 2.5-4.2MPa (1-4MPa for human), aggregate modulus of 157-287kPa (100-150kPa for human), and shear modulus of 91-147kPa (120kPa for human). Anisotropy indices ranged from 11.2-49.4 and 6.3-11.2 for tensile stiffness and strength (approximately 10 for human), respectively. Regional differences in mechanical and biochemical properties within the minipig medial meniscus were observed; specifically, GAG, PYR, PYR/COL, radial stiffness, and Young's modulus anisotropy varied by region. The posterior region of the medial meniscus exhibited the lowest radial stiffness, which is also seen in humans and corresponds to the most prevalent location for meniscal lesions. Overall, similarities between minipig and human menisci support the use of minipigs for meniscus translational research.

6.1. Introduction

Damage to the knee meniscus can result from trauma or age-related degeneration; meniscal lesions are the most common intra-articular knee injury and account for the most frequent cause of orthopedic surgical procedures in the U.S. [1]. Specifically, up to 20% of orthopedic procedures involve surgery on the meniscus, leading to approximately 850,00 patients per year [2]. The medial meniscus is about 4-times more likely to be damaged and undergo surgery compared to the lateral meniscus [3]. Additionally, the meniscus is a fibrocartilaginous tissue that is nearly avascular and, thus, is generally not amenable to repair. Differences in injury prevalence between medial and lateral menisci can result from differences in structural properties and, thus, functionality, making it

important to consider these properties during every step of developing new therapies, such as tissue engineered menisci.

Options for the management of meniscal injuries vary with respect to disease severity and type, ranging from physical therapy to invasive surgical intervention [4–6]. Meniscectomy, the partial or complete removal of the knee meniscus, can relieve pain but is reserved for cases in which meniscus repair is unlikely (e.g., tears in the avascular portion) [7,8]. Removal of either meniscus greatly predisposes a patient to osteoarthritis [9]. Thus, novel regenerative solutions for knee meniscus repair and replacement are required. Toward demonstrating efficacy of novel meniscal therapies, appropriate animal models will be needed to traverse the regulatory process. These animals should have menisci with morphological, biomechanical, and biochemical properties that are comparable to humans; similarities in gait, joint anatomy, and joint biomechanics should also be considered to facilitate translation [10].

Engineered meniscal tissues are expected to experience complex loading patterns within the knee. For example, human medial menisci have been shown to have mechanical properties that vary by topographical location [11]. Additionally, knee menisci have anisotropic tensile properties, or different mechanical properties when tested in circumferential versus radial directions; this difference in mechanical properties stems from circumferentially aligned collagen fibers that convert compressive forces into tensile hoop stresses. It is posited that tissue engineered implants should closely resemble the native tissue toward restoring function in vivo; thus, acquisition of complete design parameters from native tissue is crucial. Furthermore, engineered implants would require testing in a large animal model to show safety and efficacy prior to human trials [12].

Although characterization studies of human and farm pig knee menisci have been conducted [11,13,14] and bovine cells have been used to tissue engineer menisci [15–17], neither farm pig nor bovine models may be suitable for preclinical testing due to these animals being vastly different from humans in terms of weight. More frequently, animal models such as the goat, sheep, dog, and rabbit have been used for meniscus studies [18–21]. An emerging large animal model is the minipig, which has been proposed as a possible model that can be incorporated into future guidance documents for meniscus repair [10], but data on the knee menisci of minipigs are lacking.

The minipig model, specifically the Yucatan breed, is often used in biomedical research [22–25] and has been gaining popularity in orthopedic research and musculoskeletal science [26–29]. Yucatan minipigs share physiological similarities with humans. For example, minipig neural vascularization patterns, central nervous system physiology, and weights are comparable to humans [30–33]; additionally, adult pig menisci have been shown to have similar vascularization patterns to humans [34]. In contrast to farm pigs, minipigs are more suitable for long-term studies because their smaller size leads to reductions in needs related to handling, housing, surgery, anesthesia, and food [35]. Particularly important is that the minipig weight gain throughout a study is not as drastic as farm pigs. For example, a Yucatan minipig weighs approximately 20-30kg at sexual maturity (5-6 months old) and has a typical growth rate of 3-5kg per month, while Yorkshire/Landrace hybrid pigs at sexual maturity (5-6 months) weigh well over 100kg and continue to grow at 10-20kg per month [36]. Because the Yucatan minipig provides physiological similarities to humans, requires less resources for surgery and handling, and change less over a study's period as compared to farm pigs,

its potential as a large animal model for meniscus research should be investigated, particularly through characterization of morphological, mechanical, and biochemical properties of native tissue.

This work characterized the medial and lateral knee menisci of Yucatan minipigs through extensive analyses of structure-function relationships within the native tissue. Minipig knee menisci were investigated by gross morphology, histology, mechanical testing under tension and compression, and biochemical analyses. Furthermore, motivated by topographical differences in properties in human menisci, different regions of the minipig menisci were examined for mechanical anisotropy and degree of collagen crosslinking to provide greater insight on the native tissue's function. Because skeletally mature minipigs are similar in weight to humans and because regional differences in mechanical properties have been observed in human menisci, we hypothesized that 1) gross morphological dimensions of minipig menisci would fall within human menisci ranges, 2) as with humans, regional differences in mechanical properties would be observed in the minipig menisci, and 3) regional differences in mechanical properties would correspond to differences in collagen, glycosaminoglycan (GAG), and crosslink content. The data here will serve to advance our understanding of the regional structure-function relationships of minipig knee menisci, to provide benchmarks to assist the creation of novel regenerative solutions for human meniscal lesions, and to provide critical information regarding the suitability of the minipig as a model for investigations of the knee meniscus.

6.2. Materials and methods

6.2.1 Animals, knee meniscus gross morphology, histology, and macroscopic characterization

Knee menisci were obtained from eight healthy, skeletally mature, 16-18-month-old male and female Yucatan minipigs that were sacrificed due to reasons unrelated to this study. The menisci were excised and subsequently frozen in PBS-containing protease inhibitors 10 mmol/L N-ethylmaleimide and 1 mmol/L phenylmethylsufonyl fluoride (Sigma) at -20°C. Menisci were thawed and photographed, and the dimensions were measured using ImageJ (NIH; Figure 6.1A, 6.2) before dividing each meniscus into three regions (anterior, central, posterior). Pieces for mechanical testing and biochemical analysis were resected from the white-red zone of each region (Figure 6.1B), while histology samples comprised of a cross section taken from the central region of each meniscus. For histology, construct samples were fixed in 10% neutral buffered formalin, then embedded in paraffin and sectioned at 5μm. Safranin-O/fast green, picrosirius red, and hematoxylin and eosin (H&E) stains were conducted to visualize GAG, collagen, and cell distributions, respectively (Figure 6.3).

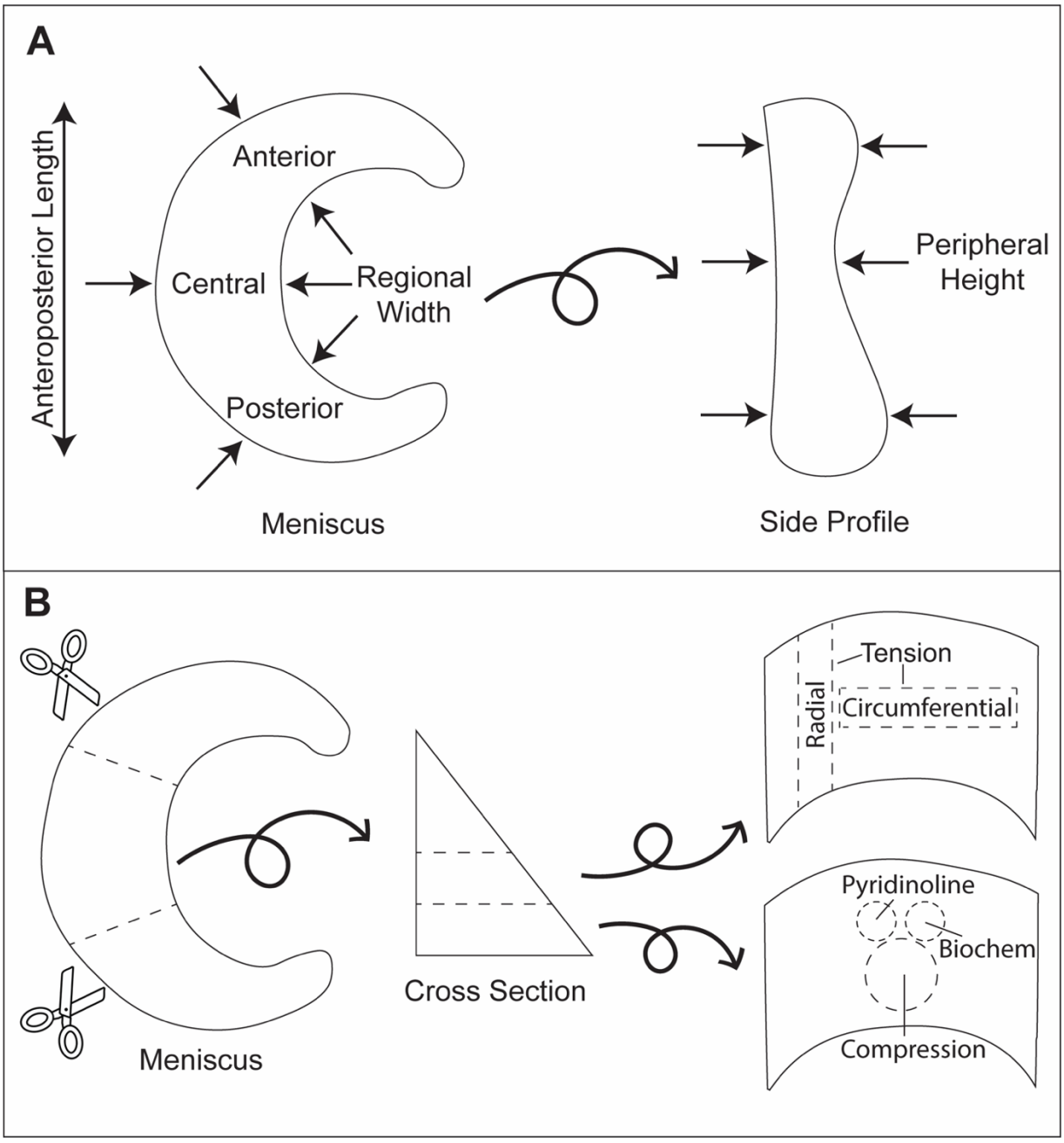

Figure 1: Gross morphology measurements and division of minipig knee menisci for mechanical and biochemical analyses. a) Arrows indicate the locations where measurements were taken for anteroposterior length, regional width, and peripheral height. b) Each meniscus was cut into three regions (anterior, central, posterior). Subsequently, each section was cut into layers from which tensile (circumferential and

radial directions), compressive (creep indentation), biochemistry, and mass spectrometry samples were collected.

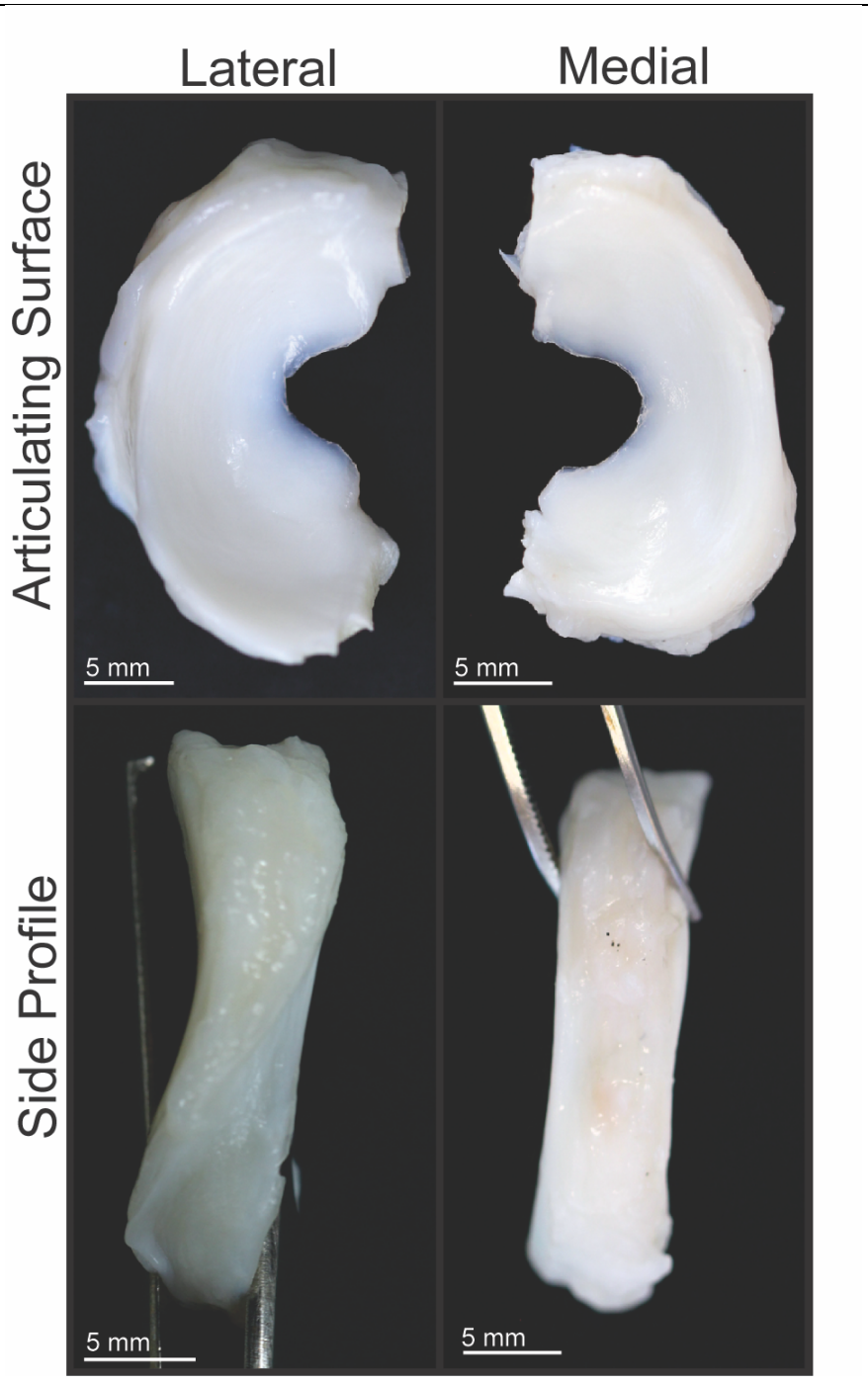

Figure 6.2: Gross morphology of Yucatan minipig knee menisci. Articulating surfaces and side profiles of medial and lateral menisci are shown.

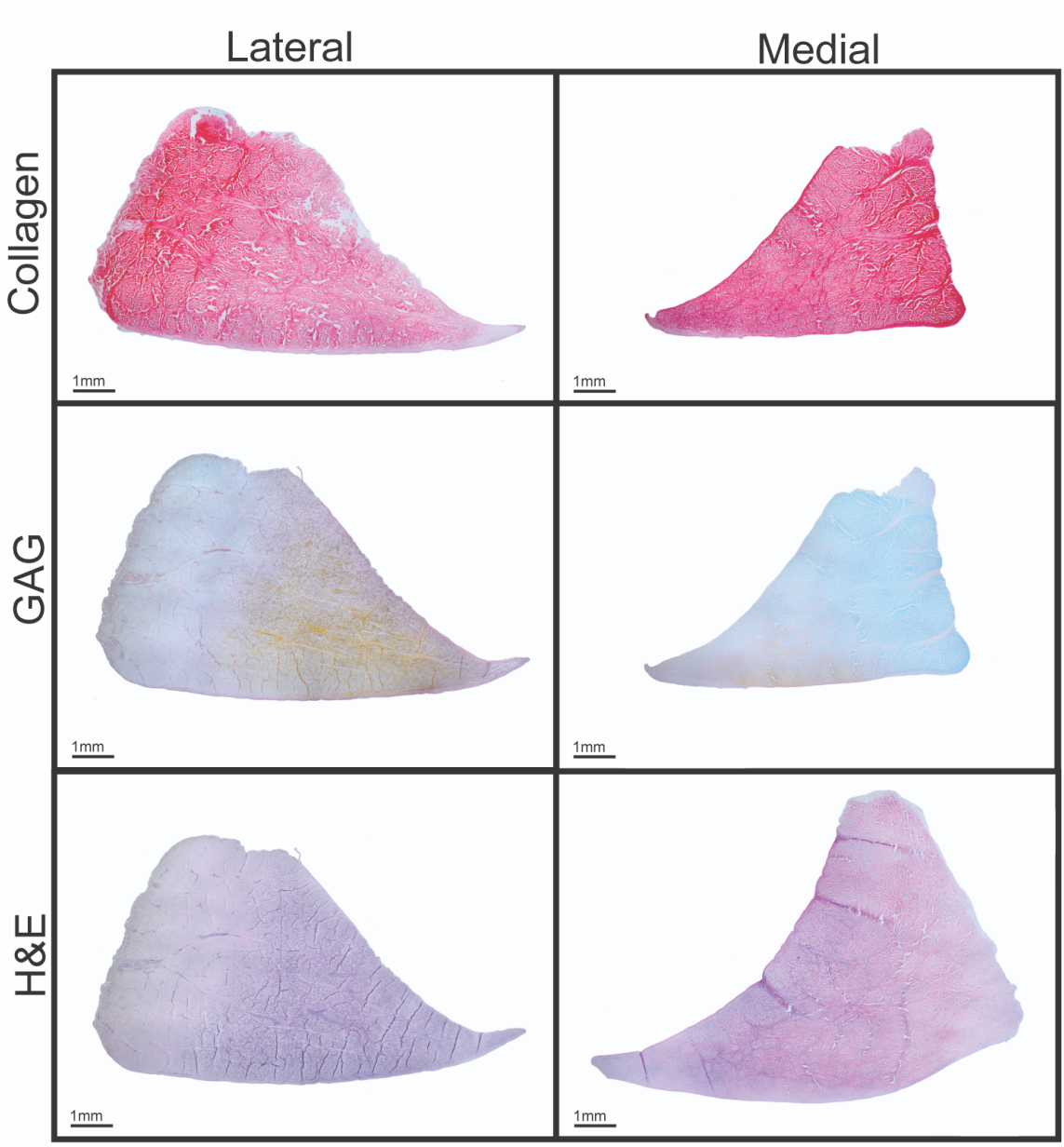

Figure 6.3: Histological staining of Yucatan minipig knee menisci. Cross sections of menisci stained for collagen (picrosirius red), GAG (Safranin-O), and cell content (H&E) are shown.

6.2.2 Tensile and compressive testing

Tensile properties were assessed using uniaxial, strain-to-failure testing in circumferential and radial directions. Samples were cut into rectangular strips and photographed, and the dimensions were measured with ImageJ. Samples were then clamped within a uniaxial testing machine (Instron model 5565) and subjected to a 1% s-1 strain rate until failure. Young's modulus (EY) was calculated from the linear portion of the stress-strain curve, and ultimate tensile strength (UTS) was calculated from the maximum stress.

Compressive properties were assessed via creep indentation testing of punches measuring 3 mm in diameter and placed into an automated indentation machine while submerged in phosphate buffered saline (PBS), as previously described [37,38]. Briefly, tissue punches were tested using a 0.5 mN tare load followed by a 0.04-0.05 N test load to maintain ~10% applied strain. The loads were applied to the surface of specimens through a 1.0 mm diameter, flat-ended, porous tip, perpendicular to the surface at the center of the sample. The sample surface is assumed to be a semi-infinite half space, which allows the single measurement point to be representative of the whole sample. The tissue was allowed to reach creep equilibrium while the deformation was recorded over time. Using the analytical solution for the axisymmetric Boussinesq problem with Papkovich potential functions, preliminary estimations of the aggregate modulus of the samples were obtained. Using the linear biphasic theory followed by a finite element model, intrinsic biomechanical properties of the samples such as aggregate modulus, shear modulus, Poisson's ratio, and permeability were calculated [39,40].

6.2.3 Analysis of tissue biochemical content

Biochemistry samples were weighed wet, then frozen and lyophilized to acquire dry weights. Collagen content was measured with the use of a Sircol standard (Biocolor) and

a modified chloramine-T colorimetric hydroxyproline assay [41]. GAG content was quantified using the Blyscan Glycosaminoglycan assay kit (Biocolor). All quantification measurements for collagen and GAG content were performed with a GENios spectrophotometer/spectrofluorometer (TECAN).

Quantification of pyridinoline crosslink content was performed via a liquid chromatography mass spectrometry (LC-MS) assay¬ [42]. Lyophilized samples were hydrolyzed in 6N HCl at 105°C for 18 hours. After evaporation, dried hydrolysates were resuspended in 25% (v/v) acetonitrile and 0.1% (v/v) formic acid in water, centrifuged at 15,000g for 5 minutes, and the supernatant was transferred to a LCMS autosampler vial. Liquid chromatography was carried out on a Cogent Diamond Hydride HPLC Column (2.1mm x 150mm, particle size 2.2µm, pore size 120Å, MicroSolv) and a pyridinoline standard (BOC Sciences) as previously described [15].

6.2.4 Statistical analysis

For each biomechanical, biochemical, and morphological test, n=5-7 samples were used. To identify outliers within groups, a ROUT test was applied using GraphPad Prism software; no outliers were identified. A Shapiro-Wilk test was applied using alpha=0.01 to confirm that data within groups were normally distributed. Data were first analyzed using a Student's t-test comparing aggregated data from all regions of the medial and of the lateral menisci to discern differences between the two sides. This level of analysis was motivated by literature showing that properties within medial and lateral menisci are different across multiple species. Next, a single factor analysis of variance (ANOVA) or Kruskal-Wallis test was used when appropriate to determine, for each meniscus, whether the properties differed by region; the levels consisted of anterior, central, and posterior

regions. A Tukey's HSD post hoc test was performed when merited. All statistics were performed with $p<0.05$. All data are presented as means ± standard deviations. For all figures, a connecting letters report shows statistical significance as indicated by groups not sharing the same letters.

6.3. Results

6.3.1 Gross morphology and histology

The Yucatan minipig medial and lateral menisci were semi-lunar and wedge shaped (Figures 6.2 & 6.3), with anteroposterior lengths of 23.2mm and 24.8mm, respectively; no significant difference in length was found between the two groups (Table 6.1). Significant difference was observed in width; medial meniscus width ranged from 7.7-10.2mm across its regions while lateral meniscus width ranged from 8.4-11.4mm. The posterior region was significantly wider than other regions for both menisci. Peripheral height also differed significantly; the medial and lateral meniscus peripheral heights varied from 6.4-6.6mm and 6.4-8.4 mm, respectively. The anterior and posterior regions of the lateral meniscus exhibited significantly higher peripheral heights when compared to the central region; there were no significant differences in peripheral heights among medial meniscus regions.

Table 1: Morphological properties of minipig menisci. Student's *t*-test showed a significant difference between medial and lateral menisci in hydration, width, and peripheral height values. For comparison of regions within each meniscus, Tukey's HSD test showed significant differences among regions for both menisci in width, while the lateral meniscus exhibited differences in peripheral height values among its regions. Values marked with different letters within each category are significantly different

among groups (p<0.05), n=7-8 per group. Human values of morphological properties from the literature are shown for comparison [13,45].

Meniscus	Region	Hydration (%)	Average Hydration (%)	Antero-Posterior Length (mm)	Width (mm)	Average Width (mm)	Peripheral height (mm)	Average Peripheral Height (mm)
Medial (Minipig)	Anterior	65.8±2.7	64.0±2.8^{B}	23.2±1.3	8.6±0.8^{B}	8.8±0.9^{B}	6.6±0.7	6.5±0.8^{B}
	Central	62.3±3.3			7.7±0.9^{B}		6.4±1.0	
	Posterior	64.2±1			10.2±0.6^{A}		6.6±0.9	
Lateral (Minipig)	Anterior	68.5±2.5	67.8±3.5^{A}	24.8±2.4	9.4±0.7^{B}	9.7±0.9^{A}	7.9±0.7^{A}	7.5±1.3^{A}
	Central	67.8±3.5			8.4±0.9^{B}		6.4±0.8^{B}	
	Posterior	67.1±4.9			11.4±1.1^{A}		8.4±1.4^{A}	
Medial (Human)	Anterior	N/A	70-75	39.8±3.7	8.5±0.6	10.6±0.8	5.5±0.3	5.8±0.3
	Central				8.3±0.5		5.0±0.5	
	Posterior				14.8±0.8		7.0±0.7	
Lateral (Human	Anterior	N/A		33.3±3.5	11.5±0.4	11.6±0.2	6.4±0.9	6.3±0.4
	Central				11.6±0.5		6.3±0.5	
	Posterior				11.7±0.3		6.2±0.8	

6.3.2 Tissue biomechanics

Biomechanical data revealed no significant differences in circumferential Young's modulus between medial and lateral menisci or among their regions, which ranged from 99.4-114.1MPa in the medial meniscus and 78.4-116.2MPa in the lateral meniscus (Figure 6.4A); additionally, circumferential UTS ranged from 18.2-25.9MPa, though no

significant difference among regions in either meniscus was shown (Figure 6.4B). Radial Young's modulus was not significantly different between menisci and ranged from 2.5-10.9MPa; however, the anterior region of the medial meniscus was significantly higher than the medial posterior region. No significant differences among regions in the lateral meniscus were observed (Figure 6.4C). UTS in the radial direction ranged from 2.5-4.2MPa. There were no significant differences between menisci or among regions within either meniscus (Figure 6.4D).

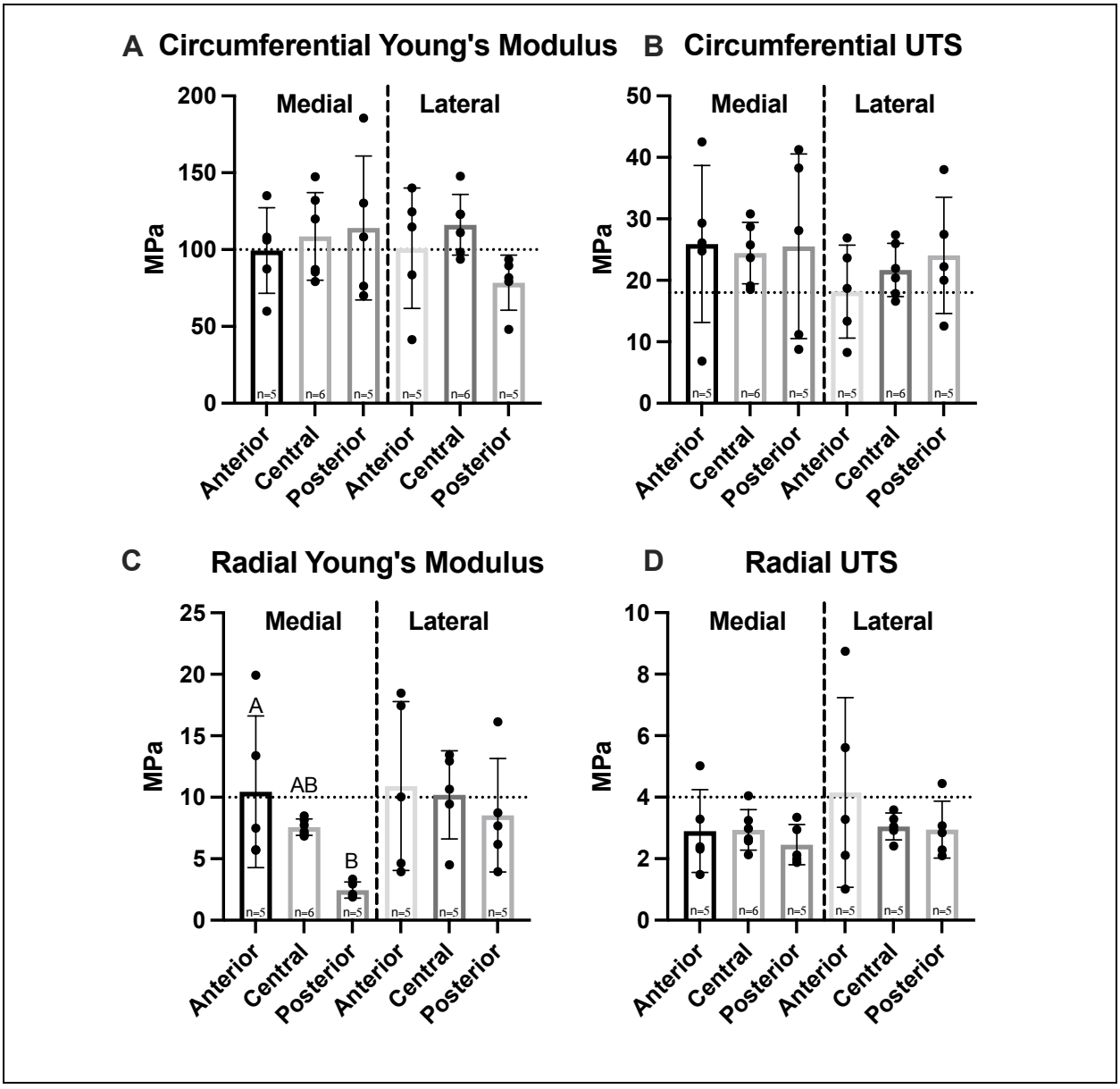

Figure 6.4: Tensile properties of Yucatan minipig knee menisci. (A, B) Young's Modulus and UTS of medial and lateral menisci are shown for the circumferential and radial directions, respectively. No significant difference was seen in circumferential stiffness and strength; (C, D) radial stiffness in the anterior region of the medial meniscus was significantly higher than the posterior region, though no significant difference was seen in radial tensile strength. All data are presented as means ± standard deviations. Statistical significance is indicated by bars not sharing the same letters within the same meniscus; additionally, horizontal dotted lines on the Y-axis represent human meniscus values from the literature for comparison to the minipig [47,51].

Compressive mechanical testing showed a significant difference in permeability values between medial and lateral menisci; however, no significant differences were observed among regions in either meniscus for the values of aggregate modulus, shear modulus, permeability, and Poisson's ratio (Figure 6.5). Aggregate and shear modulus values ranged from 157-287kPa and 91-147kPa, respectively; both moduli trended highest in the anterior region of each meniscus and trended lowest in the posterior region.

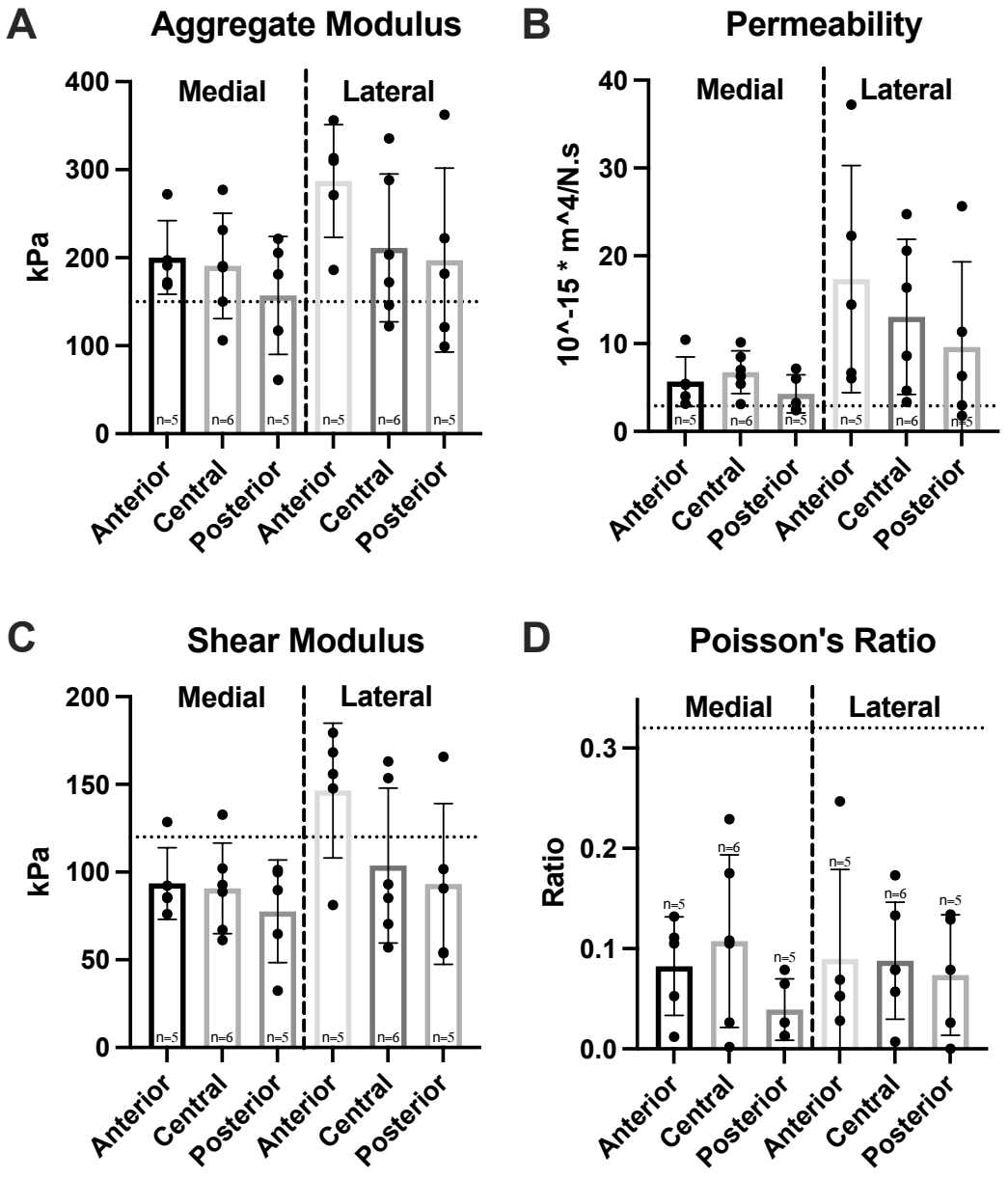

Figure 6.5: Compressive properties of Yucatan minipig knee menisci. (A-D) Aggregate modulus, permeability, shear modulus, and Poisson's ratio are shown for medial and lateral menisci, respectively. Student's *t*-test showed a significant difference between medial and lateral menisci in permeability values. One-factor ANOVA showed no significant differences in any compressive property among regions of the same

meniscus. All data are presented as means ± standard deviations. Statistical significance is indicated by bars not sharing the same letters within the same meniscus; additionally, horizontal dotted lines on the Y-axis represent human meniscus values from the literature for comparison to the minipig [11,48,51].

6.3.3 Tissue biochemistry

A significant difference in hydration percentages was observed between medial and lateral menisci, which ranged from 64.0-67.8% (Table 6.1). Biochemical analysis showed collagen (COL) and GAG throughout both menisci, with concentrations per wet weight (WW) ranging from 23.9-31.3% COL/WW and 1.20-2.57% GAG/WW, respectively (Figures 6.6A & 6.6C). There were no significant differences between menisci in collagen content normalized to wet weight or dry weight (DW). Significantly less COL/WW was observed in the anterior region of the medial meniscus compared to its other regions, while no significant differences among regions in the lateral meniscus were observed. COL/DW in the medial meniscus was significantly higher in the posterior region compared to the anterior; no significant differences in COL/DW were found among regions in the lateral meniscus (Figure 6B). Significant differences between menisci were observed for GAG/WW and GAG/DW. In the medial meniscus, the anterior region had significantly more GAG/WW and GAG/DW than the posterior region; no significant differences in GAG/WW or GAG/DW were seen among regions in the lateral meniscus (Figures 6.6C & 6.6D).

Pyridinoline (PYR) crosslink content normalized to WW was not significantly different between medial and lateral menisci and ranged from 0.38-0.58ng/μg. The central region of the medial meniscus contained significantly more PYR/WW compared to the

anterior; there were no significant differences in PYR/WW content among lateral meniscus regions (Figure 6.6E). In addition, there were no significant differences in PYR/DW between menisci or among their regions (Figure 6.6F). Finally, PYR/COL ranged from 1.45-1.96ng/μg and was not significantly different between medial and lateral menisci (Figure 6.6G).

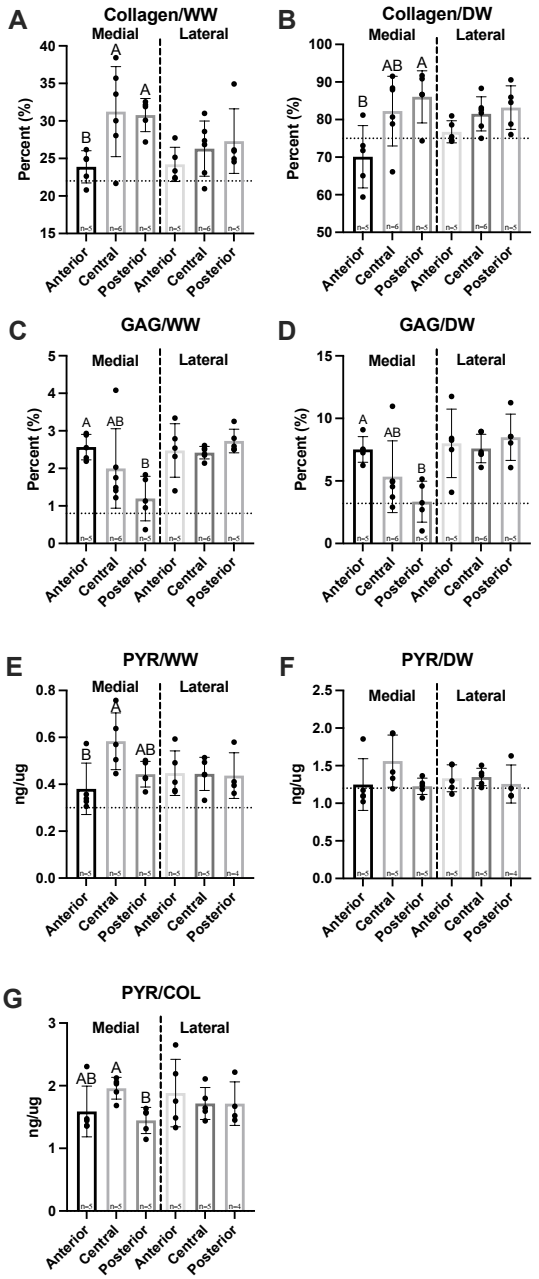

Figure 6.6: Biochemical properties of Yucatan minipig menisci. (A-F) Collagen, GAG, and pyridinoline crosslink content are shown normalized to wet and dry weights, respectively, in addition to (G) crosslinks normalized to collagen content. Student's *t*-test shows significant differences between medial and lateral menisci in GAG content. One-factor ANOVA showed pyridinoline crosslinks normalized to collagen content was significantly higher in the central region of the medial meniscus compared to its posterior region; no significant differences were seen among regions in the lateral meniscus. All data are presented as means ± standard deviations. Statistical significance is indicated by bars not sharing the same letters within the same meniscus; additionally, horizontal dotted lines on the Y-axis represent human meniscus values from the literature for comparison to the minipig [51,52,56]

6.3.4 Anisotropy

For the assessment of anisotropy, tensile properties of each region in both medial and lateral menisci were collected from two testing directions – circumferential and radial. Circumferential values were then divided by radial values to produce an anisotropy index. A significant difference between medial and lateral menisci was observed for tensile Young's modulus but not for UTS. The Young's modulus anisotropy index ranged from 11.2-49.9 and was significantly different among regions in the medial meniscus; the posterior region of the medial meniscus was significantly higher than other regions in the medial meniscus, while there were no significant differences among regions in the lateral meniscus (Figure 6.7A). UTS anisotropy levels ranged from 6.3-11.2 and no significant differences between menisci or among regions in either meniscus were found (Figure 6.7B).

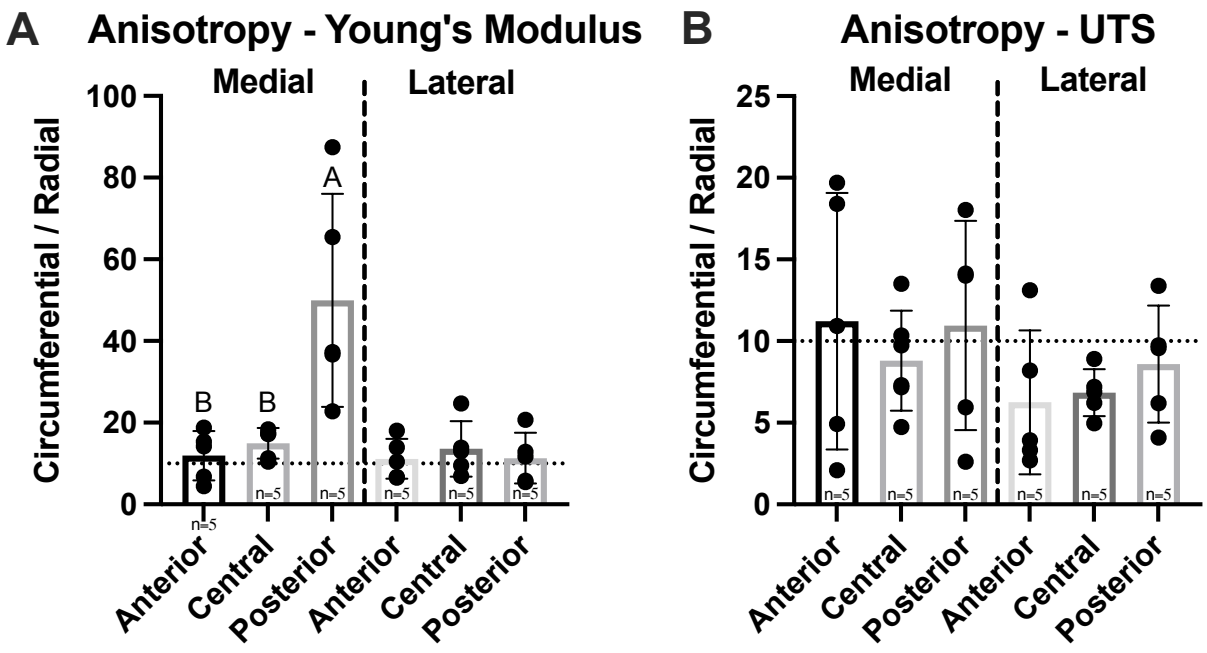

Figure 6.7: Anisotropy index of Yucatan minipig meniscus tensile properties. (A, B) Anisotropy indices are shown for tensile Young's modulus and UTS, respectively. Student's t-test showed a significant difference in Young's modulus anisotropy values between menisci. One-factor ANOVA showed the posterior region of the medial meniscus was significantly more anisotropic in tensile stiffness than its other regions, while no significant differences were seen among regions of the lateral meniscus. All data are presented as means ± standard deviations. Statistical significance is indicated by bars not sharing the same letters within the same meniscus; additionally, horizontal dotted lines on the Y-axis represent human meniscus values from the literature for comparison to the minipig [51].

6.4. Discussion

The objective of this study was to characterize the knee menisci of Yucatan minipigs because the minipig has been proposed as a large animal model for translational cartilage

and meniscus research. This was performed through an extensive analysis of structure-function relationships within the native tissue by region, which was motivated by known regional differences in human menisci. The data may provide design criteria to tissue engineers who aim to create repair and replacement technologies for the knee meniscus and to researchers that aim to test novel meniscal technologies in large animals. Notably, previously unexplored characteristics, such as the degree of collagen crosslinking within minipig menisci, were elucidated using an LC-MS assay. With regard to the hypothesis that gross morphological properties would be comparable to human menisci ranges, it was found that the regional width and peripheral height of minipig menisci fell within human ranges. Additional hypotheses that regional differences in mechanical properties would be observed and that regional differences in mechanical properties would correspond to differences in structural characteristics were also supported by the data. Support for these hypotheses is significant because the data imply that analogous products designed for human menisci would likely be functional in the minipig, allowing for human meniscal products to be tested in this animal.

Morphological features of the Yucatan minipig menisci were measured to assess the similarity between native minipig and human tissue; morphologically similar tissues between species could allow for translation of surgical techniques in addition to engineered meniscus implants. This study found minipig menisci to be comparable to human menisci, which measure 33.3-39.8mm in anteroposterior length, 8.5-14.8mm in peripheral height, and 5-7mm in regional width, respectively. For example, values measured for the minipig menisci dimensions were within ranges seen in human menisci for 2 out of 3 properties - average peripheral height and average regional width [13,43];

the lateral minipig meniscus trended higher in anteroposterior length than the medial meniscus and is approximately 28% shorter in length than the lateral human meniscus [44]. Despite this difference, minipig anteroposterior lengths are comparable to other animal models that have been used in knee meniscus research such as sheep, goats, and farm pigs that measure 22-26mm on average [21,45]. Additionally, the minipig and human both exhibit higher peripheral height values in the lateral meniscus compared to the medial side (Table 6.1). The posterior regions of both minipig menisci were significantly wider than their respective anterior and central regions, similar to human menisci; the posterior region of the lateral minipig meniscus, the widest by average in this study, was only 2% smaller than the average width reported for the lateral meniscus in the human. Additionally, comparable to what is seen in humans [20,46], histology of minipig meniscus cross sections showed a collagen network throughout the tissue, a positive staining for GAG, and cells dispersed throughout the tissue (Figure 6.3). Overall, minipig knee menisci provide gross morphological similarities to humans in terms of their peripheral height and regional width, which could allow for the ready implantation and, eventually, translation of engineered tissues for their repair or replacement.

The knee meniscus functions by developing tension when under compressive load, highlighting the importance of both mechanical properties for the meniscus. It was found that there were no significant differences in tensile stiffness and strength in the circumferential or radial directions between medial and lateral menisci (Figure 6.4). Additionally, no significant differences in circumferential tensile properties among meniscus regions were observed, replicating what is seen in humans; at their peak, minipig meniscus circumferential stiffness and strength are 81% and 138% of the peak

values recorded in humans, respectively [47]. Radial stiffness of minipig menisci were on par to those of human menisci; values averaged across both medial and lateral menisci and regions were 8.3MPa for the minipig and 10.8MPa for humans [47] (Figure 6.4C). In terms of compressive properties, only permeability was significantly different between medial and lateral menisci; this difference between menisci was not seen in human tissue in a study that measured compressive properties using stress-relaxation [48]. Additionally, the homogeneity seen among regions in Yucatan minipig menisci (Figure 6.5) is not reflected in the human, albeit a similar trend was identified; the anterior region of the human medial meniscus is stiffer than its central and posterior regions, and is 80% as stiff as the anterior region of the medial meniscus in the Yucatan minipig [11]. Biomechanical properties crucial to meniscus functionality, such as circumferential and radial tensile properties, were comparable between minipigs and humans; because of this, it is plausible that a meniscus implant with mechanical properties akin to those of human menisci can survive within the minipig knee environment during translational studies.

For humans, longitudinal tears occur more often in the medial posterior meniscus when compared to the anterior region [49]. It has been suggested that the posterior region of the human medial meniscus bears more load than the anterior region and, thus, experiences larger radial stresses that lead to longitudinal tears [50]. In the minipig, this study showed that the posterior region exhibited significantly lower radial stiffness than the anterior region (Figure 6.4C), which also corresponded to differences in composition (Figure 6.5). Thus, although there are currently no data on meniscal tears in minipigs, the data here would suggest that, with its lower mechanical properties, the minipig may share

similarities with humans in having menisci that are more prone to injuries in the medial posterior region. The mechanical data obtained here may further be supported by differences in structure, such as the density or thickness of radially aligned collagen fibers [49], which warrant additional structural studies.

Because regional differences in mechanical properties of knee menisci have been identified in humans and other species such as cows, farm pigs, rabbits, and baboons [11,47,49], it is crucial to investigate the biochemical composition of minipig menisci toward understanding their mechanical function. Minipig and human menisci share similar levels of hydration, with 67.8% hydration in the anterior region of the minipig lateral meniscus being just under the literature value of 72% for human menisci [51]. Collagen accounts for 23.9-31.3% per wet weight of minipig meniscus tissue (Figure 6.6B), and human menisci contains 22% COL/WW [52]. In terms of GAG content, values in the minipig meniscus reached as high as 2.73% GAG/WW (Figure 6.6C), which is approximately 3-times higher than in humans [52]. Notably, the posterior region of the medial meniscus contained significantly less GAG per wet and dry weights than the anterior region. Although there were no significant differences in compressive properties among regions in the medial meniscus, the posterior region had the lowest aggregate and shear moduli values. Overall, minipig meniscus collagen and GAG content were on par with or slightly exceeded levels seen in the human.

In addition to measuring collagen and GAG content, quantifying pyridinoline crosslinks is crucial to understanding the structure-function relationship of the minipig knee meniscus because these crosslinks have been shown to correlate with tensile properties of menisci and other collagenous tissues [53–55]. Pyridinoline crosslink

content normalized to dry weight trended highest in the central region of the medial minipig meniscus and was measured at approximately 0.16%, which is higher than levels obtained in human menisci using an HPLC fluorescence detection assay at 0.12% [56]. It should be noted that values in the present study were obtained using an LC-MS method, which has been shown to be more precise and accurate than HPLC fluorescence detection methods [57–61]. Pyridinoline crosslink content, for example, has been quantified using LC-MS techniques in bovine articular cartilage, showing crosslink levels of 0.12% of total dry weight, which were on par with values recorded in this study [62]. The posterior region of the medial meniscus contained significantly fewer crosslinks normalized to collagen content compared to the central region (Figure 6.6G), which may contribute to the low radial tensile stiffness in the posterior region. Overall, the medial meniscus contained regional variability in biochemical content while the lateral meniscus was more homogeneous throughout; this is reflected in the mechanical properties and anisotropy indices of the medial meniscus.

The anisotropic organization of ECM within the meniscus is crucial to the tissue's function. Circumferential tensile stiffness and strength of menisci have been reported to be approximately 10-fold higher than those of the radial direction in many species [63]. Tensile anisotropy indices were also measured, defined as circumferential tensile properties normalized to those in the radial direction [15], in this study for Yucatan minipig menisci tensile stiffness and strength. These ranged from 11.2-49.9 and 6.3-11.2, respectively, and were similar to those previously reported [63]. The medial meniscus however, contained a significantly higher anisotropy index for tensile stiffness in its posterior region compared to other regions (Figure 6.7A), likely stemming from the low

tensile properties in the radial direction. It is worth noting, though, that radial tensile values in this region of the minipig were still on par with those reported for the same meniscal region in humans [47]. In summary, the posterior region of the minipig meniscus, thus, has a higher degree of anisotropy, less crosslinked collagen, and lower radial tensile properties compared to other medial regions; these findings correspond to a region in the human medial meniscus where more injuries have been reported [49], showing the clinical relevance of using the minipig as a large animal model.

While this study elucidated that minipig menisci morphological, mechanical, and biochemical properties fall within native human tissue ranges, it is important to note that additional investigations into minipig meniscus properties could further validate these findings. Meniscus structure-function relationships have been shown to vary by zone (i.e., outer red-red zone versus inner white-white zone) in pigs and other species [20]. Compressive properties and GAG content, for example, have been shown to be higher in the inner white-white zone of human and porcine menisci when compared to the outer red-red zone [64–66]; because this study collected biochemical samples from the middle white-red zone, additional studies are warranted to compare outer and inner zones. Furthermore, as this study utilized menisci from both male and female minipigs, sex-specific differences that may exist in meniscus properties were not able to be elucidated. Identifying sex-based differences for meniscus properties, should they exist, might allow for better understanding of meniscal function and pathophysiology in humans; fibrocartilages such as the TMJ disc, for example, have a higher frequency of injury in female patients when compared to male patients [67]. Additionally, human meniscus characteristics such as GAG content have been shown to decrease with age [68];

investigation into minipig menisci at different stages of development could provide further insight into appropriate models to consider in preclinical research. These factors, investigated with an adequate number of experimental samples to generalize the findings, could thus provide crucial insight into minipig meniscus structure-function relationships.

The prevalence and economic impact of meniscal injuries motivate tissue engineers to create novel regenerative solutions. For these new implant technologies to successfully translate from the benchtop to the clinic they must first undergo extensive preclinical testing in a large animal model. It is crucial to find an appropriate animal model with similar structural, mechanical, and biochemical characteristics to humans and, ideally, a docile temperament to facilitate post-surgical care. Minipigs such as the Yucatan breed have been proposed as animal models for studies involving injuries to articular cartilage and the knee meniscus. Engineered meniscal implants should aim to recapitulate native tissue properties to increase their chances of survival in the native knee's biomechanical environment. The characterization this study provides shows that the Yucatan minipig meniscus is comparable to humans in terms of morphological, mechanical, and biochemical properties. In addition, human meniscus injury patterns were considered when identifying an analogous location where they may occur in minipigs. These findings provide design criteria for tissue engineers that aim to create regenerative solutions to meniscal injuries and support use of the Yucatan minipig as a large animal model for translating meniscal therapies.

References

[1] Salata, M. J., Gibbs, A. E., and Sekiya, J. K., 2010, “A Systematic Review of Clinical Outcomes in Patients Undergoing Meniscectomy,” Am. J. Sports Med., 38(9), pp. 1907–1916.

[2] Logerstedt, D. S., Snyder-Mackler, L., Ritter, R. C., and Axe, M. J., 2010, “Knee Pain and Mobility Impairments: Meniscal and Articular Cartilage Lesions,” J. Orthop. Sports Phys. Ther., 40(6).

[3] Baker, B. E., Peckham, A. C., Pupparo, F., and Sanborn, J. C., 1985, “Review of Meniscal Injury and Associated Sports,” Am. J. Sports Med., 13(1), pp. 1–4.

[4] Herrlin, S., Hållander, M., Wange, P., Weidenhielm, L., and Werner, S., 2007, “Arthroscopic or Conservative Treatment of Degenerative Medial Meniscal Tears: A Prospective Randomised Trial,” Knee Surgery, Sport. Traumatol. Arthrosc., 15(4), pp. 393–401.

[5] Katz, J., Brophy, R., Chaisson, C., Chaves, L., Cole, B., and Dahm, D., 2013, “Surgery versus Physical Therapy for a Meniscal Tear and Osteoarthritis,” N. Engl. J. Med., 368(18), pp. 1675–1684.

[6] Maffulli, N., Longo, U. G., Campi, S., and Denaro, V., 2010, “Meniscal Tears,” Open Access J. Sport. Med., 1, pp. 45–54.

[7] Barber-Westin, S. D., and Noyes, F. R., 2014, “Clinical Healing Rates of Meniscus Repairs of Tears in the Central-Third (Red-White) Zone,” Arthroscopy, 30(1), pp. 134–146.

[8] Xu, C., and Zhao, J., 2015, “A Meta-Analysis Comparing Meniscal Repair with Meniscectomy in the Treatment of Meniscal Tears: The More Meniscus, the Better Outcome?,” Knee Surgery, Sport. Traumatol. Arthrosc., 23(1), pp. 164–170.

[9] Rangger, C., Kathrein, A., Klestil, T., and Glötzer, W., 1997, “Partial Meniscectomy and Osteoarthritis. Implications for Treatment of Athletes.,” Sports Med., 23(1), pp. 61–68.

[10] Donahue, R. P., Gonzalez-Leon, E. A., Hu, J. C., and Athanasiou, K. A., 2019, “Considerations for Translation of Tissue Engineered Fibrocartilage from Bench to Bedside,” J. Biomech. Eng., 141(7).

[11] Sweigart, M. A., Zhu, C. F., Burt, D. M., Deholl, P. D., Agrawal, C. M., Clanton, T. O., and Athanasiou, K. A., 2004, “Intraspecies and Interspecies Comparison of the Compressive Properties of the Medial Meniscus,” Ann. Biomed. Eng., 32(11), pp. 1569–1579.

[12] Donahue, R. P., Gonzalez-Leon, E. A., Hu, J. C., and Athanasiou, K., 2018, “Considerations for Translation of Tissue Engineered Fibrocartilage from Bench to Bedside.,” J. Biomech. Eng.

[13] Takroni, T., Laouar, L., Adesida, A., Elliott, J. A., and Jomha, N. M., 2016, “Anatomical Study: Comparing the Human, Sheep and Pig Knee Meniscus,” J. Exp. Orthop., 3(1).

[14] Sweigart, M. A., and Athanasiou, K. A., 2005, “Biomechanical Characteristics of the Normal Medial and Lateral Porcine Knee Menisci,” Proc. Inst. Mech. Eng. Part H J. Eng. Med., 219(1), pp. 53–62.

[15] Gonzalez-Leon, E. A., Bielajew, B. J., Hu, J. C., and Athanasiou, K. A., 2020, “Engineering Self-Assembled Neomenisci through Combination of Matrix Augmentation and Directional Remodeling,” Acta Biomater., 109, pp. 73–81.

[16] Hadidi, P., and Athanasiou, K. A., 2013, “Enhancing the Mechanical Properties of Engineered Tissue through Matrix Remodeling via the Signaling Phospholipid Lysophosphatidic Acid,” Biochem. Biophys. Res. Commun., 433(1), pp. 133–138.

[17] Huey, D. J., and Athanasiou, K. A., 2011, “Tension-Compression Loading with Chemical Stimulation Results in Additive Increases to Functional Properties of Anatomic Meniscal Constructs,” PLoS One, 6(11), pp. 1–9.

[18] Deponti, D., Giancamillo, A. Di, Scotti, C., Peretti, G. M., and Martin, I., 2015, “Animal Models for Meniscus Repair and Regeneration,” J. Tissue Eng. Regen. Med., 9(5), pp. 512–527.

[19] Bansal, S., Keah, N. M., Neuwirth, A. L., O’Reilly, O., Qu, F., Seiber, B. N., Mandalapu, S., Mauck, R. L., and Zgonis, M. H., 2017, “Large Animal Models of Meniscus Repair and Regeneration: A Systematic Review of the State of the Field,” Tissue Eng. Part C. Methods, 23(11), pp. 661–672.

[20] Chevrier, A., Nelea, M., Hurtig, M. B., Hoemann, C. D., and Buschmann, M. D., 2009, “Meniscus Structure in Human, Sheep, and Rabbit for Animal Models of Meniscus Repair,” J. Orthop. Res., 27(9), pp. 1197–1203.

[21] Brzezinski, A., Ghodbane, S. A., Patel, J. M., Perry, B. A., Gatt, C. J., and Dunn, M. G., 2017, “The Ovine Model for Meniscus Tissue Engineering: Considerations of Anatomy, Function, Implantation, and Evaluation,” Tissue Eng. Part C. Methods, 23(12), pp. 829–841.

[22] Melnick, G., Ferrone, M., Cheng, Y., Conditt, G. B., Guérios, E. E., Rousselle, S. D., Granada, J. F., and Kaluza, G. L., 2020, “Long-Term Performance and Biocompatibility of a Novel Bioresorbable Scaffold for Peripheral Arteries: A Three-Year

Pilot Study in Yucatan Miniswine," Catheter. Cardiovasc. Interv. Off. J. Soc. Card. Angiogr. Interv., 95(7), pp. 1277–1284.

[23] Khoshnevis, M., Carozzo, C., Bonnefont-Rebeix, C., Belluco, S., Leveneur, O., Chuzel, T., Pillet-Michelland, E., Dreyfus, M., Roger, T., Berger, F., and Ponce, F., 2017, "Development of Induced Glioblastoma by Implantation of a Human Xenograft in Yucatan Minipig as a Large Animal Model," J. Neurosci. Methods, 282, pp. 61–68.

[24] Khoshnevis, M., Carozzo, C., Brown, R., Bardiès, M., Bonnefont-Rebeix, C., Belluco, S., Nennig, C., Marcon, L., Tillement, O., Gehan, H., Louis, C., Zahi, I., Buronfosse, T., Roger, T., and Ponce, F., 2020, "Feasibility of Intratumoral 165Holmium Siloxane Delivery to Induced U87 Glioblastoma in a Large Animal Model, the Yucatan Minipig," PLoS One, 15(6).

[25] Poupin, N., Tremblay-Franco, M., Amiel, A., Canlet, C., Rémond, D., Debrauwer, L., Dardevet, D., Thiele, I., Aurich, M. K., Jourdan, J., Savary-Auzeloux, I., and Polakof, S., 2019, "Arterio-Venous Metabolomics Exploration Reveals Major Changes across Liver and Intestine in the Obese Yucatan Minipig," Sci. Rep., 9(1).

[26] Bansal, S., Miller, L. M., Patel, J. M., Meadows, K. D., Eby, M. R., Saleh, K. S., Martin, A. R., Stoeckl, B. D., Hast, M. W., Elliott, D. M., Zgonis, M. H., and Mauck, R. L., 2020, "Transection of the Medial Meniscus Anterior Horn Results in Cartilage Degeneration and Meniscus Remodeling in a Large Animal Model," J. Orthop. Res., 38(12), pp. 2696–2708.

[27] Kremen, T. J., Stefanovic, T., Tawackoli, W., Salehi, K., Avalos, P., Reichel, D., Perez, M. J., Glaeser, J. D., and Sheyn, D., 2020, "A Translational Porcine Model for

Human Cell-Based Therapies in the Treatment of Posttraumatic Osteoarthritis After Anterior Cruciate Ligament Injury," Am. J. Sports Med., 48(12), pp. 3002–3012.

[28] Nordberg, R. C., Espinosa, M. G., Hu, J. C., and Athanasiou, K. A., 2021, "A Tribological Comparison of Facet Joint, Sacroiliac Joint, and Knee Cartilage in the Yucatan Minipig," Cartilage.

[29] Cone, S. G., Warren, P. B., and Fisher, M. B., 2017, "Rise of the Pigs: Utilization of the Porcine Model to Study Musculoskeletal Biomechanics and Tissue Engineering During Skeletal Growth," Tissue Eng. Part C. Methods, 23(11), pp. 763–780.

[30] Moriguchi, Y., Tateishi, K., Ando, W., Shimomura, K., Yonetani, Y., Tanaka, Y., Kita, K., Hart, D. A., Gobbi, A., Shino, K., Yoshikawa, H., and Nakamura, N., 2013, "Repair of Meniscal Lesions Using a Scaffold-Free Tissue-Engineered Construct Derived from Allogenic Synovial MSCs in a Miniature Swine Model," Biomaterials, 34(9), pp. 2185–2193.

[31] Kim, H., Song, K. D., Kim, H. J., Park, W., Kim, J., Lee, T., Shin, D., Kwak, W., Kwon, Y., Sung, S., Moon, S., Lee, K., Kim, N., Hong, J. K., Eo, K. Y., Seo, K. S., Kim, G., Park, S., Yun, C., Kim, H., Choi, K., Kim, J., Lee, W. K., Kim, D., Oh, J., Kim, E., Cho, S., Lee, H., Kim, T., and Kim, H., 2015, "Exploring the Genetic Signature of Body Size in Yucatan Miniature Pig," PLoS One, 10(4), p. e0121732.

[32] Walpole, S. C., Prieto-Merino, D., Edwards, P., Cleland, J., Stevens, G., and Roberts, I., 2012, "The Weight of Nations: An Estimation of Adult Human Biomass," BMC Public Heal. 2012 121, 12(1), pp. 1–6.

[33] Vodička, P., Smetana, K., Dvořánková, B., Emerick, T., Xu, Y. Z., Ourednik, J., Ourednik, V., and Motlík, J., 2005, “The Miniature Pig as an Animal Model in Biomedical Research,” Ann. N. Y. Acad. Sci., 1049, pp. 161–171.

[34] Peretti, G. M., Gill, T. J., Xu, J.-W., Randolph, M. A., Morse, K. R., and Zaleske, D. J., 2004, “Cell-Based Therapy for Meniscal Repair,” Am. J. Sports Med., 32(1), pp. 146–158.

[35] Mardas, N., Dereka, X., Donos, N., and Dard, M., 2014, “Experimental Model for Bone Regeneration in Oral and Cranio-Maxillo-Facial Surgery,” J. Investig. Surg., 27(1), pp. 32–49.

[36] “Swine Models | Premier BioSource” [Online]. Available: http://www.premierbiosource.com/swine-models. [Accessed: 25-Oct-2021].

[37] Brown, W. E., Huey, D. J., Hu, J. C., and Athanasiou, K. A., 2018, “Functional Self-Assembled Neocartilage as Part of a Biphasic Osteochondral Construct,” PLoS One, 13(4).

[38] Espinosa, M. G., Otarola, G. A., Hu, J. C., and Athanasiou, K. A., 2021, “Vibrometry as a Noncontact Alternative to Dynamic and Viscoelastic Mechanical Testing in Cartilage,” J. R. Soc. Interface, 18(185), p. 20210765.

[39] Athanasiou, K. A., Agarwal, A., Muffoletto, A., Dzida, F. J., Constantinides, G., and Clem, M., 1995, “Biomechanical Properties of Hip Cartilage in Experimental Animal Models,” Clin. Orthop. Relat. Res., 316(316), pp. 254–266.

[40] Elder, B. D., Kim, D. H., and Athanasiou, K. A., 2010, “Developing an Articular Cartilage Decellularization Process toward Facet Joint Cartilage Replacement,” Neurosurgery, 66(4), pp. 722–727.

[41] Cissell, D. D., Link, J. M., Hu, J. C., and Athanasiou, K. A., 2017, “A Modified Hydroxyproline Assay Based on Hydrochloric Acid in Ehrlich’s Solution Accurately Measures Tissue Collagen Content,” Tissue Eng. Part C Methods, 23(4), pp. 243–250.

[42] Naffa, R., Watanabe, S., Zhang, W., Maidment, C., Singh, P., Chamber, P., Matyska, M. T., and Pesek, J. J., 2019, “Rapid Analysis of Pyridinoline and Deoxypyridinoline in Biological Samples by Liquid Chromatography with Mass Spectrometry and a Silica Hydride Column,” J. Sep. Sci., 42(8), pp. 1482–1488.

[43] Erbagci, H., Gumusburun, E., Bayram, M., Karakurum, G., and Sirikci, A., 2004, “The Normal Menisci: In Vivo MRI Measurements,” Surg. Radiol. Anat., 26(1), pp. 28–32.

[44] Yoon, J. R., Kim, T. S., Wang, J. H., Yun, H. H., Lim, H., and Yang, J. H., 2011, “Importance of Independent Measurement of Width and Length of Lateral Meniscus during Preoperative Sizing for Meniscal Allograft Transplantation,” Am. J. Sports Med., 39(7), pp. 1541–1547.

[45] Proffen, B. L., McElfresh, M., Fleming, B. C., and Murray, M. M., 2012, “A Comparative Anatomical Study of the Human Knee and Six Animal Species,” Knee, 19(4), pp. 493–499.

[46] Fedje-Johnston, W., Tóth, F., Albersheim, M., Carlson, C. S., Shea, K. G., Rendahl, A., and Tompkins, M., 2021, “Changes in Matrix Components in the Developing Human Meniscus,” Am. J. Sports Med., 49(1), pp. 207–214.

[47] Tissakht, M., and Ahmed, A. M., 1995, “Tensile Stress-Strain Characteristics of the Human Meniscal Material,” J. Biomech., 28(4), pp. 411–422.

[48] Morejon, A., Norberg, C. D., De Rosa, M., Best, T. M., Jackson, A. R., and Travascio, F., 2021, “Compressive Properties and Hydraulic Permeability of Human

Meniscus: Relationships With Tissue Structure and Composition," Front. Bioeng. Biotechnol., 8.

[49] Skaggs, D. L., Warden, W. H., and Mow, V. C., 1994, "Radial Tie Fibers Influence the Tensile Properties of the Bovine Medial Meniscus," J. Orthop. Res., 12(2), pp. 176–185.

[50] Ahmed, A. M., and Burke, D. L., 1983, "In-Vitro Measurement of Static Pressure Distribution in Synovial Joints--Part I: Tibial Surface of the Knee," J. Biomech. Eng., 105(3), pp. 216–225.

[51] Makris, E. A., Hadidi, P., and Athanasiou, K. A., 2011, "The Knee Meniscus: Structure-Function, Pathophysiology, Current Repair Techniques, and Prospects for Regeneration," Biomaterials, 32(30), pp. 7411–7431.

[52] Herwig, J., Egner, E., and Buddecke, E., 1984, "Chemical Changes of Human Knee Joint Menisci in Various Stages of Degeneration," Ann. Rheum. Dis., 43(4), pp. 635–40.

[53] Eleswarapu, S. V., Responte, D. J., and Athanasiou, K. A., 2011, "Tensile Properties, Collagen Content, and Crosslinks in Connective Tissues of the Immature Knee Joint," PLoS One, 6(10).

[54] Williamson, A. K., Chen, A. C., Masuda, K., Thonar, E. J., and Sah, R. L., 2003, "Tensile Mechanical Properties of Bovine Articular Cartilage: Variations with Growth and Relationships to Collagen Network Components," J. Orthop. Res., 21(5), pp. 872–880.

[55] Chan, B. P., Fu, S. C., Qin, L., Rolf, C., and Chan, K. M., 1998, "Pyridinoline in Relation to Ultimate Stress of the Patellar Tendon during Healing: An Animal Study," J. Orthop. Res., 16(5), pp. 597–603.

[56] Takahashi, M., Suzuki, M., Kushida, K., Hoshino, H., and Inoue, T., 1998, “The Effect of Aging and Osteoarthritis on the Mature and Senescent Cross-Links of Collagen in Human Meniscus,” Arthrosc. - J. Arthrosc. Relat. Surg., 14(4), pp. 366–372.

[57] Bandeira, R. D. da C. C., Uekane, T. M., da Cunha, C. P., Rodrigues, J. M., de la Cruz, M. H. C., de Oliveira Godoy, R. L., and Fioravante, A. de L., 2013, “Comparison of High Performance Liquid Chromatography with Fluorescence Detector and with Tandem Mass Spectrometry Methods for Detection and Quantification of Ochratoxin A in Green and Roasted Coffee Beans,” Brazilian Arch. Biol. Technol., 56(6), pp. 911–920.

[58] Wang, H., Walaszczyk, E. J., Li, K., Chung-Davidson, Y. W., and Li, W., 2012, “High-Performance Liquid Chromatography with Fluorescence Detection and Ultra-Performance Liquid Chromatography with Electrospray Tandem Mass Spectrometry Method for the Determination of Indoleamine Neurotransmitters and Their Metabolites in Sea Lamprey Pl,” Anal. Chim. Acta, 721, pp. 147–153.

[59] Milićević, D., Jurić, V., Stefanović, S., Baltić, T., and Janković, S., 2010, “Evaluation and Validation of Two Chromatographic Methods (HPLC-Fluorescence and LC-MS/MS) for the Determination and Confirmation of Ochratoxin A in Pig Tissues,” Arch. Environ. Contam. Toxicol., 58(4), pp. 1074–1081.

[60] Bielajew, B. J., Hu, J. C., and Athanasiou, K. A., 2020, “Collagen: Quantification, Biomechanics, and Role of Minor Subtypes in Cartilage,” Nat. Rev. Mater., 5(10), pp. 730–747.

[61] Bielajew, B. J., Hu, J. C., and Athanasiou, K. A., 2021, “Methodology to Quantify Collagen Subtypes and Crosslinks: Application in Minipig Cartilages,” Cartilage.

[62] Espinosa, M. G., Otarola, G. A., Hu, J. C., and Athanasiou, K. A., 2021, “Cartilage Assessment Requires a Surface Characterization Protocol: Roughness, Friction, and Function,” Tissue Eng. Part C Methods, 27(4), pp. 276–286.

[63] Fithian, D. C., Kelly, M. A., and Mow, V. C., 1990, “Material Properties and Structure-Function Relationships in the Menisci.,” Clin. Orthop. Relat. Res., (252), pp. 19–31.

[64] Scott, P. G., Nakano, T., and Dodd, C. M., 1997, “Isolation and Characterization of Small Proteoglycans from Different Zones of the Porcine Knee Meniscus,” Biochim. Biophys. Acta, 1336(2), pp. 254–262.

[65] Nakano, T., Dodd, C. M., and Scott, P. G., 1997, “Glycosaminoglycans and Proteoglycans from Different Zones of the Porcine Knee Meniscus,” J. Orthop. Res., 15(2), pp. 213–220.

[66] Tanaka, T., Fujii, K., and Kumagae, Y., 1999, “Comparison of Biochemical Characteristics of Cultured Fibrochondrocytes Isolated from the Inner and Outer Regions of Human Meniscus,” Knee Surg. Sports Traumatol. Arthrosc., 7(2), pp. 75–80.

[67] Warren, M. P., and Fried, J. L., 2001, “Temporomandibular Disorders and Hormones in Women,” Cells. Tissues. Organs, 169(3), pp. 187–192.

[68] Clark, C. R., and Ogden, J. A., 1983, “Development of the Menisci of the Human Knee Joint. Morphological Changes and Their Potential Role in Childhood Meniscal Injury,” J. Bone Joint Surg. Am., 65(4), pp. 538–547.

Chapter 7: Tissue engineering toward knee meniscus regeneration in a Yucatan minipig model

Abstract

Treatments for injuries pertaining to the knee meniscus, the tissue that is most commonly treated in orthopaedic surgical procedures, are rarely reparative, and their long-term durability remains unpredictable. Meniscectomy can temporarily relieve pain but virtually guarantees the emergence of osteoarthritis. To address the lack of effective regenerative techniques for the knee meniscus, scaffold-free tissue-engineered implants were created using allogeneic, passaged costal chondrocytes. Efficacy in repairing a partial thickness meniscal lesion was examined in Yucatan minipigs using a novel surgical technique inspired by methods utilized in the repair of the temporomandibular joint disc. Two pilot studies were first conducted to validate the surgical method. A full study showed that treatment with an implant was safe and did not incur a systemic immune response. Additionally, implant treatment increased the stiffness of the interface between meniscal and repair tissue in the pocket holding the implant by 51% over controls; no differences in defect repair tissue mechanical or biochemical properties were identified between control and treatment groups. Gross morphological analysis showed 100% repair tissue filling in the defect for all animals within both control and treatment groups; additionally, damage to articular cartilage on medial femoral and tibial condyles was identified in all animals. Finally, histological analysis at t=8 weeks did not reveal signs of an implant within

In preparation for submission as: Gonzalez-Leon, EA, Salinas, EY, Wang, D, Hu, JC, & Athanasiou, KA. *Tissue engineering toward knee meniscus regeneration in a Yucatan minipig model*.

menisci in the treatment group. Thus, while this study developed a novel surgical procedure for implantation of neocartilage constructs within the meniscus, and showed safety and partial efficacy of the treatment, improvements to the surgical procedure in future studies is recommended to ensure retention of the implant and prevent robust healing in control defects. Ultimately, this tissue-engineering strategy paves the way for developing clinical treatments for meniscal lesions.

7.1. Introduction

The knee meniscus can sustain damage resulting from trauma resulting from physical activity, or age-related degeneration; meniscal lesions are the most common intra-articular knee injury and account for approximately 20% of all orthopedic surgical procedures in the U.S. [1]. Approximately 850,00 patients per year receive surgery involving the meniscus [2], and the medial meniscus is 4-times more likely to be damaged and undergo surgery compared to the lateral meniscus [3]. Additionally, because the meniscus is a fibrocartilaginous tissue that is nearly devoid of vascularity, it is generally not amenable to repair.

Management of meniscal injuries can vary with respect to disease severity and type; options range from physical therapy to surgical intervention [4–6]. Meniscectomy, the partial or complete removal of the knee meniscus, temporarily relieves pain but often leads to degenerative changes of the joint [7–9]. Few clinical options are available for meniscus repair, and these are mainly based on products made of synthetic materials, such as the collagen meniscus implant (CMI); while short-term efficacy has been shown with these approaches, long-term efficacy of these synthetic implants can be unpredictable [10]. Meniscus allografts have also been proposed as a solution for

replacement of knee menisci, but they can face complications such as size mismatching; additionally, contact mechanics and kinematics are not restored to levels of the intact knee with this approach [11–13]. Thus, novel regenerative solutions for knee meniscus repair and replacement are required.

Tissue engineering is a promising strategy that may offer solutions for patients suffering from a meniscal lesion by repairing and limiting further tissue damage, as well as the possibility of full replacements. Neomenisci and neocartilage, for example, have been created using the self-assembling process and have been shown to attain robust mechanical and biochemical properties with the use of mechanical and biochemical stimuli during culture [14–17]. Application of bioactive factors such as TGF-β1, glycosaminoglycan-cleaving enzyme C-ABC, and crosslinking agent LOXL2 treatments (together termed “TCL”) during the culture of tissue engineered fibrocartilage led to significant improvements of tensile properties [18]. Costal chondrocytes from minipig floating rib cartilage have also been used to create robust neocartilage at high passages with the use of TCL treatment; additionally, these neocartilage constructs treated with TCL have been used to repair the temporomandibular joint (TMJ) disc of Yucatan minipigs using a novel surgical technique [19]. The knee meniscus and TMJ disc are both anisotropic, fibrocartilaginous tissues function primarily under tension; thus, the knee meniscus may benefit from similar tissue engineering and surgical approaches.

The Yucatan minipig has been gaining popularity in orthopedic research [20–22], and has recently been identified as a large-animal model fit for translational meniscus research; Yucatan minipigs share physiological similarities with humans and have several structure-function properties within human meniscal tissue ranges [23]. For example,

minipig weights are comparable to humans [23,24]; additionally, the posterior region of the minipig medial meniscus exhibits the lowest radial stiffness when compared to the medial anterior and central regions, which is also seen in humans and corresponds to the most prevalent location for meniscal lesions. In contrast to farm pigs, minipigs are more suitable for long-term studies because their smaller size leads to reductions in needs related to handling, housing, surgery, anesthesia, and food [25]. Because the Yucatan minipig provides physiological, structural, and biochemical similarities to humans, and requires fewer resources for surgery and handling compared to farm pigs, it can serve as a large animal model for meniscus research, particularly through the implantation of self-assembled tissues toward regenerating meniscal lesions.

To implant self-assembled neocartilage toward regenerating meniscal lesions in vivo, novel surgical methods may be required. While arthroscopic procedures have been used to fix meniscal lesions that are more amenable to repair (i.e., tears within the outer red-red and white-red zones) [26], self-assembled neocartilage constructs might not be able to be delivered arthroscopically due to their dimensions and mechanical stiffness that prevents folding. Another fibrocartilage that has been repaired via implantation of self-assembled neocartilage is the TMJ disc, for which a novel surgical method termed the intralaminar fenestration technique was developed. The technique consists of creating two laminae within the disc, acting as a pocket for the implant; importantly, no sutures were placed on articulating surfaces, thus avoiding potential wear on the corresponding condyles. Use of the intralaminar fenestration technique for implanting engineered discal tissue was successful in repairing a partial thickness perforation [19]. Similar techniques might be required in the knee meniscus to ensure that the implant remains in place.

Additionally, bilateral surgeries have been utilized in Yucatan minipig orthopedic research [27–29]; utilizing both limbs during a preclinical study would reduce the animals required while maintaining an adequate number of samples for a statistically powered study. Thus, while the Yucatan minipig has been identified as a suitable animal model for meniscus research, novel surgical methods are required to deliver self-assembled implants toward regeneration of meniscal lesions.

This work examined the reparative capacity of allogeneic, tissue-engineered implants in the minipig medial meniscus compared to empty defect controls (untreated group) using a non-homologous approach (i.e., rib cartilage to meniscus). A novel surgical method inspired by methods previously used to repair the TMJ disc in the minipig model was employed to accommodate delivery of a self-assembled neocartilage implant into the knee joint. Minipig knee menisci were investigated by gross morphology, histology, mechanical testing under tension, and biochemical analyses. Pilot studies were conducted to validate whether the surgical technique was able to consistently create a defect in the correct anatomical location, and whether the implant would be retained within the meniscus. We hypothesized that 1) menisci receiving an implant would contain repair tissue within the defect that has more robust mechanical and biochemical properties than repair tissue in control meniscus defects, 2) native tissue interfaces with repair tissues (within the pocket and defect, respectively) would have more robust tensile properties in menisci receiving an implant compared to untreated controls, and 3) the implant would be identifiable within the meniscal body after 8 weeks. The data here will serve to advance the understanding of tissue-engineering efforts toward regeneration of meniscal lesions,

and, thus, assist the translation of regenerative technologies from the bench to the clinic by informing future meniscal surgical procedures in minipigs.

7.2. Materials and methods

Minipig costal chondrocyte harvest

Mini pig costal chondrocytes were harvested from the costal cartilage of juvenile (6-8 months) Yucatan minipigs (Figure 7.1; S&S Farms, California, USA). The perichondrium was first removed from the costal cartilage before mincing. Next, the minced cartilage was digested in a solution of 0.2% w/v collagenase and 3% fetal bovine serum (FBS) for 18 hours. After isolation, cells were frozen at -80°C for 24 hours in Dulbecco's modified Eagle's medium (DMEM) supplemented with 20% fetal bovine serum and 10% dimethyl sulfoxide medium at 5 million cells per milliliter before being stored in liquid nitrogen until seeding.

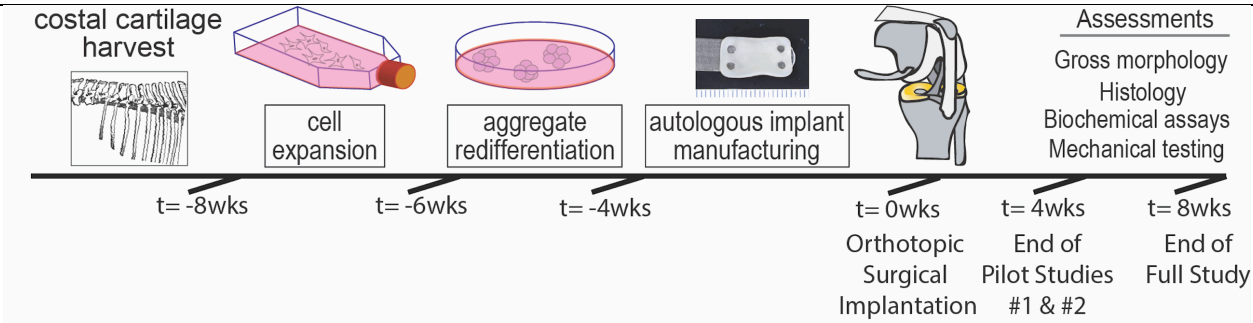

Figure 7.1: Formation of tissue-engineered implants from costal chondrocytes and experimental timeline.

Costal chondrocyte expansion and self-assembly of implants

Minipig costal chondrocytes were thawed in a water bath at 37°C, rinsed in wash media, centrifuged at 400g, and resuspended in warm chondrogenic media (CHG) with 2% FBS.

The cells were counted and brought to 1e6 cells/ml in CHG + 2% FBS + growth factors (1ng/ml TGF-β1 + 5ng/ml bFGF + 10ng/ml PDGF). Finally, 2.5ml of the cell solution plus 27.5 ml of CHG+2% FBS were seeded per T225 flask, and the flasks were placed in an incubator at 10% CO2. Chondrogenic medium and growth factors were changed every 3-4 days. Cells were passaged once they reached approximately 95% confluency, as previously described [19].

Once the cells were expanded to passage 3, they were placed into aggregate rejuvenation for 11 days, as described previously (Figure 7.1) [30]. The aggregates were then digested using 0.05% trypsin-EDTA solution and, subsequently, 2% collagenase solution (with 3% FBS in CHG) to liberate the chondrocytes. Subsequently, 8x13mm agarose (2%) wells were created using an acrylic well-maker as described previously [31]. Each well was seeded with 7 million chondrocytes suspended in 250µl of CHG; after 4 hours, the cells were fed with 2.5 mL CHG. Medium in the wells was replaced every day for the first 2 days. On day 3, the neocartilage was removed from the wells, placed in 6-well plates, and CHG (5mL) was replaced every other day. The total culture duration time was 35 days.

Each construct received the following biochemical treatment regimen: 1) TGF-β1 continuously throughout culture at 10 ng/mL, 2) a one-time C-ABC treatment, added to medium with a 0.05 M sodium acetate activator, at day 7 of culture at 2 U/mL for a duration of 4 hours, and 3) LOXL2 applied continuously from days 7 until implantation at 0.15 ng/mL as previously described [32–34]. All constructs were cultured for 5 weeks at 37ºC and 10% CO2.

7.2.1 Animals, surgical procedure, and post-operative care

The work was initiated by a pilot study to examine the feasibility of the surgical method to create a defect and implant self-assembled neocartilage within the anterior body of the minipig medial meniscus. Subsequently, due to the creation of the defect in the incorrect location in the first pilot study, a second pilot study investigated and validated changes to the surgical approach. The Full study was informed by the two pilot studies and utilized the surgical approach from Pilot Study #2.

Pilot Study #1

Two healthy, skeletally mature, 16-18-month-old male and female Yucatan minipigs were used in this study. Animals arrived one week prior to surgery to acclimate to their housing pens.

Surgical approach: Preparation for surgery, including the administration of anesthesia, was performed with assistance by ULAR Veterinary Services. Initial induction was with Telazol 10mg/kg IM injection with addition of xylazine 2mg/kg IM. Dosages were subject to the discretion of the veterinarian An IV catheter was placed in the ear vein and was used for administration of IV fluids (LRS 5-10ml/kg/hr). In addition, isoflurane delivered by mask was used during the IV catheter and induction period. Once in the appropriate depth of anesthesia, the minipig was intubated; general anesthesia was maintained with isoflurane (1-3%) accompanied with mechanical ventilation. Pre-emptive analgesia was delivered with Meloxicam 0.4mg/kg IM as well as sustained release buprenorphine at 0.2mg/kg subcutaneously. Vitals monitoring was achieved with capnography, a thermometer, and pulse oximetry. A heated water pad was used to keep the pigs at a temperature of 37-38 degrees Celsius. Once the minipig was anesthetized, 2-4ml of blood was collected for analysis of complete blood count (CBC) and blood phenotyping

chemistry panel (BPCP) to establish a baseline of properties for all minipigs. Additional blood samples for CBC and the BPCP were collected for each animal directly prior to euthanasia to determine the possible systemic effect of the implant.

Under general anesthesia, the knees were surgically prepared and draped. With the minipig in dorsal recumbency, a medial parapatellar approach was taken to access the right knee joint. The patella and patellar tendon were not distracted, and cruciate ligaments and joint surface cartilage integrity were maintained. A #11 scalpel blade was used to create approximately 6mmx4mm pockets in the anterior body of the medial and lateral menisci, as well as two laminae as previously described in the TMJ [19]. Using a 2-mm biopsy punch, a partial-thickness defect was created through the top lamina (articulating meniscal surface). Neocartilage constructs measuring approximately 4mmx3mm were implanted within the two laminae in the medial meniscus, while the lateral meniscus did not receive an implant. Finally, the outer portion of the medial meniscus was closed using 6-0 nylon suture before closing the leg with 2-0 PDS suture (Ethicon). The pilot study duration was 4 weeks.

Pilot Study #2

Two healthy, skeletally mature, 16-18-month-old male and female Yucatan minipigs were used in this study. Animals arrived one week prior to surgery to acclimate to their housing pens.

Surgical approach: Preparation for surgery was performed as described above. Under general anesthesia, the knees were surgically prepared and draped. With the minipig in dorsal recumbency, a medial parapatellar approach was taken to access the right knee

joint. The patella and patellar tendon were not distracted, and cruciate ligaments and joint surface cartilage integrity was maintained. Subsequently, destabilization of the medial meniscus was created by cutting through the anterior root (Figure 7.2A). Then, the meniscal-tibial attachment was trimmed using a scalpel to allow for additional movement and extrusion of the medial meniscus (Figure 7.2B). A 6600 Beaver blade was used to make approximately 6mmx4mm pockets in the anterior body of the medial meniscus via the creation of two laminae (Figure 7.2C). Using a 3-mm biopsy punch, a partial-thickness defect was created through the top lamina (articulating meniscal surface) (Figure 7.2D). Neocartilage constructs measuring approximately 5mmx3-4mm were implanted within the two laminae for the treatment group (Figure 7.2F), while the control group did not receive an implant. Finally, the outer portion of the medial meniscus was closed using 6-0 nylon suture (Figure 7.2G) and was restabilized using a Mini QUICKANCHOR bone anchor with #2 Ethibond (V-5) suture (Mitek) before closing the leg with 2-0 PDS suture (Figure 7.2H; Ethicon). The second pilot study duration was 4 weeks.

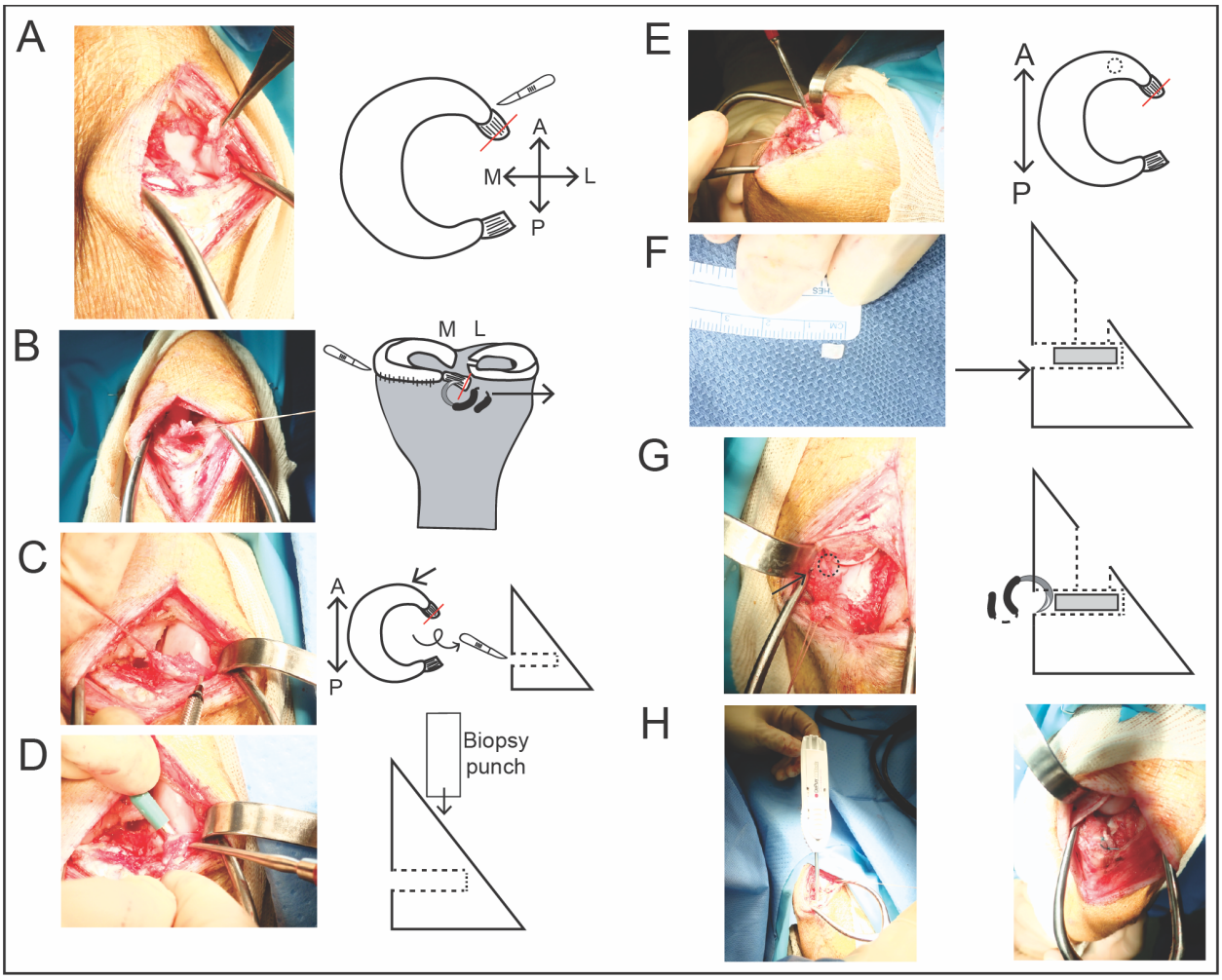

Figure 7.2: Schematic and intraoperative images demonstrating the intralaminar fenestration surgical technique in the minipig knee meniscus. A) the medial meniscus is destabilized at the anterior root, B) suture is sewed through the anterior root to pull the meniscus outward while cutting the tibial attachment, C) the intralaminar fenestration technique is used to create a pocket within two laminae in the meniscus, D) a 3mm hole punch is used to create a defect in the white-red zone, E) a freer elevator tool is depicted within the pocket and is seen through the defect, F) an implant measuring approximately 3mmx5mm is inserted into the pocket between two laminae, G) the

pocket is closed by suturing the two laminae at the outer edge of the meniscus, H) a bone anchor is used to re-stabilize the meniscus.

Full study

Six healthy, skeletally mature, 16-18-month-old male Yucatan minipigs were used in this study. Animals arrived one week prior to surgery to acclimate to their housing pens.

Surgical approach: Surgery preparation, in addition to the procedure used to create defects within the medial meniscus, was performed as described in Pilot Study #2.

Minipigs were then subjected to a bilateral surgical procedure in which one knee received a neocartilage implant and the other knee served as a control; the legs receiving an implant were alternated between animals to remove bias. The Full Study duration was 8 weeks.

7.2.2 Post-operative care

Minipigs were placed in a custom-made, IACUC-approved, sling immediately after surgery to prevent the minipig from injuring itself while awakening from anesthesia, and to prevent the immediate loading of the operated knee joint, as previously described [35]. The cage in which the minipigs were placed while suspended in the sling was also equipped with additional padding that was covered in plastic to prevent the minipig from injuring itself post-surgery. Minipigs were recovered in pens approximately 3-4 hours after surgery. Floors of recovery and of pens for housing were covered in anti-slip mats.

In terms of postoperative analgesia, animals received Meloxicam 0.4 mg/kg IM or Banamine (Flunixin) 2.2 mg/kg once daily for 3 days and then as needed per ULAR vet

services' recommendation. An additional dosage of buprenorphine was given 2-3 days postoperatively if needed.

7.2.3 Activity monitors

Actigraph wGT3X activity monitors were attached onto a custom-made belt, which was then draped around the abdomen of n=2 minipigs 5 days before surgery. Monitors were removed during surgery and then placed on the animals again once they were placed back in their recovery pens; monitors remained attached for 17 days after surgery.

7.2.4 Euthanasia

Minipigs were humanely euthanized 8 weeks after implantation with an intramuscular injection of Telazol/Xylazine followed by an IV injection of pentobarbital (Euthasol) at a dose of 1 ml (390 mg/4.5 kg); minipigs in pilot studies were euthanized 4 weeks after implantation. Knee joints were removed en bloc and transported to the laboratory to be processed for assessment of gross morphological and functional properties.

7.2.5 Knee meniscus gross morphology, histology, and macroscopic characterization

The menisci were excised and subsequently covered in gauze soaked in PBS-containing protease inhibitors 10 mmol/L N-ethylmaleimide and 1 mmol/L phenylmethylsufonyl fluoride (Sigma) and stored at 4°C until testing. Menisci in addition to femoral and tibial condyles were photographed before dividing each meniscus. Pieces for mechanical testing and their dimensions were measured using ImageJ (NIH; Figure 7.3); tensile samples were collected from the repair tissue within the defect, the interface between repair and native tissue, and the laminae interface. Samples for biochemical analysis were resected from the repair tissue found within the defect. Histology samples comprised of a cross section taken from each meniscus at the outer edge of the defect. For histology,

construct samples were fixed in 10% neutral buffered formalin, then embedded in paraffin and sectioned at 5μm. Safranin-O/fast green, picrosirius red, and hematoxylin and eosin (H&E) stains were conducted to visualize GAG, collagen, and cell distributions, respectively.

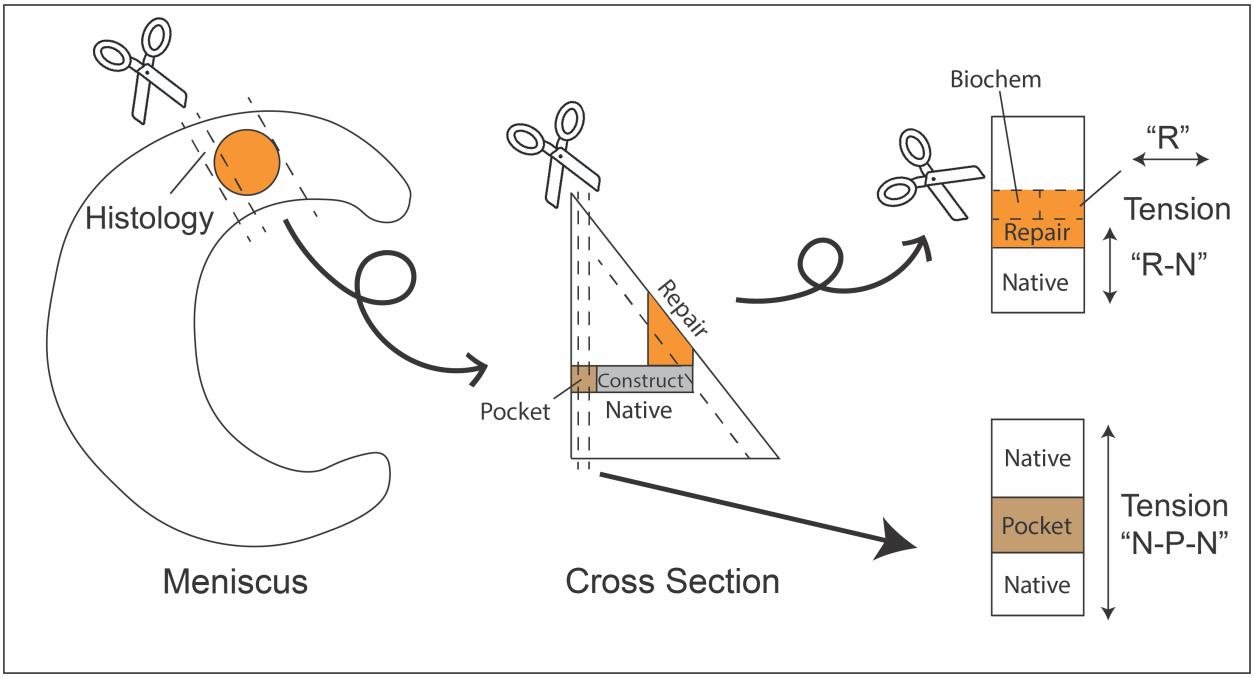

Figure 7.3: Division of minipig knee menisci for mechanical, biochemical, and histological analyses. The outer edge of each defect was used for histology. Strips from the cross section were taken for tensile testing of defect Repair (R) tissue in the circumferential direction in addition to Native-Repair (N-R) and Native-Pocket-Native (N-P-N) interfaces. Biochemistry samples were collected from leftover R tissue after tensile testing.

7.2.6 Tensile testing

Tensile properties were assessed using uniaxial, strain-to-failure testing. The following tissues and interfaces were tested: defect repair tissue (R), native-pocket-native (N-P-N) interface, and native-repair (N-R) tissue interface (Figure 7.3). R samples were tested in

the circumferential direction only due to the limited amount of tissue available. Samples were cut into rectangular strips and photographed, and the dimensions were measured with ImageJ. Samples were then clamped within a uniaxial testing machine (Instron model 5565) and subjected to a 1% s-1 strain rate until failure. Young's modulus was calculated from the linear portion of the stress-strain curve, and ultimate tensile strength (UTS) was calculated from the maximum stress.

7.2.7 Analysis of tissue biochemical content

Biochemistry samples consisted of repair tissue within the meniscal defects; samples were weighed wet, then frozen and lyophilized to acquire dry weights. Collagen content was measured with the use of a Sircol standard (Biocolor) and a modified chloramine-T colorimetric hydroxyproline assay [36]. GAG content was quantified using the Blyscan Glycosaminoglycan assay kit (Biocolor). All quantification measurements for collagen and GAG content were performed with a GENios spectrophotometer/spectrofluorometer (TECAN).

7.2.8 Safety assessments

Blood samples taken from minipigs pre-surgery and directly before euthanasia were shipped overnight to the UC Davis Comparative Pathology Laboratory (UC Davis CPL), where they were subjected to a complete blood count (CBC) and a blood phenotyping chemistry panel (BPCP).

7.2.9 Statistical analysis

For each biomechanical, biochemical, and morphological test, n=6 samples were used. A single factor analysis of variance (ANOVA) was used to determine whether the properties differed by group. Additionally, a Student's t-test was used to compared CBC

and BPCP data at t=0 and t=8 weeks. A Tukey's HSD post hoc test was performed when merited. All statistics were performed with $p<0.05$. All data are presented as means ± standard deviations. For all figures, a connecting letters report shows statistical significance as indicated by groups not sharing the same letters.

7.3. Results

7.3.1 Gross morphology and histology

Pilot Study #1

The Yucatan minipig medial menisci retained their semi-lunar and wedge shape; it was found post-sacrifice that the defect was created in the anterior root as opposed to the anterior body of the meniscus (Figure 7.4). Considerable fibrovascular scar tissue was observed in both animals at the anterior root where the defects were created. Defects were not able to be identified underneath the scar tissue. Because the defect was not in the correct anatomical location, and neither the defect nor implant were identifiable, histological samples were not taken from these animals.

Pilot Study #2

The Yucatan minipig medial menisci retained their semi-lunar and wedge shape and showed signs of translucent, red-hued repair tissue within all the defects for both animals (Figure 7.4); defects were placed in the white-red zone of the anterior body of the medial meniscus as intended. When creating the meniscal pocket using the intralaminar fenestration technique, one animal accidentally received a through-and-through incision. One animal had an oval-shaped defect while the other exhibited a defect with jagged, non-uniform edges. Damage to the medial femoral condyle was identified in one of two

animals, while both animals showed signs of damage to underlying articular cartilage on the tibial plateau. The self-assembled neocartilage construct was identified via histological visualization within one of two animals used in the pilot study, which exhibited less intense collagen staining compared to surrounding native tissue.

Full Study

The Yucatan minipig medial menisci retained their semi-lunar and wedge shape and showed signs of excellent repair tissue within all defects for both control and implant groups (Figure 7.5); repair tissue had a translucent, smooth appearance and a light-pink or gray hue, and reached the defect edges on the articulating surface. Defects were circular- or oval-shaped in Control and Implant groups. Additionally, all medial femoral condyles and tibial plateaus exhibited damage to the articular cartilage for both control and implant groups (Figure 6). The implant was not clearly identified in the Implant group gross morphologically or histologically after 8 weeks, though signs of the pocket created using the intralaminar fenestration technique was visible (Figures 7.7 & 7.8).

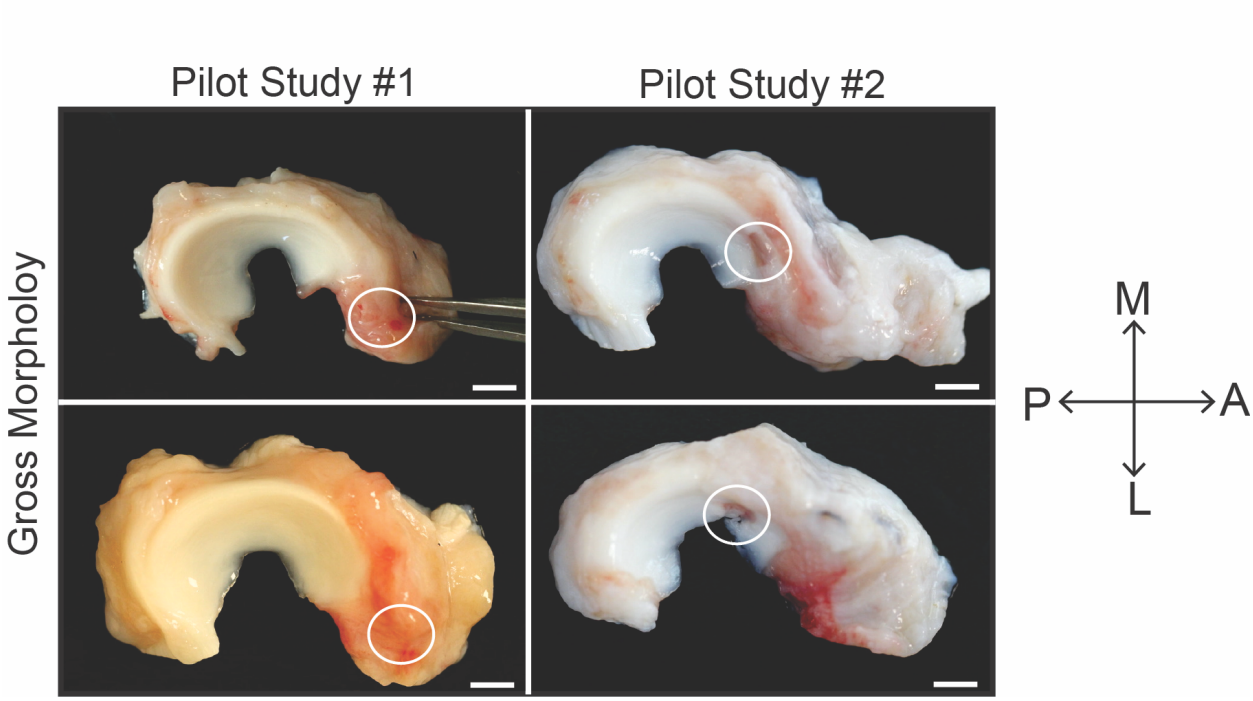

Figure 7.4: Gross morphology of Yucatan minipig knee menisci – Pilot Study #1 and Pilot Study #2. Gross morphology of n=2 menisci are shown for each surgical set. Scale bar represents 5mm and circles represent the defect location.

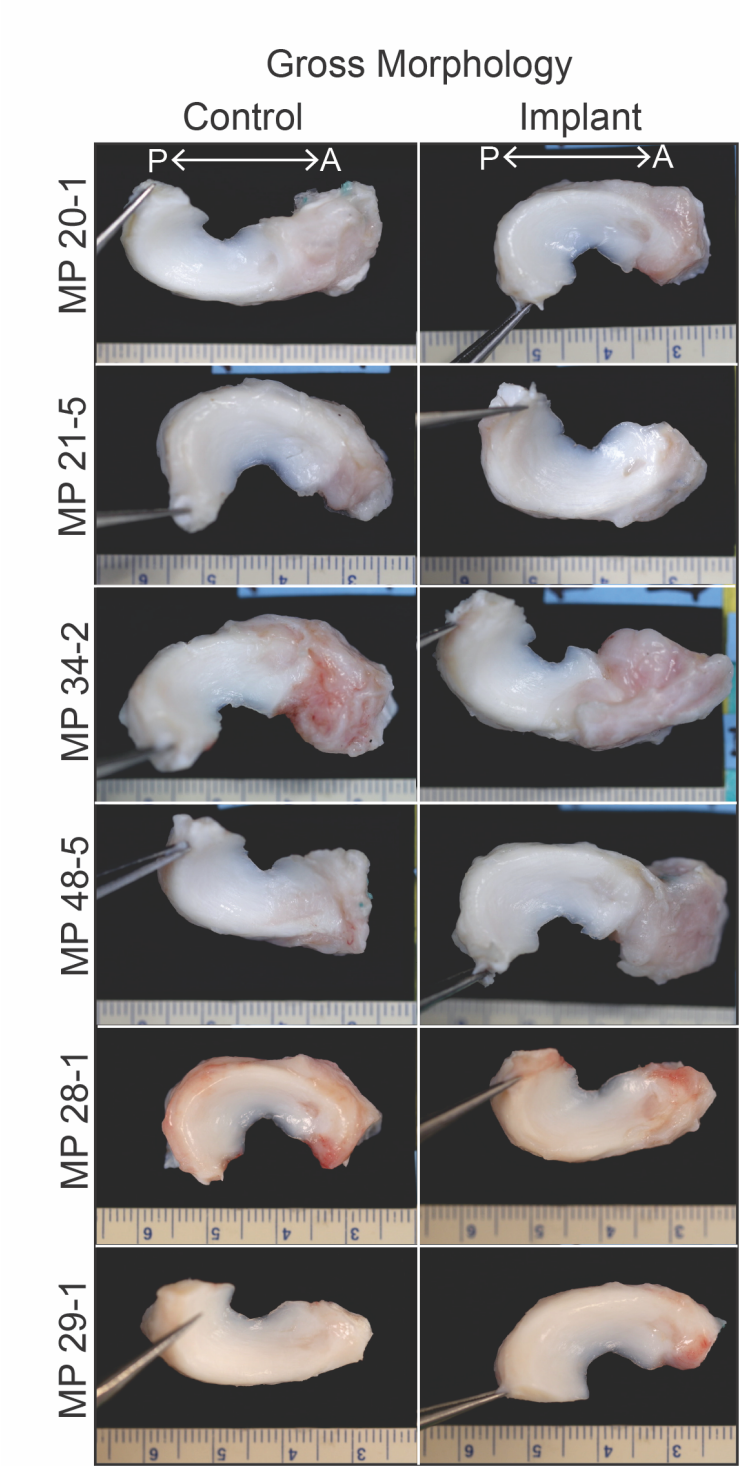

Figure 7.5: Gross morphology of Yucatan minipig knee menisci – Full Study. Gross morphology of Control and Implant groups are shown. Arrows denote anterior (A) and posterior (P) directions.

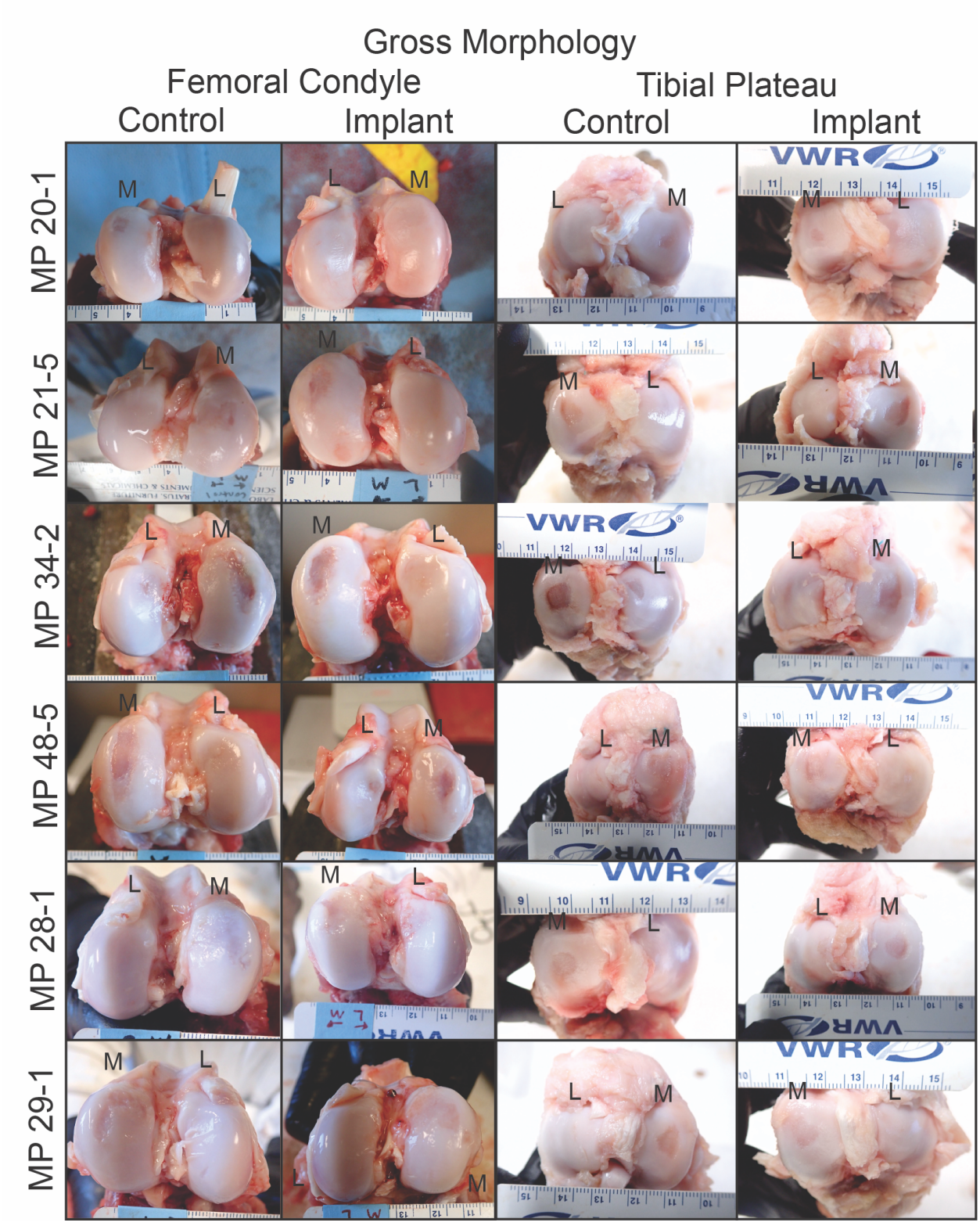
Gross Morphology
Femoral Condyle
Tibial Plateau
Control
Implant
Control
Implant
MP 20-1
MP 21-5
MP 34-2
MP 48-5
MP 28-1
MP 29-1

Figure 7.6: Gross morphology of Yucatan minipig femoral condyles. Gross morphology of femoral condyles from Control and Implant groups are shown. “M” and “L” denoted medial and lateral condyles, respectively.

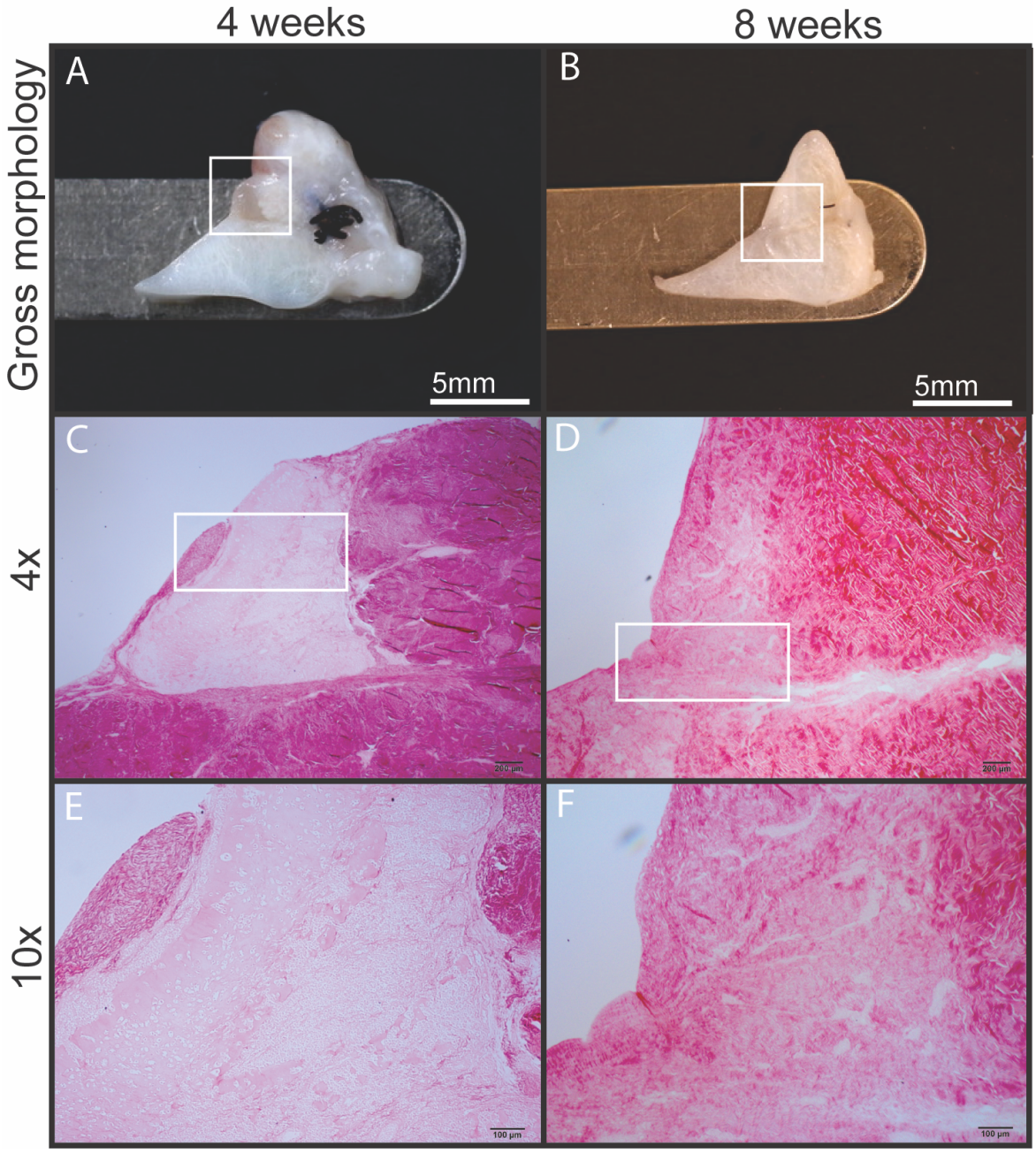

Figure 7.7: Histological assessment of integration of the tissue-engineered implants within Yucatan minipig knee menisci. (A and B) Gross morphology of the sections obtained from the minipig menisci treated with tissue-engineered implants, 4 and 8 weeks after implantation, respectively; pieces of the black suture used to close the pocket can be seen. (C and D) Low-magnification picrosirius red histology of the meniscus cross section containing a tissue-engineered implant, which appears as a pink band at 4 weeks and is not clearly outlined at 8 weeks, respectively. (E and F) Higher magnification of the H&E sections containing implants at 4 and 8 weeks after implantation, respectively.

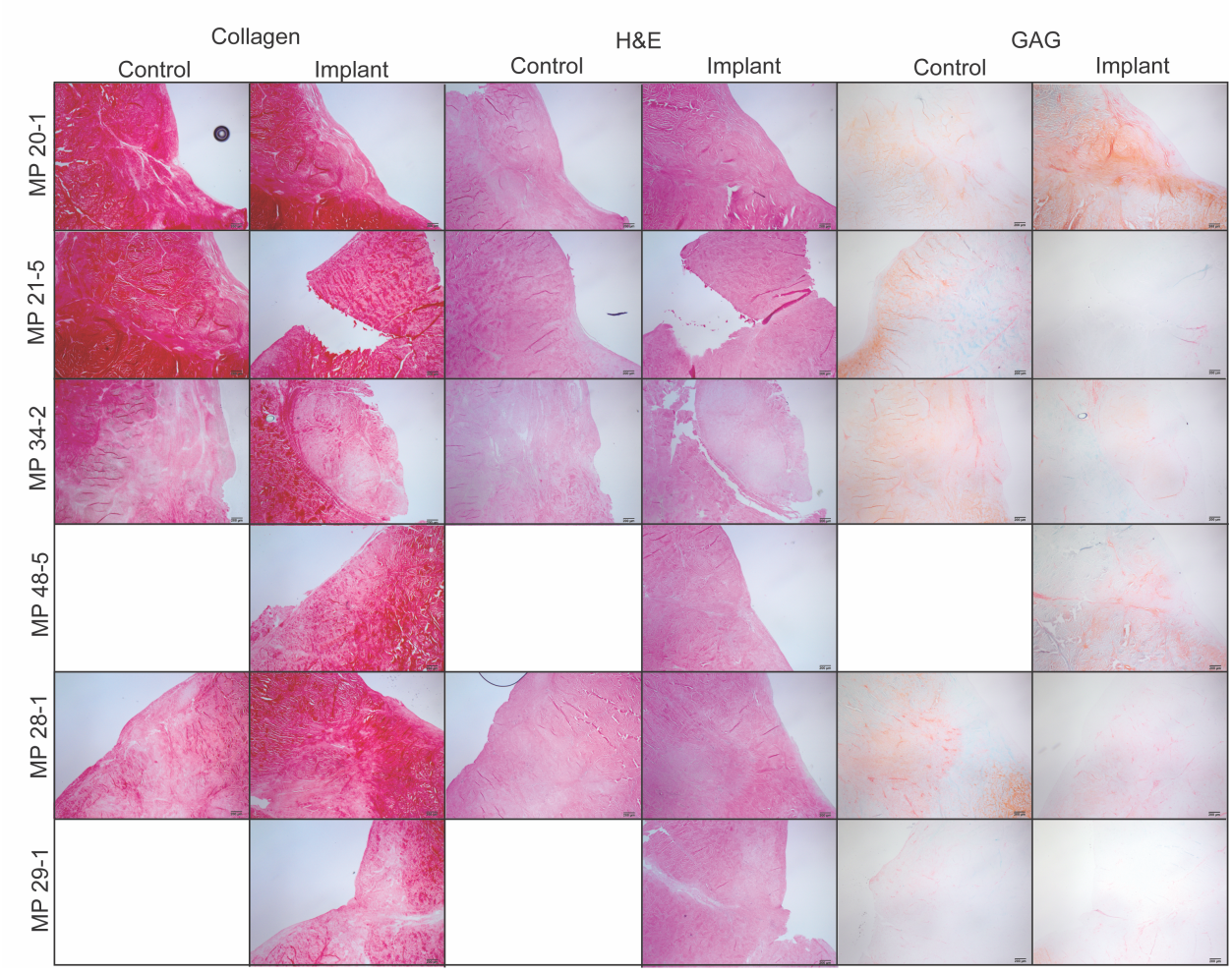

Figure 7.8: Histological staining of Yucatan minipig knee menisci for the Full Study. Cross sections of menisci stained for collagen (picrosirius red), GAG (Safranin-O), and cell content (H&E) are shown. Samples that are missing images resulted from the loss of tissue during sectioning.

7.3.2 Tissue biomechanics

Pilot Studies

Because the defect was not created in the intended anatomical location, and neither the defect nor implant were identifiable, samples for mechanical testing were not taken from animals used in Pilot #1. In Pilot #2, the repair tissue (R) sample collected from the meniscus that showed healing within the defect contained Young's modulus and UTS values of 4.2 MPa and 2.9 MPa, respectively.

Full Study

Biomechanical data revealed no significant differences in Young's modulus between Control and Implant groups for R and R-N samples (Figure 7.9), while the Implant group had significantly higher values than the Control group for N-P-N samples (6.15±0.85 MPa vs. 4.08±1.0 MPa, respectively; p=0.003) (Figure 10). Constructs at t=0 weeks in vitro trended higher in Young's modulus and UTS values than constructs cultured for t=8 weeks, but no significant statistical difference was observed.

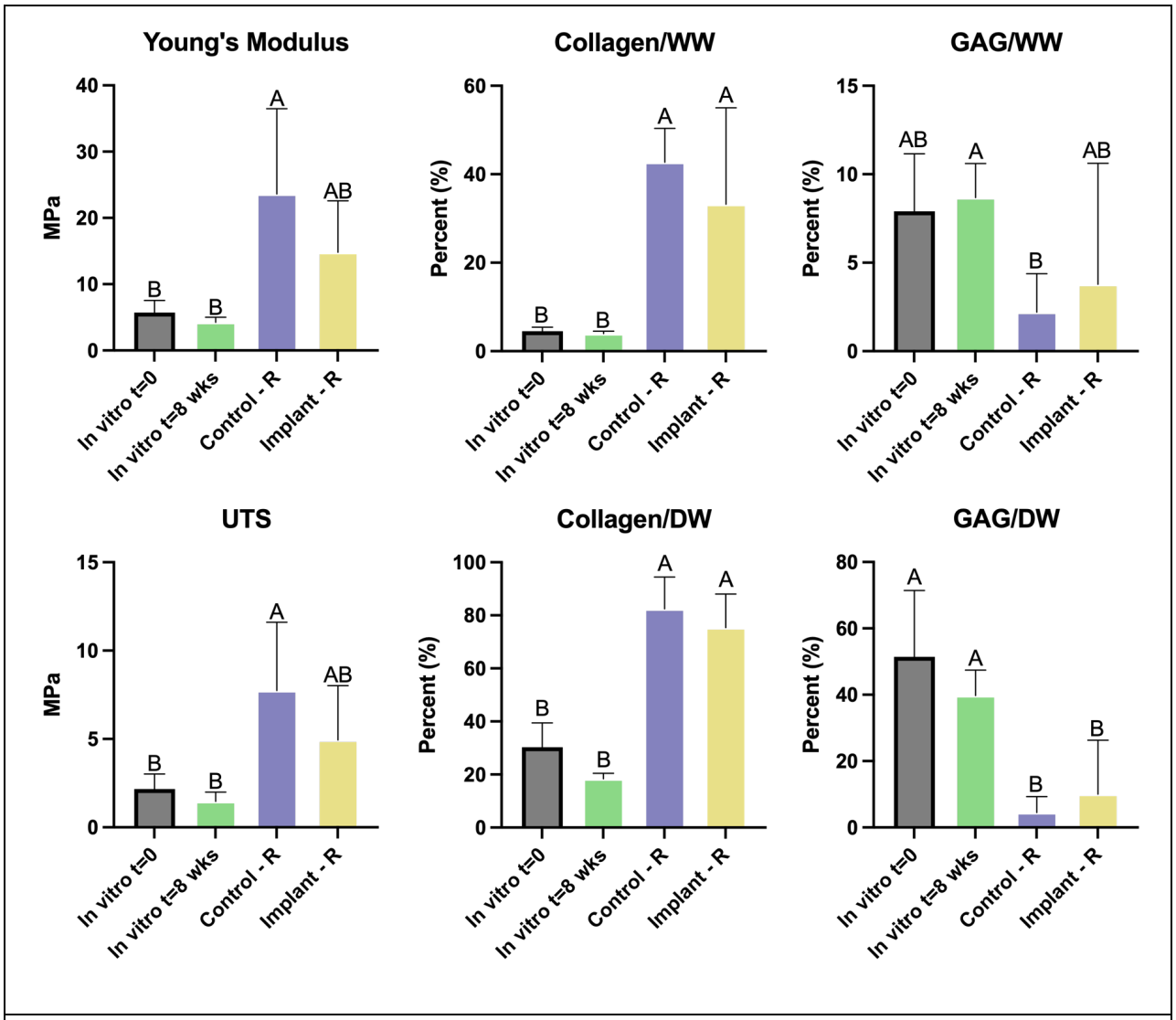

Figure 7.9: Tensile and biochemical properties of repair tissue. Young's Modulus and UTS of repair tissue within the defects are shown for the circumferential directions. No significant difference was seen in tensile Young's modulus and UTS between R samples from Control and Implant groups; R samples from the Control group were significantly higher in Young's modulus and UTS values compared to in vitro controls at t=0 and t=8 weeks. Repair tissue in Control and Implant groups exhibited higher collagen content and lower GAG content compared to t=0 and t=8wks controls, respectively; no significant difference in collagen or GAG content was seen between R samples in Control and

Implant groups. All data are presented as means ± standard deviations. For all figures, statistical significance is indicated by bars not sharing the same letters.

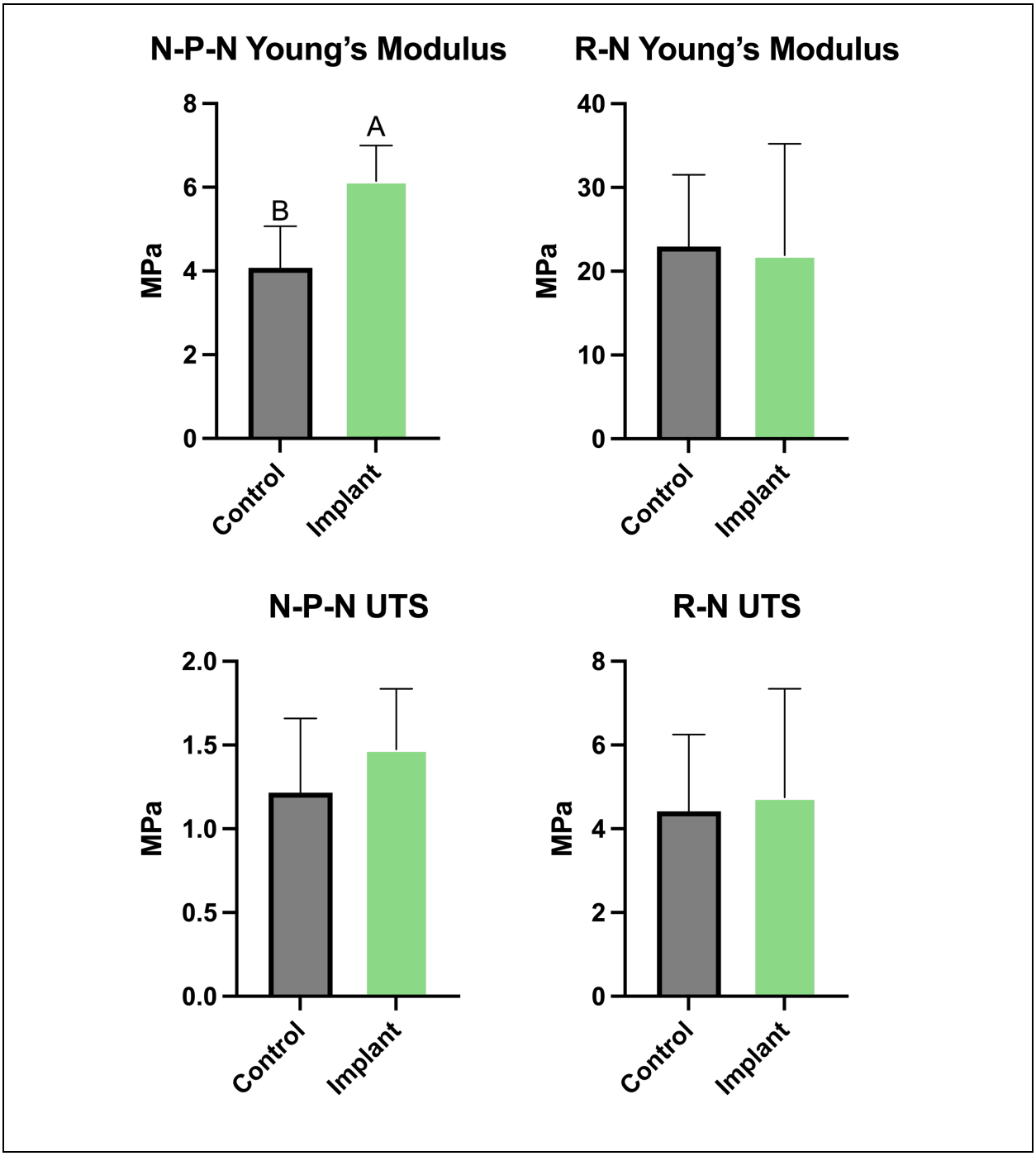

Figure 7.10: Tensile properties of Yucatan minipig menisci repair tissue interfaces. Young's modulus and ultimate tensile strength (UTS) of N-P-N and N-R interfaces are shown. N-P-N interface Young's modulus was higher in Implant group samples compared to untreated Controls. All data are presented as means ± standard deviations.

7.3.3 Tissue biochemistry

Pilot Studies

Because the defect was not created in the intended anatomical location in Pilot Study #1, and neither the defect nor implant were identifiable, samples for biochemical testing were not taken from these animals. Pilot Study #2 utilized n=1 for the Implant group without controls as references, statistical analysis of tissue mechanical properties could not be performed. However, repair tissue collagen (COL) content normalized to WW and DW measured 4.0% and 11.4%, respectively.

Full Study

In vitro constructs at t=0 weeks and t=8 weeks were both significantly higher in hydration percentages than repair tissue from Control and Implant groups, respectively (84.4±3.8% and 78.3±0.94% vs 46.7±14.6% vs. 49.3±29.5%, respectively). Control and Implant groups exhibited higher collagen (COL) content per wet weight (WW) and dry weight (DW) than t=0 weeks and t=8 weeks in vitro constructs (Figure 7.9). Control and Implant groups contained 42.7±7.6% and 33.3±21.8% COL/WW, respectively, in addition to 82.5±12.0% and 75.4±12.7% COL/DW, respectively. Additionally, Control and Implant groups contained significantly less GAG/WW and GAG/WW than t=0 weeks and t=8

weeks constructs. Control and Implant groups contained 2.2±2.2% and 3.8±6.8% GAG/WW, respectively as well as 4.5±4.8% and 10.1±16.2% GAG/DW, respectively.

7.3.4 Activity monitors

Full Study

Activity monitor data provided step counts for n=2 minipigs from 5 days before surgery until 17 days after surgery. Average step count before surgery was 3180±864 steps per day; on days 1, 5, 10, and 15 step counts were 231±252, 1460±112, 1594±1099, and 1870±1395 steps per day, respectively (Supplementary Figure 7.1). One of two minipigs (MP 29-1) was able to recover to pre-surgical activity as denoted by step count, while a positive trend toward reaching baseline activity levels was identified in MP 28-1.

7.3.5 Complete Blood Count (CBC)

CBC values for Pilot Study #1 and Pilot Study #2 were not assessed for changes between t=0 weeks and t=4 weeks (n=2; Supplementary Table 7.1, 7.3). For assessment of changes between the t=0 weeks and t=8 weeks, CBC values at both timepoints were compared. No significant difference was identified between both timepoints for 16 of 20 CBC values, including white blood cell (WBC) among others, indicating that they remained stable throughout the duration of the study (Table 7.1). Red blood cells (RBC) significantly increased from t=0 to t=8 weeks (5.37±0.49 M/ul vs. 6.57±0.59 M/ul, respectively; p=0.01) in addition to hemoglobin (9.58±1.03 g/dL vs. 11.28±0.67 g/dl, respectively; p=0.01), and hematocrit (30.48±3.72% vs. 36.28±1.97%, respectively; p=0.02); platelet content significantly decreased from t=0 to t=8 weeks (418±102 K/ul vs. 255±89 K/ul, respectively; p=0.03). Hemoglobin content at t=0 weeks was the only

parameter outside of porcine reference ranges provided by UC Davis CPL that are meant to serve as general guidelines.

Table 7.1: Full Study CBC data. CBC values from t=8 weeks normalized to values from t=0 are shown. Student's *t*-test shows significant differences between time points for red blood cell, hemoglobin, hematocrit %, and platelet content.

Minipig	**20-1**	**21-5**	**34-2**	**48-5**	**28-1**
WBC	1.04	1.09	0.80	0.79	1.77
Absolute Neutrophil cells	1.51	1.34	0.89	0.84	1.63
Absolute Lymphocyte cells	0.63	0.83	0.90	0.67	1.42
Absolute Monocyte cells	0.37	1.73	0.60	0.95	1.46
Absolute Eosinophil cells	4.80	0.17	0.09	0.29	11.87
Absolute Basophil cells	1.33	0.67	0.14	0.00	n/a

Neutrophil %	1.45	1.23	1.11	1.07	0.92
Lymphocyte %	0.60	0.76	1.12	0.86	0.80
Monocyte %	0.37	1.57	0.75	1.22	0.82
Eosinophil %	4.45	0.16	0.10	0.37	6.61
Basophil %	1.09	0.51	0.14	0.24	12.75
RBC	1.17	1.34	1.26	1.06	1.31
Hemoglobin	1.07	1.20	1.20	1.09	1.37
Hematocrit %	1.17	1.39	1.31	1.05	1.10
MCV	1.00	1.04	1.04	0.99	0.84
MCH	0.92	0.90	0.95	1.03	1.04
MCHC	0.92	0.86	0.92	1.04	1.24
RDW %	1.04	1.04	1.02	0.98	1.41
Platelets	0.37	0.73	0.74	0.51	0.68
MPV	1.08	0.95	1.16	0.97	1.46
WBC	1.04	1.09	0.80	0.79	1.77

7.3.6 Blood phenotyping chemistry panel (BPCP)

BPCP values for Pilot Study #1 and Pilot Study #2 were not assessed for changes between t=0 weeks and t=4 weeks (n=2; Supplementary Table 7.2, 7.4). For assessment of changes between the t=0 weeks and t=8 weeks, BPCP values at both timepoints were

compared. Nine out of 15 BPCP values remained stable for the duration of the study (Table 7.2). Blood urea nitrogen significantly increased from t=0 to t=8 weeks (15.4±2.3 mg/dl vs. 23.6±1.6 mg/dl, respectively; $p<0.0001$) in addition to albumin (4.03 ±0.28 g/dl vs. 4.44±0.19 g/dl, respectively; $p=0.01$), and total protein content (5.68±0.26 g/dl vs. 6.44±0.21 g/dl, respectively; $p<0.001$); glucose significantly decreased from t=0 to t=8 weeks (71.4±7.75 mg/dl vs. 53.0±16.4 mg/dl, respectively; $p=0.03$), as well as total bilirubin (0.09±0.07 mg/dl vs. 0.02±0.03 mg/dl, respectively; $p=0.04$) and chloride (101.5±1.3 mmol/L vs. 98.5±2.01 mmol/L, respectively; $p=0.01$). Albumin and blood urea nitrogen content at both t=0 and t=8 weeks were the only parameters outside the range of porcine reference ranges provided by UC Davis CPL.

Table 7.2: Full Study BPCP data. BPCP values from t=8 weeks normalized to values from t=0 are shown. Student's *t*-test shows significant differences in albumin, blood urea nitrogen, glucose, total bilirubin, total protein, and chloride content between the two time points.

Minipig	**20-1**	**21-5**	**34-2**	**48-5**	**28-1**	**29-1**
Alanine Transaminase	0.85	1.08	1.05	0.77	1.00	1.32
Albumin	1.14	1.17	1.13	1.02	1.08	1.07
Alkaline Phosphatase	1.32	0.99	1.29	1.34	0.77	1.07
Amylase	1.22	1.30	1.09	1.16	1.29	0.94
Aspartate Transaminase	0.73	0.83	0.96	1.14	1.61	1.98

Blood Urea Nitrogen	1.52	1.89	1.24	1.37	1.46	1.95
Calcium	1.03	1.02	1.06	1.00	0.95	0.99
Creatinine	0.98	0.98	0.76	1.06	0.90	0.89
Glucose	0.67	0.44	0.60	1.15	1.17	0.56
Phosphorus	0.96	0.89	1.01	1.07	1.27	1.23
Total Bilirubin	n/a	n/a	n/a	n/a	0.30	0.61
Total Protein	1.15	1.16	1.17	1.08	1.10	1.15
Chloride	0.98	0.97	0.93	0.95	1.00	0.98
Potassium	1.15	1.20	1.33	1.15	0.92	0.91
Sodium	0.99	0.99	0.97	0.98	1.07	1.03

7.4. Discussion

The objective of this study was to examine the reparative capacity of allogeneic, tissue-engineered implants in medial menisci of Yucatan minipigs using a non-homologous approach over 8 weeks. This was performed through an extensive analysis of gross morphological and histological properties of excised menisci, as well as mechanical and biochemical properties of repair tissues and interfaces found within defects. Toward this, several prior steps had to be completed, including creation of an appropriate defect model and development of surgical techniques; pilot studies served to validate a surgical technique that allowed for consistent creation of a defect in the anterior body of the meniscus without perturbing large collagenous structures such as the medial cruciate ligament (MCL). Using the defect model developed in the pilots, we proceeded to examine the hypothesis that the tissue-engineered implants would improve healing. Unfortunately,

for this defect model, this hypothesis was not supported because all empty defects were also fully filled with repair tissue. Further analysis showed that the quality of the repair tissue did not differ significantly between the menisci in Control and Implant groups in terms of mechanical and biochemical properties, indicating that future work would need to apply the constructs to a more appropriate defect model to examine the hypothesis. Despite this, however, the Full Study showed that the implants were safe, as indicated by CBC and BPCP results reported at t=0 and t=8 weeks. Additionally, with regard to the hypothesis that native tissue interfaces with repair tissues (within the pocket and defect; N-P-N and R-N, respectively) would have more robust tensile properties in menisci receiving an implant compared to untreated controls was partially supported by the data; only the N-P-N interface within the Implant group was higher in tensile Young's modulus values compared to the Control menisci. These data imply that tissue-engineered neocartilage implants aid in the healing response of separated or torn meniscal edges, and that additional improvements to the surgical method used in this study are needed to ensure that the implant is consistently retained within the native meniscus. Other factors related to the surgical procedure, such as the size and shape of the defect that is created, should also be considered for improvement as control defects exhibited excellent healing responses; ideally, a critical size defect should be created to properly evaluate the regenerative capacity of self-assembled neocartilage in minipig meniscal lesions.

When one is in the translational pathway to develop a potential product for clinical use, both the safety and efficacy of the approach should be considered. In terms of safety, allogeneic implants used in a non-homologous approach to repair meniscal defects did not cause a systemic immune response that negatively affected minipig health. CBC data

showed that 16 of 20 parameter values remained stable throughout the duration of the study (Table 7.1); despite this, the only parameter that was outside of reference porcine ranges provided by UC Davis CPL was hemoglobin content at t=0 (9.58±1.03 g/dL, reference range: 10.0-16.0 g/dL) and was elevated to within reference ranges by t=8 weeks. Additionally, BPCP data showed that 9 out of 15 parameter values remained stable throughout the duration of the study (Table 7.2). Of these BPCP parameters that did not remain stable over 8 weeks, only 2 parameters were outside of porcine reference ranges, namely albumin and blood urea nitrogen content. At both t=0 and t=8 weeks, values for albumin (4.03±0.28 g/dL and 4.44±0.19 g/dL, respectively) and blood urea nitrogen content (15.35±2.31 mg/dL and 23.62±1.56 mg/dL, respectively) were higher than porcine reference ranges (1.9-3.6 g/dL and 7-14 mg/dL, respectively). Reference ranges provided by UC Davis CPL are meant to serve as general guidelines, however, and are not specifically tailored toward the Yucatan minipig; ideally, comparison to untreated controls is recommended by UC Davis CPL. As all animals received an implant in this study due to the use of a bilateral approach, control animals that did not receive an implant were not investigated and could facilitate more direct comparison of safety data between implant-treated and untreated animals in future studies. Additionally, activity monitor data from the Full Study showed that minipig activity progressed toward presurgical levels within the first two weeks after undergoing surgery (Supplementary Figure 7.1). All safety measurements thus exhibited the exceptional profile of the neocartilage constructs.

In terms of efficacy, several design criteria were considered when creating the novel surgical technique used in the Full Study. For example, criteria included 1) the ability

to create a defect in the correct anatomical location consistently, 2) the preservation of large collagenous structures, such as the MCL, to maintain proper joint function, 3) pocket creation for the implant that closes without the use of sutures on the articulating surface of the meniscus, 4) retention of the implant within the meniscal pocket for the duration of the study, and 5) creation of a defect that does not spontaneously heal in menisci that do not receive an implant. Conducting pilot studies to validate the surgical method were crucial to informing methods used in the Full Study. Pilot Study #1 for example, did not satisfy the first criterion since the defect was created in the anterior root; this suggested that the meniscus needs to be pulled out farther from under the femoral condyle during surgery to consistently place defects in the anterior body of the tissue (Figure 7.4). Subsequently, in Pilot Study #2, the medial meniscus was destabilized, and the tibial attachment was trimmed to allow for better manipulation of the meniscus from under the femoral condyles. This allowed for better visualization of the defect location and facilitated creation of the pocket on the outer edge of the meniscus. Delivery of the implant within the intended location was ensured with this method, and one out of two animals exhibited robust repair tissue healing within the defect that propagated up to the articulating surface (Figure 7.4). The implant was also visualized in one of two animals via histological analysis; because no control menisci were investigated in Pilot Study #2 to minimize the number of animals used, four out of five design criteria for the surgical technique were satisfied. Ultimately, lessons learned in pilot studies allowed for the surgical method to be carried over for further validation in a full, statistically powered study.

Gross morphological features of the Yucatan minipig menisci were observed to assess the degree to which defects were filled with repair tissue, and whether femoral

condyles exhibited signs of damage to articular cartilage. Pilot Study #2 showed repair tissue within defects in n=2 medial menisci at t=4 weeks, which both received implants, despite only one exhibiting filling to the top of the defect with repair tissue (Figure 7.4); the through-and-through incision that was accidentally made when creating the pocket in the animal that exhibited less defect healing might have prevented retention of the implant and, thus, the intended healing response. In the Full Study, it was found that all samples from Control and Implant groups had defects 100% filled with repair tissue that propagated up to the top articulating meniscal surface (Figure 7.5). Additionally, all medial femoral condyles from Control and Implant groups exhibited damage to the articular cartilage (Figure 7.6). Because defects in the untreated Control group exhibited robust filling with repair tissue, future studies could employ the use of larger defects, or create defects of a different shape (i.e., rectangular versus circular) to ensure more stress concentrations and, thus, a greater degree of degeneration. For example, full thickness, 4mm circular defects created within the anterior body of the medial meniscus in a previous study using minipigs did not heal [37]; a smaller, 3mm defect size was chosen for this study to prevent the implant from dislodging through the defect and into the joint space. Additionally, partial thickness defects were used in all surgical sets in this study to recapitulate the intralaminar fenestration technique used to repair minipig TMJ discs [19]. Partial thickness defects in human menisci, which are more commonly seen emanating from the superior surface similar to this study, have also been shown to heal without the use of surgical repair techniques [38,39]. The degeneration of articular cartilage on the femoral condyles could partly stem from the initial destabilization of the meniscus; a destabilized medial meniscus within a Yucatan minipig model previously led to

fibrovascular scar tissue at the anterior root where the incision was made in addition to femoral condyle damage [20], which were also seen in this study. Thus, despite defects in Control and Implant groups being completely filled after 8 weeks, which left criterion #5 of our surgical model unsatisfied, gross morphological signs of fibrous scar tissue at the anterior root and articular cartilage damage indicate that meniscal function is not fully recapitulated with this surgical model.

Histological evaluation of meniscal samples allowed for the visualization of repair tissue within the pocket and defect, and was used to qualitatively identify whether the implant remained in place for treatment groups. Pilot Study #2 first provided signs that the implant was retained within the pocket at 4 weeks post-surgery in at least one of two animals and showed that the implant integrated with the surrounding native tissue (Figure 7.7); the implant showed less intense staining for collagen than native tissue, as expected. The pocket created with the intralaminar fenestration technique was visible in the Full Study, though the implant was not identified (Figure 7.8); this contrasts with results when the intralaminar fenestration technique was used in a TMJ model, where the implant could be identified by gross morphological and histological analysis at 8 weeks post-surgery [19]. This could result from implant not being properly retained within the pocket, or from considerable remodeling of the implant within the in vivo environment. To ensure that the implant is retained within the native tissue, improvements to the surgical procedure may be required. For example, custom-made tools could be manufactured to create more consistent pocket dimensions as opposed to using a Beaver blade; there is a possibility of the implant migrating within the pocket if the dimensions are much larger than the implanted construct. A different kind of pocket, such as embedding the implant

within a vertical longitudinal or horizontal tear, might also be more effective than methods used in this study and could provide insight into the repair capacity of self-assembled implants for different injury models; different pocket creation methods may aid in the retention of the implant. Thus, future studies investigating the repair capacity of neocartilage implants within meniscal defects could benefit from incremental improvements to surgical methods outlined in this study.

The knee meniscus, an anisotropic fibrocartilaginous tissue, resists compressive forces by developing tension along circumferentially aligned collagen fibers; because of the harsh mechanical environment within the knee joint, regenerated tissues should aim to recapitulate the function of native tissue. Tensile stiffness and strength of defect repair tissue in the Implant group reached up to 18% and 27% of native minipig values in the circumferential direction, respectively [23]. Other studies in dogs have also shown meniscal repair tissue to be mechanically inferior to the native tissue [40]. Collagen content between Control and Implant groups did not significantly differ, though levels in the Implant group reached up to 106% and 88% of native COL/WW and COL/DW values, respectively [23]. This may imply that collagen fibers within the repair tissue, despite reaching or nearing native levels, might be fragmented, are not fully aligned in the circumferential direction, have not fully matured, or are of a different collagen subtype than is seen in healthy tissue [41]; knee menisci are composed mainly of collagen type I, and, thus, future studies might benefit from a comprehensive proteomic analysis to understand repair tissue composition in this model. GAG/WW and GAG/DW in repair tissue did not significantly differ between Control and Implant groups, and samples from the Implant group reached as high as 147% of native tissue GAG/WW values. Thus, while

biochemical content of repair tissue reached or exceeded native tissue values, the structure of this tissue might not truly recapitulate the native meniscus as shown by its mechanical properties.

Another important factor to consider when evaluating the effectiveness of a regenerative solution is the strength of interfaces between native and repair tissues. This study found that neocartilage implants significantly improved N-P-N interface stiffness by 51% over untreated controls for the Full Study, while there were no significant improvements to the N-R interface (Figure 7.10). Because the implant tends to extrude toward the outer edge of the meniscus when closing the pocket, it is possible that the implant was not directly under the fenestration and thus only increased the healing response of the pocket. Samples akin to the N-P-N group in this study were tested in tension in a TMJ study conducted in minipigs in which self-assembled neocartilage was used toward healing a partial thickness defect [19]; the interface samples in the TMJ study also saw improvements in tensile stiffness in animals that received implants. The increased integration quality of the two laminae between which the implant was embedded in the treatment group compared to controls may imply that the neocartilage acts as a substrate and source of active, healthy cells that are depositing matrix; because the implant was not identified at the end of the Full Study, future time-point studies could facilitate an understanding of how the implant may migrate or remodel within the meniscal pocket. This finding, in addition to the pocket exhibiting healing in animals from Pilot Study #2 (Figure 7.7), suggests that this regenerative approach to meniscal lesions could be applied specifically to longitudinal or horizontal tears in which two torn ends of the meniscus would need to be fused back together. Another study that implanted a collagen

matrix embedded with mesenchymal stem cells (MSCs) within two torn ends of a vertical longitudinal defect in sheep also found a higher incidence of healing in the treatment group compared to controls, showing the potency of cell-based implants toward healing and fusing torn meniscal edges [42]. Thus, the Implant treatment was not only safe but also enhanced the integration and healing of the horizontal incision made during the creation of the meniscal pocket, although more work needs to be done to determine its efficacy for partial thickness defects and other injury models such as full thickness defects and vertical longitudinal tears.

The prevalence and economic impact of meniscal injuries motivate tissue engineers to create novel regenerative solutions and encourage collaboration with orthopedic surgeons toward developing surgical methods that accommodate implantation of these technologies. For these new implant technologies to successfully translate from the benchtop to the clinic they must first undergo extensive preclinical testing in a large animal model; aside from the importance of finding an appropriate animal model, it is crucial to develop surgical techniques that will allow for survival of the implant and, subsequently, a robust healing response. The investigation into the effectiveness of self-assembled neocartilage toward regenerating injured meniscal tissue using a novel surgical technique showed that implantation of self-assembled neocartilage constructs within the meniscus results in an exceptional safety profile and increased tensile properties of the interface between native and pocket repair tissues. Additionally, 3 out of 5 surgical design criteria were able to be satisfied in the Full Study. Thus, more robust methods are required to ensure survival of the implanted tissue and satisfy remaining criteria; additionally, critical defect models, such as full thickness defects which do not

typically heal without surgical intervention, are needed to prevent full healing of empty defects and examine efficacy of the tissue engineering approach. This may require alteration to the surgical approach used in this study or other existing methods; tissue engineered implants would also benefit from attaining properties closer to that of native tissue, which could increase their likeliness for survival in vivo. Ultimately, these findings provide a foundation for tissue engineers and orthopedic surgeons to build upon toward finding regenerative solutions to meniscal injuries.

References

[1] Salata, M. J., Gibbs, A. E., and Sekiya, J. K., 2010, “A Systematic Review of Clinical Outcomes in Patients Undergoing Meniscectomy,” Am. J. Sports Med., 38(9), pp. 1907–1916.

[2] Logerstedt, D. S., Snyder-Mackler, L., Ritter, R. C., and Axe, M. J., 2010, “Knee Pain and Mobility Impairments: Meniscal and Articular Cartilage Lesions,” J. Orthop. Sports Phys. Ther., 40(6).

[3] Baker, B. E., Peckham, A. C., Pupparo, F., and Sanborn, J. C., 1985, “Review of Meniscal Injury and Associated Sports,” Am. J. Sports Med., 13(1), pp. 1–4.

[4] Herrlin, S., Hållander, M., Wange, P., Weidenhielm, L., and Werner, S., 2007, “Arthroscopic or Conservative Treatment of Degenerative Medial Meniscal Tears: A Prospective Randomised Trial,” Knee Surgery, Sport. Traumatol. Arthrosc., 15(4), pp. 393–401.

[5] Katz, J., Brophy, R., Chaisson, C., Chaves, L., Cole, B., and Dahm, D., 2013, “Surgery versus Physical Therapy for a Meniscal Tear and Osteoarthritis,” N. Engl. J. Med., 368(18), pp. 1675–1684.

[6] Maffulli, N., Longo, U. G., Campi, S., and Denaro, V., 2010, “Meniscal Tears,” Open Access J. Sport. Med., 1, pp. 45–54.

[7] Barber-Westin, S. D., and Noyes, F. R., 2014, “Clinical Healing Rates of Meniscus Repairs of Tears in the Central-Third (Red-White) Zone,” Arthroscopy, 30(1), pp. 134–146.

[8] Xu, C., and Zhao, J., 2015, “A Meta-Analysis Comparing Meniscal Repair with Meniscectomy in the Treatment of Meniscal Tears: The More Meniscus, the Better Outcome?,” Knee Surgery, Sport. Traumatol. Arthrosc., 23(1), pp. 164–170.

[9] Rangger, C., Kathrein, A., Klestil, T., and Glötzer, W., 1997, “Partial Meniscectomy and Osteoarthritis. Implications for Treatment of Athletes.,” Sports Med., 23(1), pp. 61–68.

[10] Yoon, J. R., Kim, T. S., Wang, J. H., Yun, H. H., Lim, H., and Yang, J. H., 2011, “Importance of Independent Measurement of Width and Length of Lateral Meniscus during Preoperative Sizing for Meniscal Allograft Transplantation,” Am. J. Sports Med., 39(7), pp. 1541–1547.

[11] Wang, D., Gonzalez-Leon, E., Rodeo, S. A., and Athanasiou, K. A., 2021, “Clinical Replacement Strategies for Meniscus Tissue Deficiency,” Cartilage, 13(1_suppl), pp. 262S-270S.

[12] Novaretti, J. V., Lian, J., Sheean, A. J., Chan, C. K., Wang, J. H., Cohen, M., Debski, R. E., and Musahl, V., 2019, “Lateral Meniscal Allograft Transplantation With Bone Block and Suture-Only Techniques Partially Restores Knee Kinematics and Forces,” Am. J. Sports Med., 47(10), pp. 2427–2436.

[13] Kim, J. G., Lee, Y. S., Bae, T. S., Ha, J. K., Lee, D. H., Kim, Y. J., and Ra, H. J., 2013, “Tibiofemoral Contact Mechanics Following Posterior Root of Medial Meniscus Tear, Repair, Meniscectomy, and Allograft Transplantation,” Knee Surg. Sports Traumatol. Arthrosc., 21(9), pp. 2121–2125.

[14] Huey, D. J., and Athanasiou, K. A., 2011, “Tension-Compression Loading with Chemical Stimulation Results in Additive Increases to Functional Properties of Anatomic Meniscal Constructs,” PLoS One, 6(11), pp. 1–9.

[15] Gonzalez-Leon, E. A., Bielajew, B. J., Hu, J. C., and Athanasiou, K. A., 2020, “Engineering Self-Assembled Neomenisci through Combination of Matrix Augmentation and Directional Remodeling,” Acta Biomater., 109, pp. 73–81.

[16] Huey, D. J., and Athanasiou, K. A., 2011, “Maturational Growth of Self-Assembled, Functional Menisci as a Result of TGF-B1 and Enzymatic Chondroitinase-ABC Stimulation,” Biomaterials, 32(8), pp. 2052–2058.

[17] Hadidi, P., and Athanasiou, K. A., 2013, “Enhancing the Mechanical Properties of Engineered Tissue through Matrix Remodeling via the Signaling Phospholipid Lysophosphatidic Acid,” Biochem. Biophys. Res. Commun., 433(1), pp. 133–138.

[18] Makris, E. A., MacBarb, R. F., Paschos, N. K., Hu, J. C., and Athanasiou, K. A., 2014, “Combined Use of Chondroitinase-ABC, TGF-B1, and Collagen Crosslinking Agent Lysyl Oxidase to Engineer Functional Neotissues for Fibrocartilage Repair,” Biomaterials, 35(25), pp. 6787–6796.

[19] Vapniarsky, N., Huwe, L. W., Arzi, B., Houghton, M. K., Wong, M. E., Wilson, J. W., Hatcher, D. C., Hu, J. C., and Athanasiou, K. A., 2018, “Tissue Engineering toward Temporomandibular Joint Disc Regeneration,” Sci. Transl. Med., 10(44).

[20] Bansal, S., Miller, L. M., Patel, J. M., Meadows, K. D., Eby, M. R., Saleh, K. S., Martin, A. R., Stoeckl, B. D., Hast, M. W., Elliott, D. M., Zgonis, M. H., and Mauck, R. L., 2020, “Transection of the Medial Meniscus Anterior Horn Results in Cartilage Degeneration and Meniscus Remodeling in a Large Animal Model,” J. Orthop. Res., 38(12), pp. 2696–2708.

[21] Kremen, T. J., Stefanovic, T., Tawackoli, W., Salehi, K., Avalos, P., Reichel, D., Perez, M. J., Glaeser, J. D., and Sheyn, D., 2020, “A Translational Porcine Model for Human Cell-Based Therapies in the Treatment of Posttraumatic Osteoarthritis After Anterior Cruciate Ligament Injury,” Am. J. Sports Med., 48(12), pp. 3002–3012.

[22] Nordberg, R. C., Espinosa, M. G., Hu, J. C., and Athanasiou, K. A., 2021, “A Tribological Comparison of Facet Joint, Sacroiliac Joint, and Knee Cartilage in the Yucatan Minipig,” Cartilage.

[23] Gonzalez-Leon, E. A., Hu, J. C., and Athanasiou, K. A., 1AD, “Yucatan Minipig Knee Meniscus Regional Biomechanics and Biochemical Structure Support Its Suitability as a Large Animal Model for Translational Research,” Front. Bioeng. Biotechnol., 0, p. 239.

[24] Walpole, S. C., Prieto-Merino, D., Edwards, P., Cleland, J., Stevens, G., and Roberts, I., 2012, “The Weight of Nations: An Estimation of Adult Human Biomass,” BMC Public Heal. 2012 121, 12(1), pp. 1–6.

[25] Mardas, N., Dereka, X., Donos, N., and Dard, M., 2014, “Experimental Model for Bone Regeneration in Oral and Cranio-Maxillo-Facial Surgery,” J. Investig. Surg., 27(1), pp. 32–49.

[26] Cinque, M. E., DePhillipo, N. N., Moatshe, G., Chahla, J., Kennedy, M. I., Dornan, G. J., and LaPrade, R. F., 2019, “Clinical Outcomes of Inside-Out Meniscal Repair According to Anatomic Zone of the Meniscal Tear,” Orthop. J. Sport. Med., 7(7).

[27] Pfeifer, C. G., Fisher, M. B., Saxena, V., Kim, M., Henning, E. A., Steinberg, D. A., Dodge, G. R., and Mauck, R. L., 2017, “Age-Dependent Subchondral Bone Remodeling and Cartilage Repair in a Minipig Defect Model,” Tissue Eng. Part C. Methods, 23(11), pp. 745–753.

[28] Kim, I. L., Pfeifer, C. G., Fisher, M. B., Saxena, V., Meloni, G. R., Kwon, M. Y., Kim, M., Steinberg, D. R., Mauck, R. L., and Burdick, J. A., 2015, “Fibrous Scaffolds with Varied Fiber Chemistry and Growth Factor Delivery Promote Repair in a Porcine Cartilage Defect Model,” Tissue Eng. Part A, 21(21–22), pp. 2680–2690.

[29] Fisher, M. B., Belkin, N. S., Milby, A. H., Henning, E. A., Bostrom, M., Kim, M., Pfeifer, C., Meloni, G., Dodge, G. R., Burdick, J. A., Schaer, T. P., Steinberg, D. R., and Mauck, R. L., 2015, “Cartilage Repair and Subchondral Bone Remodeling in Response to Focal Lesions in a Mini-Pig Model: Implications for Tissue Engineering,” Tissue Eng. Part A, 21(3–4), pp. 850–860.

[30] Murphy, M. K., Masters, T. E., Hu, J. C., and Athanasiou, K. A., 2015, “Engineering a Fibrocartilage Spectrum through Modulation of Aggregate Redifferentiation,” Cell Transplant., 24(2), pp. 235–245.

[31] Huwe, L. W., Sullan, G. K., Hu, J. C., and Athanasiou, K. A., 2018, “Using Costal Chondrocytes to Engineer Articular Cartilage with Applications of Passive Axial Compression and Bioactive Stimuli,” Tissue Eng. Part A, 24(5–6), pp. 516–526.

[32] Lee, J. K., Huwe, L. W., Paschos, N., Aryaei, A., Gegg, C. A., Hu, J. C., and Athanasiou, K. A., 2017, “Tension Stimulation Drives Tissue Formation in Scaffold-Free Systems,” Nat. Mater., 16(8), pp. 864–873.

[33] Makris, E. A., Responte, D. J., Paschos, N. K., Hu, J. C., and Athanasiou, K. A., 2014, “Developing Functional Musculoskeletal Tissues through Hypoxia and Lysyl Oxidase-Induced Collagen Cross-Linking,” Proc. Natl. Acad. Sci., 111(45), pp. E4832–E4841.

[34] MacBarb, R. F., Makris, E. A., Hu, J. C., and Athanasiou, K. A., 2013, “A Chondroitinase-ABC and TGF-B1 Treatment Regimen for Enhancing the Mechanical Properties of Tissue-Engineered Fibrocartilage,” Acta Biomater., 9(1), pp. 4626–4634.

[35] Wang, D., Cubberly, M., Brown, W. E., Kwon, H., Hu, J. C., and Athanasiou, K. A., 2021, “Diagnostic Arthroscopy of the Minipig Stifle (Knee) for Translational Large Animal Research,” Arthrosc. Tech., 10(2), pp. e297–e301.

[36] Cissell, D. D., Link, J. M., Hu, J. C., and Athanasiou, K. A., 2017, “A Modified Hydroxyproline Assay Based on Hydrochloric Acid in Ehrlich’s Solution Accurately Measures Tissue Collagen Content,” Tissue Eng. Part C Methods, 23(4), pp. 243–250.

[37] Moriguchi, Y., Tateishi, K., Ando, W., Shimomura, K., Yonetani, Y., Tanaka, Y., Kita, K., Hart, D. A., Gobbi, A., Shino, K., Yoshikawa, H., and Nakamura, N., 2013, “Repair of Meniscal Lesions Using a Scaffold-Free Tissue-Engineered Construct Derived from Allogenic Synovial MSCs in a Miniature Swine Model,” Biomaterials, 34(9), pp. 2185–2193.

[38] Zemanovic, J. R., McLlister, D. R., and Hame, S. L., 2004, “Nonoperative Treatment of Partial-Thickness Meniscal Tears Identified during Anterior Cruciate Ligament Reconstruction,” Orthopedics, 27(7), pp. 755–758.

[39] “Non-Operative Treatment of Meniscal Tears - PubMed” [Online]. Available: https://pubmed.ncbi.nlm.nih.gov/2745476/. [Accessed: 17-Feb-2022].

[40] Roeddecker, K., Muennich, U., and Nagelschmjdt, M., 1994, “Meniscal Healing: A Biomechanical Study,” J. Surg. Res., 56(1), pp. 20–27.

[41] Ghadially, F. N., Lalonde, J. M., and Wedge, J. H., 1983, “Ultrastructure of Normal and Torn Menisci of the Human Knee Joint,” J. Anat., 136(Pt 4), pp. 773–91.

[42] Whitehouse, M. R., Howells, N. R., Parry, M. C., Austin, E., Kafienah, W., Brady, K., Goodship, A. E., Eldridge, J. D., Blom, A. W., and Hollander, A. P., 2017, “Repair of Torn Avascular Meniscal Cartilage Using Undifferentiated Autologous Mesenchymal Stem Cells: From In Vitro Optimization to a First-in-Human Study,” Stem Cells Transl. Med., 6(4), pp. 1237–1248.

Supplementary Materials

Supplementary Table 7.1: Pilot Study #1 and #2 CBC data. CBC values from t=4 weeks normalized to values from t=0 is shown. Statistical analysis was not conducted due to a lack of statistical power in each pilot (n=2).

Minipig	20-1	21-5	34-2	48-5
WBC	1.04	1.09	0.80	0.79

Absolute Neutrophil cells	1.51	1.34	0.89	0.84
Absolute Lymphocyte cells	0.63	0.83	0.90	0.67
Absolute Monocyte cells	0.37	1.73	0.60	0.95
Absolute Eosinophil cells	4.80	0.17	0.09	0.29
Absolute Basophil cells	1.33	0.67	0.14	0.00
Neutrophil %	1.45	1.23	1.11	1.07
Lymphocyte %	0.60	0.76	1.12	0.86
Monocyte %	0.37	1.57	0.75	1.22
Eosinophil %	4.45	0.16	0.10	0.37
Basophil %	1.09	0.51	0.14	0.24

RBC	1.17	1.34	1.26	1.06
Hemoglobin	1.07	1.20	1.20	1.09
Hematocrit %	1.17	1.39	1.31	1.05
MCV	1.00	1.04	1.04	0.99
MCH	0.92	0.90	0.95	1.03
MCHC	0.92	0.86	0.92	1.04
RDW %	1.04	1.04	1.02	0.98
Platelets	0.37	0.73	0.74	0.51
MPV	1.08	0.95	1.16	0.97
WBC	1.04	1.09	0.80	0.79

Supplementary Table 7.2: Pilot Study #1 and #2 BPCP data. BPCP values from t=4 weeks normalized to values from t=0 are shown. Statistical analysis was not conducted due to a lack of statistical power in each pilot(n=2).

Minipig	**67-1**	**173-4**	**108-7**	**139-4**
Alanine Transaminase	0.96	1.07	0.92	0.51
Albumin	1.07	1.14	1.08	1.06
Alkaline Phosphatase	1.39	1.51	1.15	1.38
Amylase	1.31	1.14	1.21	1.06

Aspartate Transaminase	1.20	1.72	0.79	0.48
Blood Urea Nitrogen	1.20	1.17	1.38	0.93
Calcium	0.98	0.92	1.03	0.97
Creatinine	1.14	0.74	1.11	1.32
Glucose	0.89	0.16	1.36	1.21
Phosphorus	1.50	1.32	0.90	0.94
Total Bilirubin	1.18	0.57	0.11	0.36
Total Protein	1.12	1.15	0.97	1.05
Chloride	0.98	1.01	1.06	1.04
Potassium	1.07	1.16	1.22	1.03
Sodium	1.01	1.01	1.05	1.06

Supplementary Table 7.3: Pilot Studies and Full Study CBC presurgical data.

CBC values from t=0 are shown.

Minipig	**67-1**	**173-4**	**108-7**	**139-4**	**20-1**	**21-5**	**34-2**	**48-5**	**28-1**
WBC (K/ul)	7.82	12.68	9.98	10.52	10.02	9.76	10.88	14.06	6.54
Absolute Neutrophil cells (K/ul)	4.15	7.29	5.99	5.84	4.60	5.08	6.48	8.71	3.23

Absolute Lymphocyte cells (K/ul)	3.02	3.46	3.37	4.28	4.91	3.86	2.70	4.27	2.87
Absolute Monocyte cells (K/ul)	0.32	0.29	0.22	0.27	0.43	0.30	0.75	0.82	0.28
Absolute Eosinophil cells (K/ul)	0.31	1.58	0.38	0.11	0.05	0.48	0.80	0.24	0.15
Absolute Basophil cells (K/ul)	0.02	0.06	0.03	0.01	0.03	0.03	0.14	0.02	0.00
Neutrophil %	53.02	57.46	60.01	55.56	45.86	52.03	59.60	61.92	49.38
Lymphocyte %	38.58	27.31	33.79	40.73	49.01	39.57	24.86	30.36	43.89
Monocyte %	4.15	2.31	2.18	2.57	4.30	3.12	6.89	5.82	4.35
Eosinophil %	3.97	12.48	3.76	1.03	0.51	4.94	7.33	1.73	2.33
Basophil %	0.28	0.44	0.26	0.10	0.32	0.35	1.32	0.17	0.04
RBC (M/ul)	5.65	4.76	4.88	6.67	5.17	4.73	5.92	5.81	5.24

Hemoglobin (g/dL)	9.3	8.6	7.9	9.5	10.2	8.9	10.3	10.4	8.1
Hematocrit %	29.5	26.8	26.4	34.6	30.9	24.6	29.7	33.1	34.1
MCV (fL)	52.2	56.2	54.2	51.8	59.7	52.1	50.2	57.0	65.1
MCH (pg)	16.5	18.1	16.2	14.2	19.7	18.8	17.4	17.9	15.5
MCHC (g/dL)	31.5	32.1	29.9	27.5	33.0	36.2	34.7	31.4	23.8
RDW %	17.8	17.3	18.4	19.4	16.9	19.0	19.8	18.0	14.0
Platelets (K/uL)	264	341	442	521	323	323	495	551	401
MPV (fL)	10.3	10.1	9.9	11.4	13.5	12.0	8.6	9.0	8.7
WBC (K/ul)	7.82	12.68	9.98	10.52	10.02	9.76	10.88	14.06	6.54

Supplementary Table 7.4: Pilot Studies and Full Study CBC data at study endpoints. CBC values from t=4 weeks or t=8 weeks are shown.

Minipig	**67-1**	**173-4**	**108-7**	**139-4**	**20-1**	**21-5**	**34-2**	**48-5**	**28-1**
WBC (K/ul)	14.80	9.52	6.68	9.02	10.44	10.62	8.72	11.04	11.58
Absolute Neutrophil cells (K/ul)	9.89	6.09	3.56	5.00	6.94	6.80	5.77	7.31	5.26

Absolute Lymphocyte cells (K/ul)	2.98	3.12	2.63	3.69	3.07	3.20	2.42	2.87	4.07
Absolute Monocyte cells (K/ul)	0.43	0.17	0.34	0.3	0.16	0.52	0.45	0.78	0.41
Absolute Eosinophil cells (K/ul)	1.45	0.12	0.13	0.05	0.24	0.08	0.07	0.07	1.78
Absolute Basophil cells (K/ul)	0.05	0.02	0.02	0.01	0.04	0.02	0.02	0.00	0.06
Neutrophil %	66.81	64.00	53.28	55.38	66.45	63.99	66.15	66.22	45.38
Lymphocyte %	20.11	32.76	39.43	40.87	29.36	30.14	27.76	26.00	35.14
Monocyte %	2.93	1.78	5.04	3.07	1.57	4.90	5.17	7.09	3.57
Eosinophil %	9.83	1.24	2.01	0.56	2.27	0.79	0.75	0.64	15.41
Basophil %	0.31	0.21	0.25	0.12	0.35	0.18	0.18	0.04	0.51
RBC (M/ul)	5.51	5.82	6.22	6.49	6.03	6.34	7.45	6.14	6.89

Hemoglobin (g/dL)	9.3	10.2	10.4	10.5	10.9	10.7	12.4	11.3	11.1
Hematocrit %	29.9	33.3	34.4	35.9	36.0	34.2	38.9	34.7	37.6
MCV (fL)	54.3	57.3	55.3	55.3	59.7	54.0	52.2	56.5	54.6
MCH (pg)	16.9	17.5	16.7	16.2	18.1	16.9	16.6	18.4	16.1
MCHC (g/dL)	31.1	30.6	30.2	29.2	30.3	31.3	31.9	32.6	29.5
RDW %	20.5	18.6	17.9	18.2	17.5	19.7	20.1	17.6	19.8
Platelets (K/uL)	462	529	417	468	120	235	365	282	272
MPV (fL)	13.5	12.4	10.7	10.5	14.6	11.4	10.0	8.7	12.7
WBC (K/ul)	14.80	9.52	6.68	9.02	10.44	10.62	8.72	11.04	11.58

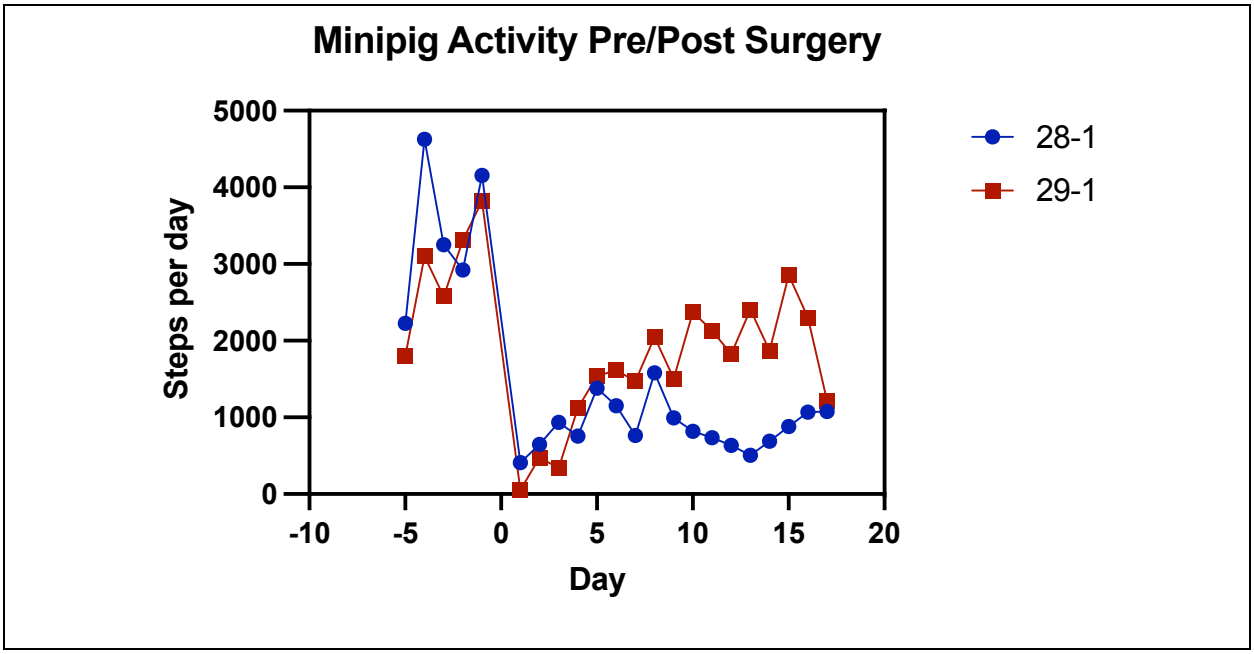

Supplementary Figure 7.1: Activity monitor data for the Full Study. Step count for n=2 minipigs from the Full Study are shown from t=-5 days pre-surgery to t=17 days post-surgery.

Conclusions

Tissue engineering, specifically of the knee meniscus, has made progress toward creating mechanically functional tissues to replace menisci injured due to trauma or degeneration. Specifically, self-assembled neomenisci and neocartilage, which have been engineered with compressive properties on par or approaching those of native tissue, have the potential to be innovative therapies to repair and replace injured menisci but still lack adequate tensile properties. Thus, this work aimed to enhance tensile properties of self-assembled neomenisci and neocartilage using bioactive factors or a combination of complementary mechanical stimuli. Also, since small-strain models do not capture functionality during native loading conditions, native and engineered menisci were modeled using hyperelastic parameters to better understand how microstructural components contribute to tissue functionality. To then facilitate the investigation of meniscus technologies *in vivo*, Yucatan minipig knee menisci were extensively characterized and were found to be suitable to translational meniscus studies. Finally, the safety and efficacy of allogeneic, self-assembled neocartilage implants toward repairing meniscal defects was studied in the Yucatan minipig. Ultimately, this work makes strides toward enhancing engineered neomenisci and neocartilage properties closer to those of native tissue, such that one day these technologies may be translated to the clinical bedside.

Because tensile properties of tissue-engineered menisci are still lacking in comparison to their compressive properties, which reach native tissue levels, a combination of complementary bioactive treatments was applied to investigate their effects on neomeniscus properties. TCL treatment had previously been shown to increase

mechanical and biochemical properties of neomenisci and fibrocartilages, while LPA had been shown to increase tensile properties and induce cytoskeletal contraction of meniscal cells. TCL+LPA was found to augment and align the mechanical properties of engineered fibrocartilaginous tissues. Higher collagen and pyridinoline crosslink content accompanied a synergistic increase in tensile properties; anisotropic mechanical properties were also observed in tissues treated with TCL+LPA, with tensile anisotropy values reaching close to 4. Anisotropic values trended higher in constructs treated with LPA, with the highest values recorded in the TCL+LPA group, while TCL treatment led to anisotropy values closer to 1. This finding was supported by second harmonic generation (SHG) signal of LPA and TCL+LPA treated constructs, which appeared more intense than control and TCL groups, indicating a higher degree of circumferentially aligned collagen fibers. Thus, the use of a combination of bioactive stimuli to achieve synergistic improvements in properties of engineered knee meniscus tissue was highlighted. The strategy of combining matrix augmentation and directional remodeling therefore is a simple and effective method to increase tensile properties of engineered neomenisci and provides a promising path toward deploying these neomenisci as functional repair and replacement tissues.

To properly understand meniscus function in relation to its structural properties, models that capture meniscal functional properties under normal loading conditions are needed. Small-strain linear analysis is typically used to model the meniscus but is largely phenomenological; however, the meniscus experiences large strains (~40%) under normal loading conditions. Hyperelastic models use large strain assumptions and were investigated with regard to modeling the native knee meniscus; ideally, a model that could

capture native and engineered meniscus function would be identified to better inform meniscus tissue engineering strategies. Native tissue extracellular matrices were thus perturbed with collagenase treatment, then the menisci underwent a series of mechanical and biochemical assays to quantify the effects of the changes to the ECM. As hypothesized, a fiber-reinforced Neo-Hookean model was found to best the best model based on goodness-of-fit. The fiber-reinforced Neo-Hookean model incorporates tissue microstructural properties into its analysis; this model also uses single fiber-family formulation, which assumes that collagen fibers are only circumferentially oriented. Three parameters are used in the fiber-reinforced Neo-Hookean, which is higher than the Neo-Hookean (one parameter) and Yeoh models (two parameters) that were also examined in this study, respectively. In our work we were able to identify that one of these parameters can be predetermined using a sensitivity analysis; thus, only two parameters were used to describe the tissue's behavior under large strain. This fiber-reinforced model was then applied to data from engineered neomenisci that had been treated with TCL+LPA in a previous study and was able to capture changes in experimental data stemming from bioactive treatments better than Neo-Hookean or Yeoh models that do not incorporate microstructural properties such as collagen and GAG. Future studies using this hyperelastic model could incorporate a better representation of the distribution of collagen fibers within the meniscus by including functional properties in the radial direction in addition to quantitative fiber alignment data to improve fidelity to experimental results. Together, these data provide a hyperelastic model that allows for deeper understanding of meniscal function with regard to its microstructural properties, and aids

tissue engineers in the design of functional neomenisci toward their use in repair and replacement technologies.

The use of mechanical stimuli in self-assembled neocartilages had previously been shown to be efficacious with a variety of mechanical stimuli, such as uniaxial tension, fluid-induced shear, or compression; however, only one type of stimulus was applied at a time. Thus, the use of uniaxial tension in combination with fluid-induced shear stress was investigated; the hypothesis that applying a combined stimulus regimen would result in improved functional properties compared to either stimulus alone or unstimulated controls was supported. Interestingly, benefits to neocartilage properties from application of uniaxial tension that were first identified in previous studies using different models were also seen in this study; specifically, the uniaxial tension regimen that was previously used in neocartilage derived from bovine and human sources was also validated in neocartilage engineered using minipig costal chondrocytes in this set of experiments. Additionally, it was shown that the order of stimulus application mattered, as only the application of tension before fluid-induced shear treatment resulted in improvements to construct mechanical properties. Importantly, neocartilage constructs had previously been used to repair fibrocartilaginous tissues such as the TMJ disc, implying that they may also be effective in the meniscus; the flat morphology of these constructs also allows for them to be used in the repair of meniscal injuries, especially in cases where two torn ends of the meniscus need to be integrated back together. Thus, this work is significant in that neocartilage functional properties were increased using a combination of two mechanical stimuli without the use of bioactive factors, which could facilitate the

implantation of these constructs in an appropriate animal model in future translational research.

Knowing the importance of using an appropriate animal model for the investigation of the efficacy of self-assembled tissues toward repairing the injured knee meniscus, Yucatan minipig were identified as a potential fit as they are becoming more frequently used in orthopedic research. Additionally, no guidance documents for translation of engineered fibrocartilage technologies exist to aid researchers through the FDA regulatory paradigm, further illustrating that “gold-standard” animal models need to be established for preclinical research. Thus, medial and lateral menisci from Yucatan minipigs were extensively characterized in terms of their gross morphological, mechanical, and biomechanical properties by region within each meniscus and compared to human values from the literature. Characterization of minipig menisci led to not only a repository of data, but also showed that several minipig meniscus morphological and functional properties fell within human ranges. For example, meniscal width and peripheral height were within human ranges, in addition to tensile and compressive properties. Biochemical content of minipig menisci, such as collagen, GAG, and crosslinks also met or exceeded values previously shown in humans. Additionally, regional investigation of these properties elucidated that GAG, PYR, PYR/COL, radial stiffness, and Young’s modulus anisotropy varied by region in the medial meniscus, while the lateral meniscus was more homogeneous throughout. Importantly, the lowest radial stiffness in the medial meniscus was obtained in the posterior region, corresponding to the most prevalent location for meniscal lesions also seen in humans. Investigation of injury models in future minipig studies could thus elucidate more robust comparisons to

human clinical data and could inform surgical techniques for the implantation of tissue-engineered repair technologies, such as self-assembled neomenisci or neocartilage constructs. Overall, similarities between minipig and human menisci supported the use of minipigs for meniscus preclinical research.

With the functional properties of native minipig menisci in mind, which largely fell within human ranges, this work then aimed to implant allogeneic, self-assembled neocartilage toward repairing defects created within the minipig knee meniscus. Pilot studies were conducted to validate the novel surgical method that was inspired by the intralaminar fenestration technique used to repair the minipig TMJ disc. A full study was then conducted that showed treatment with an implant significantly increased the tensile Young's modulus of the interface between laminae created when making the meniscal pocket by 51% over controls; however, no differences in repair tissue mechanical or biochemical properties were identified between control and treatment groups. Gross morphological analysis showed repair tissue filling up to the top surface of the defects for all animals within both control and treatment groups; additionally, damage to articular cartilage on medial femoral and tibial condyles was identified in all animals. Finally, histological analysis at t=8 weeks did not reveal signs of an implant within menisci in the treatment group despite being able to identify the implant at t=4 weeks in the second pilot study. Thus, this study demonstrated that implants exhibited an exceptional safety profile via analysis of blood samples before surgery and after the study endpoint, developed a novel surgical procedure for implantation of neocartilage constructs within the meniscus, and showed partial efficacy of implant treatment as denoted by increases to the Young's modulus of the native-pocket-native interface when compared to controls. Improvements

to the surgical procedure and defect model in future studies is recommended to ensure retention of the implant and limit healing in untreated control animals. Ultimately, this tissue-engineering strategy paves the way for developing clinical treatments for meniscal lesions.

The work developed here fits very well within the FDA pathway that a tissue-engineered, cell-based product needs to follow before submission of an investigational device exemption (IDE) and/or investigational new drug (IND) application depending on its classification. Safety and efficacy of self-assembled, allogeneic neocartilage implants used to repair meniscal lesions were investigated in an appropriate animal model, namely the Yucatan minipig. The characterization of the safety profiles of neocartilage constructs implanted into minipig menisci was initiated through extensive blood panels as discussed in Chapter 7; future studies should build upon this foundation and collect additional data on *in vivo* and *in vitro* implant safety through methods such as toxicology, pharmacology, and karyotyping. Improvements to the efficacy of the tissue engineering approach used toward repairing meniscal lesions in Chapter 7 is also needed to progress along the regulatory pathway; further development of the surgical technique to enhance implant retention, and the identification of a critically sized defect model in another animal study could facilitate these improvements. Upon completion of such studies, a pivotal large animal study needs to be performed and durability of the implant should be examined; this would be done likely in additional animal studies lasting at least 12 months. Once this is sufficiently completed, this tissue-engineered implant for repair of meniscal lesions can progress along the regulatory pathway and be considered for first-in-human studies and clinical applications.